

RD-A185 825

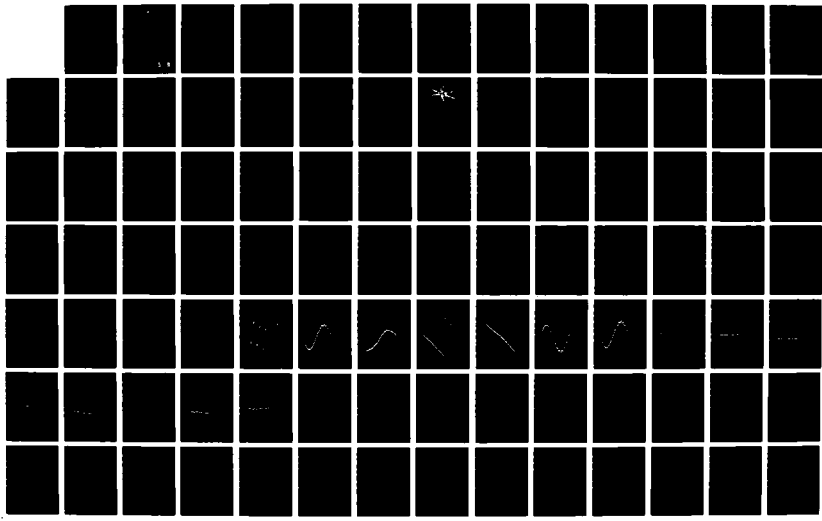
AN EVALUATION OF SEMIANALYTICAL SATELLITE THEORY
AGAINST LONG ARCS OF REA. (U) AIR FORCE INST OF TECH
WRIGHT-PATTERSON AFB OH M E FIEGER JAN 87

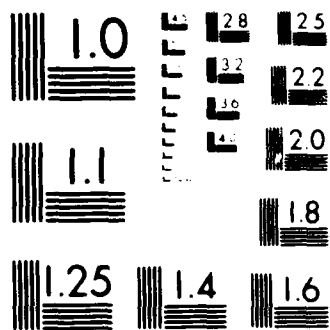
UNCLASSIFIED

AFIT/CI/NR-87-52T

1/1
F/G 22/3

NL





MICROFILM REPRODUCTION NUMBER - HART
NO. 10000000000000000000

AD-A185 825

(1)

DTIC FILE COPY

AN EVALUATION OF SEMIANALYTICAL SATELLITE THEORY

AGAINST LONG ARCS OF REAL DATA

FOR HIGHLY ECCENTRIC ORBITS

by

Martin Earl Fieger

B.S., University of Illinois
(1979)

Submitted to the Department of Aeronautics and Astronautics
in Partial Fulfillment of the Requirements of the Degree of

MASTER OF SCIENCE IN AERONAUTICS AND ASTRONAUTICS

at the

MASSACHUSETTS INSTITUTE OF TECHNOLOGY

January 1987

© The Charles Stark Draper Laboratory, Inc.

The Charles Stark Draper Laboratory, Inc. hereby grants to M.I.T.
permission to reproduce and to distribute copies of this thesis
document in whole or in part.

Signature of Author:

Martin E. Fieger

Department of Aeronautics and Astronautics
9 January 1987

Certified by:

Paul J. Cefola

Paul J. Cefola, Thesis Supervisor
Lecturer, Aeronautics and Astronautics

Accepted by:

Professor Harold J. Wachman
Chairman, Aeronautics and Astronautics Graduate Committee

DISTRIBUTION STATEMENT A

Approved for public release
Distribution Unlimited

DTIC
ELECTED
S OCT 27 1987 D
CH

87 10 14 252

AN EVALUATION OF SEMIANALYTICAL SATELLITE THEORY

AGAINST LONG ARCS OF REAL DATA

FOR HIGHLY ECCENTRIC ORBITS

by

Martin Earl Fieger

Submitted to the Department of Aeronautics and Astronautics on 9 January 1987 in partial fulfillment of the requirements for the Degree of Master of Science in Aeronautics and Astronautics.

ABSTRACT

The objective of this thesis is to test the Semianalytical Satellite Theory (SST) as implemented in The Charles Stark Draper Laboratory version of the Goddard Trajectory Determination System (GTDS) against long arcs of real data for highly eccentric orbits. The real data is in the form of North American Defense Command (NORAD) element sets and actual observations. Data are pre-processed and converted to a set of observations in a GTDS-compatible format. These observations undergo a differential correction (DC) process to generate the initial conditions for an SST ephemeris prediction. This prediction is then compared with real data to evaluate the performance of the SST.

Data available for this study included element sets and metric observations for the following objects:

<u>Object</u>	<u>Data Type</u>	<u>Period</u>
NSSC 9829 (1977-10A) Molniya 2-17	Mean elements	February 1977 - July 1986
NSSC 14095 (1983-51A) Exosat	Mean elements Observations	June 1983 - December 1985 June 1983 - December 1985
NSSC 13964 (1983-25A) Molniya 1-57	Mean elements Observations	May 1983 - September 1985 May 1983 - December 1985

The results validated the performance of the Semianalytical Satellite Theory for high eccentricity orbits. When elements sets were used as inputs to the DC, comparisons between the NORAD singly-averaged elements and the SST predictions showed good agreement. When the metric observations were used as inputs to the DC, agreement between the SST predictions and the observation data was very good.

Thesis Supervisor: Paul J. Cefola, Ph.D
Section Chief
Computer Science Division
The Charles Stark Draper Laboratory

Lecturer
Department of Aeronautics and Astronautics
Massachusetts Institute of Technology



Accession For	
NTIS GRA&I	<input checked="" type="checkbox"/>
DTIC TAB	<input type="checkbox"/>
Unannounced	<input type="checkbox"/>
Justification	
By	
Distribution/	
Availability Codes	
Dist	Avail and/or Special
A-1	

ACKNOWLEDGEMENTS

I wish to express my sincere gratitude to the Charles Stark Draper Laboratory for its support of this effort. Special thanks go to Dr. Ronald J. Proulx for his assistance during the development of the plotter utility and in the interpretation of the GTDS runs using the 8 x 8 resonant harmonic field. Mr. Wayne McClain made several valuable suggestions that were helpful in interpreting the semimajor axis comparisons. Mr. Leo Early was a saving source of information on the GTDS subroutines, especially those concerning the ORB1 files. It was also through his effort that the capability of the pre-processor for NORAD observations was expanded to include optical data. I'm grateful to USAF Lt. Col. Robert Herklotz, a fellow student at MIT, for his helpful comments and support.

I am especially grateful to Dr. Paul J. Cefola, also of Charles Stark Draper Laboratory, who served as my thesis advisor. His patience, helpfulness, and availability were extraordinary.

I'd like to express appreciation to Drs. R. Sridharan and E.M. Gaposchkin of Lincoln Laboratory for the helpful comments provided during their review of the results of this work.

The NORAD data for satellites NSSC14095 and NSSC13964 used in this investigation were obtained from the NORAD Historical Data System. I know it was not a trivial exercise to compile the data, and I'm most appreciative to Col. Jimmy Morrell of the USAF Space Command/J3S and his personnel for their efforts. I'd also like to thank Ronn Kling of Teledyne-Brown, Inc., for the mean elements for NSSC 9829. I'm grateful to Dr. Felix Hoots and Mr. Paul Major of the Directorate of Astrodynamics at Space Command for their comments on the SDP4 theory and its application.

I'm also indebted to Elba Santos for the professional appearance of this thesis. A final and special note of thanks to her.

The work in this thesis was partially supported by the Draper Laboratory IRD program (DFY86).

Permission is hereby granted by The Charles Stark Draper Laboratory, Inc., to the Massachusetts Institute of Technology and to the Air Force Institute of Technology to reproduce any or all of this thesis.

TABLE OF CONTENTS

<u>Chapter</u>	<u>Page</u>
1. INTRODUCTION.....	13
1.1 Uses of Elliptical Orbits.....	14
1.1.1 Scientific Missions.....	15
1.1.2 Military Missions.....	17
1.1.3 Transfer Orbits to Geosynchronous Orbits.....	19
1.2 Need for Long-Term Predictions.....	21
1.2.1 Mission Design.....	22
1.2.2 Catalog Maintenance.....	23
1.2.3 Satellite Constellation Evolution.....	24
1.2.4 Debris and Collision Assessments.....	25
1.2.5 Space Arms Control Issues.....	26
1.3 Application of Artificial Satellite Theory to Elliptical Orbits.....	27
1.3.1 Previous Application of Artificial Satellite Theory to Highly Elliptical Orbits.....	28
1.3.2 NORAD Prediction Models and the Implementation of SDP4.....	31
1.3.3 Semianalytical Satellite Theory.....	35
1.4 Thesis Overview.....	38
2. TEST METHODOLOGY.....	40
2.1 Pre-Processing NORAD Data to GTDS Observation Card Format...	43
2.2 SST Differential Correction Process.....	49
2.3 SST Ephemeris Prediction Process.....	50
2.4 Plotting Element Comparisons and Differences.....	51
3. TEST RESULTS.....	53
3.1 Initialization of SST Using Element Sets.....	53
3.1.1 NSSC 9829.....	53
3.1.1.1 Mission and Operations.....	54
3.1.1.2 SST DC and Ephemeris Generation.....	55
3.1.1.3 Comparison and Difference Plots.....	57

TABLE OF CONTENTS (Continued)

<u>Chapter</u>	<u>Page</u>
3.1.2 NSSC 14095.....	75
3.1.2.1 Mission and Operations.....	75
3.1.2.2 SST DC and Prediction.....	77
3.1.2.3 Comparison and Difference Plots.....	79
3.2 Initialization of SST Using Observation Data.....	96
3.2.1 NSSC 13964.....	96
3.2.1.1 Mission and Operations.....	96
3.2.1.2 SST DC and Prediction.....	97
3.2.1.3 Comparison and Difference Plots.....	107
3.2.2 Simulation of SDP4 with SST for NSSC 13964.....	108
4. CONCLUSIONS AND RECOMMENDATIONS.....	135
4.1 Conclusions.....	135
4.2 Future Work.....	138
LIST OF REFERENCES.....	209

LIST OF APPENDICES

<u>Appendix</u>	<u>Page</u>
A. Source Code for Utilities.....	140
ADCEDIT.....	141
RUNADC.....	146
SDP4.....	159
RDORB1.....	167
PLOTTER.....	171
RUNADCOB.....	185
ASTRON.....	195
PRENUT.....	205

LIST OF TABLES

<u>Table</u>	<u>Page</u>
1. NSSC 9829 Initial Operational Orbit Elements.....	54
2. NSSC 9829 Element Set Edits.....	55
3. Force Models Used for NSSC 9829.....	56
4. Results of DC for NSSC 9829.....	56
5. Results of Comparisons for NSSC 9829.....	57
6. NSSC 14095 Initial Operational Orbit Elements.....	76
7. NSSC 14095 Element Set Edits.....	77
8. Force Models Used for NSSC 14095.....	77
9. Results of DC for NSSC 14095.....	78
10. Results of Comparisons for NSSC 14095.....	79
11. NSSC 13964 Initial Operational Orbit Elements.....	97
12. Radar Observation Data Weights.....	97
13. Optical Observation Data Weights.....	98
14. Mean Dynamics Model Used for NSSC 13964.....	98
15. Short-Periodics Model Used for NSSC 13964.....	99
16. Results of DC for NSSC 13964.....	106
17. NSSC 13964 Residual Plot Key.....	106
18. Observation Summary by Type for NSSC 13964.....	107
19. Results of Comparisons for NSSC 13964.....	108
20. Mean Force Models in SDP4 Simulation.....	124
21. Short-Periodic Force Models in SDP4 Simulation.....	124
22. Results of "SDP4-Simulated" DC for NSSC 13964.....	125
23. Comparison of "SDP4-Simulated" Predictions and Full-Modelled SST Predictions for NSSC 13964 from 850102 to 850122.....	126
24. Results of SST DC with 20-Day Fit for NSSC 13964.....	126

LIST OF TABLES

<u>Table</u>	<u>Page</u>
25. Comparison of SST Predictions (Using 20-Day Fit Interval) and SST PRedicitions (Using 90-Day Fit Interval for NSSC 13964 from 850102 to 850122.....	127
26. Comparison of SST Predictions (Using 20-Day Fit Interval) and SST Predictions (Using 90-Day Fit Interval) for NSSC 13964 from 850122 to 850212.....	128
27. Comparison of Prediction Results Using Element Sets and Observations.....	137

LIST OF FIGURES

<u>Figure</u>	<u>Page</u>
1. Molniya 1 Spacecraft.....	20
2. Typical Molniya Groundtrack.....	20
3a. Test Data Flow Using NORAD Element Sets to Initialize the Semianalytical Theory.....	41
3b. Test Data Flow Using NORAD Observations to Initialize the Semianalytical Theory.....	42
4. NSSC 9829 NORAD Element Sets-1983 (OMEGA, XMO, XNC).....	45
5. Subroutine RUNADC Algorithm for Pre-Processing NORAD Element Sets.....	46
6. NSSC 9829 Semimajor Axis Comparison.....	59
7. NSSC 9829 Eccentricity Comparison.....	60
8. NSSC 9829 Inclination Comparison.....	61
9. NSSC 9829 Longitude of Ascending Node Comparison.....	62
10. NSSC 9829 Argument of Perigee Comparison.....	63
11. NSSC 9829 Radius of Perigee Comparison.....	64
12. NSSC 9829 Radius of Apogee Comparison.....	65
13. NSSC 9829 Semimajor Axis Difference.....	66
14. NSSC 9829 Eccentricity Difference.....	67
15. NSSC 9829 Inclination Difference.....	68
16. NSSC 9829 Longitude of Ascending Node Difference.....	69
17. NSSC 9829 Argument of Perigee Difference.....	70
18. NSSC 9829 Mean Anomaly Difference.....	71
19. NSSC 9829 Radius of Perigee Difference.....	72
20. NSSC 9829 Radius of Apogee Difference.....	73
21. NSSC 9829 NORAD Element Sets-1983 (XNDT2, XNDD6, BSTAR).....	74
22. NSSC 14095 Mean Anomaly Difference.....	80

LIST OF FIGURES

<u>Figure</u>	<u>Page</u>
23. NSSC 14095 Semimajor Axis Comparison.....	81
24. NSSC 14095 Eccentricity Comparison.....	82
25. NSSC 14095 Inclination Comparison.....	83
26. NSSC 14095 Longitude of Ascending Node Comparison.....	84
27. NSSC 14095 Argument of Perigee Comparison.....	85
28. NSSC 14095 Radius of Perigee Comparison.....	86
29. NSSC 14095 Radius of Apogee Comparison.....	87
30. NSSC 14095 Semimajor Axis Difference.....	88
31. NSSC 14095 Eccentricity Difference.....	89
32. NSSC 14095 Inclination Difference.....	90
33. NSSC 14095 Longitude of Ascending Node Difference.....	91
34. NSSC 14095 Argument of Perigee Difference.....	92
35. NSSC 14095 Mean Anomaly Difference.....	93
36. NSSC 14095 Radius of Perigee Difference.....	94
37. NSSC 14095 Radius of Apogee Difference.....	95
38. NSSC 13964 DC Residual (Range).....	100
39. NSSC 13964 DC Residual (Azimuth).....	101
40. NSSC 13964 DC Residual (Elevation).....	102
41. NSSC 13964 DC Residual (Range Rate).....	103
42. NSSC 13964 DC Residual (Right Ascension).....	104
43. NSSC 13964 DC Residual (Declination).....	105
44. NSSC 13964 Semimajor Axis Comparison.....	109
45. NSSC 13964 Eccentricity Comparison.....	110
46. NSSC 13964 Inclination Comparison.....	111
47. NSSC 13964 Longitude of Ascending Node Comparison.....	112

LIST OF FIGURES

<u>Figure</u>	<u>Page</u>
48. NSSC 13964 Argument of Perigee Comparison.....	113
49. NSSC 13964 Radius of Perigee Comparison.....	114
50. NSSC 13964 Radius of Apogee Comparison.....	115
51. NSSC 13964 Semimajor Axis Difference.....	116
52. NSSC 13964 Eccentricity Difference.....	117
53. NSSC 13964 Inclination Difference.....	118
54. NSSC 13964 Longitude of Ascending Node Difference.....	119
55. NSSC 13964 Argument of Perigee Difference.....	120
56. NSSC 13964 Mean Anomaly Difference.....	121
57. NSSC 13964 Radius of Perigee Difference.....	122
58. NSSC 13964 Radius of Apogee Difference.....	123
59. NSSC 13964 Radial Differences.....	129
60. NSSC 13964 Cross-Track Differences.....	130
61. NSSC 13964 Along-Track Differences.....	131
62. NSSC 13964 Radial Differences.....	132
63. NSSC 13964 Cross-Track Differences.....	133
64. NSSC 13964 Along-Track Differences.....	134

CHAPTER 1

INTRODUCTION

The objective of this thesis is to test the Semianalytical Satellite Theory (SST) as implemented in the Charles Stark Draper Laboratory version of the Goddard Trajectory Determination System (GTDS) against long arcs of real data for highly eccentric orbits. The real data is in the form of North American Defense Command (NORAD) element sets and metric observations. The orbits of primary interest will be those of two Soviet Molniya spacecraft (12-hr, high e) and of the European Space Agency satellite Exosat. Data are pre-processed and converted to a set of observations in a GTDS-compatible format. These observations undergo a differential correction (DC) process to generate the initial conditions for an SST ephemeris prediction. Processing of the real data proceeds along slightly different paths depending on whether element sets or observations are used to generate the initial conditions. This prediction is then compared with real data to evaluate the performance of the SST.

Chapter 1 reviews the use of elliptical orbits by the scientific and military communities. The need for long-term orbit predictions is described and the application of artificial satellite theory to highly elliptical orbits is reviewed.

THE SPACIAL ENVIRONMENT

designed to withstand the severe environment of space. In addition, the number and types of scientific instruments used on the various satellites have increased. The scientific instruments used on the present day satellites are more sophisticated than those used on the early satellites. The development of the various instruments has been stimulated by the increasing number of scientific publications. The instruments used on the early satellites were relatively simple and limited in their capabilities. As the number and complexity of these space systems increased, so did the need for more sophisticated instruments. The development of the various instruments has been stimulated by the increasing number of scientific publications. The instruments used on the early satellites were relatively simple and limited in their capabilities.

Of the satellites launched during the first decade of the space era, only 11 have survived. Missions of flight to the Moon and to other planetary satellites have been planned for the remaining satellites. At least 11 have been completed successfully. Some of the satellites have been lost due to damage from micrometeorites. The remainder have been lost due to various causes of mission failure, ocean survival, or due to lack of funding, safety, and funds to continue the international effort.

Approximately 40% of the various satellites have had a scientific research as their aim. Most have been designed to examine Earth and its environment. Other targets of research have been the planets, sun, and stars. Nearly all of the scientific satellites have been of the communications type. Communications satellites are designed to provide telephone, television, and other services to the public. Many of the satellites have been designed to provide information to the public about the environment.

testing new instruments or engineering techniques, and a few have been for the mapping of Earth resources [1].

The primary uses of elliptical orbits have been for scientific missions conducted by all the space-going countries of the world, military missions conducted primarily by the United States and the Soviet Union, and for transfer orbits to geosynchronous and other high altitude orbits. The major advantages of highly elliptical orbits include relatively long "stay-time" in a relatively small area of space and an independence from atmospheric drag effects during most of the orbit lifetime. These advantages have been exploited by both scientific and military investigators.

1.1.1. Scientific Missions

The great majority of scientific satellites operated in elliptical missions have been devoted to the studies of the Earth and the near-Earth environment. The primary users have been the United States, the Soviet Union, and the European Space Agency (ESA).

One of the early scientific programs was the Interplanetary Monitor Platform (IMP) program which consisted of ten United States spacecraft launched from 1963 to 1973. Its mission was to continuously measure the radiation environment in the immediate vicinity of Earth and in interplanetary space during a complete solar cycle in preparation for the Apollo program. The satellite orbits had a typical perigee height of approximately 200 km and an apogee height of approximately 200,000 km [2].

A more current satellite, the Combined Release and Radiation Effects Satellite (CRRES) has an unusual mission in that it performs related scientific experiments in both low earth orbit and a geosynchronous transfer orbit [3]. One mission objective of the CRRES is to determine how the Earth's magnetic field affects in situ microelectronic components. Another objective is to gather the data for an improved model of the Earth's radiation environment. The orbital parameters of the three year mission include a geosynchronous altitude apogee, a low inclination, and a perigee altitude of approximately 400 km.

The Soviet Union continues its active use of space, and several recent spacecraft have utilized the elliptical orbit. The Astron satellite launched in March 1983 from Tyuratam had a mission to investigate distant X-ray and ultraviolet emissions. Its orbit measured 2000 km by 200,000 km and had an orbital period of four days. It thus remained at great distances from the Earth for three and a half days of its orbit and was highly visible to Soviet ground-based tracking stations. The Prognoz series began in 1972 and has included a wide range of scientific missions. Prognoz 9 was launched in July 1983 from Tyuratam into an orbit measuring 400 km by 720,000 km to investigate remnant radiation from the "big bang". Prognoz 10 was launched in April 1985 into an orbit measuring 400 km by 200,000 km to study the shock wave boundaries created by the interaction of the solar wind plasma and the Earth's magnetosphere. Other Soviet scientific satellite programs planned for later in the decade [4] include placing the first of two pair of Prognoz-type and Magion-type satellites into an orbit measuring 500 km by 250,000 km and the second pair into an

orbit with an apogee of only 20,000 km. The first set will investigate the magnetospheric tail as the other pair observes the auroral field lines.

The ESA began utilizing the elliptical orbit in August 1975 with its Cos-B spacecraft designed as a gamma-ray observatory. It initially operated in a 0.88 eccentricity orbit of 340 km by 99,870 km and decayed in January 1986. The ISEE-2, launched in October 1977, was designed for magnetospheric exploration from a 0.91 eccentricity orbit. It is predicted to decay in September 1987 [5]. Another ESA satellite, whose orbit will be studied in detail later in this paper, is the Exosat, launched in May 1983.

1.1.2 Military Missions

The traditional military missions in space are: (1) communications; (2) reconnaissance and surveillance; (3) navigation; (4) meteorology; and (5) geodesy. Spacecraft with these missions primarily operate in one of five orbit types: (1) low Earth orbits, (LEO) below 5000 km; (2) geosynchronous orbits (GEO), at 35,700 km altitude; (3) Molniya orbits, about 500 km by 40,000 km with a 12 hour period; (4) semi-synchronous orbits, at 20,000 km with a 12 hour period; and (5) super-synchronous orbits between GEO and the Moon. Tables 1 thru 4 of [6] describe the current U.S. and Soviet military space systems. The U.S. utilizes elliptical orbits for its Satellite Data System (SDS), and the Soviets utilize elliptical orbits for their Molniya communications satellites as well as some early warning missions.

There is little open literature on the classified SDS program. Reference [7] describes it as having a three-fold mission: (1) maintain polar communication with Strategic Air Command aircraft in those areas uncovered by communication satellites in geosynchronous orbit; (2) provide a command and control link for USAF satellites; and (3) act as a relay for KH-11 photographic-reconnaissance satellites. The SDS spacecraft are launched atop the Titan 3B / Agena booster and inserted into an orbit approximately 320 km by 38,600 km, with apogee timed to occur over the polar regions. An inclination of about 63° provides greater satellite visibility at high latitudes. There were an estimated eight operational spacecraft launched between 1975 and 1981 [7].

The Soviet Union inaugurated its eminently successful domestic communication satellite system in April of 1965 with the launch of Molniya 1-1. Since then 110 of the 1600 kg spacecraft have carried the Molniya name.

Due to the enormous expanse of the Soviet Union - over 180° in longitude and over 40° in latitude to the Arctic Circle - the Soviets pioneered the use of highly elliptical orbits inclined 63° to 65° to the equator to provide reliable, nation-wide telephone, telegraph, and television communications. With perigee heights of 400 to 600 km situated over the Southern Hemisphere, Molniya satellites linger over the Soviet Union at altitudes of 39,000 to 40,000 km for approximately eight hours every revolution. By carefully positioning satellites in sequence as few as three satellites can provide around-the-clock coverage, although four or more are usually employed.

Two constellations of Molniya satellites serve the Soviet communications requirements [4]. The older Molniya 1 satellites are flown in eight orbital planes spaced 45° apart. Each satellite is positioned in its plane to ensure that every satellite in the network traces the same path over the Earth each day. This technique minimizes tracking requirements of the more than 90 Orbita ground stations. The second system is comprised of advanced Molniya 3 satellites, which are thought to be enhanced for maritime communications. The Molniya 3 network presently consists [4] of four satellites spaced 90° apart with ascending nodes near 65° and four satellites interspersed with ascending nodes near 155° . Figure 1 [4] is a diagram of the Molniya 3-21, and Figure 2 [8] shows a typical Molniya groundtrack.

The Soviet space program has other military spacecraft designed to operate in elliptical orbits. Planning for a Soviet ballistic missile early-warning satellite system that began in 1972 came to fruition in 1984 with the launch of seven new spacecraft. The constellation now consists of nine planes spaced 45° apart, with one satellite per plane, at an inclination of 63° and having an orbital period of 118 minutes [9].

1.1.3 Transfer to Geosynchronous Orbit

The geostationary transfer orbit (GTO) is also of high eccentricity. Objects in this orbit have lifetimes varying from a few months to more than 10 years, depending on the lunar-solar configuration at the time of launch. Estimation of the reentry date for such objects is less accurate

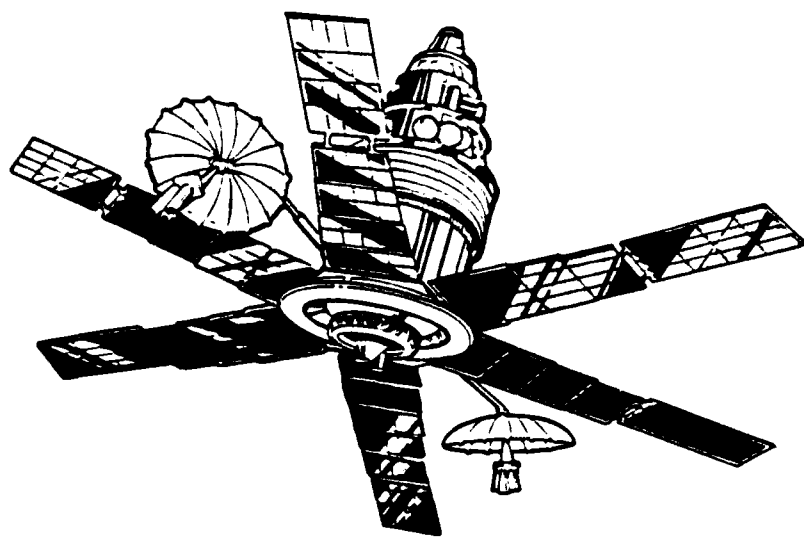


Figure 1. Molniya Spacecraft

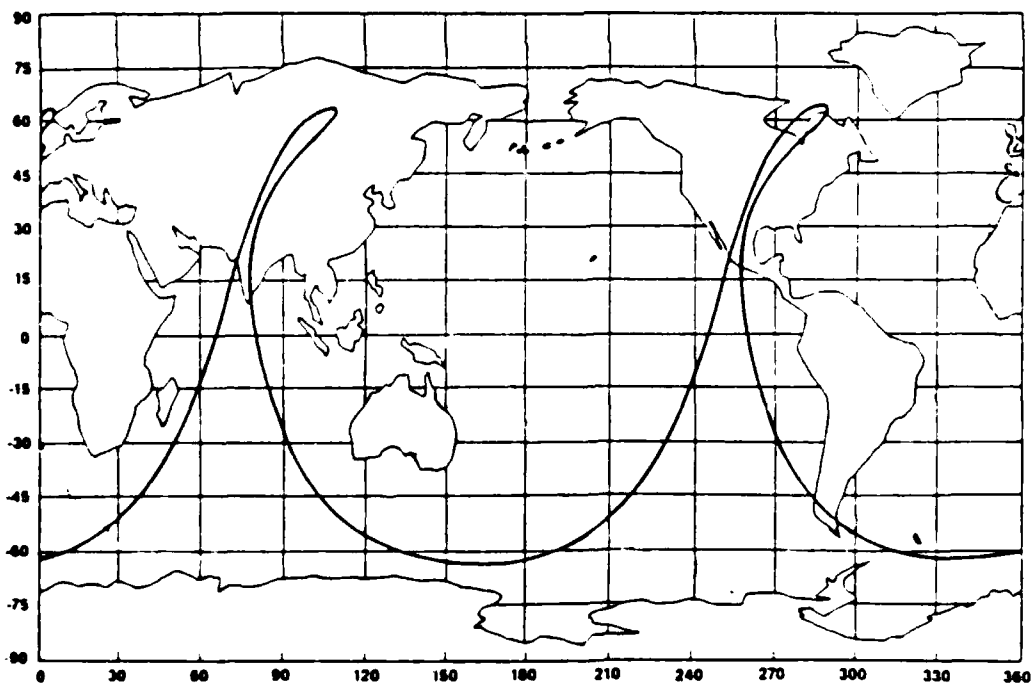


Figure 2. Typical Molniya Groundtrack

than for scientific satellites because of the increased influence of air drag at perigee due to their large size. Long-term predictions also can be particularly difficult if the lunar-solar perturbations hold the perigee height in the atmosphere, causing the satellite to pass through several resonance conditions.

One such object in the geosynchronous transfer orbit is NSSC 10723 (1978-12C), third stage for the International Ultraviolet Explorer launched in January 1978. It had an initial semimajor axis of 29,648 km and perigee height of 177 km, for an eccentricity of 0.779. It had an estimated orbital lifetime of seven years [1].

1.2 NEED FOR LONG-TERM PREDICTIONS

There are several reasons for investigating the behavior of highly elliptical orbits. The importance of accurately predicting the long-term motion of a satellite orbit is probably most evident during the mission design phase of the spacecraft. Besides the concerns that exist for the orbit evolution of a single spacecraft, there are concerns for the evolution over time for a constellation of two or more spacecraft. The need to reliably predict satellite orbits is evident in light of the increasing attention given to the problem of orbital debris and to the possibility of collisions in space. Long-term prediction of satellite orbits has also become an issue in the area of space arms control.

1.2.1 Mission Design

The orbital lifetime should be well understood prior to launch via the mission analysis process. Obviously, the satellite orbital lifetime must be longer than the satellite operational lifetime. Long-term predictions of the orbit insure the satellite has the proper orbital parameters while the spacecraft is performing its intended function. Long-term predictions are also necessary to design the satellite stationkeeping algorithms. Large and heavy satellites do not completely burn up during atmospheric re-entry; the exact time and place of re-entry must be predicted in order to warn the inhabitants of any danger (e.g., Cosmos 954 in 1978, Skylab in 1979, and Cosmos 1402 in 1983).

The most significant sources of perturbations of geocentric satellite orbits, and especially for mission design studies, are the central body oblateness, atmospheric drag, and lunar-solar gravity. The oblateness of the Earth causes a secular change in orbit orientation and is important directly because of its immediate influence on the mission, and indirectly because by changing the orbital relationship to the lunar-solar constellation, it alters the lunar-solar effects. Atmospheric drag results in a decrease in orbital energy and therefore a secular reduction of apogee. For orbits of higher eccentricity, with e approximately equal to 0.7, the gravitational perturbations due to the Sun and Moon are dominant in determining the evolution of satellite orbits. The orbital elements significantly effected by external body perturbations are the eccentricity, inclination, argument of perigee, and the longitude of the ascending node.

The perigee variations due to the Sun and Moon follow a characteristic pattern approximated by the superposition of four sine waves: (1) a very small-amplitude wave with the same periodicity as the satellite; (2) a 14-day wave of larger amplitude; (3) a 183-day wave of amplitude 5.8 times as large; and (4) a several-year period wave, usually of still larger amplitude. The four waves are usually called the short, intermediate, long, and very-long period effects [10]. The last two are important for determining orbital lifetimes of high-apogee, low-perigee orbits. The intermediate and long-period effects are related to the perturbing body's orbital motion and the very-long effect to the satellite orbit plane's changing orientation.

1.2.2 Catalog Maintenance

The responsibility for space population record-keeping is entrusted to the North American Aerospace Defense Command (NORAD). Observations on the deep space satellites are provided by four sources - the optical sensors at the Baker-Nunn camera sites, electro-optical sensors including the three Ground Based Electro-Optical Deep Space Sensor System (GEODSS) sites, deep space radar sensors, and near-Earth radars such as NAVSPASUR and PAVE PAWS when the satellites pass with range of these sensors. Observations from these sensors are used in conjunction with high-speed computers for identification and cataloging of all satellites and objects in space. The resulting element sets are then distributed to users to allow prediction of the future position and velocity of each space object.

Deep space satellites present a difficult problem in terms of catalog maintenance because many of the satellite orbits are out of range or at the very limits of present tracking capabilities [11]. Because of their slow angular motion relative to near-Earth satellites, deep space satellites are observed by fewer sensors and their orbits are therefore calculated with less data.

Reference [12] stated that the catalog of objects in space is relatively complete for objects greater than 10 cm in size, and he estimates that the population of objects 1 - 4 cm in size could be 3 to 10 times the known population. An object this size could have a mass of 100 grams and at relative velocities of the order of 10 km/sec could inflict significant damage to a satellite or an abandoned rocket stage. Reference [12] went on to state that it is possible to detect objects 1-10 cm across using space-based radar or lidar systems, but that the mass and power requirements are currently prohibitively high.

1.2.3 Satellite Constellation Evolution

The parameters of satellite constellation design include the number of satellites available, the properties of the sensor and payload (constrained by the operating altitude and attitude of the spacecraft), and the amount and type of coverage required. Methods of minimizing revisit time or maximizing coverage typically assume symmetric constellations [13]. That is, satellites in a single orbit plane are evenly distributed in mean anomaly, and individual orbit planes at common inclinations are evenly

distributed in right ascension of ascending node. Real-world perturbations can and do cause changes in the argument of perigee, longitude of the ascending node, etc. These real-world perturbations necessitate careful study of the long-term stability of the satellite constellation.

1.2.4 Debris and Collision Assessments

More than 3000 payloads and 12,000 objects have been put into orbit since 1957. The December 1984 "Satellite Situation Report", quoted in [12], listed 5408 objects in orbit, of which 5% were operational payloads, 20% were non-operational payloads, 25% were mission-related objects, and 50% were satellite breakups. Many mission-related objects - upper stages, apogee kick motors, spent rocket casings, parts of separation devices, protective covers, etc. - remain in low Earth orbit or in the geosynchronous transfer orbit. The geostationary ring, a strictly limited territory only 264,930 km long, is becoming increasingly crowded, especially near the stable points of 107° West and 76° East longitude. Trends indicating that the number of operating spacecraft will double every five years [14] accentuate the need for accurate long-term prediction of objects in these orbits.

There are several means of reducing the hazards of collision. Some are relatively easy to implement with spacecraft design changes or operational procedures. These include reducing the number of objects at separation, de-orbiting large satellites to re-enter the atmosphere, depleting residual propellants, and conducting satellite destruction tests at low

altitude to ensure rapid decay of debris. Another method, which is less costly in terms of the required spacecraft mass than deorbiting to Earth is to desynchronize upward. It is written policy of the INTELSAT board of governors to desynchronize unusable spacecraft 40 km to 50 km upward; it is written policy of NOAA to desynchronize at least 300 km upward [14]. The Soviet Union does not circularly desynchronize, but has fired to produce large eccentricity to reduce the chances of crossing on the geostationary ring.

1.2.5 Space Arms Control Issues

The requirement for long-term prediction of orbits is relevant in discussions of military space systems. The vulnerability of a satellite to attack is primarily a function of the orbit in which the satellite operates, since the orbit determines the time and cost for an Earth-launched ASAT intercept or the power for a laser or particle beam attack.

There has been general agreement that essential warning and communication capabilities should be preserved at a very high priority even in the face of a nuclear attack [6,15,16]. One possible bilateral agreement to enhance the security of some space assets most relevant to nuclear stability in an adequately verifiable way could develop "rules of the road" for space, i.e., an international agreement governing the use of space. This agreement might, for example, make it legal for any signatory nation to take some action regarding other nations' satellites coming closer than certain stated distances to specified satellites of its own. The stated

distances and specified satellites would have to be resolved according to the orbits of the satellites to be protected and according to the requirements of civilian space users.

Illustrative "rules of the road" include: (1) keep 100 km and 3° out-of-plane from foreign satellites below 5000 km; (2) keep 500 km from foreign satellites above 5000 km except those within 500 km of geosynchronous altitude; (3) allow one pre-announced close approach at a time; (4) find guilty of trespass the satellite of the nation which most recently initiated a maneuver burn [16].

1.3 APPLICATION OF ARTIFICIAL SATELLITE THEORY TO ELLIPTICAL ORBITS

The application of analytical, semianalytical, and numerical orbit propagators to the problem of long-term prediction of eccentric orbits is the subject of this section. When making any comparison, it is important to understand the two things being compared. Because one objective of this research was to test the long-term predictions of the semianalytical theory against real data in the form of NORAD mean elements, both the semianalytical and NORAD satellite theories will be reviewed. Also included is a review of previous applications of artificial satellite theory to the problem of highly elliptical orbits.

1.3.1 Previous Applications of Artificial Gravity to the Circular Orbit Elliptical Orbit

Reference (12) developed an analytical method to predict the long-term changes of orbits having moderate to large eccentricities, with the apogee and semi-major axes up to ten Earth radii. Circular orbits for the Sun and Moon were assumed, as was a linear orbital plane that coincided with the plane of the elliptipse. It was found that orbital lifetimes were determined primarily by the orbital elements. The precession of the orbital angular momentum of the Earth's orbit around the Sun was found to be very slow, precessing about the Sun at a rate of approximately one degree in 100 years.

Reference (13) added the effects of obliquity and eccentricity to the orbital longitude dependence of the dip potential. It was shown that the effect with an eccentricity higher than about 0.1, the obliquity and the effect of the dipole moment, interact with each other, which is reflected in the zero-gravity time. A constant parameter was introduced that described the behavior of the elliptical orbits near the circular orbit, provided the orbital motion was not significantly affected by the Sun.

Reference (14) derived the non-circular equilibrium orbits for the Earth-Moon orbits as functions of the obliquity and the moment of inertia, and examined in detail the long-period orbital motion of the Moon around the Earth and the Earth's influence on the Moon's motion.

orbit was due to resonance with longitude terms in the geopotential. The importance of the lunar-solar perturbations was mentioned only in passing, noting that several Molniyas had been lost to improper initial placement of the orbit node with respect to the Moon's node. The equation of motion of the mean longitude of a closely commensurate satellite due to the geopotential was a function of the unnormalized harmonic coefficients of degrees l and order m ($l \geq m$) in the geopotential expansion, the orbit semi-major axis, and the amplitudes and phase angles of the composite vectors which depend on the inclination, eccentricity, and argument of perigee of the orbit. It was shown that there were four relevant resonant terms that accounted for all but 10% of the resonant acceleration on the 12-hr satellite orbit. All but 20% of the resonant acceleration was accounted for by only two of the terms, and all but about 25% of the resonant acceleration for orbits in the vicinity of critical inclination was accounted for by a single term. For equatorial and critically-inclined orbits with specified eccentricity and argument of perigee, only one longitude for the placement at equator crossing resulted in orbits in stable equilibrium with the resultant geopotential forces. For the maximum altitude 12-hr orbit intermediate inclination ($50^\circ < i < 70^\circ$), stable orbits were available for equator crossing longitudes between 55° and 85° East provided the argument of perigee was within 100° .

Reference [20] described the basic theory for a computer program PROD (Program for Orbit Development) which predicted the long-term development of elliptic orbits under the influence of the Earth's gravitational potential and the attractions of the Sun and Moon. Effects of drag and

solar radiation pressures were not included. Reference [21] used this program to predict orbital elements for a Molniya 1 satellite and compared them to U.S. Air Force orbital 5-line elements. The PROD-predicted perigee heights were accurate to about 20 km throughout a 21-month interval.

Reference [21] also developed an analytical method for 12-hr orbits of 65° inclination and demonstrated that the lifetime must be between one and seven years. It was shown that in the absence of air drag, orbital lifetime is controlled by the variation in perigee height which, in turn, is controlled by the variation in eccentricity. This variation in eccentricity due to lunar-solar perturbations was expressed as a function of argument of perigee and longitude of the ascending node. With initial values of eccentricity and argument of perigee ($e=0.74$ and $\omega=286^\circ$) for 31 of the 65 Molniyas launched up to that time, and with an observed value of -0.25 deg/day as the rate of change of argument of perigee, the decay condition was then expressed as the intersection of two curves involving the varying value of perigee and the varying and initial values of longitude of the ascending node.

For Molniya satellites in orbits of 63° inclination, [21] found that the satellite orbits were far less amenable to analytical treatment, because the argument of perigee could librate around 270° and the inclination about 63.4° . He concluded that very long lifetimes, on the order of hundreds of years, were possible if the argument of perigee remained around 270° for cases in which the absolute value of the longitude of the ascending node was below 60° . In 1978 [22] presented a graphical method

of estimating future lifetimes of an artificial satellite based on its current rate of decay and by using an exponential atmosphere model. Effects of the asphericity of the Earth, effects of atmospheric oblateness, density changes due to the 11-year solar cycle, day-to-night, and semiannual variations were approximated by specified correction factors. Large lunar-solar perturbations (greater than 50 km) were handled with numerical integration. For high eccentricity orbits, the initial value of perigee height was corrected using the decay rate with the mass-to-area ratio of the spacecraft. These methods allowed decay date predictions up to about one year ahead with an accuracy of about 10% of the remaining lifetime.

1.3.2 NORAD Prediction Models and the Implementation of SDP4

As previously mentioned, NORAD has the responsibility of maintaining a catalog of element sets for all space objects. The element sets are then distributed to users to allow prediction of the future position and velocity of each space object. The satellite observations are obtained by the Space Detection and Tracking System (SPADATS) network of "skin-track" radars and optical sensors. The orbital element sets are based on statistical processing of the satellite observations. For the highly eccentric orbits, the observations are primarily obtained from the deep space radars (Millstone and Altair) and from the GEODSS optical sensors.

NORAD has utilized several propagation models for prediction of satellite position and velocity. They will be summarized here; a more detailed

description is available in [23]. The earliest model, SGP, was developed in 1966 for near Earth satellites. It simplified the work of Kozai for its gravitational model, including the zonal harmonics J_2 and J_4 , and it assumed the drag effect on mean motion to be a quadratic in time, resulting in a cubic variation in mean anomaly with time. The drag effect on eccentricity was modeled in such a way that perigee height remained constant.

A second propagation model, SGP4, was developed in 1970 and is used for near Earth satellites. This model was obtained by simplification of the more extensive analytical theory of Lane and Cranford which used the solution of Brouwer for its gravitational model and a power density function for its atmospheric model. The next model developed, SDP4, was an extension of SGP4 to be used for deep-space satellites (which NORAD defines as those having a period greater than 225 minutes). It is described in more detail below.

Another propagation model, developed but never implemented operationally, was SGP8. The SGP8 and SDP8 models have the same gravitational and atmospheric models as the SGP4 and SDP4 models respectively, although the form of the solution was quite different.

Since the late 1970's, SDP4 has been the model used for deep space satellites. The SDP4 theory is based upon the restricted four-body solution for resonating satellites without drag and using multiple transformations developed by Hujasak [24]. First, the four-body oblate Earth problem,

which describes the satellite motion perturbed by the point mass effects of the Moon and Sun as well as the oblate Earth is analyzed [24]. Several transformations are introduced and the transformed dynamical system is integrated analytically. He then used the method of averaging to derive a multiply-transformed dynamical system for resonating satellites of 12-hr or 24-hr orbital periods. This dynamical system was then integrated analytically except for a numerical evaluation of the main resonance effect.

Hujšák used the spherical harmonic potential of the Earth in terms of associated Legendre functions as given by [25], where the Earth potential was separated into the zonal potential and the potential due to sectoral and tesseral harmonics, the latter of which was expressed in terms of the $F_{lmp}(i)$ and $G_{lpq}(e)$ inclination and eccentricity functions. The specific tesseral resonance terms included in SDP4 for the 12 hr orbits are of degree and order:

2,2	5,2
3,2	5,4
4,4	

The gravitational potential of the Moon or Sun was represented by a single term of the expanded series of Legendre functions of the phase angle between the satellite and the third body.

The dynamical system was a function of two fast variables, mean anomaly and Greenwich sidereal time, and satisfied the conditions for application

of the method of averaging. The resultant first-order short-periodic variations due to J_2 are given in Appendix F of [24]. Second-order, short-periodic variations were ignored. Second and third transformations were then applied to remove the mean anomalies of the Moon and Sun. The triply-transformed dynamical system for non-resonating satellites was then expressable as the sum of zonal expressions and third body effects (see Appendices D and E of [24]) which varied slowly with time.

For the problem of resonance, [24] suggested a change of variables which resulted in a dynamical system which was a function of a single fast variable, namely, the sidereal time. The singly-averaged four-body oblate Earth potential under resonance conditions was then derived using the method of averaging. A resonating triply-averaged potential was then derived after averaging over the lunar and solar mean anomalies.

In the early 1990's USAF Space Command plans to convert to a new, more accurate ephemeris prediction model called HANDE [26] to predict satellite position and velocity and to maintain the National Space Surveillance Center (NSSC) catalog. The HANDE model was developed in [27] and was designed for both near-Earth and deep space satellites. The method includes the zonal harmonics J_2 , J_3 , and J_4 for its gravitational model and a dynamic atmosphere [28] for its physical atmospheric model. It includes lunar and solar effects as well as resonance terms for satellites with 1/2 day and 1 day periods. HANDE, as all the NORAD ephemeris models, produces predictions in an Earth-centered non-rotating coordinate

system based on the true equator and mean equinox of the epoch of the element set. The HANDE theory is unique relative to previous NORAD theories in that the external user only needs the ephemeris reduction portion of the theory.

1.3.3 Semianalytical Satellite Theory

Advanced applications of space for both military and scientific missions require fast, reliable orbit predictions for artificial satellites. Orbit predictions using special perturbation theories, based upon the numerical integration of the osculating equations of motion, are accurate but slow, since they often require a hundred or more steps per satellite orbit to give good results. Orbit predictions using general perturbation theories are fast but contain large errors due to the neglect of certain perturbations. The SDP4 model, for example, truncates the zonal potential after J_4 , limits the third-body potential expansion to a single term, assumes truncated resonance effects based on a 12-hr or 24-hr orbit, and assumes a power density function for its atmospheric model.

Semianalytical Satellite Theory (SST) is an alternative to special and general perturbation theories. In SST, perturbations that can be expressed in terms of a disturbing potential have that potential expressed in nearly singularity-free equinoctial elements. The perturbations are then put in Lagragian Variation of Parameter (VOP) form. This allows only small deviations from Keplerian motion to be considered. Those perturbations which cannot be expressed in terms of potential, such as drag and solar radiation pressure, are expressed in Gaussian VOP equations.

SST then uses the Generalized Method of Averaging [29,30] to separate long-period and secular terms from the short-periodic components of the satellite motion. It is usually sufficient to perform this separation of the so-called "mean" elements from the short-periodic terms only to first order in small parameters of the perturbations; however some second order and coupling terms have been included.

The analytical or numerical averaging technique which separates these mean components results in a smooth mean satellite motion. For perturbations expressed in terms of a potential this separation is primarily accomplished by averaging all the perturbative effects over a fast angular variable for a satellite period. For non-potential perturbations this averaging takes place over the satellite period instead of a cycle of an angular variable.

A low-order integration technique, e.g., the fourth-order Runge-Kutta method, with stepsizes of one day is usually sufficient to integrate the averaged satellite motion for the high eccentricity cases. Interpolators are used to produce accurate mean orbital elements for any time of interest. Reversing the averaging transformation results in the short-periodic component of motion. This short-period term is added to the mean motion to obtain the satellite osculating state. The fact that the calculation of this short-period term is usually only required for the particular time of the desired osculating output is one of the major advantages of the SST. This is because the mean motion already allows the full dynamics to

be recovered. The short-period portion of the theory also includes an interpolator concept so that closely spaced output requirements can be treated efficiently.

The SST used in this investigation has been implemented in the CSDL version of the Goddard Trajectory Determination System (GTDS), a multi-purpose computer system originally formulated to support space missions and various research and development project requirements at NASA Goddard Space Flight Center [31]. The Draper version includes an array of force models that can be called upon to achieve varying levels of orbit determination accuracy for different satellite orbits. Shown below are the force models developed for the semianalytical propagator.

Mean Element Dynamics

Recursive zonals (closed form (c.f.)) and $J_2^2 e^1$

Recursive tesseral resonance (e^n , $n > 20$)

Recursive lunar-solar (single averaging)(c.f.)

Recursive lunar-solar (double averaging)(c.f.)

Solid Earth tide (c.f.)

Atmospheric Drag (and J_2 /drag coupling)(numerical)

Solar radiation pressure (numerical)

Short Periodics

Recursive zonals (c.f.) and $J_2^2 e^1$

Recursive tesseral m-dailies (c.f.)

Recursive tesseral linear combinations ($e^n, n > 20$)

Recursive J_2 secular/tesseral m-daily coupling (c.f.)

Recursive lunar-solar (c.f.)

Atmospheric drag (numerical)

Solar radiation pressure (numerical)

Numerous studies for several types of orbits have confirmed the accuracy of the theory [32,33,34], and a portable version has also been developed [35].

1.4 THESIS OVERVIEW

The primary objective of this thesis is to test the semianalytical satellite theory as implemented in the CSDL version of the GTDS against long arcs of real data of highly eccentric orbits. Of primary interest will be the orbits of two Soviet Molniya spacecraft and the orbit of the European Space Agency satellite Exosat. The data for the satellites will be in the form of NORAD observations and element sets. Chapter 1 has reviewed the uses of elliptical orbits and the need for long-term predictions. It has also reviewed the application of artificial satellite theory to highly elliptical orbits.

Chapter 2 addresses the test methodology of this investigation. The primary topics include:

1. Pre-processing NORAD data
2. Determining an initial state using an SST DC

3. Generating the SST prediction file

4. Evaluating the SST prediction

Chapter 3 describes the results obtained using real data for specific orbits using the methodology of Chapter 2. The data available for this study includes observations and element sets for the following objects:

<u>Object</u>	<u>Data Type</u>	<u>Period</u>
NSSC 9829 (1977-10A)	Mean elements	February 1977 - September 1986
Molniya 2-17		
NSSC 14095 (1983-51A)	Mean elements	June 1983 - December 1985
Exosat	Observations	June 1983 - December 1985
NSSC 13964 (1983-25A)	Mean elements	May 1983 - September 1985
Molniya 1-57	Observations	May 1983 - December 1985

The rationale for the dynamics modelling chosen in each case for the differential correction and for the semianalytic propagator is given, and an analysis of the comparison and difference plots is made.

Chapter 4 summarizes the results of the previous chapters and presents some ideas for future study.

CHAPTER 2

TEST METHODOLOGY

The primary objective of this thesis is to test the semianalytical satellite theory as implemented in the CSDL version of the GTDS against long arcs of real data for highly eccentric orbits. Of primary interest will be the orbits of two Soviet Molniya spacecraft and the orbit of the European Space Agency satellite Exosat. The data for the satellites is in the form of NORAD element sets and actual observations. Chapter 1 reviewed how elliptical orbits have been used by the scientific and military communities, described the need for long-term predictions, and reviewed the application of artificial satellite theory to highly elliptical orbits. Chapter 2 addresses test methodology.

The primary topics of this methodology include:

1. Pre-processing NORAD data
2. Determining an initial state using an SST DC
3. Generating the SST prediction file
4. Evaluating the SST prediction

The overall framework of this effort is shown in Figure 3a and Figure 3b. Figure 3a illustrates the data flow in which a relatively short arc of

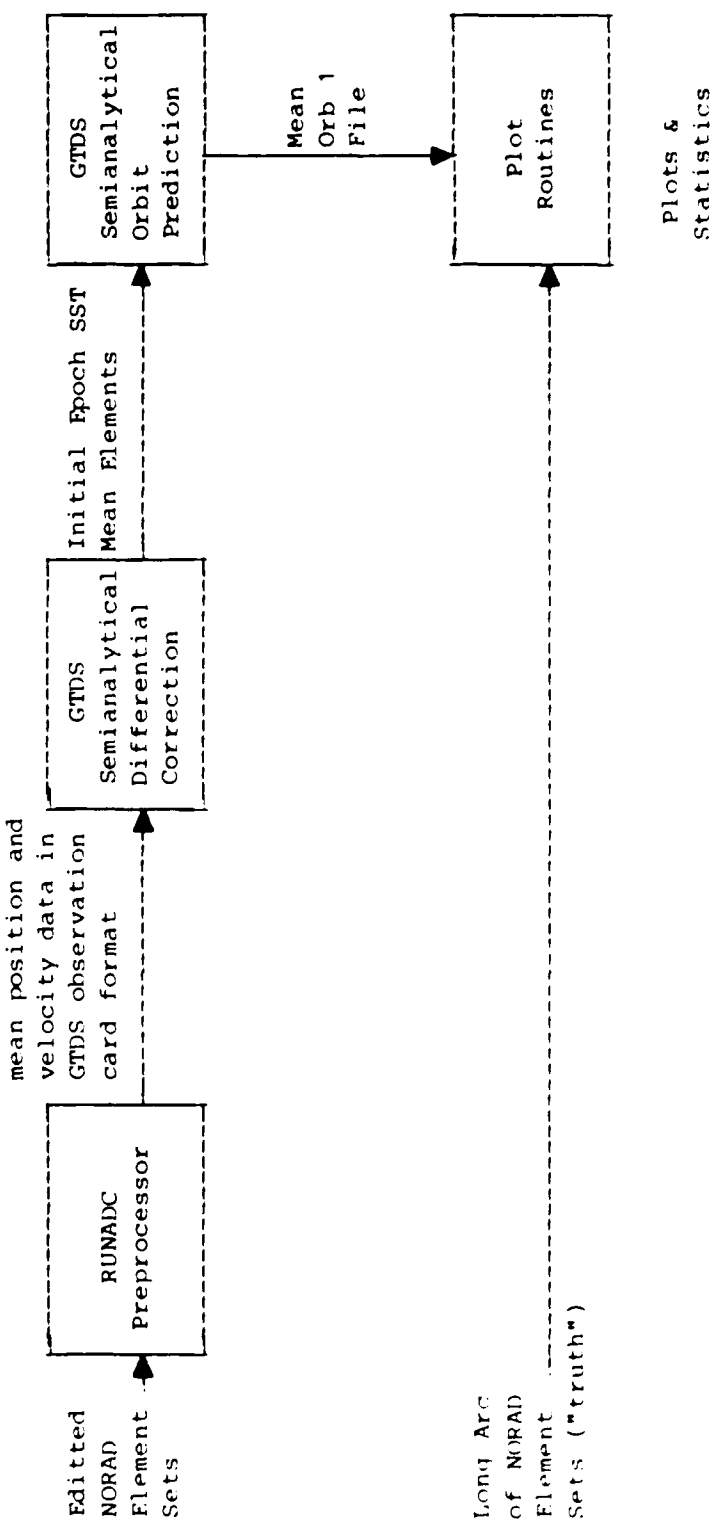


Figure 3a. Test data flow using NORAD Element Sets to initialize the Semianalytical Theory

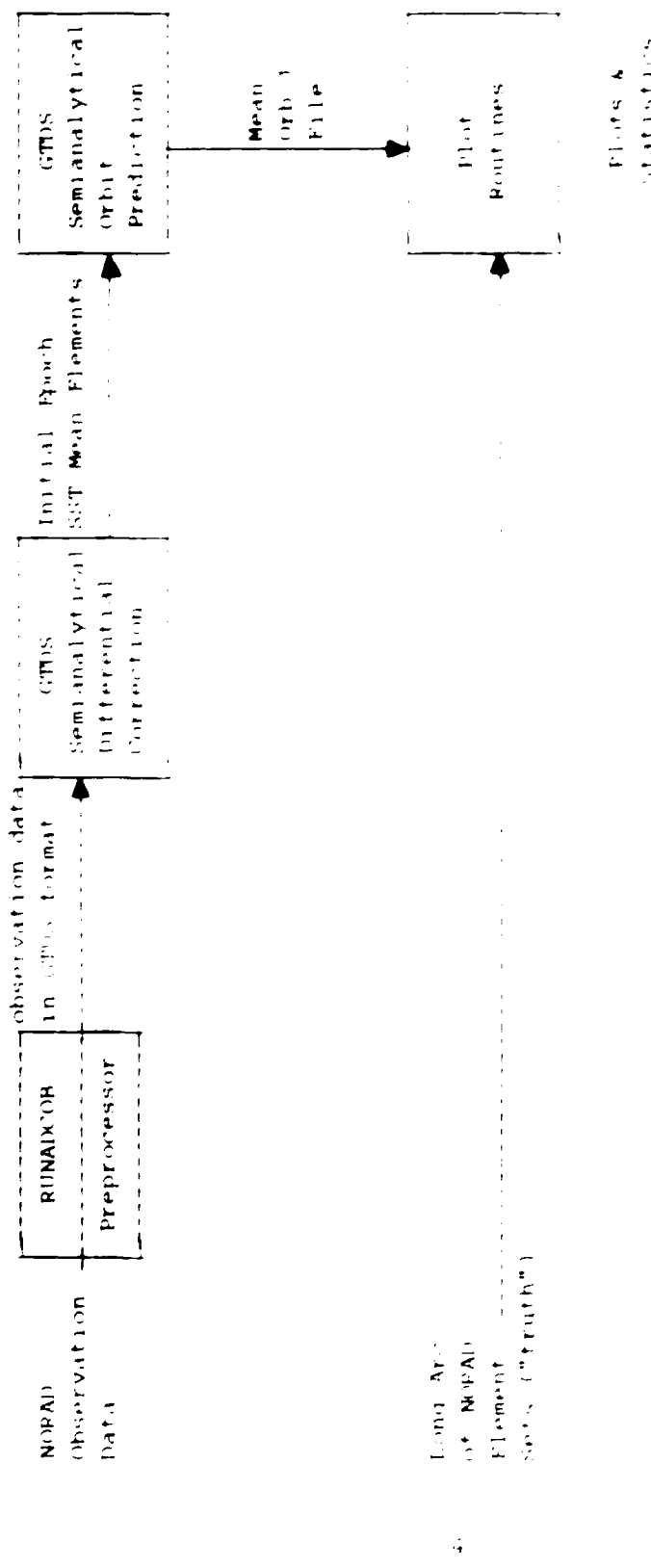


Figure 1. Test data flow using NOPAL observation data to validate the semi-analytical theory

NORAD element sets are converted to mean position and velocity. The mean position and velocity data are used as lumped observations in the DC to determine initial values of the mean elements for the SST prediction. The results of this prediction are compared with a long arc of NORAD element sets.

An alternative approach is to use the NORAD observation data from the HDS to determine initial values for the SST mean element set (Figure 3b). Software used to convert range, azimuth, elevation, and range-rate data from NORAD observation format to GTDS observation format had been built previously. For this study, the pre-processing capability was expanded to include optical data. The results of the SST prediction are again compared with a long arc of NORAD element sets.

2.1 PRE-PROCESSING NORAD DATA TO GTDS OBSERVATION CARD FORMAT

Processing of NORAD data proceeds along slightly different paths depending on whether element sets or observations are used in the DC. Element sets are received from the NORAD Historical Data System (HDS) in transmission card format [23] and include values for:

Epoch	Epoch time (YYDDD.DDDDDDDDD)
XNUT2	One half the mean motion rate (rev/day ²)
XDUT6	one sixth the second derivative of mean motion (rev/day ³)
BSTAR	Drag factor (earth radius ⁻¹)
KINCL	Inclination (degrees)

XNODE	Right ascension of node (degrees)
EO	Eccentricity
OMEGA	Argument of perigee (degrees)
XMO	Mean anomaly (degrees)
XNO	Mean motion (rev/day)

A graphical utility written in IBM FORTRAN 77 called ADCEDIT plots each element against the day of any selected year of data. This allows "noisy" element sets to be edited.

The program source code is listed in Appendix A. The routine creates a deck of data cards and a deck of control cards required for the CSDL plotting program PLOT4B [36]. Figure 4 is an example that plots the argument of perigee, mean anomaly, and mean motion for NSSC 9829 for 1983. The element set that caused the spike was consequently edited from further pre-processing.

The next step in the pre-processing of element set data is to generate position and velocity in GTDS observation format [31]. This is accomplished by a modified version of the NORAD SDP4 routines described in [23]. DRIVER has been replaced by the utility RUNADC, and subroutine SDP4 has been slightly modified. The subroutines ACTAN, DEEP, THETAG, and FMOD2P were unchanged.

The algorithm for RUNADC is shown in Figure 5, and its source code is listed in Appendix A. An input card reads the satellite designator, the NORAD generator type, and the data card format. Error messages are issued

SV 9829

NORAD MEAN ELEMENTS

◊ 1983

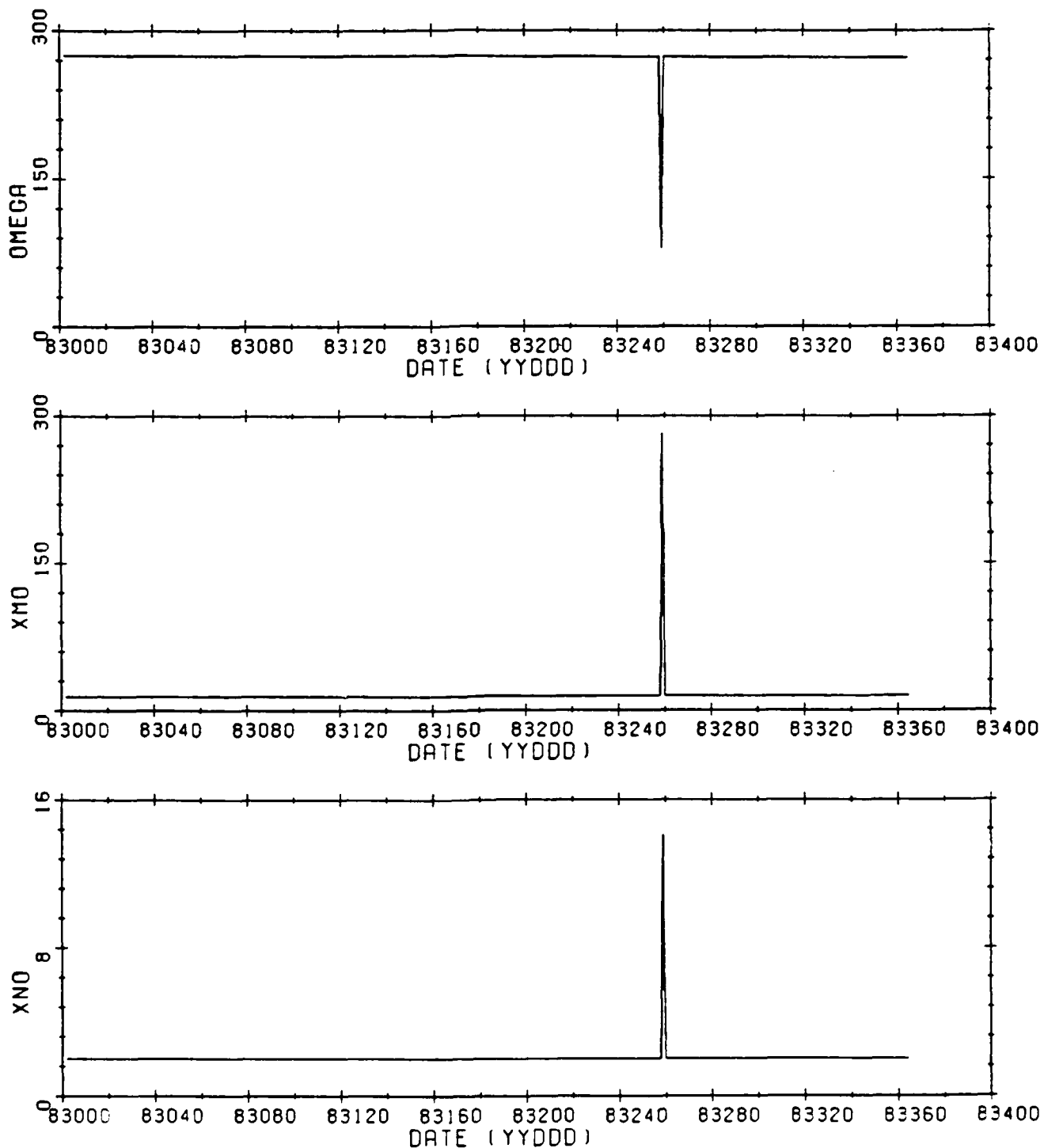


Figure 4. NSSC 9829 NORAD Element Sets-1983 (OMEGA, XMO, XNO)

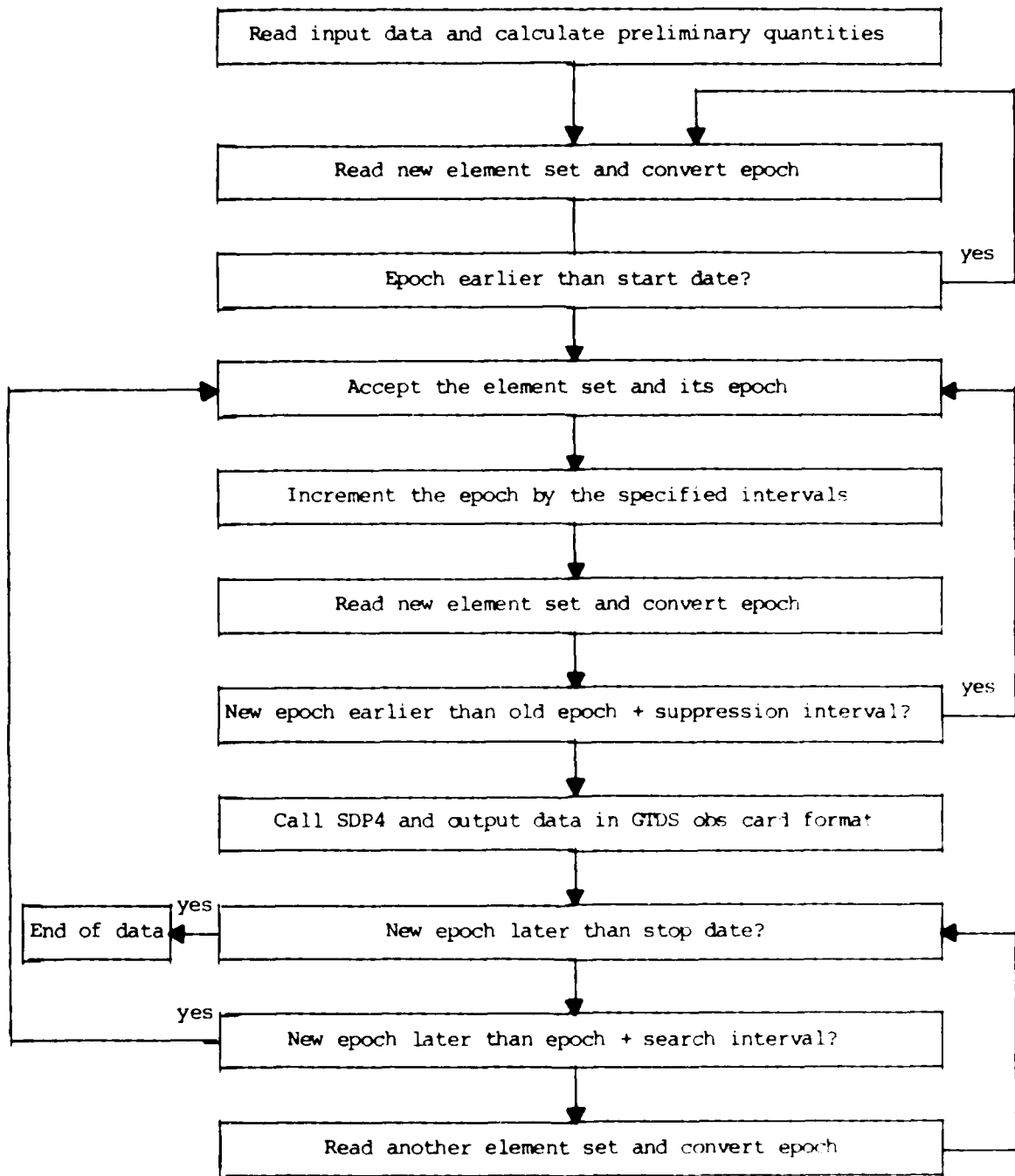


Figure 5. Subroutine RUNADC Algorithm for Pre-Processing NORAI Element Sets

if the generator type is not 'SDP4' or the data card format is other than 'TRANS'. The input card also contains the type of output desired (mean or osculating), the start date and end date for the GTDS observation card file and another temporary dataset of NORAD elements, a search interval, and a suppression interval.

The first NORAD element card is read and examined to see if its epoch occurs after the start date specified on the input card. When a satisfactory epoch is found, the data is examined to see if the next epoch occurs within the suppression interval, typically 12-15 hours, specified on the input card. The suppression interval helps ensure that the element set is the final element set in a NORAD differential correction. The element set is then input into the routine SDP4. "TSINCE" is set equal to zero because the SDP4 subroutine will not be used to generate predictions. That is, the position and velocity observation data are generated by SDP4 at the time epoch attached to the input element set. Also, the J_2 short-periodic model included in the original SDP4 may be circumvented by specifying 'mean' as the type of output motion desired. The utility thus generates single-averaged, or 'mean' data. This simplifies the GTDS DC process because only the mean dynamics need to be included. These mean position and velocity data are written in GTDS observation card format and used to calculate Keplerian and equinoctial elements. These data are written into a temporary data set of "NORAD" points which will be later plotted with the "GTDS" predictions. The next element set accepted by the

pre-processor will occur after the search interval, typically 5-7 days. This search interval was necessary to limit the number of GTDS observation cards. Element sets are accepted until the specified end date is reached.

The observation cards thus created serve as the input to the GTDS differential correction program which is used to determine the initial conditions for the ephemeris prediction using the semianalytical theory.

The procedure of using the element sets to initialize the DC has the advantage that the position and velocity observations require little auxiliary data (such as observation noise and bias, station location, etc.). The disadvantage of this procedure is that the elements sets contain errors originating in the original observations and in the processing used to generate the element sets. Determination of the initial SST mean elements may require the NORAD element set error statistics, and this data is not maintained in the HDS.

When actual NORAD observations are used to determine the initial conditions for the DC, pre-processing is necessary to transform the data from NORAD to GTDS format. For radar observations, which may include range, azimuth, elevation, and range rate, the pre-processing is primarily a matter of converting time and units. For the optical data, the NORAD HDS provides the right ascension and declination data in a true equator mean equinox of date coordinate system. This data must be transformed to the Mean of 1950.0 coordinate system before it can be used with the GTDS optimal observation model.

Pre-processing of the observations is performed by the CSDL utility RUNADCOB. For optical observations, RUNADCOB utilizes another subroutine ASTRON to convert to the Mean of 1950.0 coordinate system. The precession and nutation matrices for the coordinate transformation are calculated by the subroutine PRENUT whose algorithms originated in the NORAD SACEPH program. Listings of RUNADCOB, ASTRON, and PRENUT are found in Appendix A. The observation cards produced by RUNADCOB serve as the input to the GTDS DC program.

2.2 SST DIFFERENTIAL CORRECTION PROCESS

The primary purpose of the GTDS Differential Correction (DC) program is to estimate the satellite orbit and auxilliary parameters (such as the drag coefficient, solar pressure coefficient, etc.). The estimation algorithm used in the DC program is called the weighted least squares with a priori algorithm or the Bayesian weighted least squares algorithm [31]. It minimizes the sum of the squares of the weighted residuals between actual and computed observations, while simultaneously constraining the model parameters to satisfy the a priori conditions to within a specified uncertainty. Both first- and second-order statistics (i.e., the mean and covariance matrices) are determined for the estimated variables.

The user provides the DC program with the initial estimate of the solve-for vector at a specified epoch. (For this effort, the initial estimate for the elements was taken from the NORAD element set data.) The program

can accept a variety of observation types in one of several input coordinate systems. Observation uncertainties, atmospheric model, and spacecraft area and mass parameters may also be specified. The DC program can access the complete semianalytical theory as described in Section 1.3.3.

2.3 SST EPHEMERIS PREDICTION PROCESS

The function of the ephemeris generation program GTDS EPHEM is to compute, from prescribed initial conditions, the value at a specified time of the vehicle state and, optionally, the state partial derivatives. In order to meet varying precision and efficiency requirements, several orbital theories have been provided, ranging from a first-order analytic theory to a high-precision Cowell-type numerical integration. The state partial derivatives can be computed by precision numerical integration of variational equations. The state partial derivatives with respect to the initial state, i.e., the state transition matrix, can optionally be generated by a two-body analytic approximation.

GTDS EPHEM includes the complete semianalytical theory as described in Section 1.3.3. The user selects the appropriate model for the orbit under study and inputs the initial elements at epoch. The GTDS EPHEM program can accept the input conditions in one of several coordinate systems. A desired atmospheric model, spacecraft area, and mass parameters may also be specified.

The GTDS EPHEM program writes the prediction file of mean position and velocity data into an ORB1 file. The FORTRAN utility RDORB1 reads position and velocity, calculates the corresponding Keplerian and equinoctial elements, and writes this "GTDS" data into a file with the same format as the file of "NORAD" points. A copy of RDORB1 is included in Appendix A.

2.4 PLOTTING ELEMENT COMPARISONS AND DIFFERENCES

Comparison and difference plots of the "GTDS" predictions and the "NORAD" points are created using the CSDL plotting program PLOT4B [36]. Because of limitations of PLOT4B it was necessary to interpolate the "GTDS" predictions (spaced regularly in time) to the "NORAD" output from the modified SDP4 routine (spaced irregularly in time). This interpolation is performed by program PLOTTER.

The FORTRAN utility PLOTTER reads the set of position and velocity components, the Keplerian elements, and the equinoctial elements from the temporary dataset of "GTDS" predictions created by the RDORB1 utility. It first reads the input control cards containing the satellite designator, the time interval at which the GTDS predictions are spaced, the comparison start date, the start day of the plot and the final day of the plot in number of days since the start date, the FORTRAN file numbers of the two data sets, and the gravitational constant.

The angular velocities of mean anomaly and mean longitude are used to convert the "sawtooth" values of longitude of ascending node, argument of perigee, mean anomaly, and mean longitude to linearized values. These linearized values for the angular elements can then be used to perform a five-point Lagragian interpolation of the SST predictions to the times corresponding to the NORAD mean elements. The numerical difference between each SST prediction and NORAD mean element is calculated, and first-order statistics (mean difference and standard deviation) are computed for the entire comparison interval.

The radial, cross-track, and along-track errors using the "NORAD" points as the estimated trajectory and the "GTDS" predictions as the true trajectory are then calculated. Unit vectors for these errors are defined by:

$$\text{Radial error } \hat{H} = \frac{\hat{r}}{|\hat{r}|}$$

$$\text{Cross-track error } \hat{C} = \frac{\hat{r} \times \hat{v}}{|\hat{r} \times \hat{v}|}$$

$$\text{Along-track error } \hat{L} = \frac{(\hat{r} \times \hat{v}) \times \hat{r}}{|(\hat{r} \times \hat{v}) \times \hat{r}|}$$

The program then writes PLOT4B control cards and data cards for comparison plots, difference plots, and error plots. A copy of the source code for PLOTTER is found in Appendix A.

CHAPTER 3

TEST RESULTS

The primary objective of this thesis was to test the semianalytical satellite theory as implemented in the CSDL version of the GTDS against long arcs of real data for highly eccentric orbits. Chapter 2 addressed the test methodology used in this investigation and described the software development that was undertaken to interface the NORAD data to the GTDS format and then to interface GTDS predictions and NORAD elements to a simple plotting program package. The present chapter summarizes the comparisons between the SST predictions and the NORAD real data using a 9-year arc of element sets for NSSC 9829, the Soviet Molniya 2-17 spacecraft, an 18-month arc of element sets for NSSC 14095, the ESA Exosat, and an 18-month arc of observations for NSSC 13964, the Soviet Molniya 1-57 spacecraft. Comparison and difference plots are given for all three satellites.

3.1 INITIALIZATION OF SST USING ELEMENT SETS

3.1.1 NSSC 9829

3.1.1.1 Mission and Operations

The NSSC 9829 spacecraft, Molniya 2-17, was launched 11 February 1977. The spacecraft entered a supra-semi-synchronous transfer orbit with a period of 735 minutes [1] and was allowed to drift westward to its operational location. Its initial operational orbital parameters on 1 May 1977 [1] are shown in Table 1.

Table 1. NSSC 9829 Initial Operational Orbit Elements	
Element	Value
Semimajor axis	26554 km
Apogee height	39853 km
Perigee height	498 km
Eccentricity	0.7410
Inclination	62.9°
Argument of perigee	280°
Period	717.67 minutes
NORAD Coordinates	

The analysis for this satellite was based solely on element set data. However, a review of the graphs created by ADCEDIT indicated there were no apparent maneuvers during the period of the available NORAD data.

Figure 4 is a plot of argument of perigee, mean anomaly, and mean motion for NSSC 9829 for 1983. The "spikes" on all three plots clearly indicate a bad element set. These "spikes" typify the element sets that were deleted from further pre-processing and comparisons. These element sets are listed in Table 2.

Table 2. NSSC 9829 Element Set Edits

Element set date (YYDDD.DDDDDDDD)	Questionable Element
77191.32816013	XNDT2
77196.31168989	XNDT2
77298.97607433	BSTAR
77312.93081504	XNDD6
79211.99956568	XNDT2, XINCL
79271.81988559	XNDT2
81256.60694402	XINCL
81273.55533913	BSTAR
81275.54929572	BSTAR
82228.57192200	XNDT2, XINCL, EO, OMEGA
82245.01890805	XNDT2, BSTAR
83259.82751893	XNDT2, XINCL, EO, OMEGA, XMO, XNO

It should be noted that the percentage of element sets edited was extremely small (about 1% of the 9 year arc).

3.1.1.2 SST DC and Prediction

The initial estimate for the vehicle state was taken from a NORAD mean element set. Six months of data were used in the fit, and the epoch was chosen to minimize noise in the mean motion rate and to ensure perigee was outside the main portion of the atmosphere. Table 3 summarizes the force models employed in the SST DC and prediction. The initialization procedure automatically computes the maximum powers of a/R and e to be included in the power series expansions [37]. Drag terms were not included because perigee height was outside the main portion of the atmosphere, and solar pressure terms were not included because early runs showed their contribution was minimal.

Table 3. Force Model used for NSSC 9829

Zonals: J_2 thru J_{10} , e^5 , GEM 9

Tesseral resonance: GEM 9, (2,2) through (6,6), e^{20}

Non-central bodies:

Moon $(a/r)^9$, e^7

Sun $(a/r)^3$, e^3

Solve-for parameters: mean equinoctial elements

Drag: off

Solar pressure: off

The a priori values and the final values for the Keplerian elements and their standard deviations are shown in Table 4. The assumed observations standard deviations were 20 km for each position coordinate and 20 m/sec for each velocity coordinate.

Table 4. Results of DC for NSSC 9829

Epoch: Aug 3, 1979, 23 hours, 42 min, 12.000 sec

Element	A priori Value	Final Value	Standard Deviation
a (km)	26556.8740	26556.9582	1.67468E-03
e	0.6992405	0.6990986	8.42488E-05
i ($^\circ$)	63.144666	63.173001	0.59929
Ω ($^\circ$)	190.635924	190.619681	0.42451
ω ($^\circ$)	281.54328	281.59624	1.2282
M ($^\circ$)	13.30040	13.29315	0.20159

Weighted RMS: 0.2893

Mean of 1950.0 Coordinates

The final values of the Keplerian elements and the epoch indicated in Table 4 were used as initial conditions for an SST prediction. The same force models shown in Table 3 were used to create an ephemeris prediction file of about 2330 days.

3.1.1.3 Comparison and Difference Plots

The results of comparing of the "NORAD" points to the "GTDS" predictions using the GEM 9 Earth gravitational model and a 6 x 6 harmonic field are shown in Figures 6-20. Figures 6-12 are comparison plots of the "NORAD" and "GTDS" predictions for the Keplerian elements for the approximately 2330 days of available NORAD elements following the indicated epoch of August 1979. The mean difference and standard deviation after 326 comparisons for the Keplerian and equinoctial elements are shown in Table 5.

Table 5. Results of Comparisons for NSSC 9829

Element	Mean Difference	Standard Deviation
Semimajor axis (km)	.25046	.19496
Eccentricity	0.22437E-03	0.38909E-03
Inclination (°)	0.33941E-01	0.87707E-01
Longitude of ascending node (°)	0.22964	0.13148
Argument of perigee (°)	0.11699	0.10242
Mean anomaly (°)	1.0960	0.78569
Radius of perigee (km)	5.9652	10.348
Radius of apogee (km)	5.9333	10.242
H	0.96150E-03	0.77753E-03
K	0.98751E-03	0.70091E-03
P	0.16495E-02	0.17350E-02
Q	0.16255E-02	0.11163E-02
Mean longitude (°)	0.99281	0.74933
Norad Coordinates		

The slowly varying Keplerian element histories (Figures 6-10) and the mean anomaly difference (Figure 18) clearly demonstrate the ability of the semianalytical theory to predict the dominant motion experienced by the NORAD element sets.

Gravitational models and tesseral resonance terms other than those listed in Table 3 were used in various DC runs. In each case the semimajor axis difference exhibited a frequency very similar to the resonance period exhibited by the semimajor axis difference plot (Figure 13). A marked improvement was noted when a 6x6 field with GEM 9 coefficients was used to generate the semianalytical prediction in Figures 6-12.

When an 8x8 field with GEM 9 coefficients was used, the DC converged very unsatisfactorily with an overall weighted RMS value of 2.071 over the 6 month fit span (compare this to the weighted RMS value of 0.2893 shown in Table 4).

Consideration of this poor fit led to several Precise Conversion of Elements (PCE) runs by R. Proulx (CSDL) which generated predictions using a Cowell numerical integration scheme. These predictions very closely resembled the SST predictions using the 8x8 field. It was at this point that usage of actual NORAD observations to improve the fit was considered. This led to the method of initialization of the SST prediction using observation data which is described in Section 3.2.

SV09829 SEMIMAJOR AXIS

MEAN DIFFERENCE: 0.25046

SIGMA: 0.19496

AFTER 326 COMPARISONS

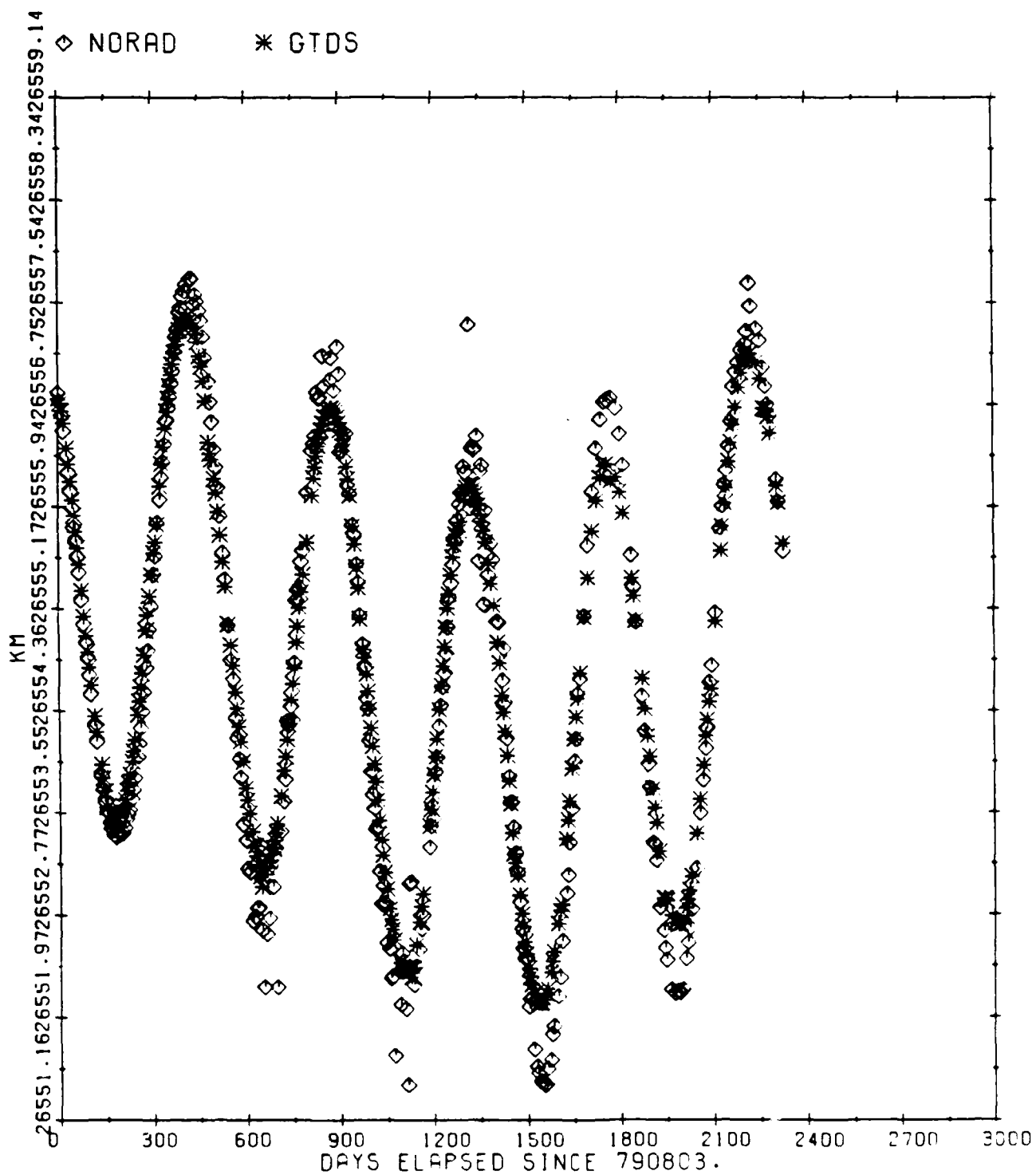


Figure 6. NORAD 9829 Semimajor Axis Comparison

SV09829 ECCENTRICITY

MEAN DIFFERENCE: 0.22437E-03 SIGMA: 0.38909E-03 AFTER 326 COMPARISONS

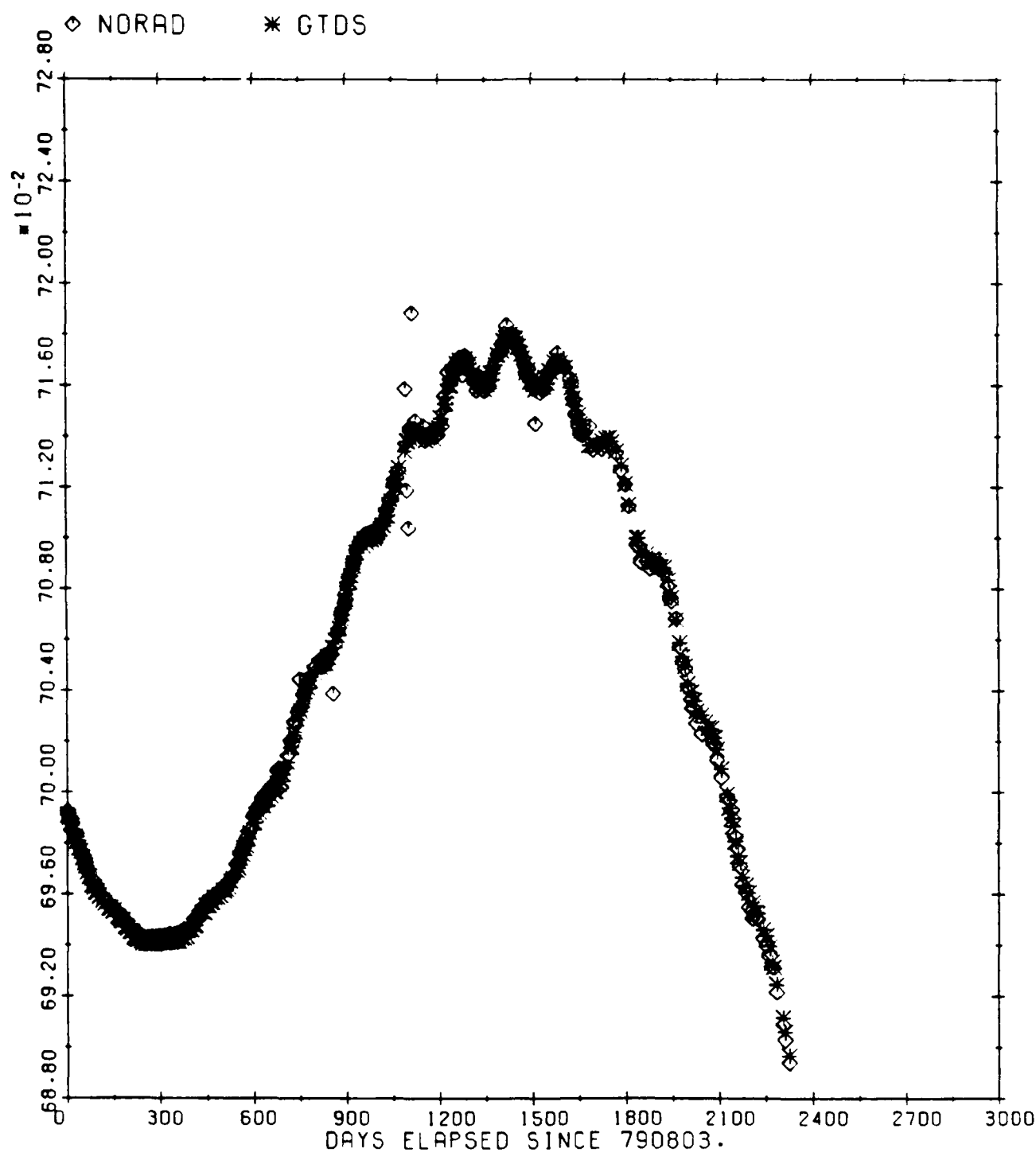


Figure 7. NSSC 9829 Eccentricity Comparison

SV09826 INCLINATION

MEAN DIFFERENCE: 0.33941E-01 SIGMA: 0.87707E-01 AFTER 326 COMPARISONS

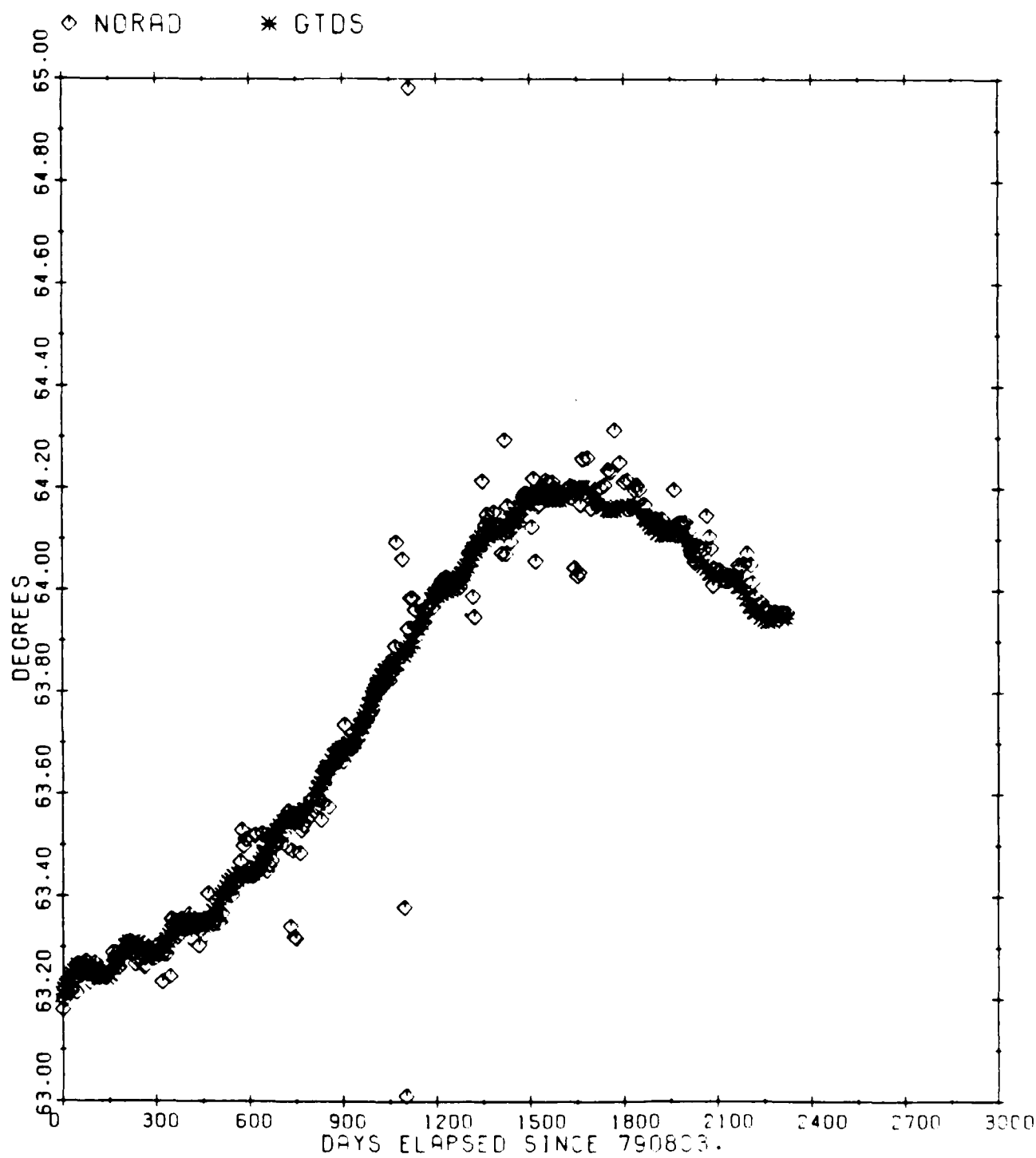


FIGURE 8. NO. 09826 Inclination Comparison

SV09829 LONGITUDE OF ASCENDING NODE

MEAN DIFFERENCE: 0.22964 SIGMA: 0.13148 AFTER 326 COMPARISONS

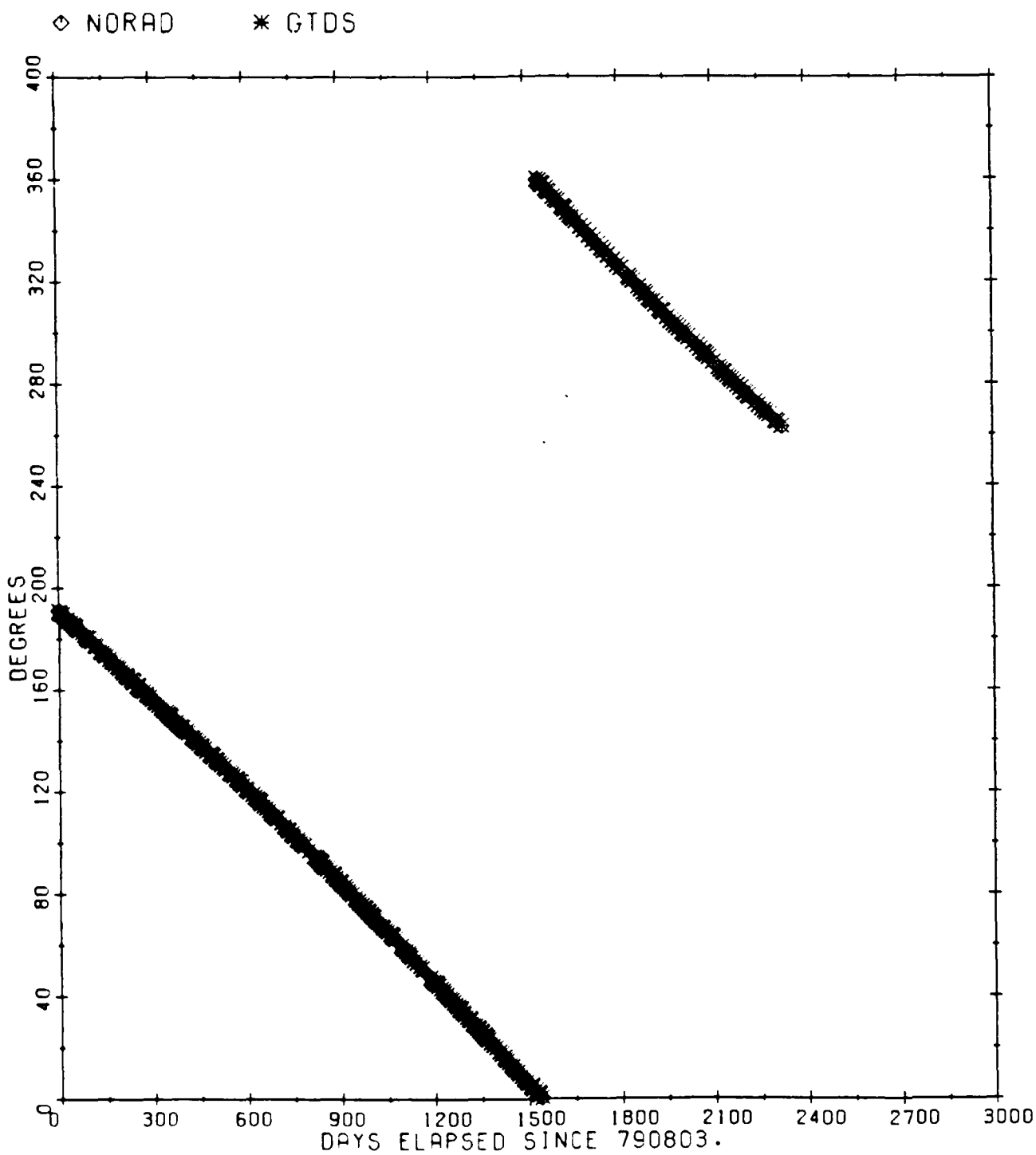


Figure 6. NORAD/GTDS Longitude of Ascending Node Comparison

SV09829 ARGUMENT OF PERIGEE

MEAN DIFFERENCE: 0.11699 SIGMA: 0.10242 AFTER 326 COMPARISONS

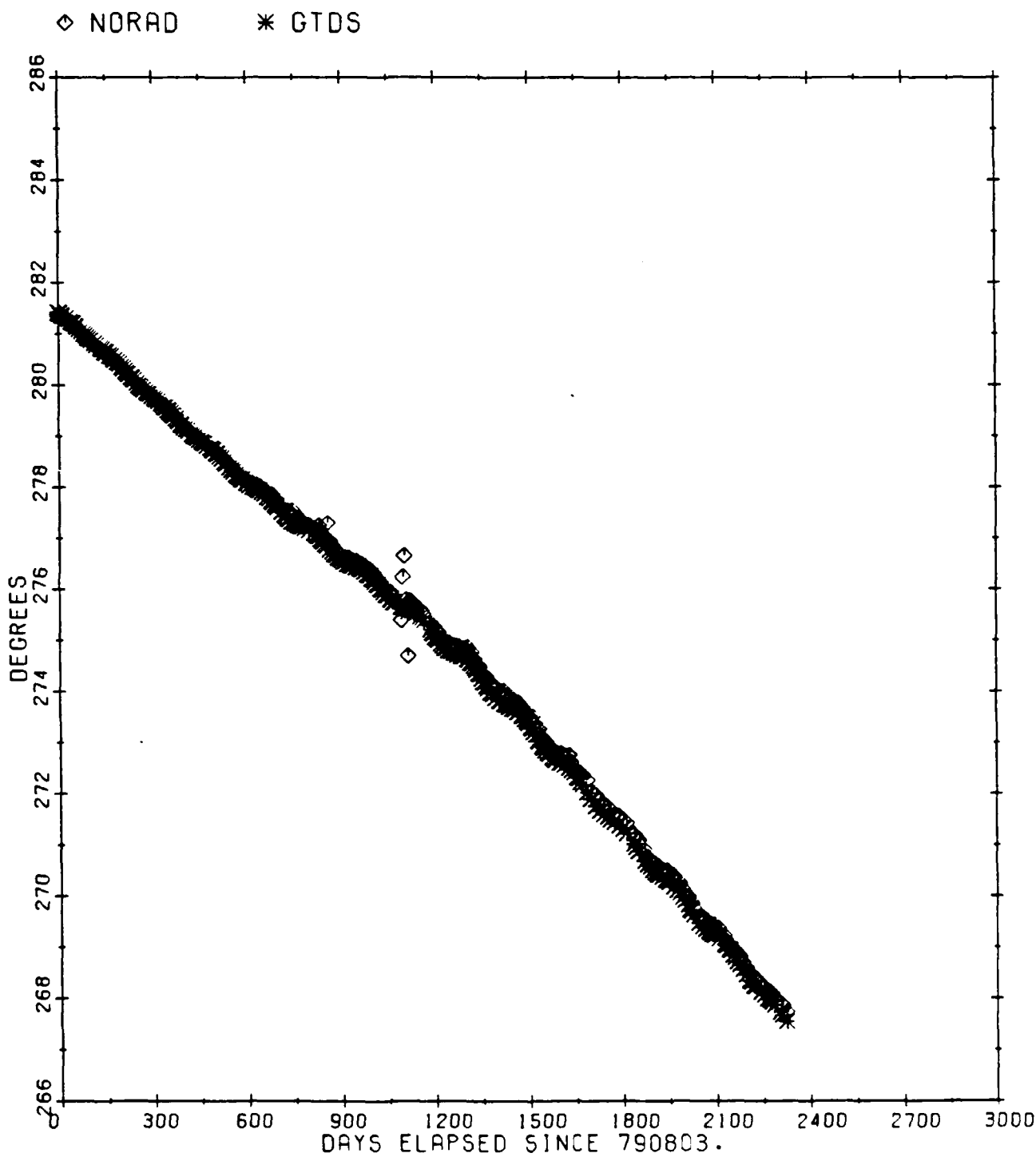


Figure 10. NSSC 9829 Argument of Perigee Comparison

SV09829 RADIUS OF PERIFOCUS

MEAN DIFFERENCE: 5.9652 SIGMA: 10.348 AFTER 326 COMPARISONS

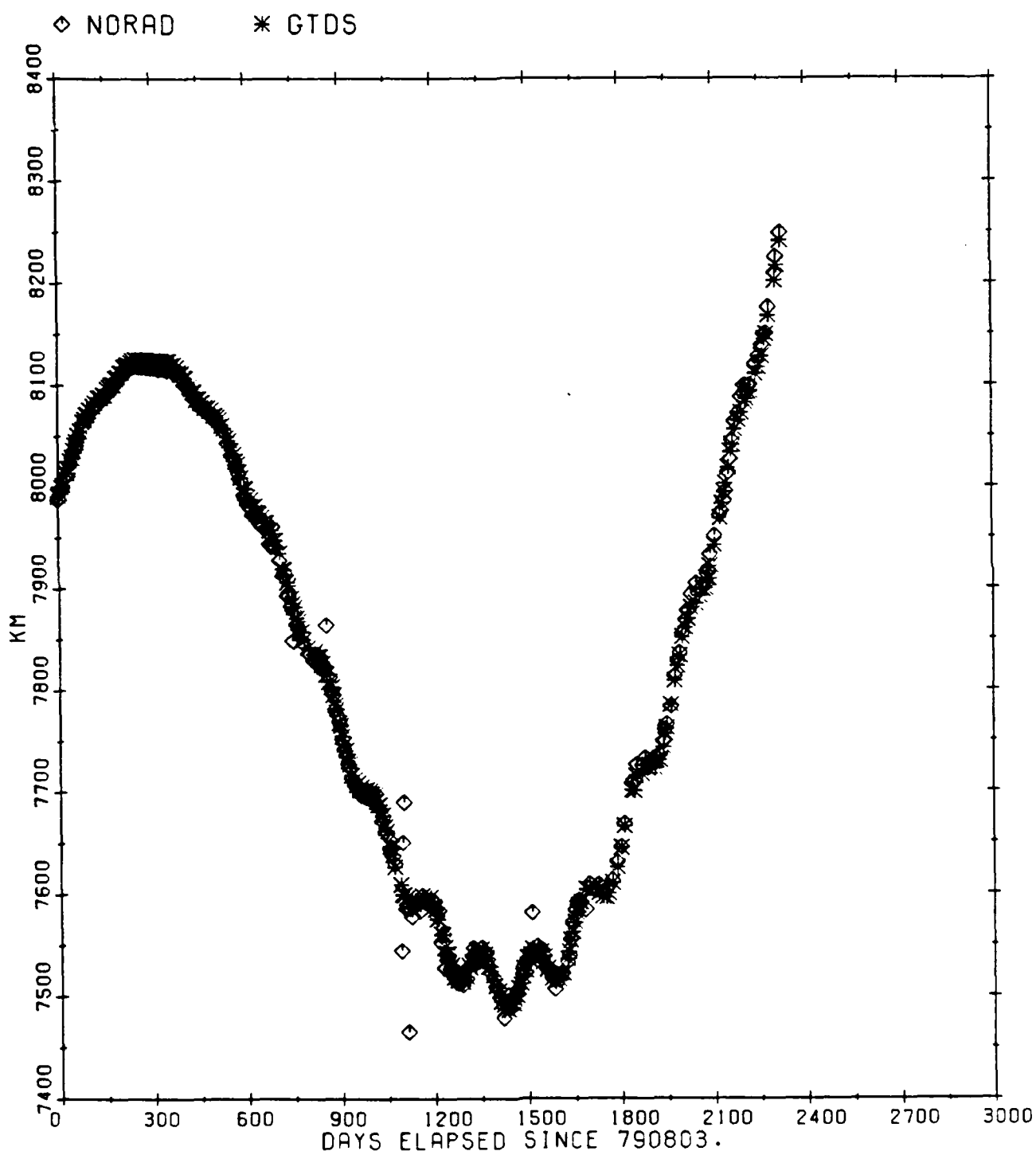


Figure 11. NSSC 9829 Radius of Perigee Comparison

SV09829 RADIUS OF APOFOCUS

MEAN DIFFERENCE: 5.9333

SIGMA: 10.242

AFTER 326 COMPARISONS

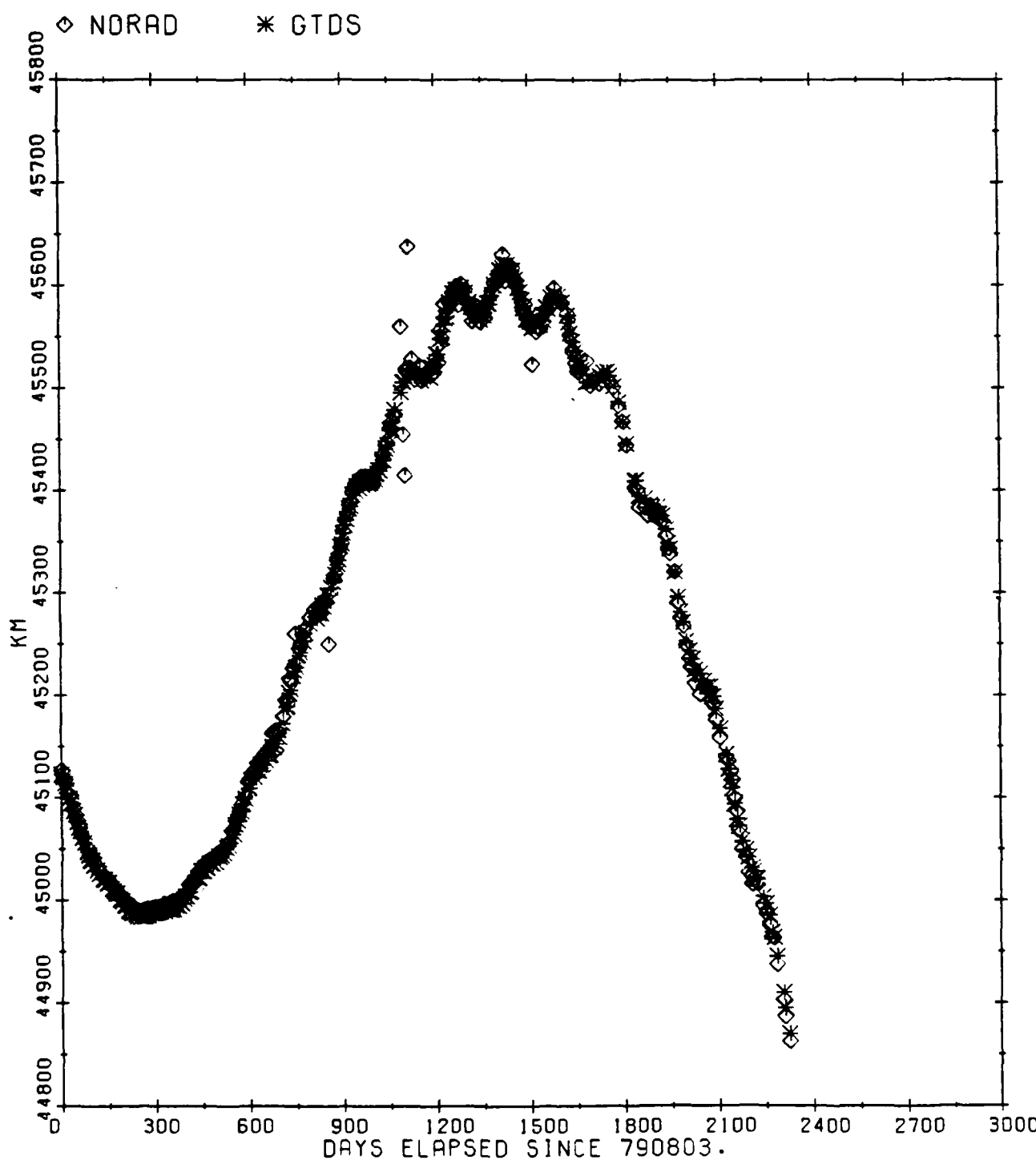


Figure 12. NSSC 9829 Radius of Apogee Comparison

SV09829 SEMIMAJOR AXIS

COMPARISON DIFFERENCE: DELTA = GTDS-NORAD

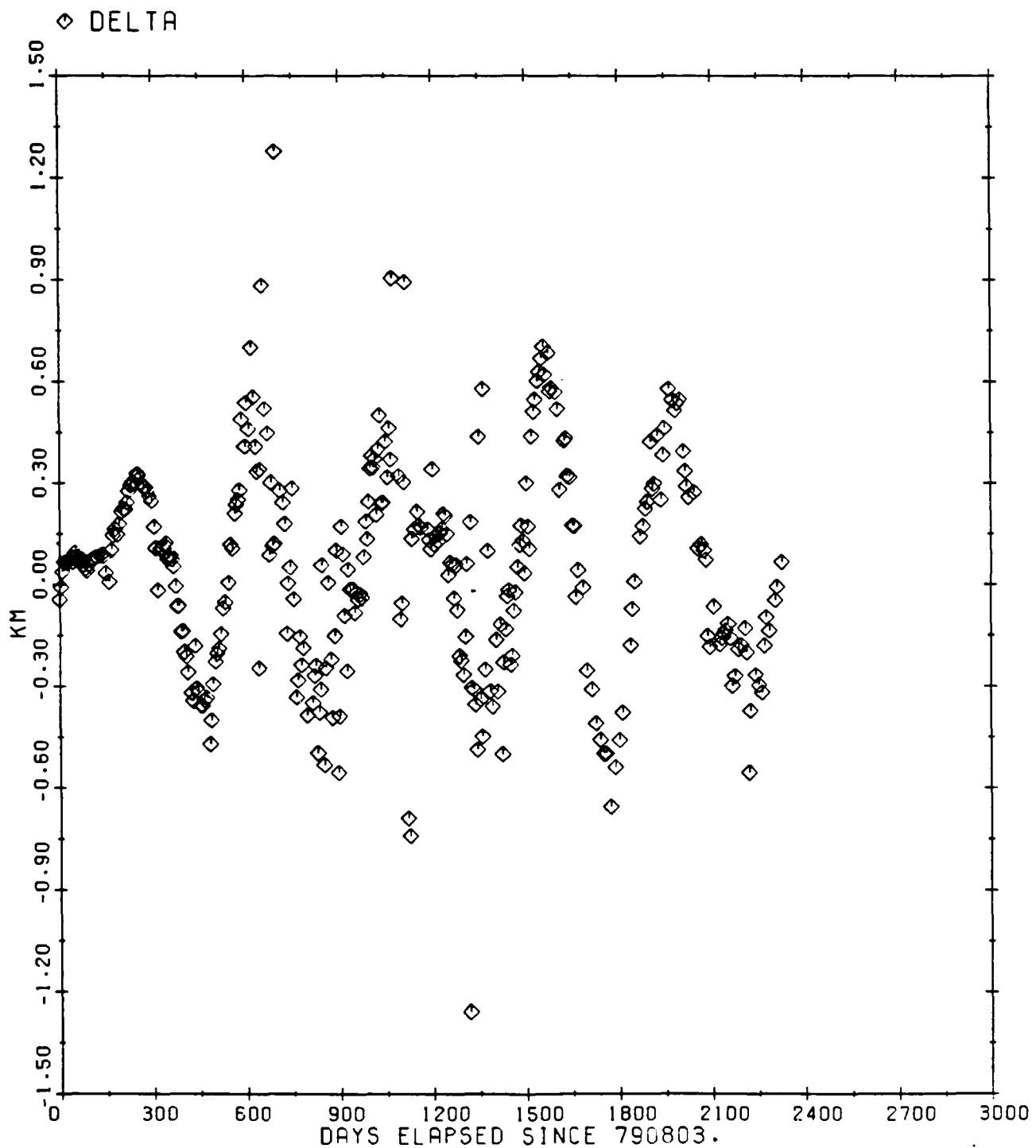


Figure 13. NSSC 9829 Semimajor Axis Difference

SV09829 ECCENTRICITY

COMPARISON DIFFERENCE: DELTA = GTDS-NORAD

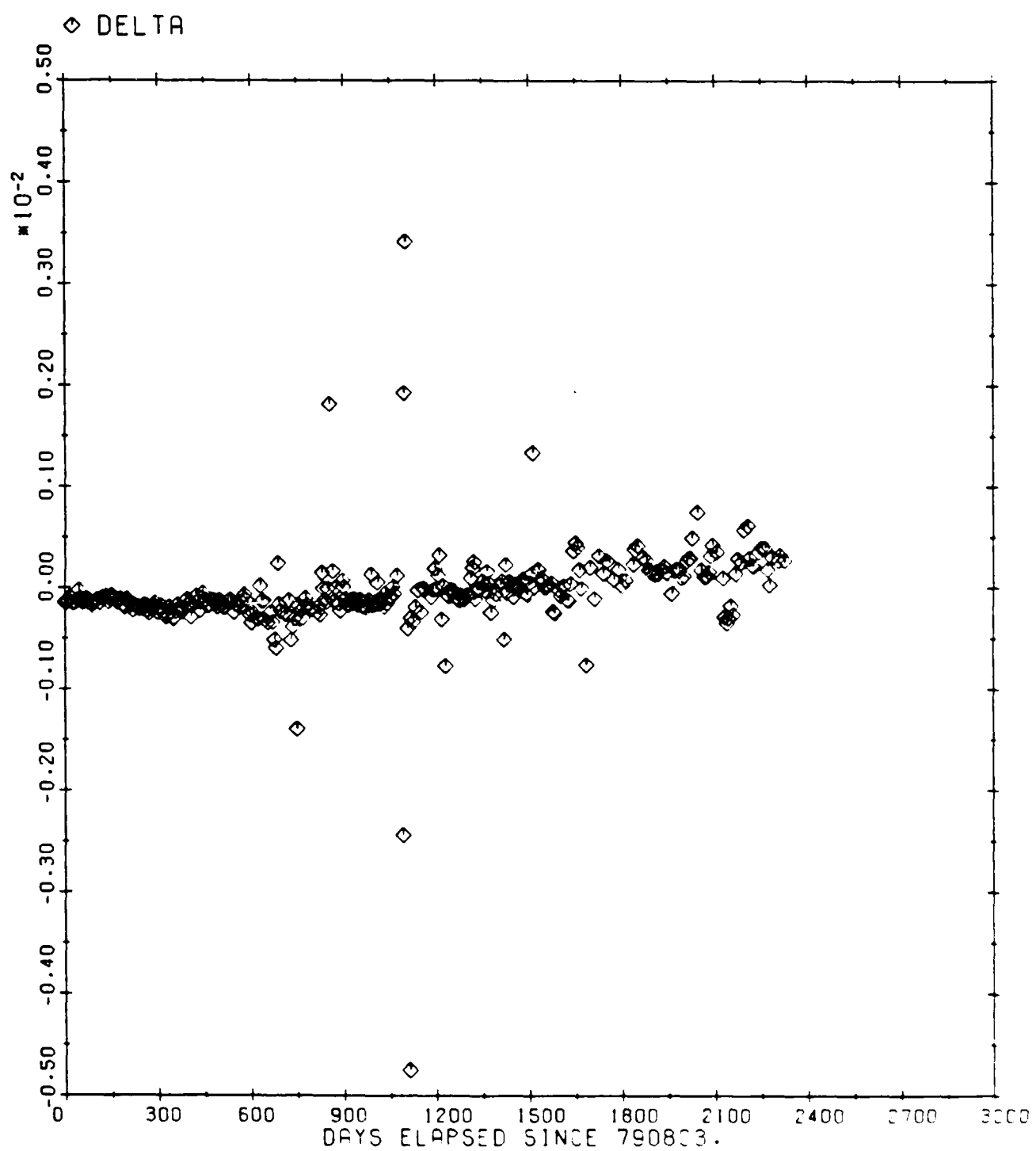


Figure 14. NUSC 9829 Eccentricity Difference

SV09829 INCLINATION

COMPARISON DIFFERENCE: DELTA = GTDS-NORAD

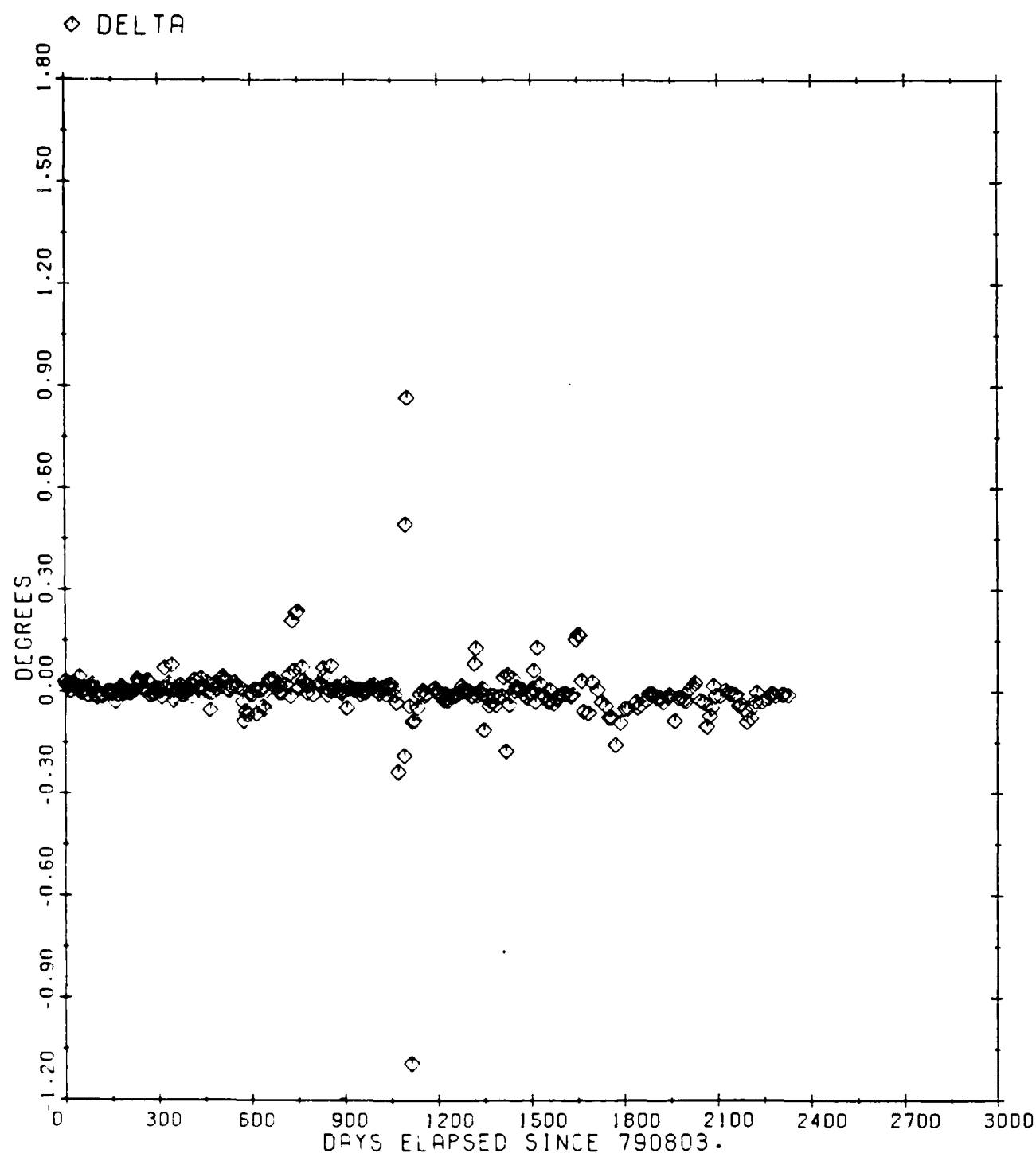


Figure 18. NAV 09829 Inclination Difference

SV09829 LONGITUDE OF ASCENDING NODE

COMPARISON DIFFERENCE: DELTA = GTDS-NORAD

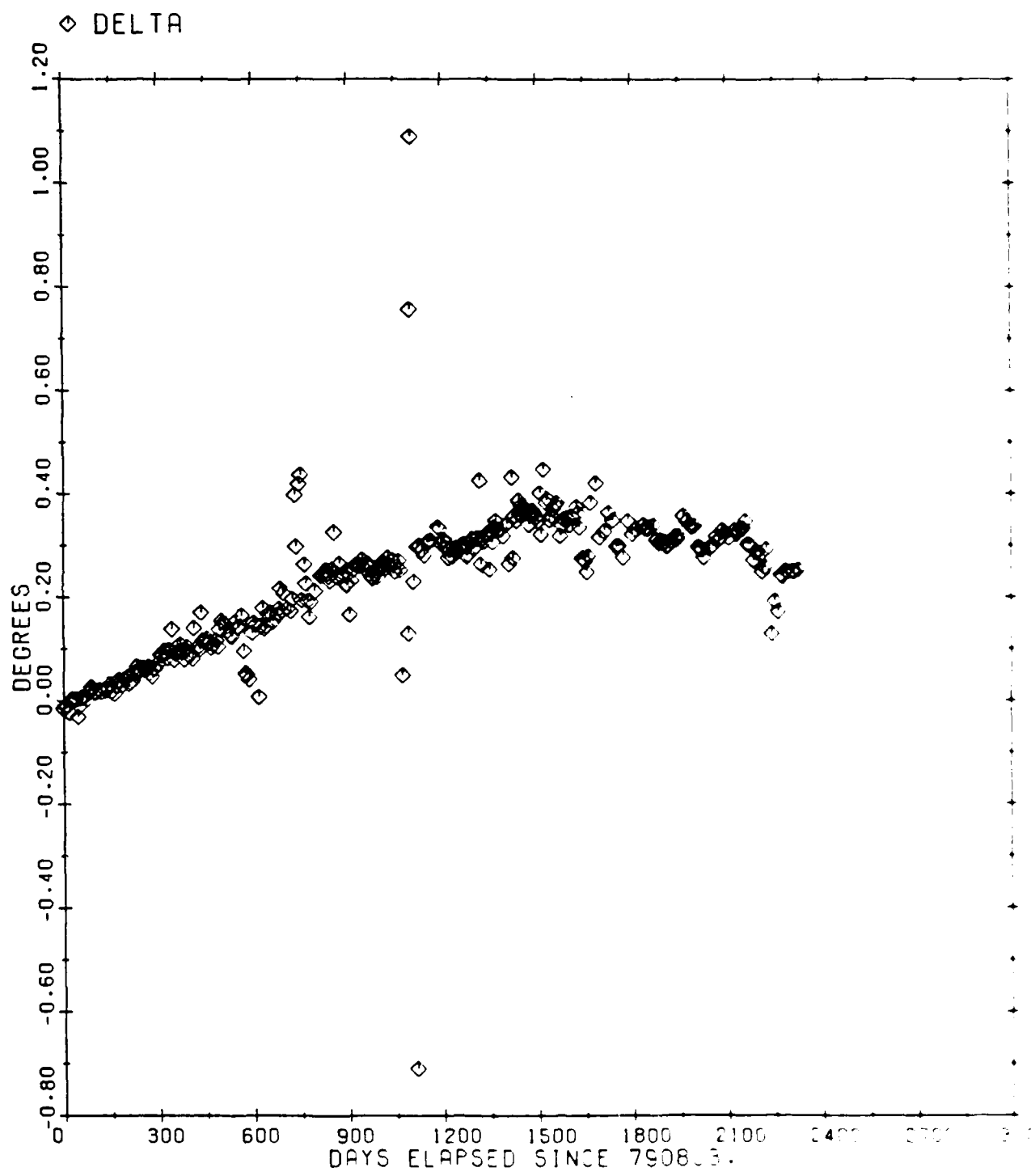
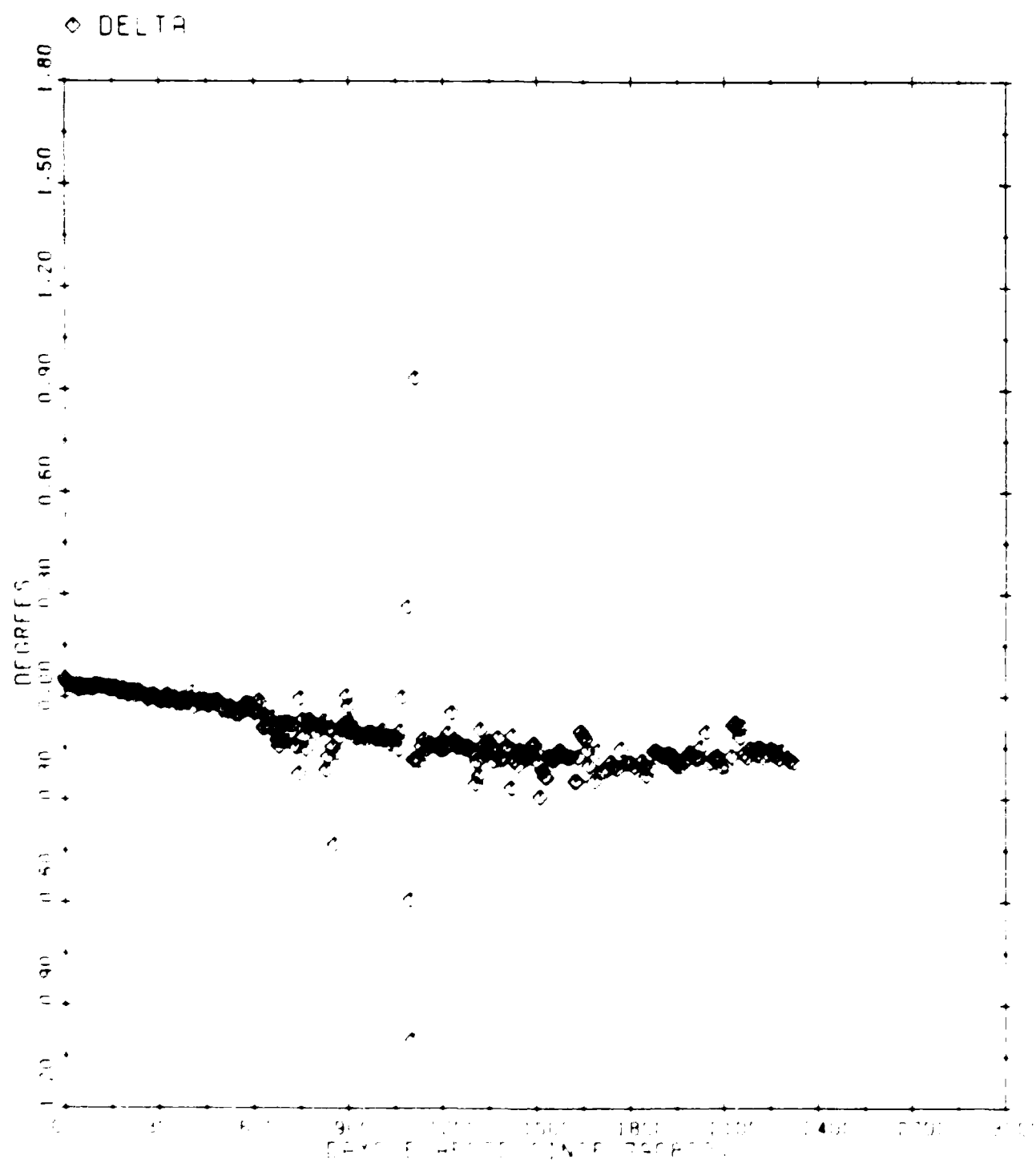


Figure 16. NSSC 9829 Longitude of Ascending Node Difference

SV09826 ARGUMENT OF PERIGEE

COMPARISON DIFFERENCE: DELTA = GTDS-NORAC



GTDS/NORAC ARGUMENT OF PERIGEE DIFFERENCE

SV09829 MEAN ANOMALY

COMPARISON DIFFERENCE: DELTA = GTDS-NORAD

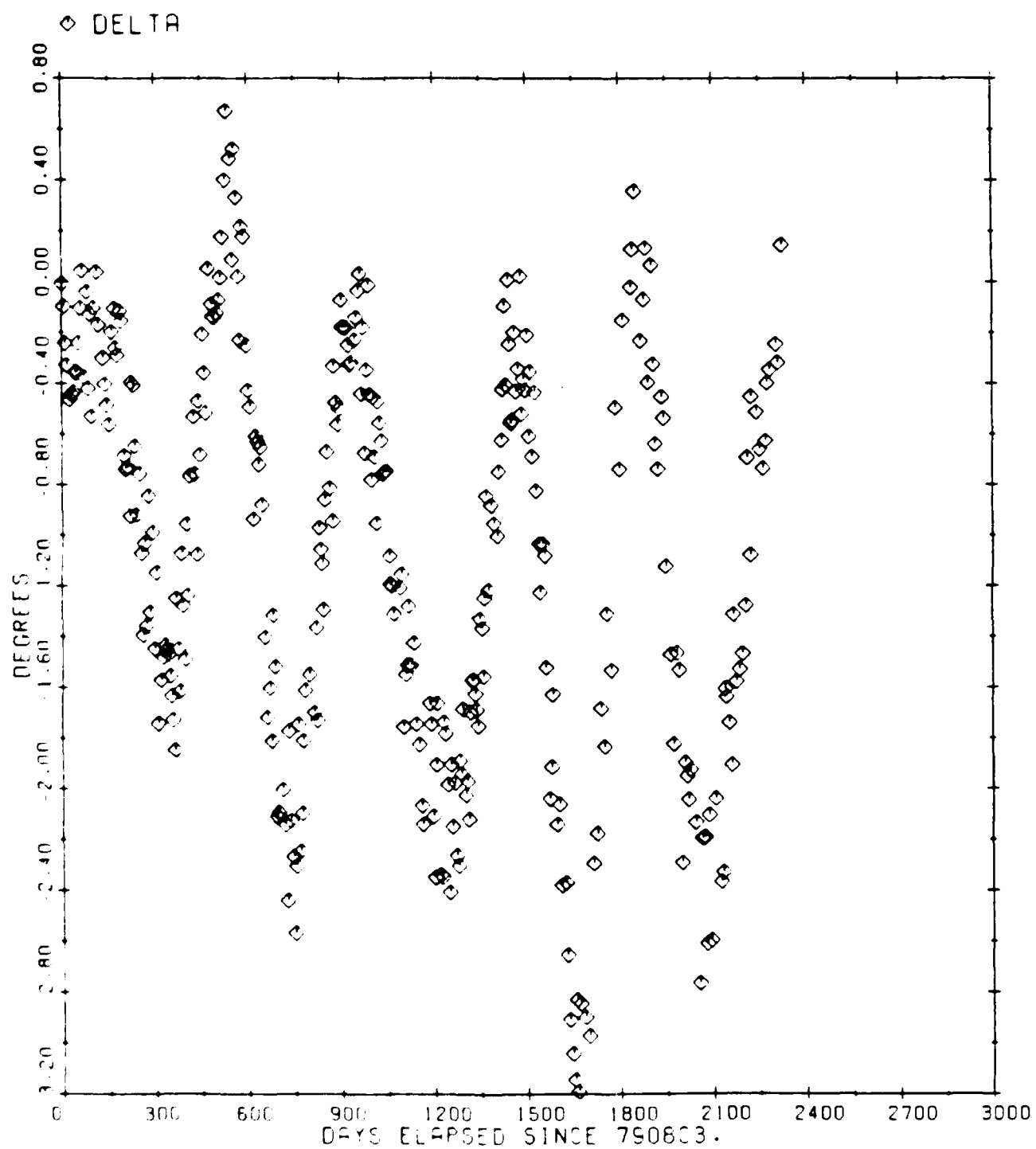


Figure 1c. SV09829 Mean Anomaly Difference

SV09829 RADIUS OF PERIFOCUS

COMPARISON DIFFERENCE: DELTA = GTDS-NORAD

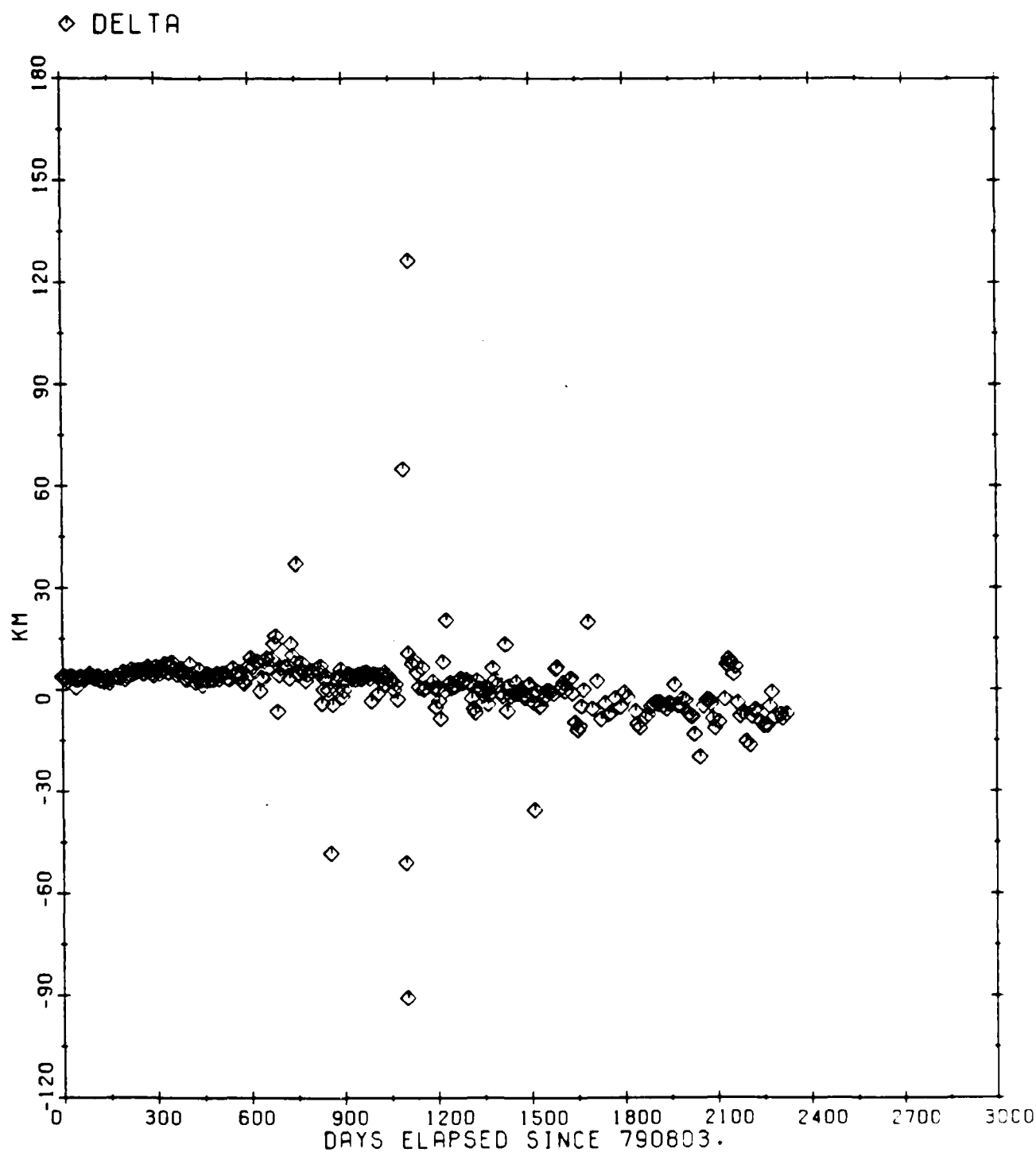


Figure 19. NSSC 9829 Radius of Perigee Difference

SV09829 RADIUS OF APOFOCUS

COMPARISON DIFFERENCE: DELTA = GTDS-NORAD

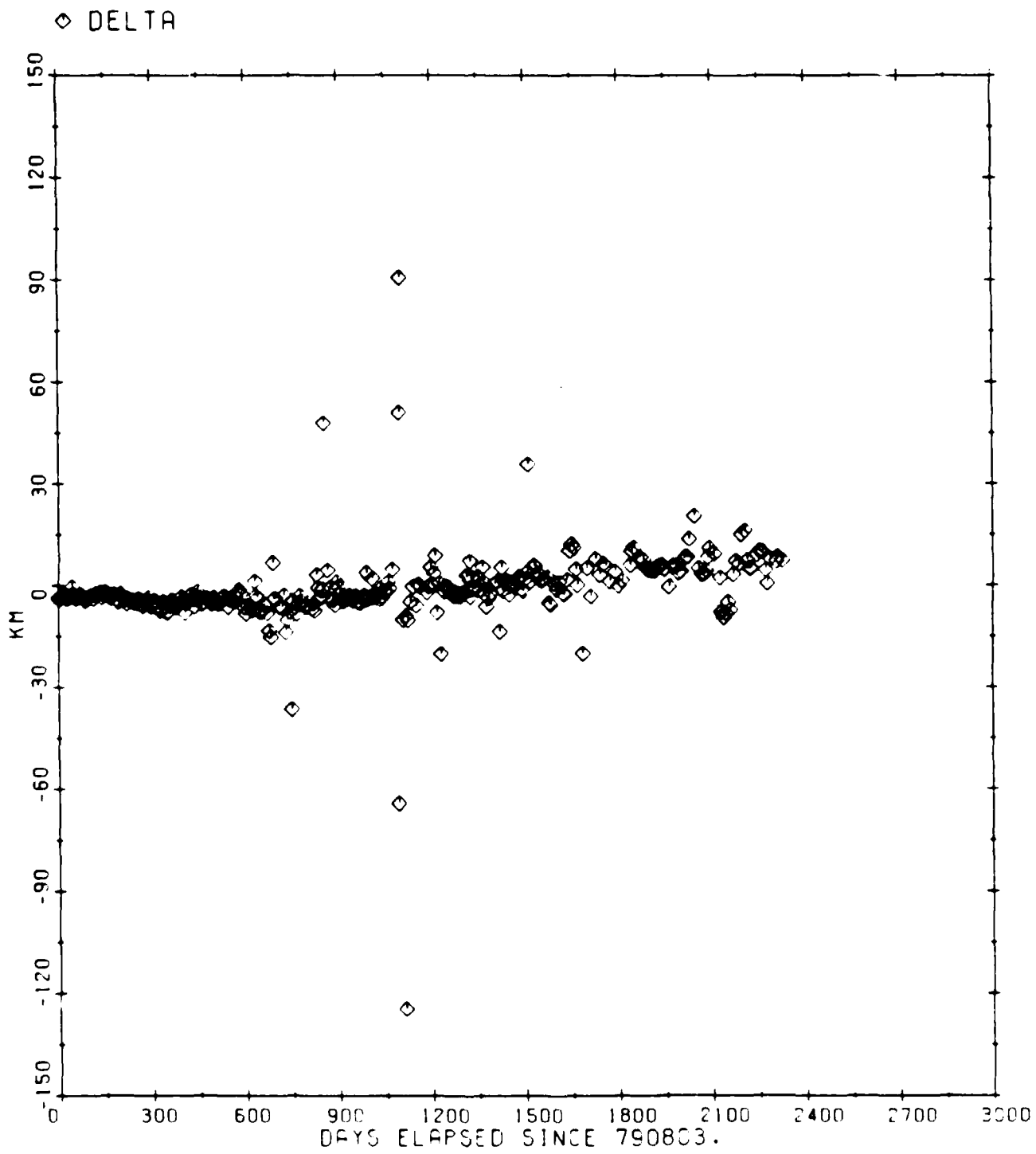
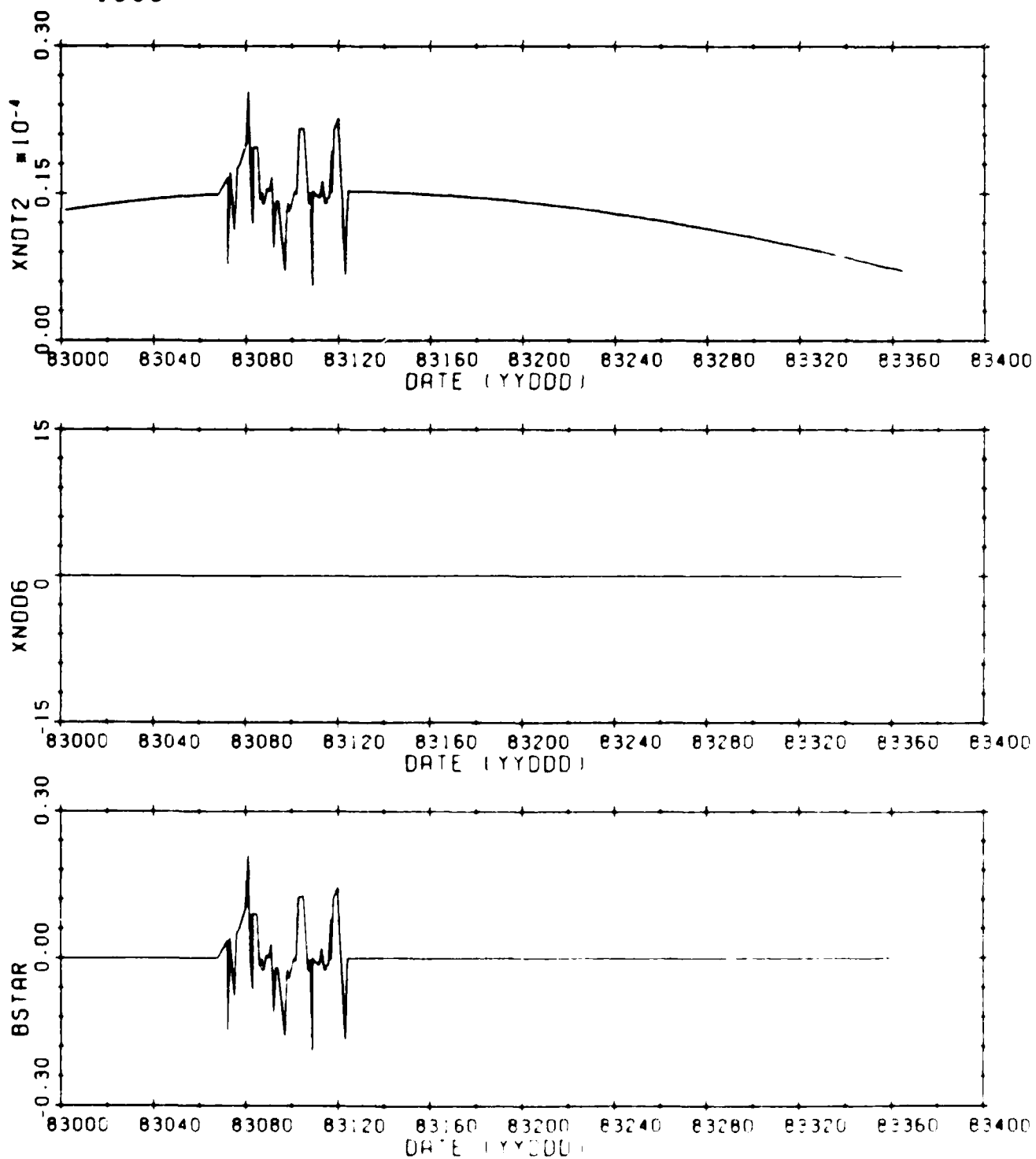


FIGURE 21. NO. C 9829 Radius of Apoee Difference

SV 9829

NORAD MEAN ELEMENTS

◊ 1983



The NSS 19829 difference plots for eccentricity and inclination (Figures 14 and 15) show essentially no secular trend. The small secular trend noted in the difference plot for longitude of the ascending node (Figure 16) may correspond to J_2^2 effects in the gravitational model. Note also the large standard deviation for the ascending node (Table 4).

In nearly all the comparison plots (Figures 6-12) there are several "noisy" NORAD predictions at approximately 1.5 days after epoch. These correspond to the "discontinuities" seen in the NORAD element set plots for mean motion rate and the drag factor (Figure 21). The reason the mean motion rate and drag factor should exhibit this behavior is not well understood.

Figure Number 14

Section 7. Mission and Operations

The European Space Agency (ESA) Spacelab-1 Experiment was launched on 29 May 1983. The Experiment was the first of three Spacelab flights. The primary objectives of the payload's primary payloads were the low-energy imaging telescope, the micrometeorite experiment, and the gravitational field spectrometer.

The design lifetime of Exosat was two years without orbital maneuvers, and sufficient onboard propellant was available to perform perigee height maneuvers to allow an orbital lifetime increase of up to 12 months. Initial orbital parameters [36] are shown in Table 6.

Table 6. NSSC 14095 Initial Operational Orbit Elements

Element	Value
Apogee height	2×10^5 km
Perigee height	500 km
Inclination	72.5°
Argument of perigee	286.5°
Period	99 hours

The high eccentricity of the orbit ($e=0.935$) allowed the spacecraft to remain above the radiation belts at 50,000 km for 80 hours of its 99 hour period, permitting uninterrupted observations for 72 hours per orbit and continuous coverage from a single ground station.

In the first months of operation, various anomalies occurred, with the spacecraft switching from star pointing mode to slow-iterating. Sun safety mode, and considerable mass of propane attitude control gas was lost. Later, in January 1990, the X-axis gyro malfunctioned and in the following week numerous anomalies involving the triggering of safety modes occurred, with the resultant loss of a large amount of control gas fuel.

The real data for Exosat consisted of 131 NORAD element sets. Of these, 96 were ESA-provided mean element sets. The utility AD-EDIT was used to examine the element set data, and the following element sets were edited prior to input to the preprocessor:

Table 7. NSSC 14095 Element Set Edits	
Element set date (YYDDD.DDDDDDD)	Questionable element
83276.9999999	XNDT2, XNDD6, XINCL, XNODE, EO, OMEGA
85167.9999999	XNDT2, XNDD6, XINCL, XNODE, EO, OMEGA
85293.9999999	XNDT2, XNDD6, XNO

3.1.2.2 SST DC and Prediction

As was the case for NSSC 9829, the initial estimate for the vehicle state for NSSC 14095 was taken from a NORAD mean element set. Six months of data were used in the fit, and epoch was chosen to ensure a perigee outside the main portion of the atmosphere. Table 8 lists the force models utilized in the SST DC and prediction. The maximum powers of a^R and e included in the power series expansions are larger than those included for NSSC 9829 (Table 3) because of the longer period and higher eccentricity of the Exosat orbit. Drag effects were not included because perigee height was outside the atmosphere, and solar pressure effects were shown to be minimal.

Table 8. Force Model used for NSSC 14095
Zonal: J_2 through J_{10} , e^4 , GEM 9
Tesseral resonances: off
Non-central bodies:
Moon (a/r) ¹³ , e^{18}
Sun (a/r) ⁴ , e^4
Solve-for parameters: mean equinoctial elements
Drag: off
Solar pressure: off

The a priori values and the final values for the Keplerian elements and their standard deviations are shown in Table 9. The assumed observation standard deviations were 40 km for each position coordinate and 40 m/sec for each velocity coordinate.

Table 9. Results of DC for NSSC 14095			
Epoch: Aug 19, 1983, 23 hours, 59 min, 59.000 sec			
Element	<i>a</i> priori Value	Final Value	Standard Deviation
$a(\text{km})$	102351.2699	102368.2782	0.25212
e	0.928471	0.926001	1.52616E-4
$i(^{\circ})$	71.98431	72.12634	1.2160
$\omega(^{\circ})$	185.5514	184.9844	4.3266
$\vartheta(^{\circ})$	283.5979	283.6980	1.4847
$M(^{\circ})$	233.4717	233.6411	2.6055
Weighted RMS: 2.357			
Mean of 1950.0 Coordinates			

It is interesting to compare the standard deviation obtained for the mean semimajor axis (252 meters) with the standard deviation obtained for the mean semimajor axis for NSSC 9829 (1.67 meters).

The final values of the Keplerian elements and the epoch indicated in Table 9 were used as initial conditions for an SST prediction. The same force models shown in Table 8 were used to create an ephemeris prediction file of about 84 days.

3.1.2.3 Comparison and Difference Plots

Figures 23-29 are comparison plots of the "NORAD" and "GTDS" predictions for the Keplerian elements for the approximately 250 days of available NORAD data following the indicated epoch of August 1983.

This prediction length was chosen because plots of the longer prediction length (840 days) revealed two distinct changes in slope of the comparison plot for mean anomaly (Figure 22). This suggested that the Exosat performed maneuvers during May 1984 and February 1985. The mean difference and standard deviation after 27 comparisons for the Keplerian and equinoctial elements are:

Table 10. Results of Comparisons for NSSC 14095

Element	Mean Difference	Standard Deviation
Semimajor axis (km)	77.274	149.98
Eccentricity	0.12844E-02	0.73346E-03
Inclination (°)	0.10235	0.75591E-01
Longitude of ascending node (°)	0.38547	0.27984
Argument of perigee (°)	0.12361	0.10469
Mean anomaly (°)	0.28861	0.53563
Radius of perigee (km)	133.69	82.289
Radius of apogee (km)	185.80	248.62
H	0.12355E-02	0.10365E-02
K	0.42946E-02	0.32847E-02
P	0.46902E-02	0.33793E-02
Q	0.17882E-02	0.14650E-02
Mean longitude (°)	0.46272	0.47961

Figures 30-37 are the plots of the difference between the "GTDS" predictions and the "NORAD" points for the Keplerian elements plotted against the number of days since August 1983.

SV14095 MEAN ANOMALY

COMPARISON DIFFERENCE: DELTA = GTDS-NORAD

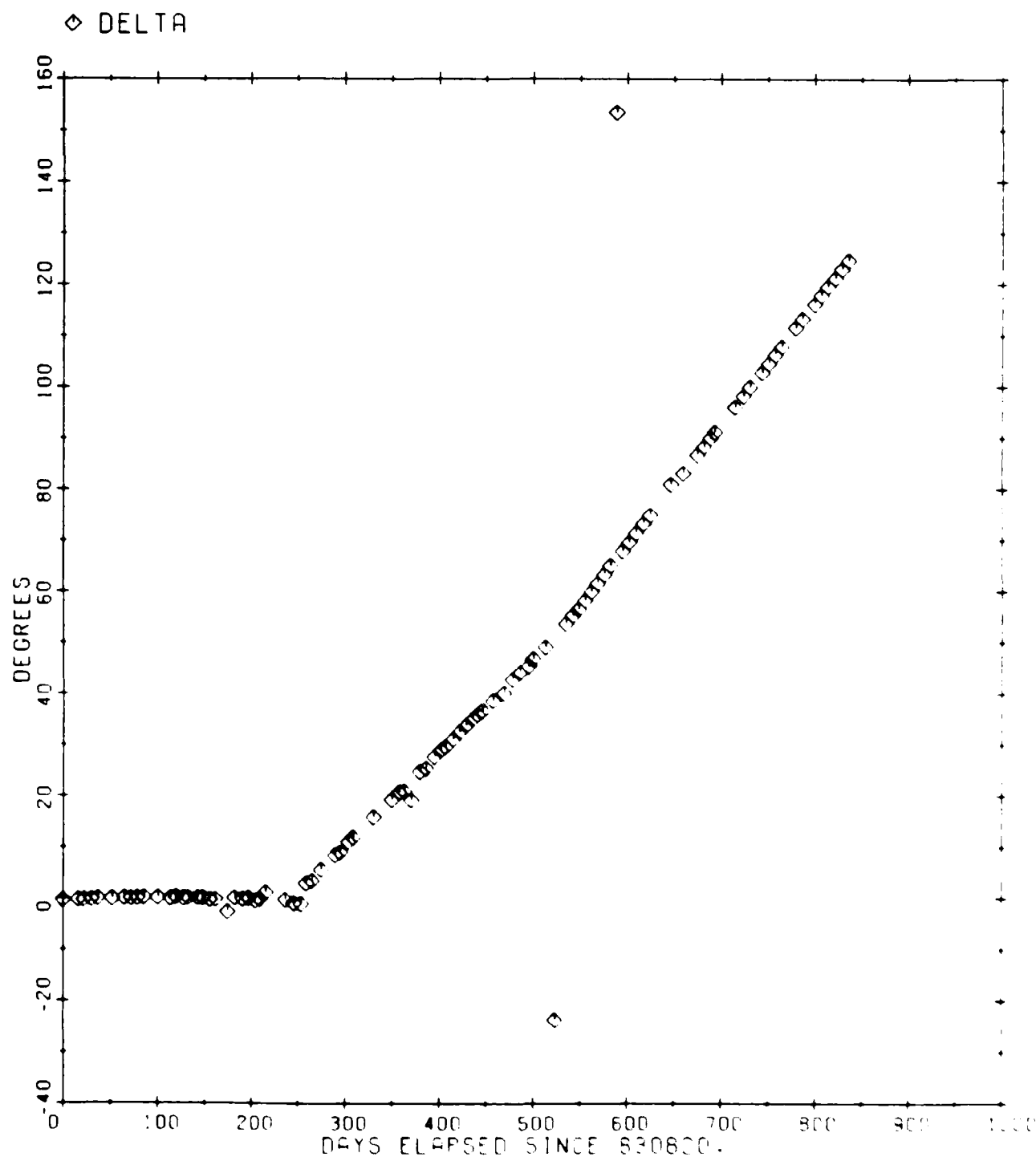
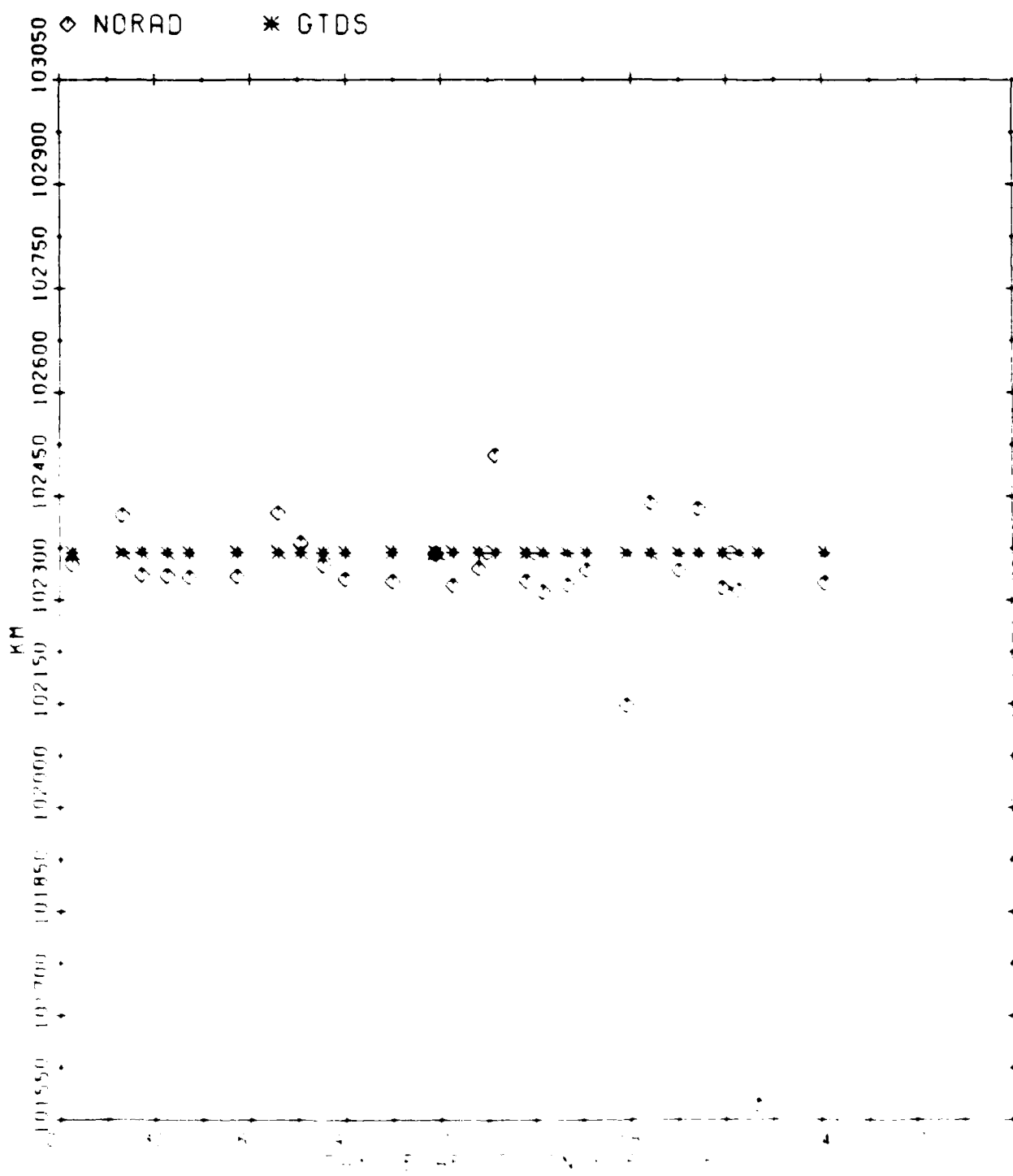


Figure 14-14. SV14095 Mean Anomaly Comparison.

SV14095 SEMIMAJOR AXIS

MEAN DIFFERENCE: 77.274 SIGMA: 149.98 AFTER 27 COMPARISONS



SV14095 ECCENTRICITY

MEAN DIFFERENCE: 0.12844E-02 SIGMA: 0.73346E-03 AFTER 27 COMPARISONS

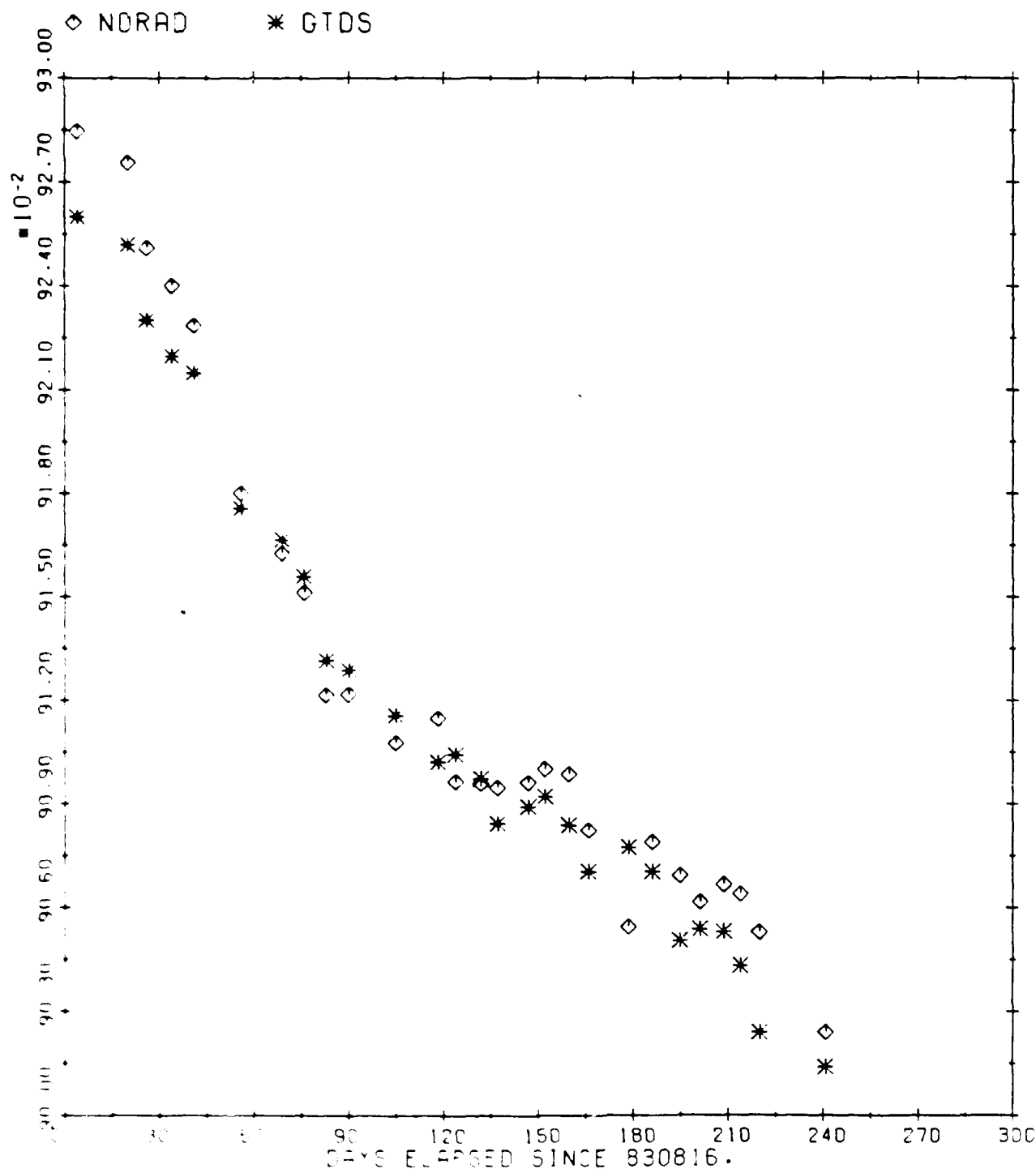
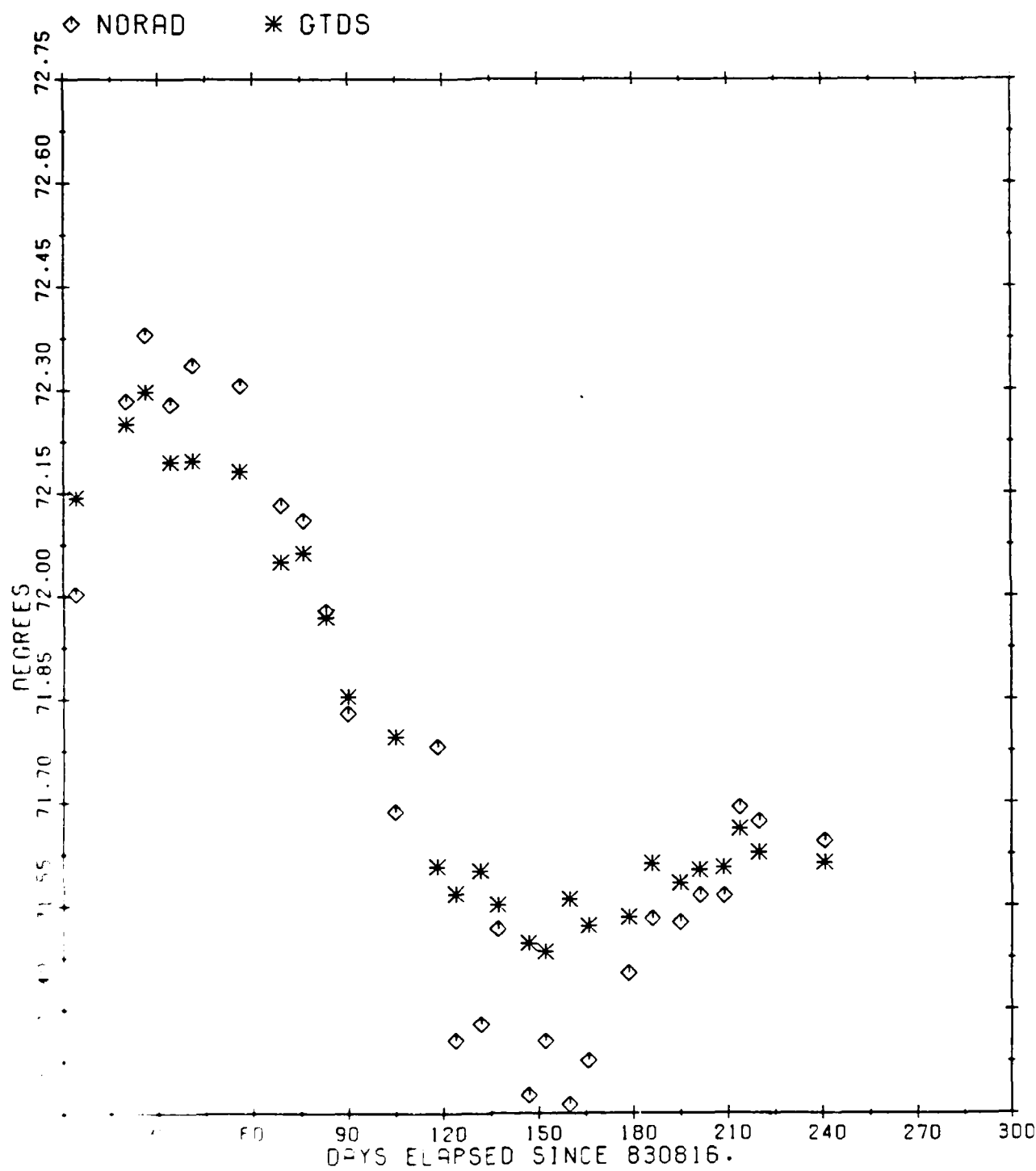


FIG. NO. 14 C Eccentricity Comparison

SV14095 INCLINATION

MEAN DIFFERENCE: 0.10235 SIGMA: 0.75591E-01 AFTER 27 COMPARISONS



SV14095 Inclination Comparison

SV:14095 LONGITUDE OF ASCENDING NODE

MEAN DIFFERENCE: 0.38547 SIGMA: 0.27984 AFTER 27 COMPARISONS

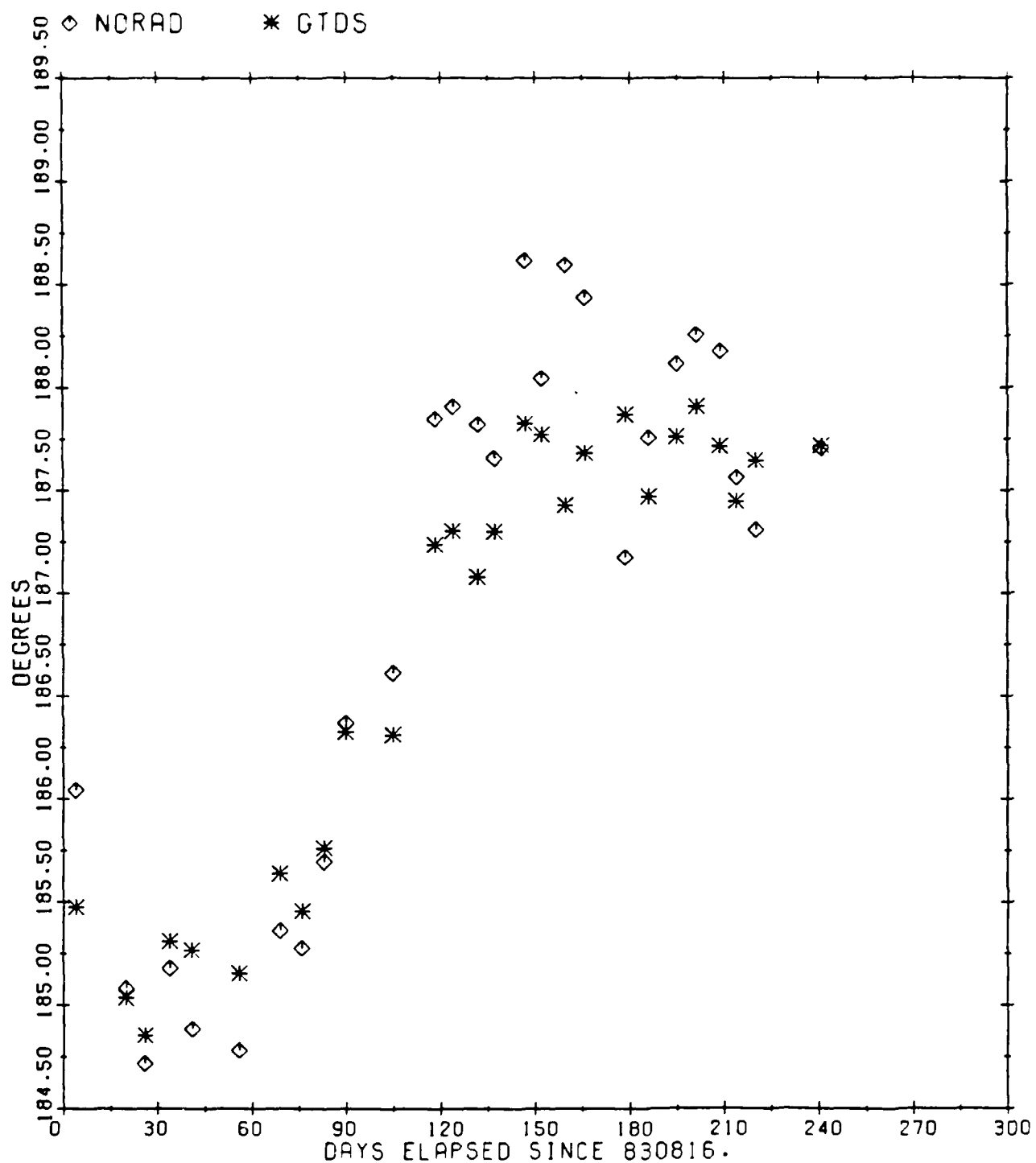


Figure 26. NSSC 14095 Longitude of Ascending Node Comparison

SV14095 ARGUMENT OF PERIGEE

MEAN DIFFERENCE: 0.12361

SIGMA: 0.10469

AFTER 27 COMPARISONS

◊ NORAD * GTDS

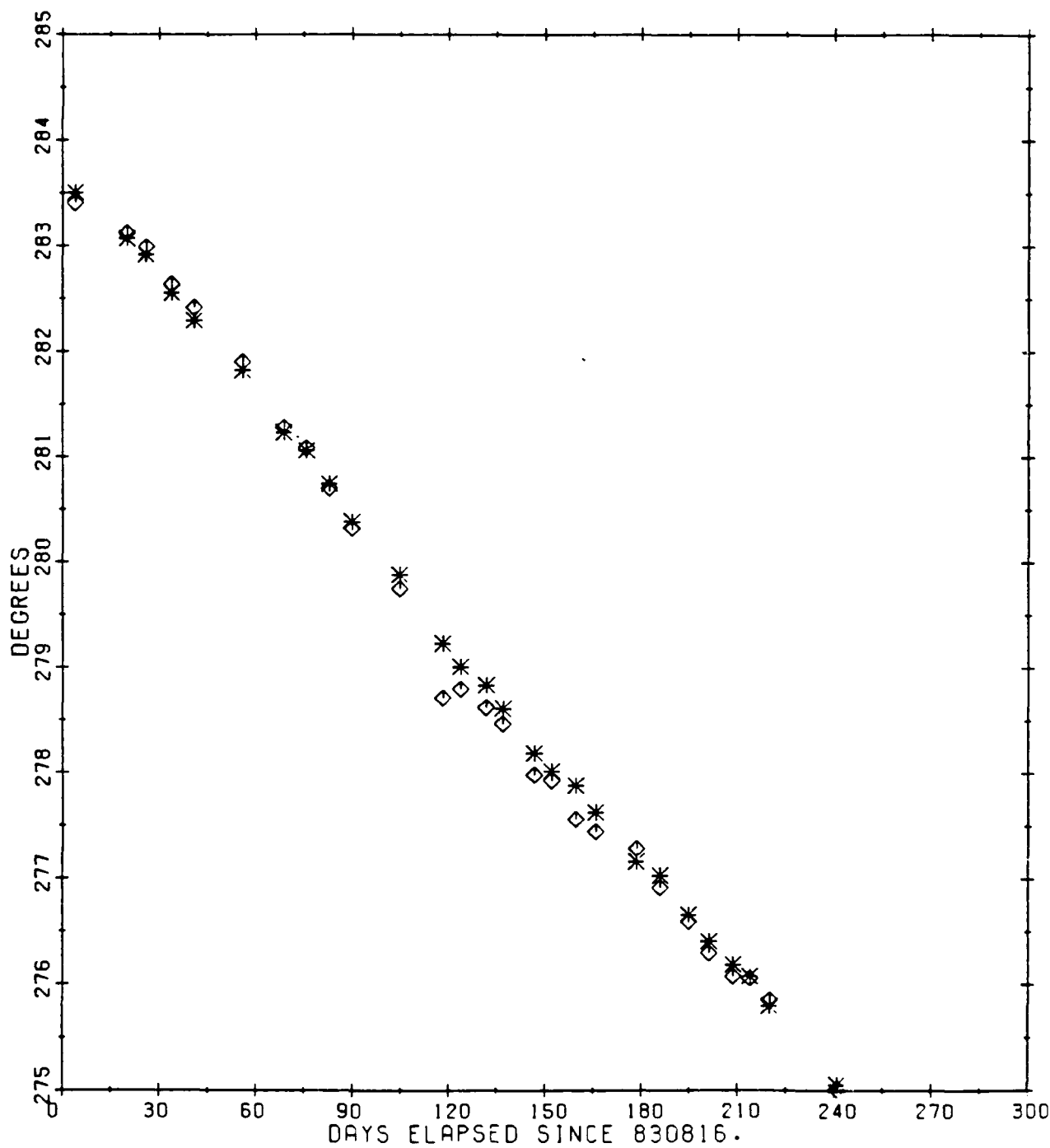


Figure 27. NSFC 14095 Argument of Perigee Comparison

SV14095 RADIUS OF PERIFOCUS

MEAN DIFFERENCE: 133.69

SIGMA: 82.289

AFTER 27 COMPARISONS

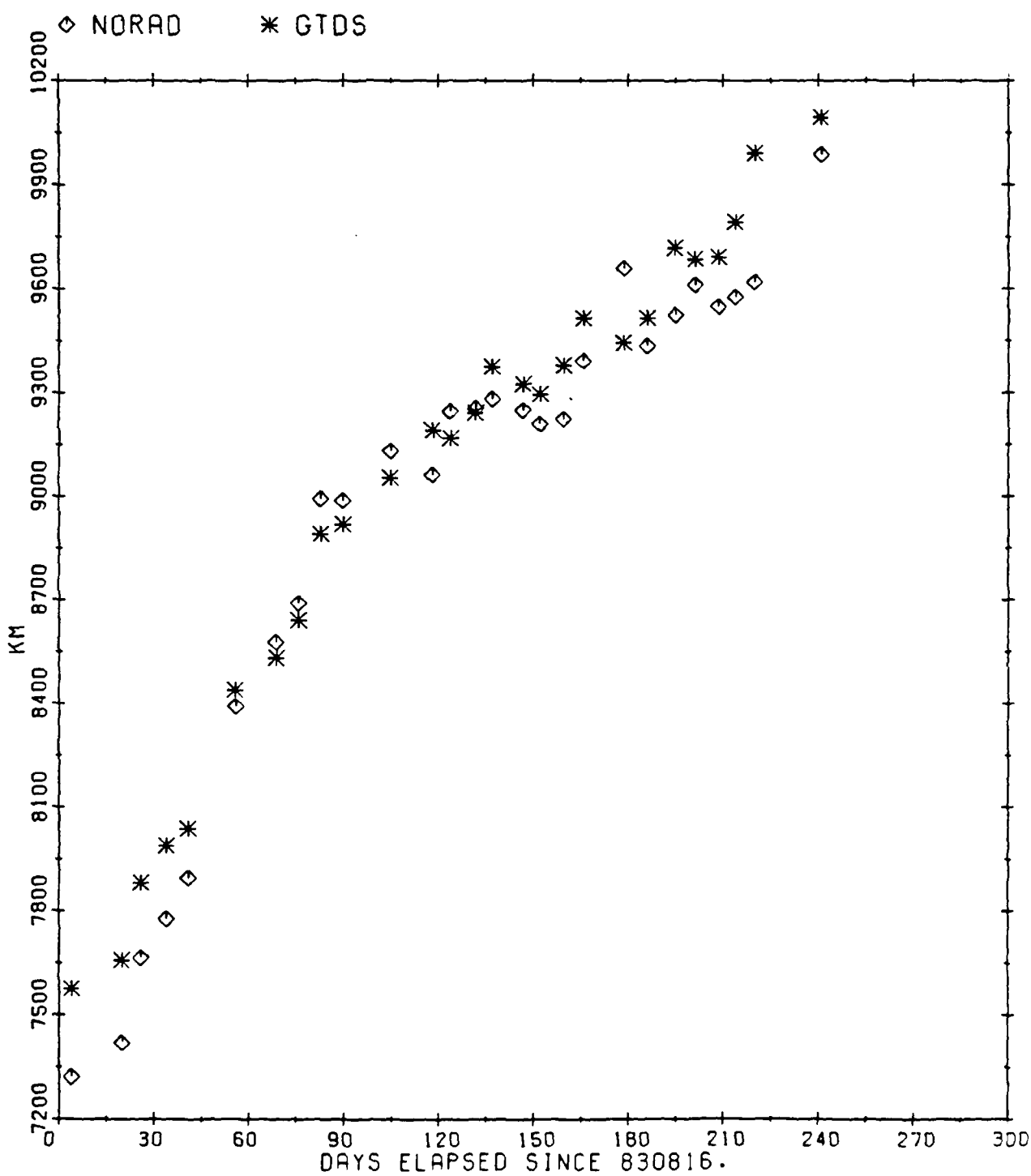


Figure 28. NSSC 14095 Radius of Perigee Comparison

SV14095 RADIUS OF APOFOCUS

MEAN DIFFERENCE: 185.80 SIGMA: 248.62 AFTER 27 COMPARISONS

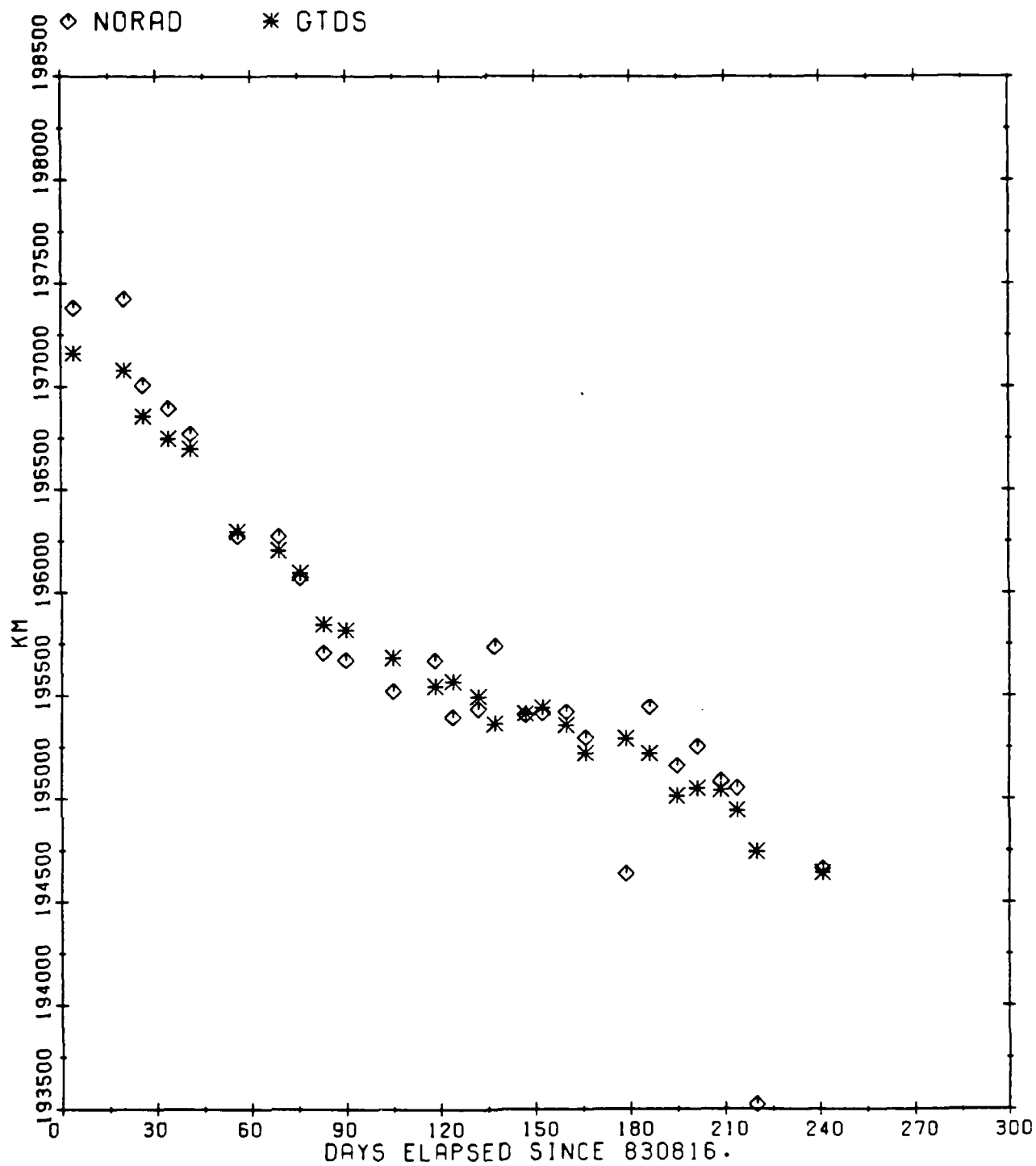


Figure 29. NSSC 14095 Radius of Apogee Comparison

SV14095 SEMIMAJOR AXIS

COMPARISON DIFFERENCE: DELTA = GTDS-NORAD

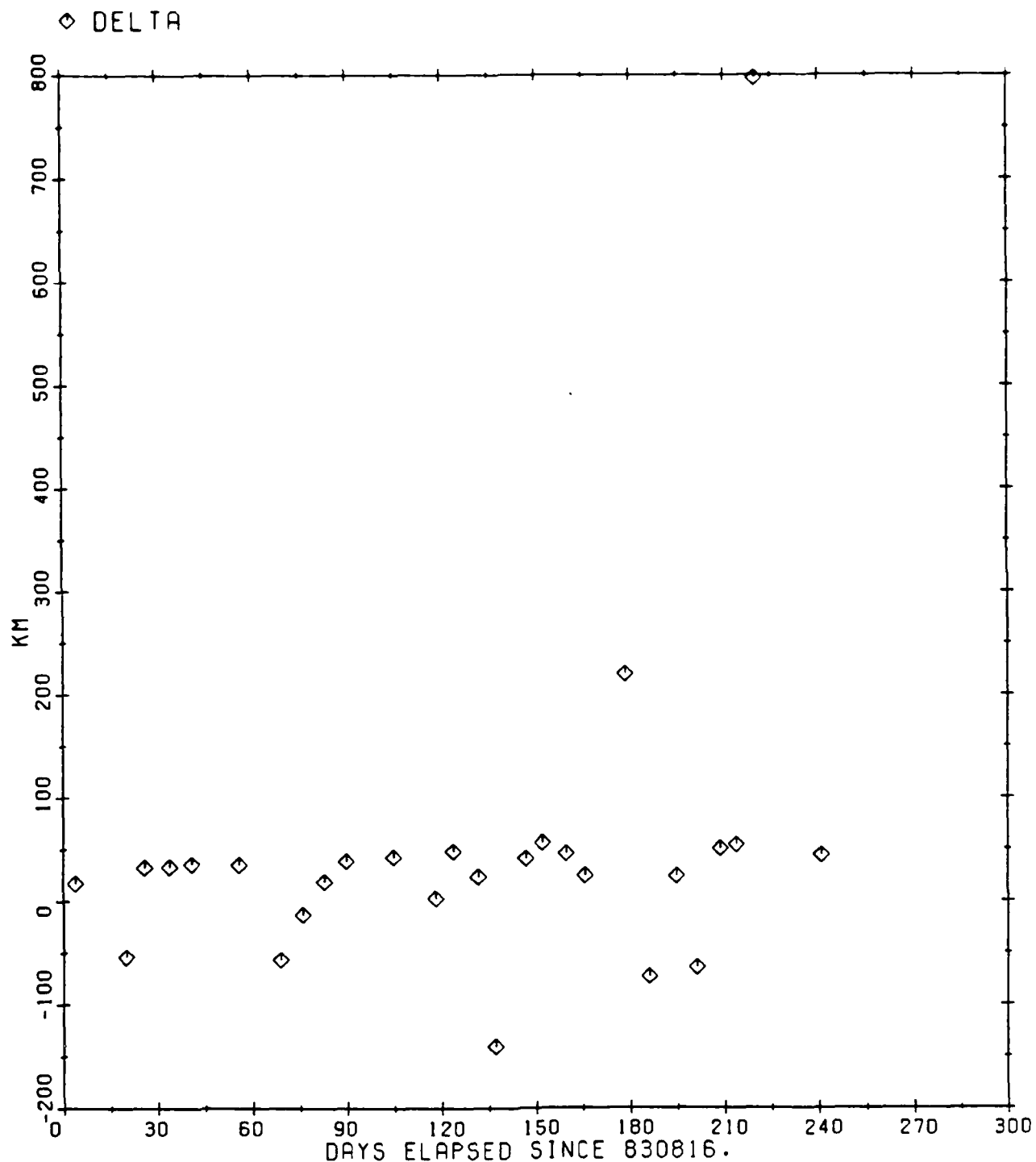


Figure 30. NSSC 14095 Semimajor Axis Difference

SV14095 ECCENTRICITY

COMPARISON DIFFERENCE: DELTA = GTDS-NORAD

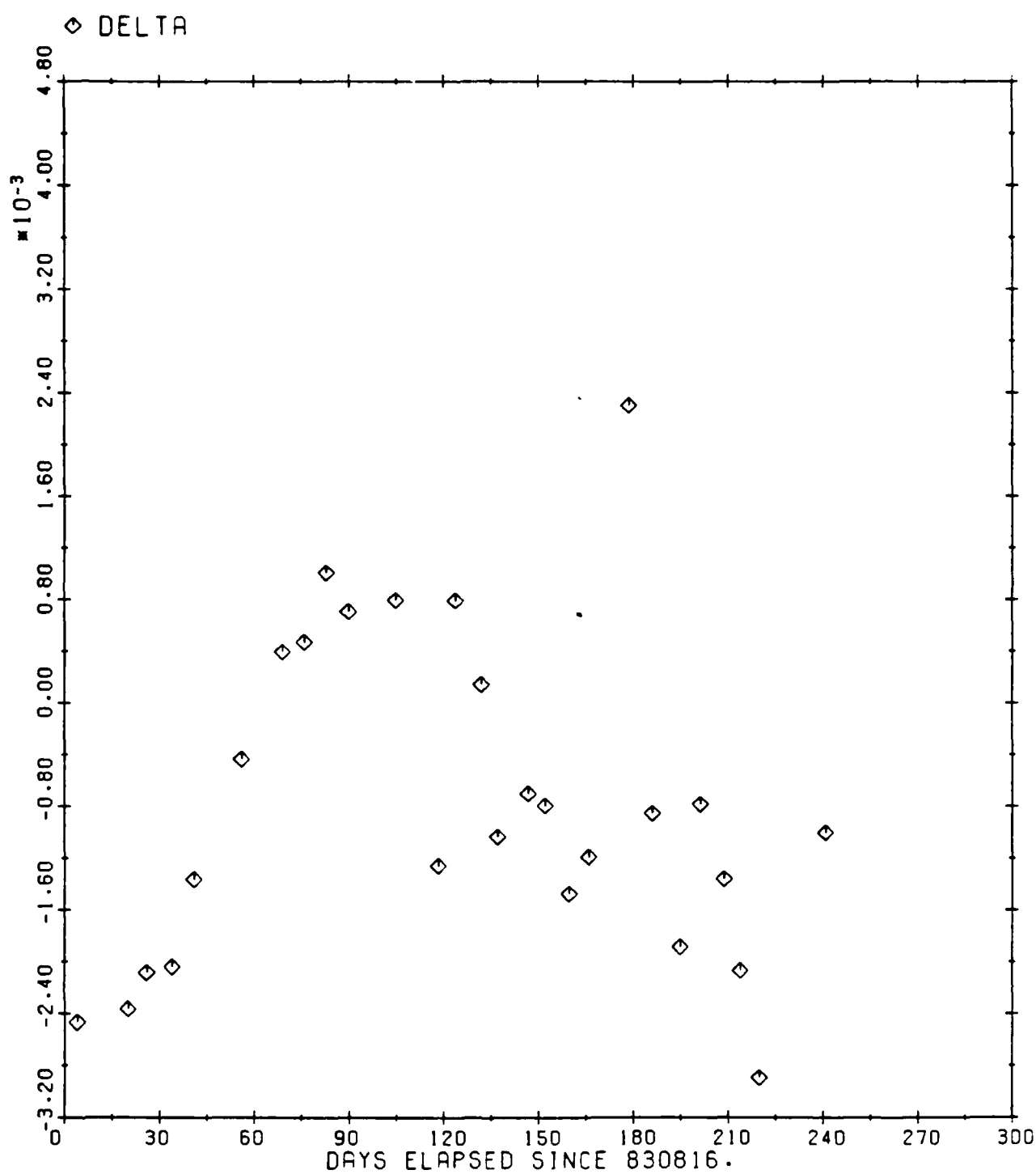


Figure 31. NSSC 14095 Eccentricity Difference

SV14095 INCLINATION

COMPARISON DIFFERENCE: DELTA = GTOS-NORAD

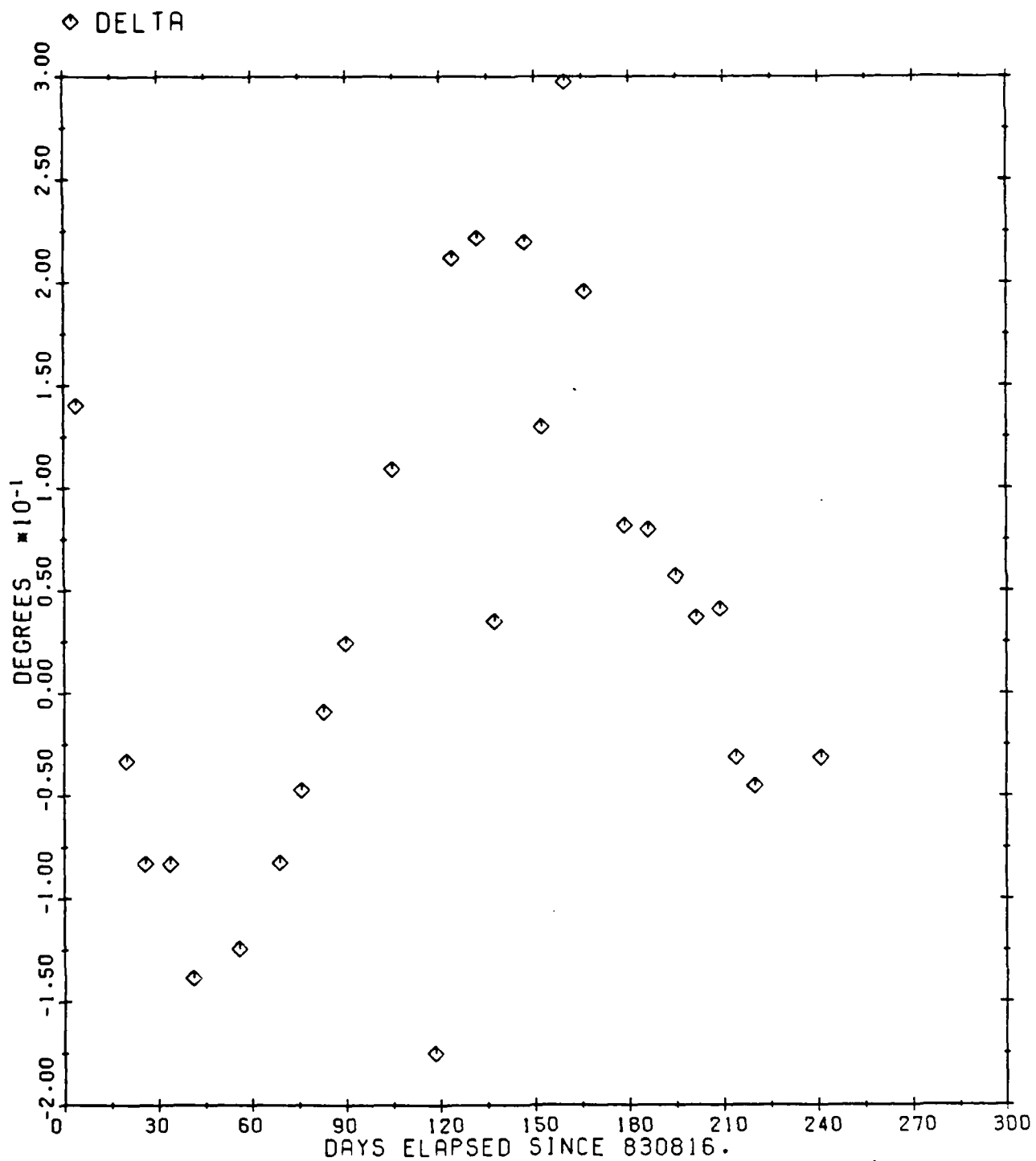


Figure 32. NSSC 14095 Inclination Difference

SV14095 LONGITUDE OF ASCENDING NODE

COMPARISON DIFFERENCE: DELTA = GTDS-NORAD

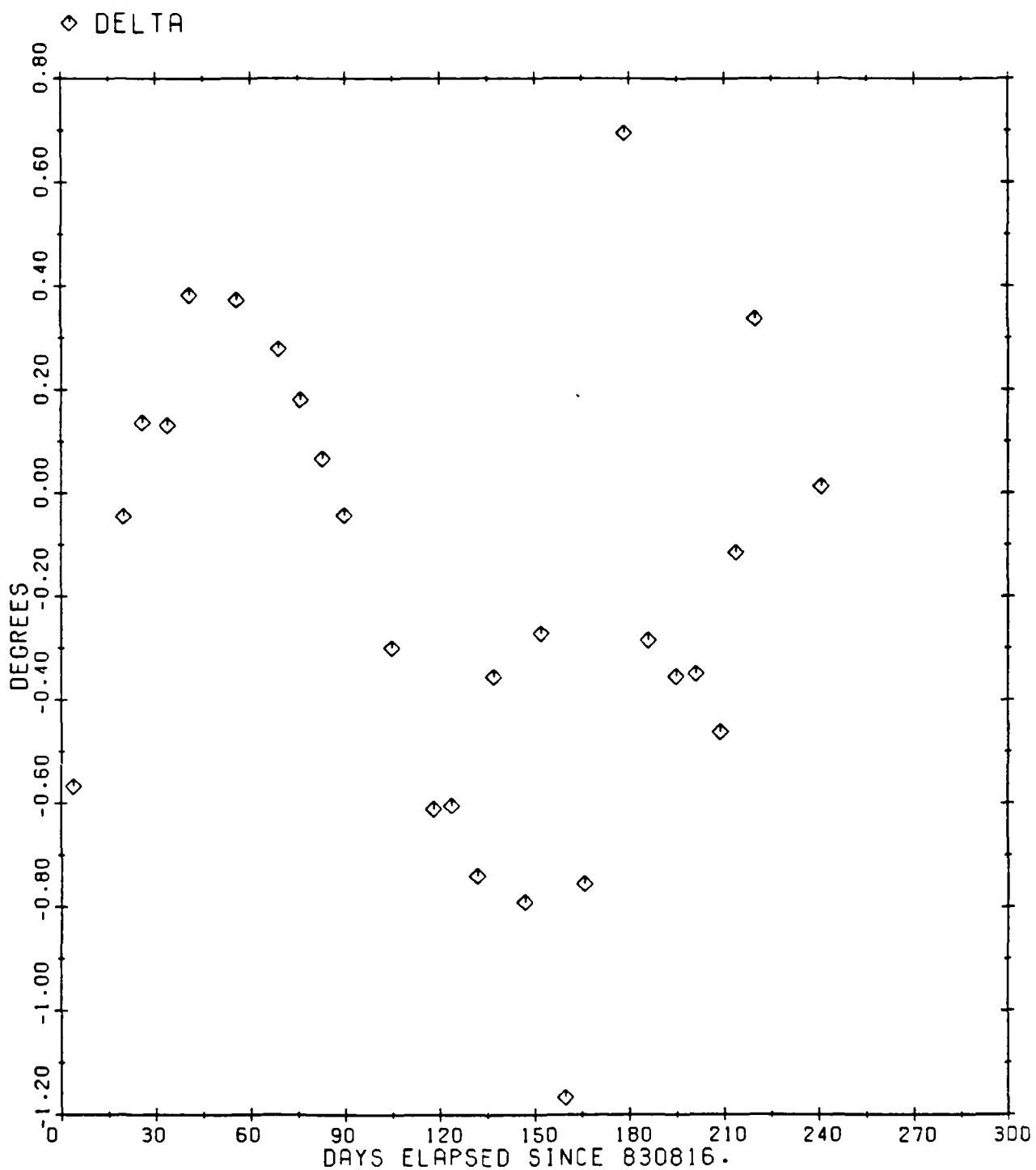


Figure 33. NSSC 14095 Longitude of Ascending Node Difference

SV14095 ARGUMENT OF PERIGEE

COMPARISON DIFFERENCE: DELTA = GTDS-NORAD

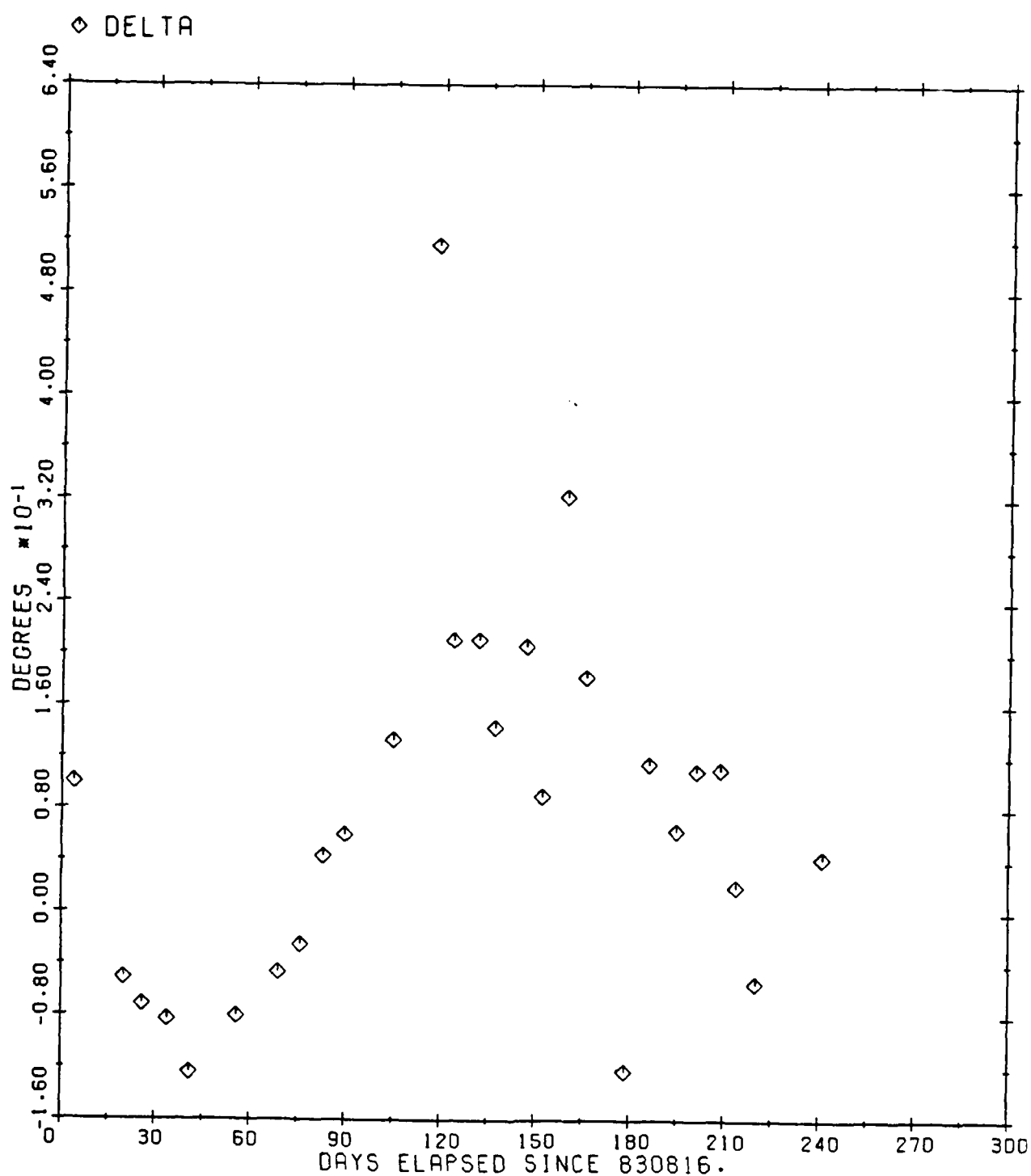


Figure 34. NSSC 14095 Argument of Perigee Difference

SV14095 MEAN ANOMALY

COMPARISON DIFFERENCE: DELTA = GTDS-NORAD

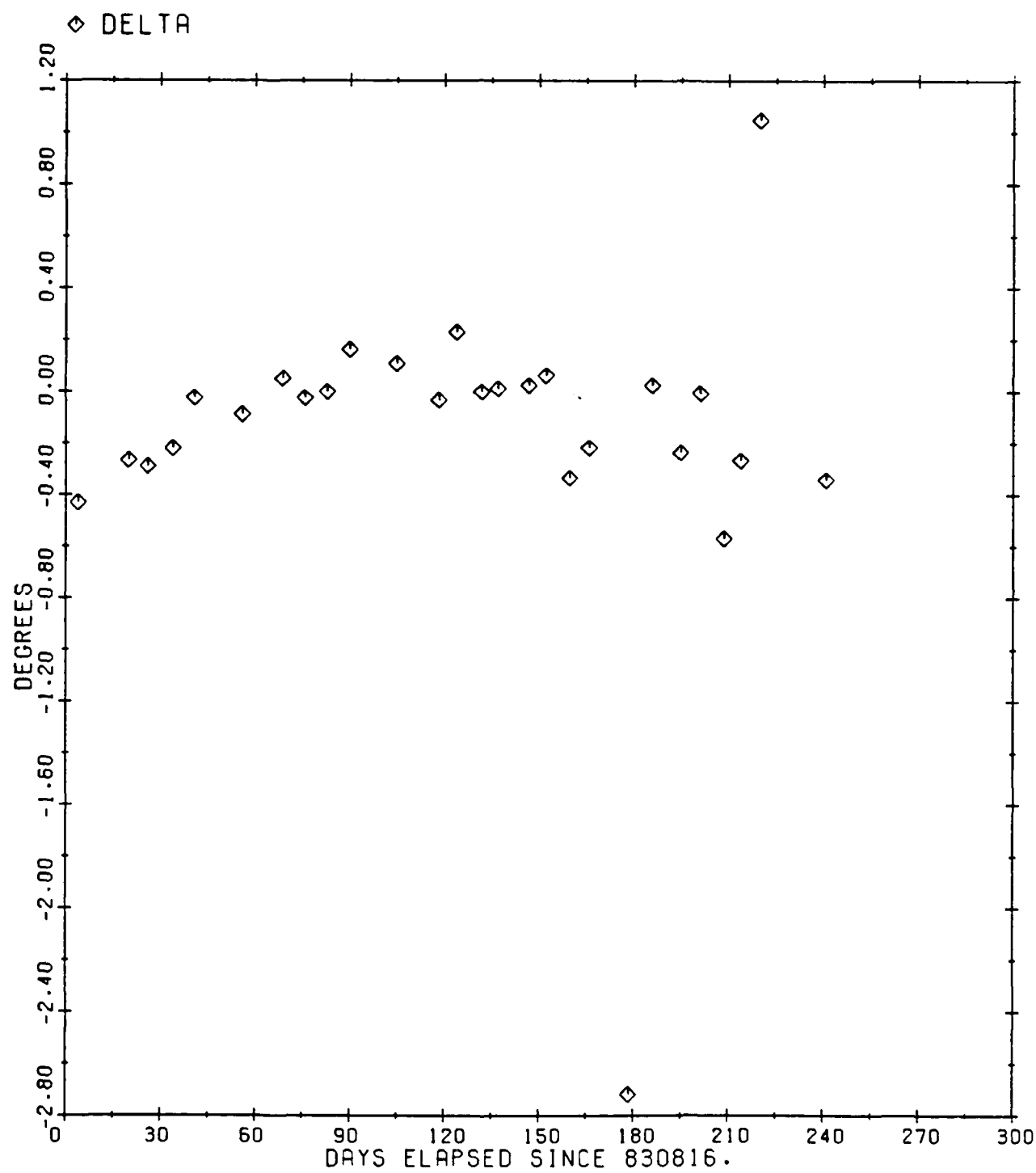


Figure 35. NSSC 14095 Mean Anomaly Difference

SV14095 RADIUS OF PERIFOCUS

COMPARISON DIFFERENCE: DELTA = GTDS-NORAD

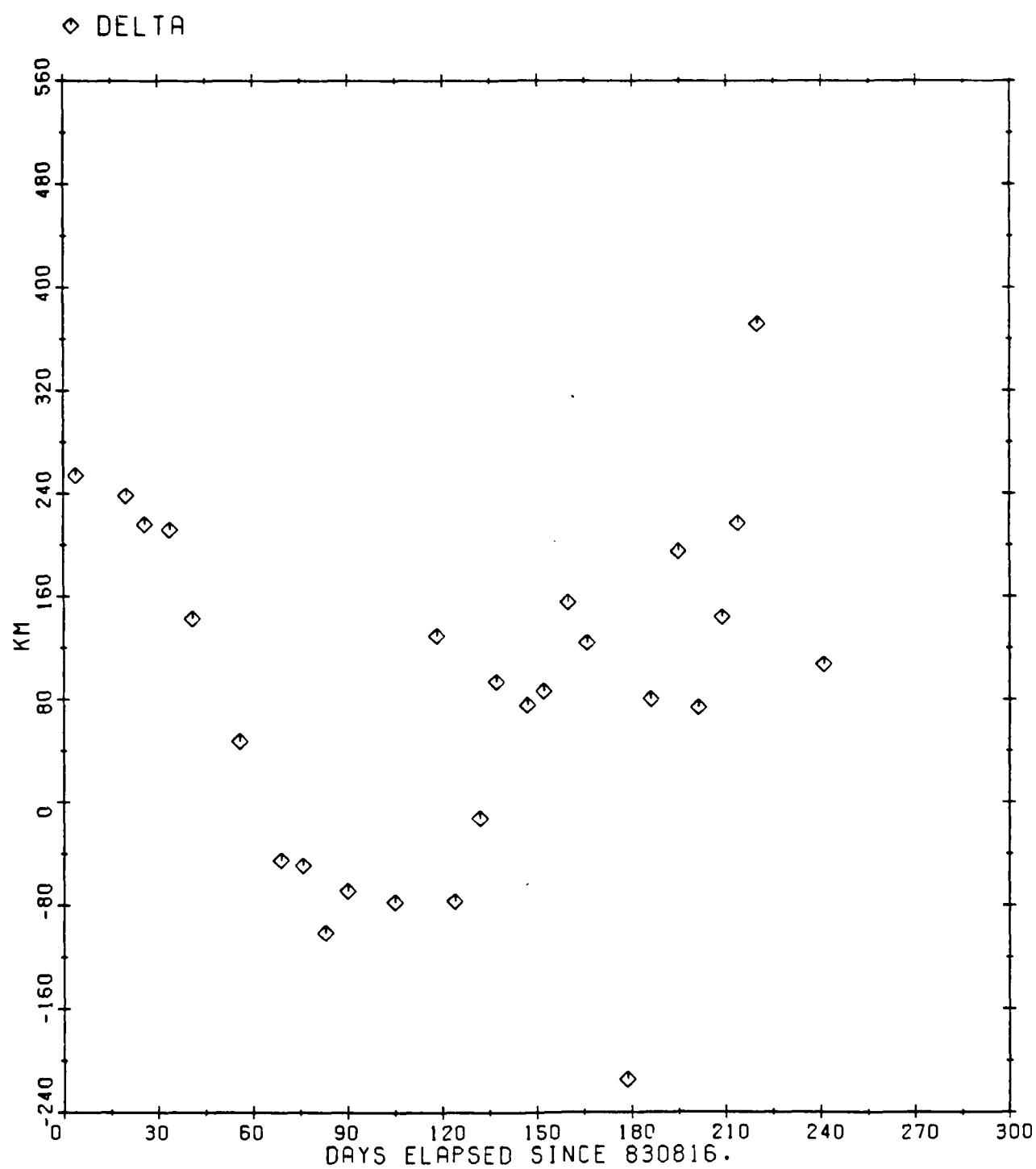


Figure 36. NSSC 14095 Radius of Perigee Difference

SVIAGE RADIUS OF APOGEE

COMPARISON DIFFERENCE: DELTA = GIOES-NORRAC

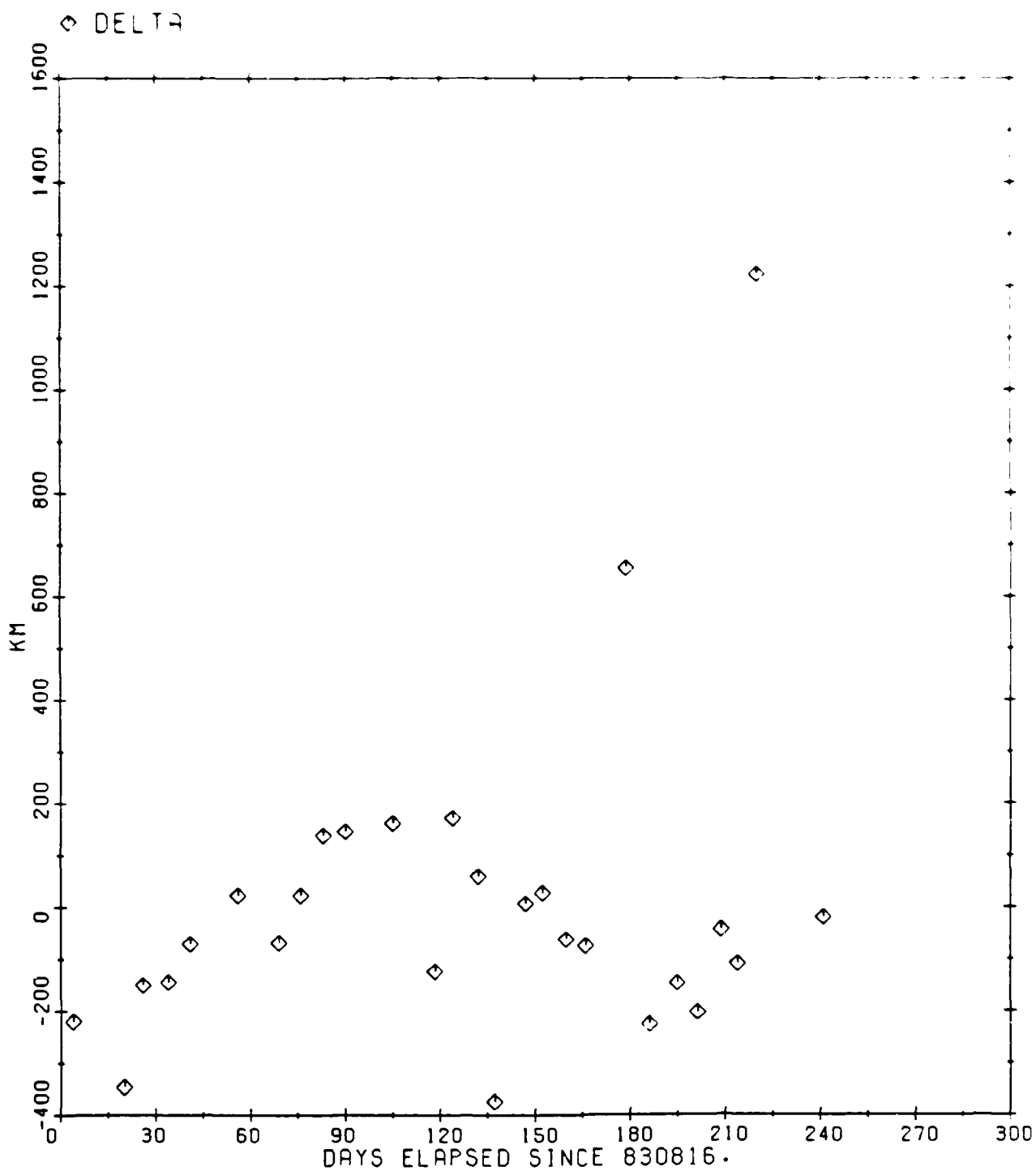


Figure 37. NSSC 14095 Radius of Apogee Difference

periods, varying Keplerian element histories (Figures 23-27) and mean anomaly differences. Figure 35^a demonstrate the relatively good agreement between the SST and NORAD predictions. The comparison difference plot for semi-major axis (Figure 30^a) exhibits no secular drift, although there appears to be a slight oscillation with a period of about 60 days. The difference plots for eccentricity, inclination, longitude of ascending node, and argument of perigee (Figures 31-34) exhibit a slight systematic error with a period of about one year. Secular trends in this prediction interval (only 10 days) are much more difficult to detect than when long intervals of data are available, as was the case with NSSC 9829.

3.2 INITIALIZATION OF SST USING OBSERVATION DATA

As was mentioned in Section 3.1.1.3, a six-month DC that included an 8x8 field with 3DM-4 coefficients resulted in a very unsatisfactory overall weighted RMS value. Subsequent testing validated the SST models. It was at that point that the use of actual NORAD observations was considered. Observational data was available for NSSC 13964.

3.2.1 NSSC 13964

3.2.1.1 Mission and Operations

The NSSC 13964 spacecraft, Molniya 1-57, was launched 2 April 1983 as a replacement for Molniya 1-52. Its initial transfer orbit had a period of 700 minutes [40], indicating the spacecraft drifted eastward to its operational location. Its initial operational orbital elements [9] for 7 April 1983 are shown in Table 11.

MD-A185 825

AN EVALUATION OF SEMIANALYTICAL SATELLITE THEORY
AGAINST LONG ARCS OF REA. (U) AIR FORCE INST OF TECH
WRIGHT-PATTERSON AFB OH M E FIEGER JAN 87

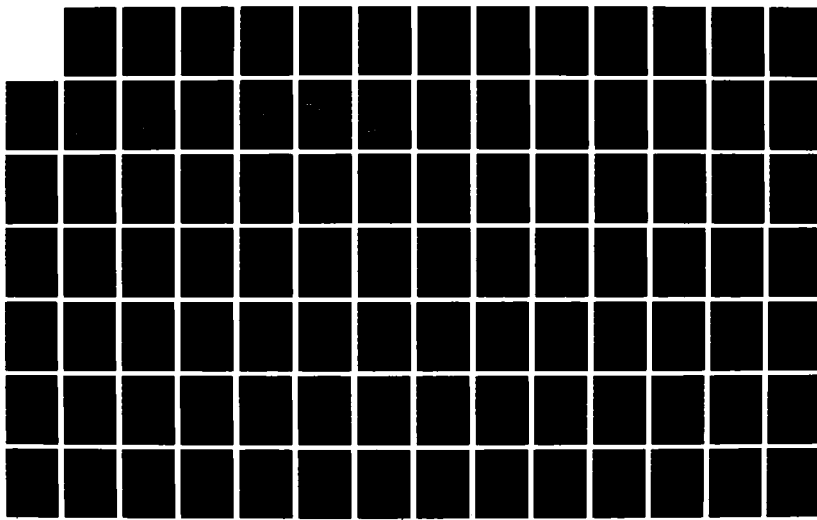
2/3

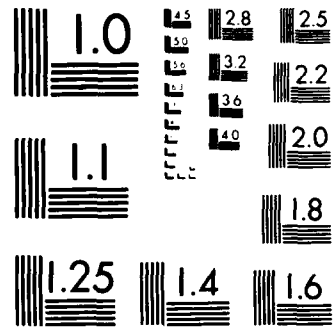
UNCLASSIFIED

AFIT/CI/NR-87-52T

F/G 22/3

NL





MICROCOPY RESOLUTION TEST CHART
NATIONAL BUREAU OF STANDARDS 1963-A

Table 11. NSSC 13964 Initial Operational Orbit Elements

Element	Value
Apogee height	39,877 km
Perigee height	482 km
Inclination	62.93 degrees
Period	717.85 minutes

3.2.1.2 SST DC and Prediction

The NORAD observation data was comprised of radar observations and optical data. The observation weights that were used are given in Tables 12 and 13. These result from [41, 42, 43]. Also, the range and range-rate weights have been heuristically adjusted to consider the particular short-periodic model chosen for use in these semianalytical DC runs. A NORAD mean element set was used as an initial estimate for the DC run. Processing included the first three months of 1985 observations. Tables 14 and 15 list the force models utilized in the SST DC and prediction. It was necessary to include short-periodics modelling because the real data was in the form of actual observations.

Table 12. Radar Observation Data Sigmas

Station	Range (m)	Azimuth (mdeg)	Elevation (mdeg)	Range-rate (cm/s)
Eglin (399)	67.	17.	15.	n/a
Altair (666)	60.	31.	17.	15.
Millstone (369)	35.	9.1	8.3	10.

Table 13. Optical Observation Data Sigmas

Station	Right Ascension (mdeg)	Declination (mdeg)
Primary Telescope (231, 232, 221, 222, 211, 212)	5.5	5.5
Secondary Telescope (233, 223, 213)	6.9	6.9

Table 14. Mean Dynamics Model used for NSSC 13964

Zonals: J_2 through J_8 , e^5 , WGS72 (12x12)

Tesseral resonance: WGS72 (12x12), (2,2) through (8,8), e^{20}

Non-central bodies:

Moon: $(a/r)^9$, e^7

Sun: $(a/r)^3$, e^3

Solve-for parameters: mean equinoctial elements,
solar radiation coefficient

Drag: off

Solar pressure: on (Area = 3 m^2 , mass = 250 kg)

Table 15. Short-Periodics Model used for NSSC 13964

Zonals: J_2 through J_4 , WGS72 (12x12)

Tesseral m-dailies: 4x4

J_2 secular/m-daily coupling: off

High-frequency tesseral: off

Non-central bodies:

Moon: $(a/r)^{10}$, e^{10}

Sun: $(a/r)^4$, e^4

Drag: off

Solar pressure: off

It was assumed that an 8x8 field would be an improvement over the 6x6 field included for NSSC 9829 (see Table 3). Solar pressure effects were also included. As before, the number of terms included in the power series expansions was automatically selected by the GTDS software. The short-periodics model of Table 15 was based on a sizing analysis for the short-periodic perturbations for 12-hr, high eccentricity orbits [44].

The a priori values and the final values for the Keplerian elements and the solar radiation coefficient C_r , and the corresponding standard deviations are shown in Table 16. The assumed observation standard deviations were given in Tables 12 and 13. The converged iteration residual plots are shown in Figures 38-43. (The NORAD station numbers corresponding to the plot designators are found in Table 17.)

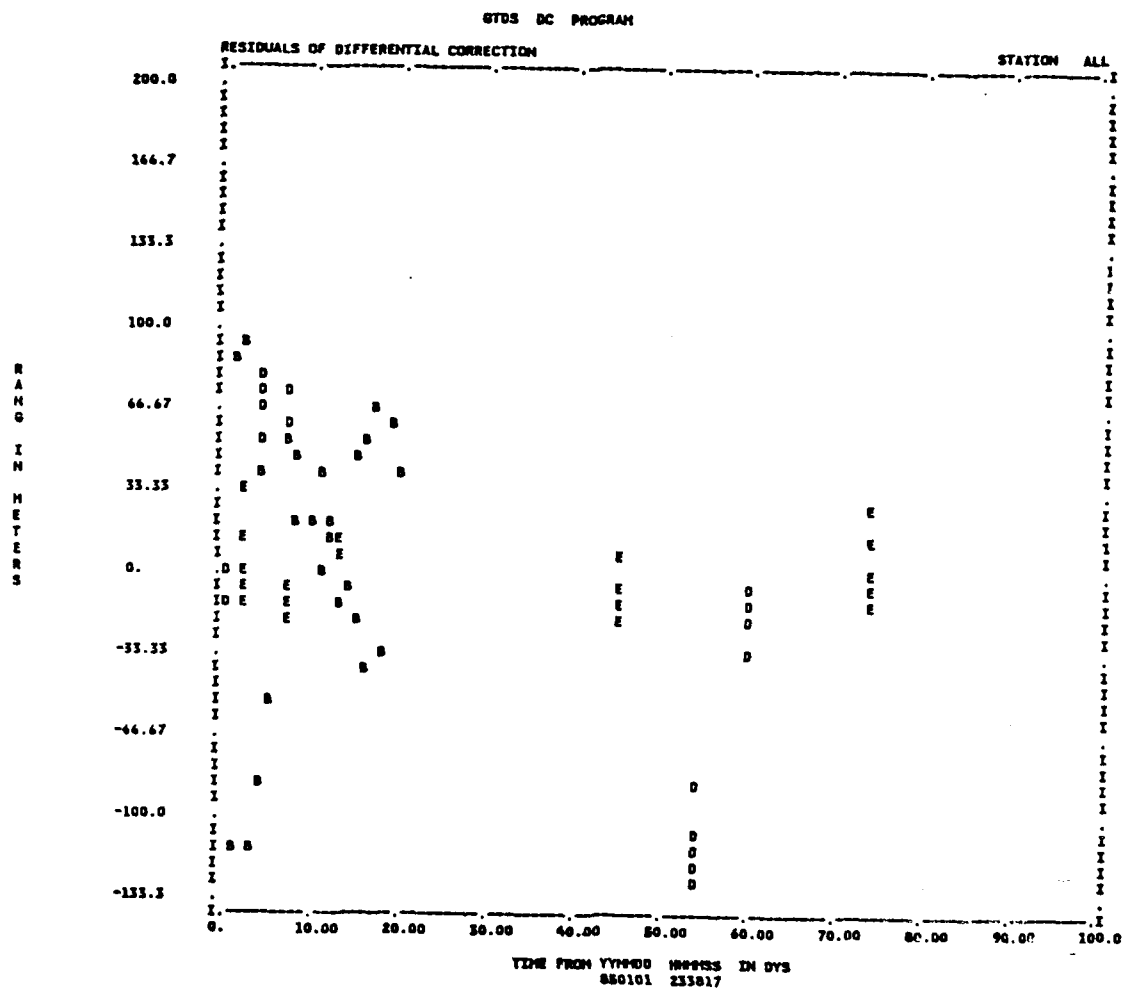


Figure 38. NSSC 13964 DC Residual (Range)

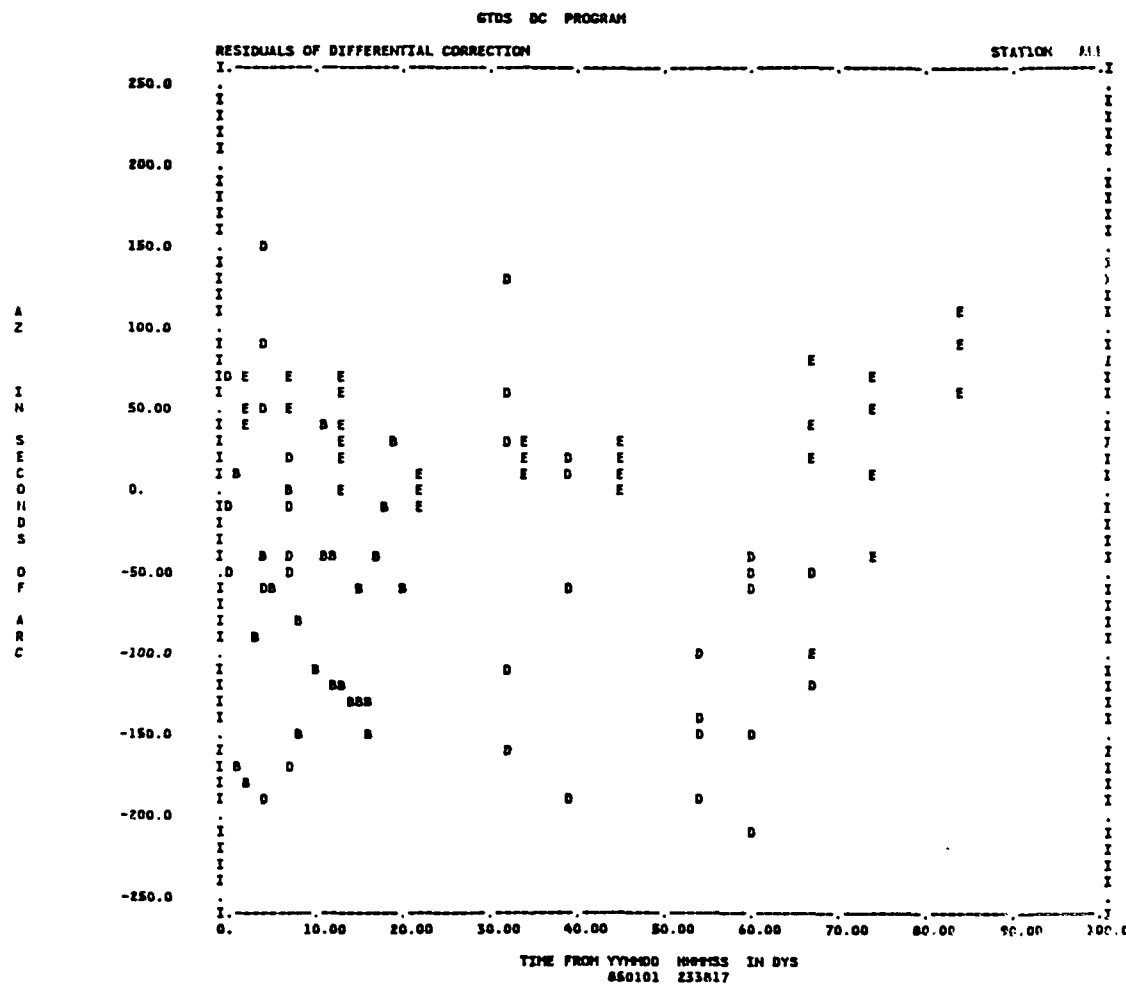


Figure 39. NSSC 13964 DC Residual (Azimuth)

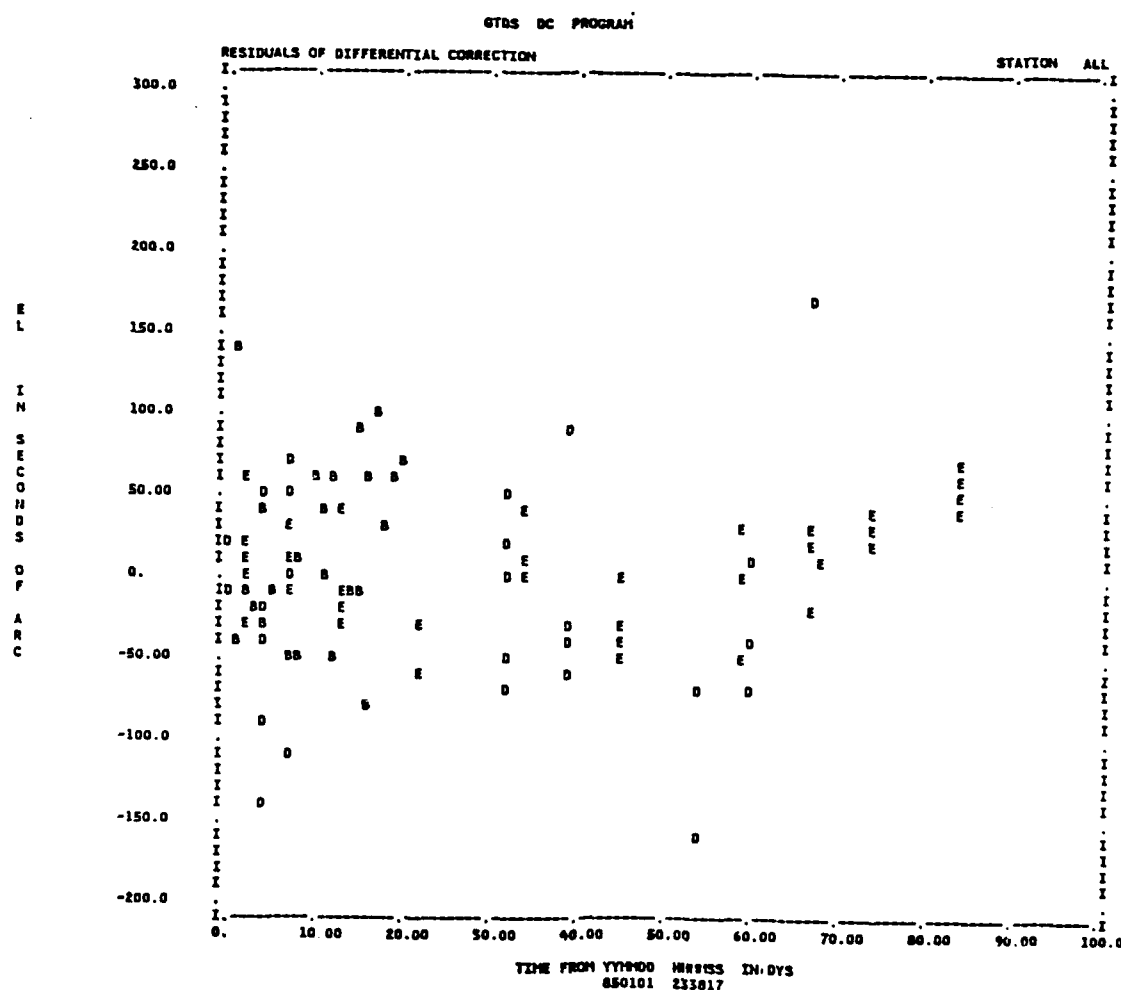


Figure 40. NSSC 13964 DC Residual (Elevation)

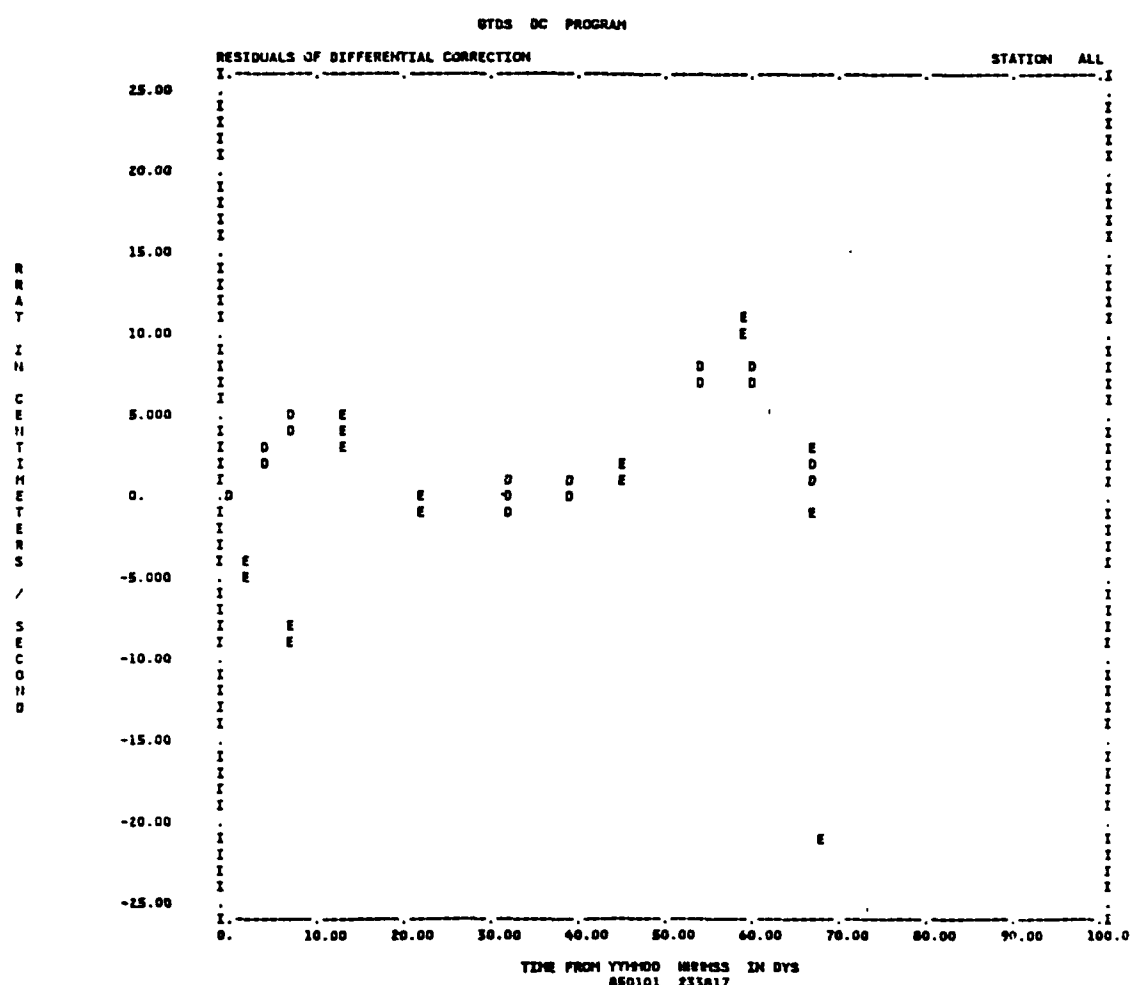


Figure 41. NSSC 13964 DC Residual (Range Rate)

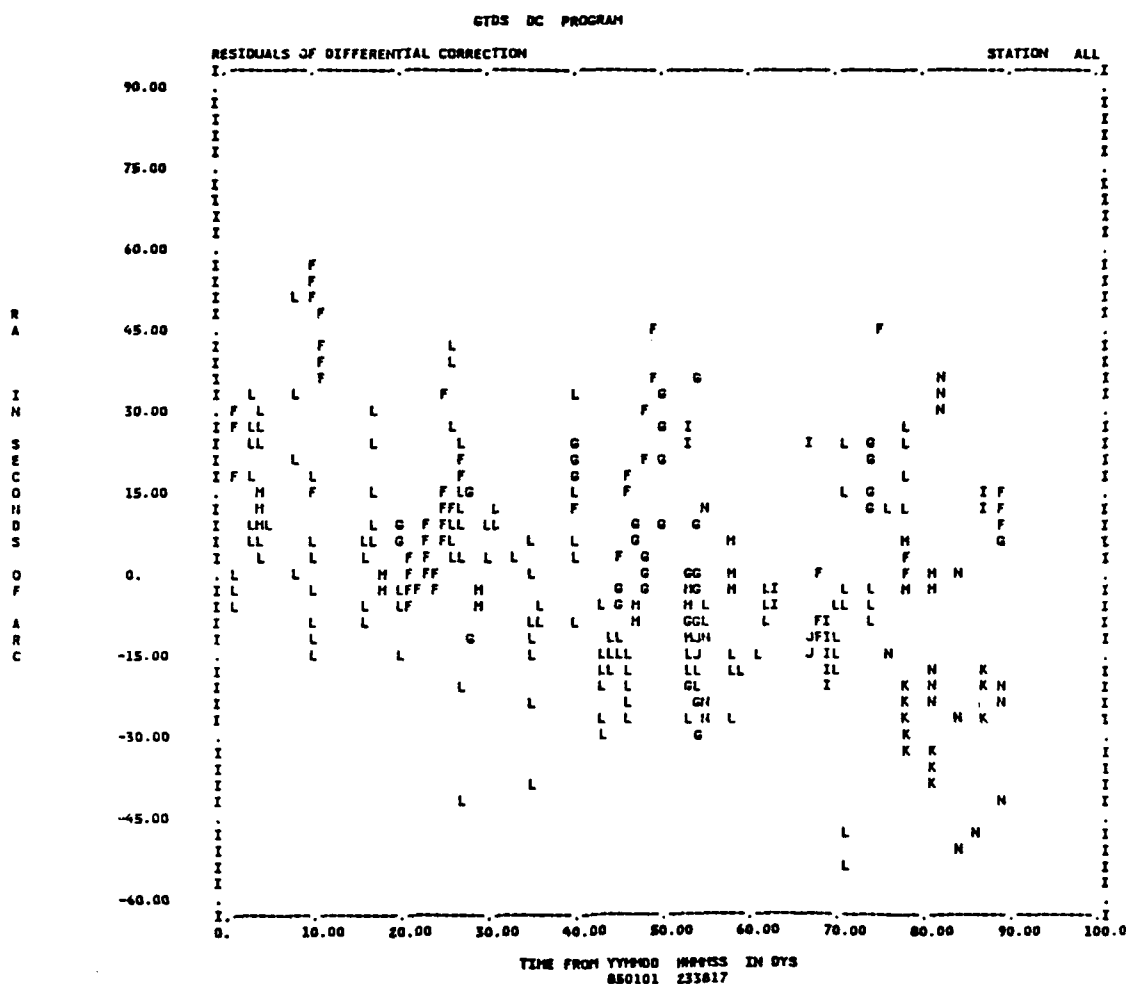


Figure 42. NSSC 13964 DC Residual (Right Ascension)

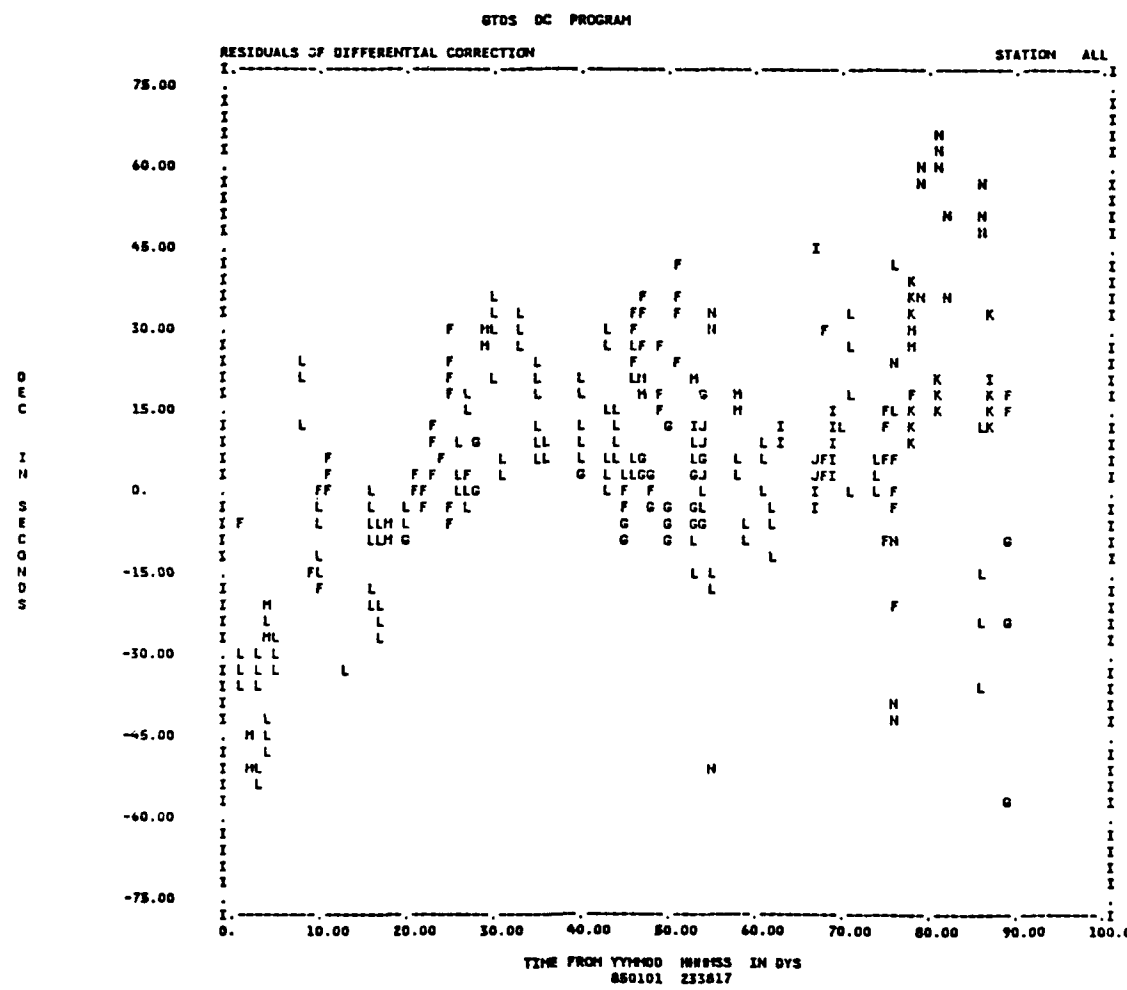


Figure 43. NSSC 13964 DC Residual (Declination)

Table 16. Results of DC for NSSC 13964			
Epoch: Jan 1, 1985, 23 hours, 38 min, 17.903 sec			
Element	A priori Value	Final Value	Standard Deviation
a(km)	26554.300	26554.302	4.37195E-05
e	0.7179000	0.7179169	2.61725E-07
i($^{\circ}$)	63.09000	63.09183	1.02427E-02
Ω ($^{\circ}$)	163.31300	163.31333	1.24113E-02
ω ($^{\circ}$)	279.65000	279.65431	7.33589E-03
M($^{\circ}$)	12.627000	12.627693	2.28709E-03
C_x	1.2000000	1.3425221	0.758E-03
Weighted RMS: 0.92677			
Mean of 1950.0 Coordinates			

Table 17. Residual Plot Key	
Residual Plot Symbol	NORAD Station Number
B	399
D	666
E	369
F	231
G	232
H	233
I	221
J	222
K	223
L	211
M	212
N	213

The percentage of each observation type accepted by the DC is shown in Table 18.

Table 18. Observation Summary by Type for NSSC 13964

Type	Total Number	Number Accepted
Range	131	73 (55%)
Azimuth	131	100 (76%)
Elevation	131	107 (81%)
Range Rate	102	68 (66%)
Right Ascension	501	434 (86%)
Declination	501	474 (94%)

A comparison of Table 16 and Table 4 demonstrates how the use of observation data improved the determination of initial conditions. The standard deviation for the mean semimajor axis improved from a value of 1.67m to a value of 0.0437m.

3.2.1.3 Comparison and Difference Plots

The final values of the Keplerian elements and the solar radiation coefficient indicated in Table 16 were used as initial conditions for an SST prediction. The force model of Table 14 was used to create an ephemeris prediction file of about 250 days. Figures 44-50 are comparison plots of the "NORAD" and "GTDS" predictions for the Keplerian elements. The mean differences and standard deviations after 126 comparisons are shown in Table 19.

Figures 51-58 are the plots of the difference between the "GTDS" predictions and the "NORAD" points for the Keplerian elements. Note that the comparison difference plot for semimajor axis (Figure 51) exhibits none of the resonance period error exhibited by NSSC 9829 using element sets

(Figure 13). The remaining difference plots (Figures 52-58) show no secular trends, with the exception of argument of perigee (Figure 55).

Table 19. Results of Comparisons for NSSC 13964

Element	Mean Difference	Standard Deviation
Semimajor axis (m)	67.695	64.706
Eccentricity	0.76003E-04	0.86377E-04
Inclination ($^{\circ}$)	0.78965E-02	0.82670E-02
Longitude of ascending node ($^{\circ}$)	0.15868E-01	0.10429E-01
Argument of perigee ($^{\circ}$)	0.17679E-01	0.11293E-01
Mean anomaly ($^{\circ}$)	0.19882	0.13963
Radius of perigee (km)	2.0123	2.2880
Radius of apogee (km)	2.0611	2.3298
H	0.11456E-03	0.11290E-03
K	0.19659E-03	0.12057E-03
P	0.17967E-03	0.11745E-03
Q	0.89706E-04	0.78150E-04
Mean longitude ($^{\circ}$)	0.19429	0.13477

The magnitudes of the differences between the SST predictions and the NORAD points are much less for the case where observation data were used. (Compare Table 19 with Table 5.) This clearly demonstrates that the ability of the semianalytical theory to predict dominant motion is enhanced by initialization with observation data.

3.2.2 Simulation of SDP4 with SST for NSSC 13964

An effort was made to account for the errors between the SST predictions and the NORAD mean elements seen for the Molniya orbits. This was accomplished by configuring the SST with the dynamic modelling used in SDP4 and performing a DC over a short interval of observation data for

SV13964 SEMIMAJOR AXIS

MERN DIFFERENCE: 0.67695E-01 SIGMA: 0.64706E-01 AFTER 126 COMPARISONS

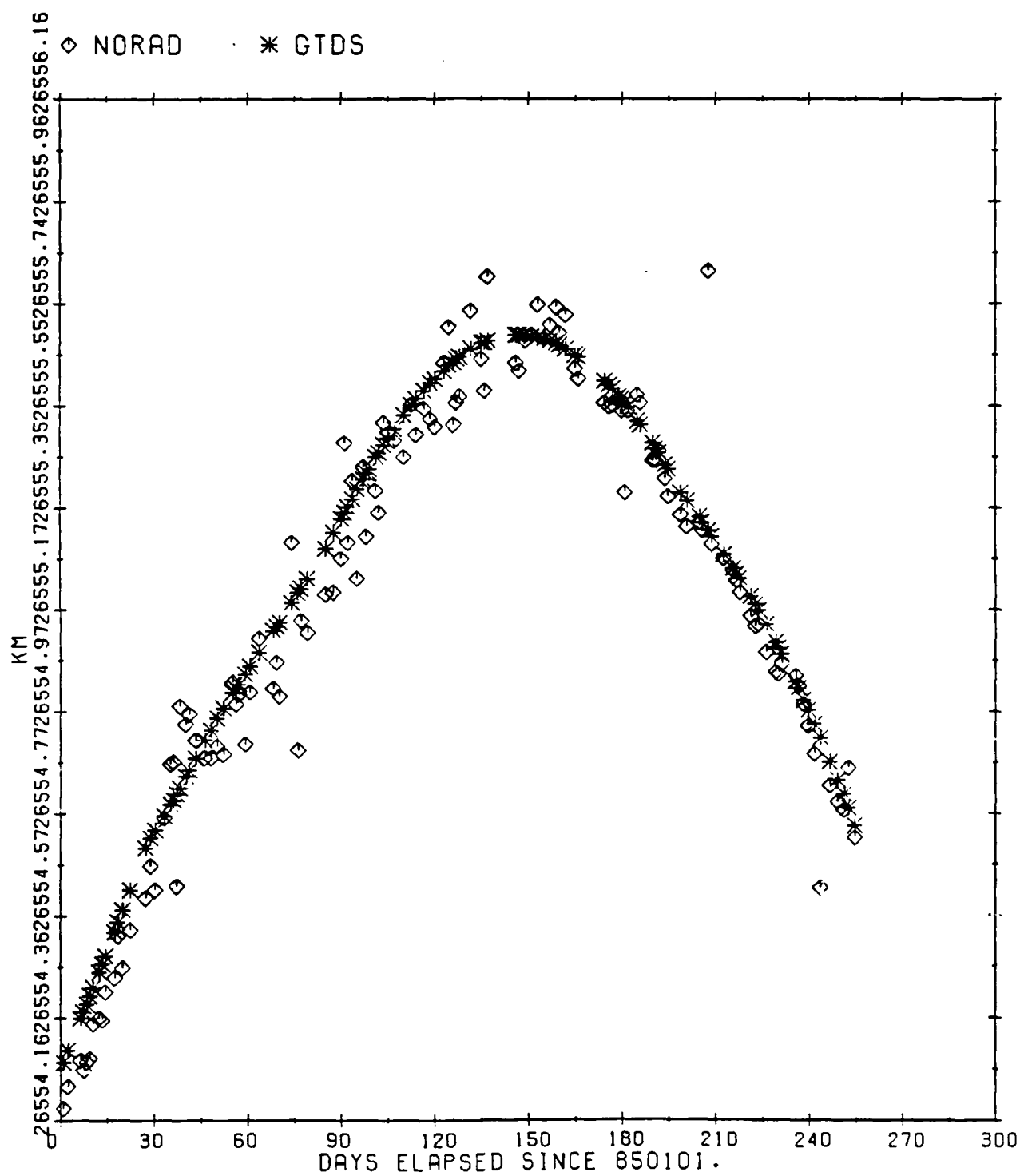


Figure 44. NSSC 13964 Semimajor Axis Comparison

SV13964 ECCENTRICITY

MEAN DIFFERENCE: 0.76003E-04 SIGMA: 0.86377E-04 AFTER 126 COMPARISONS

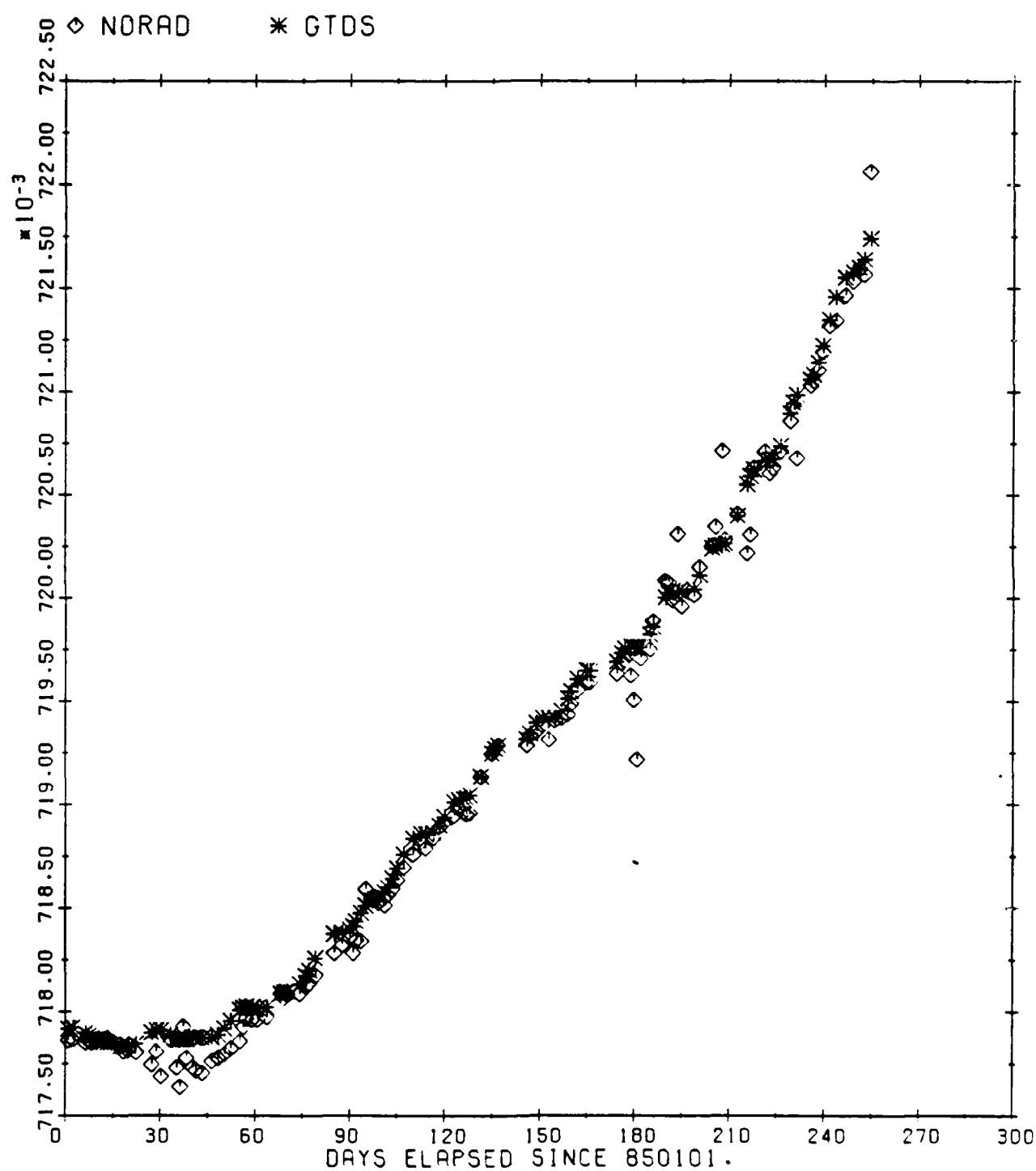


Figure 45. NSSC 13964 Eccentricity Comparison

SV13964 INCLINATION

MEAN DIFFERENCE: 0.78965E-02 SIGMA: 0.82670E-02 AFTER 126 COMPARISONS

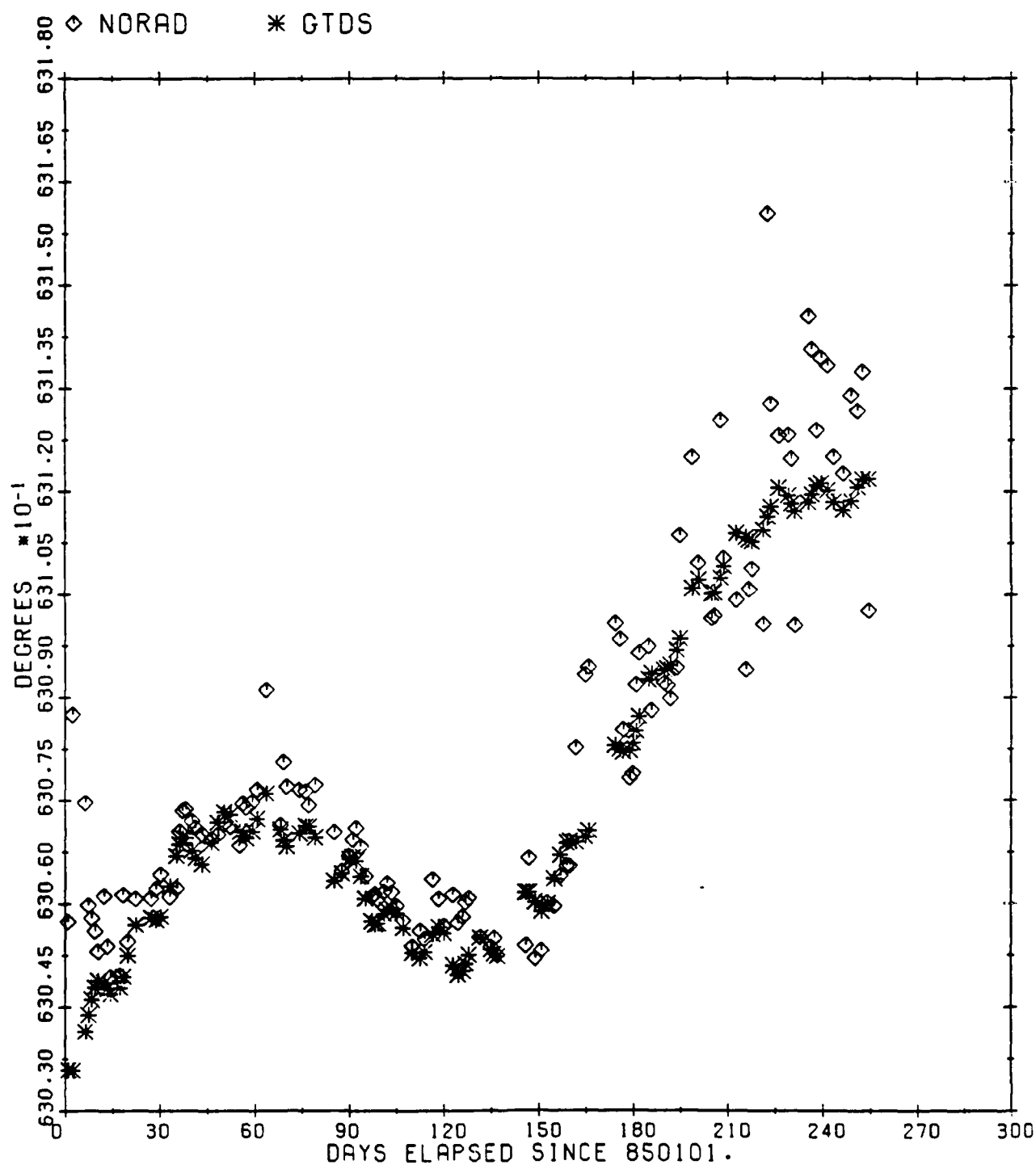


Figure 46. NSSC 13964 Inclination Comparison

SV13964 LONGITUDE OF ASCENDING NODE

MEAN DIFFERENCE: 0.15868E-01 SIGMA: 0.10429E-01 AFTER 126 COMPARISONS

◊ NORAD * GTDS

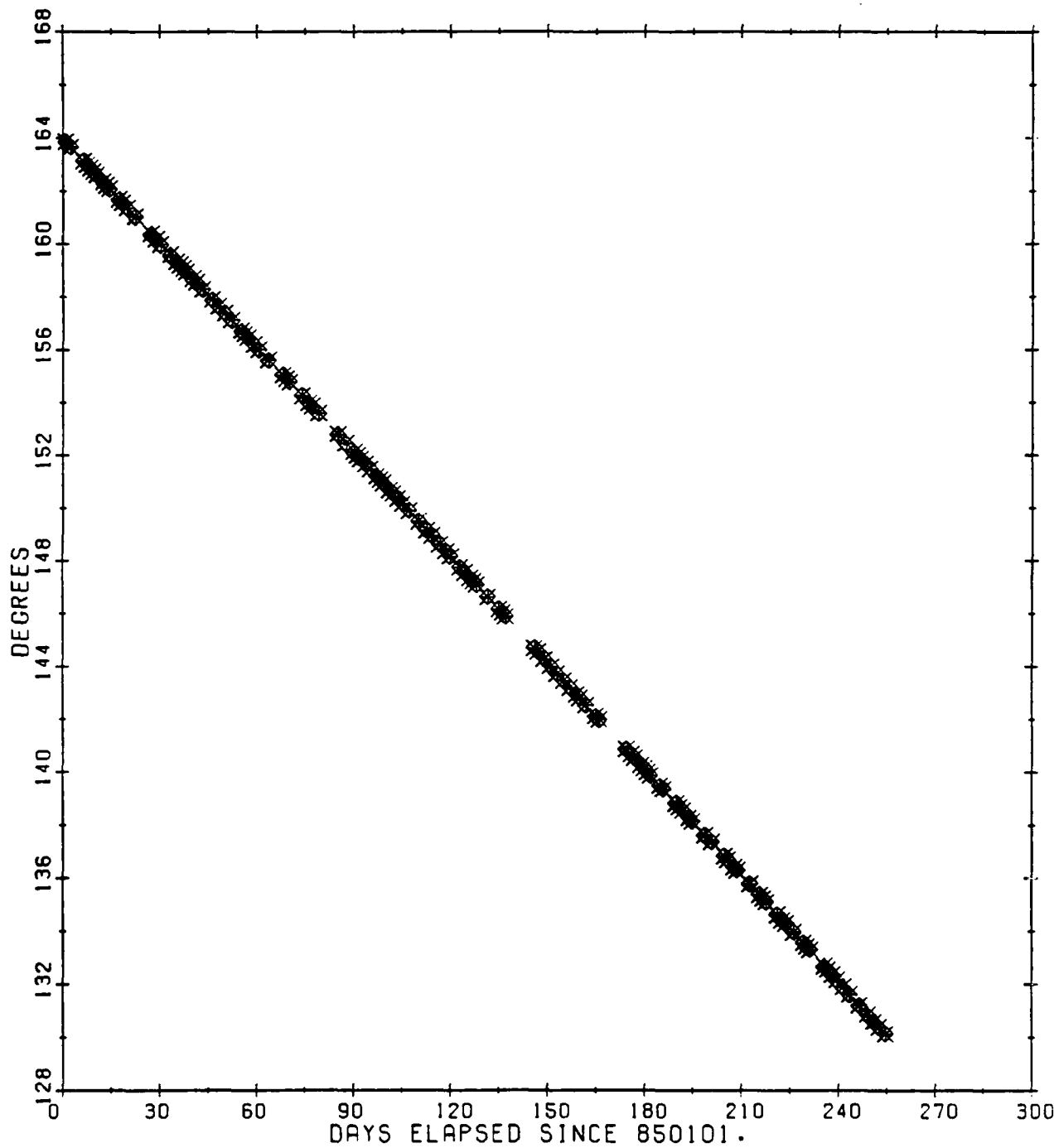


Figure 47. NSSC 13964 Longitude of Ascending Node Comparison

SV13964 ARGUMENT OF PERIGEE

MEAN DIFFERENCE: 0.17679E-01 SIGMA: 0.11293E-01 AFTER 126 COMPARISONS

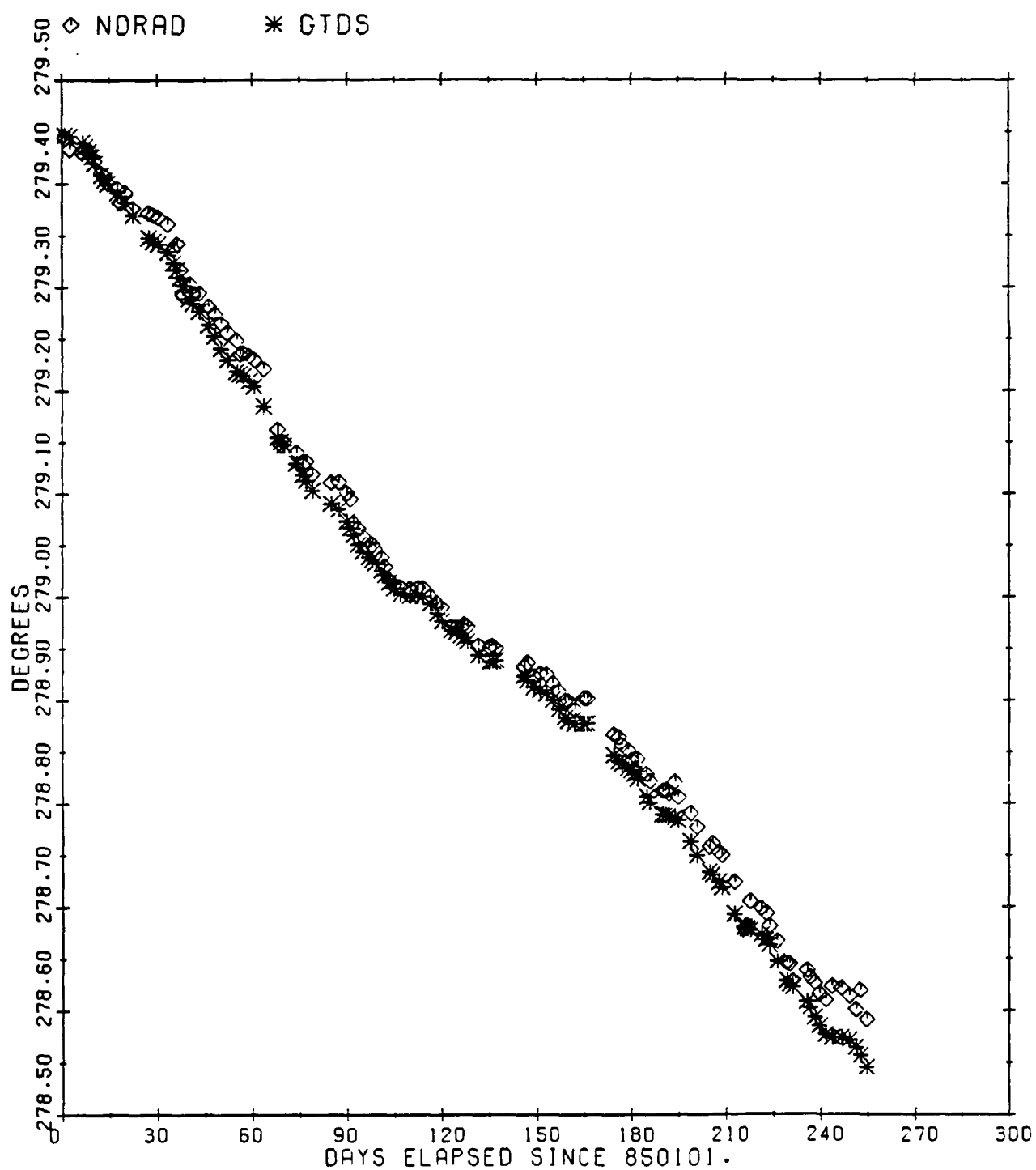


Figure 48. NSSC 13964 Argument of Perigee Comparison

SV13964 RADIUS OF PERIGEE

MEAN DIFFERENCE: 2.0123 SIGMA: 2.2880 AFTER 126 COMPARISONS

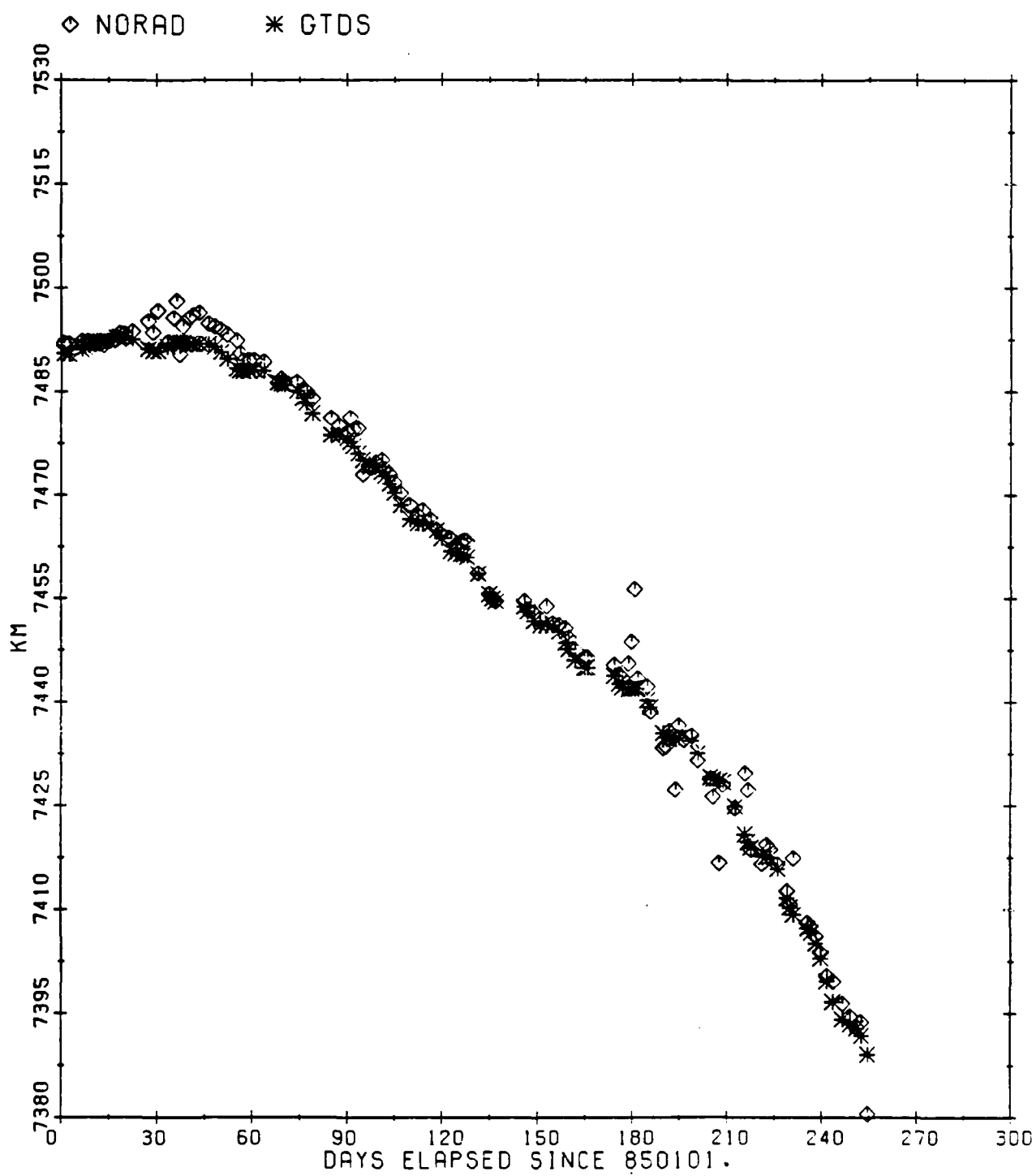


Figure 49. NSSC 13964 Radius of Perigee Comparison

SV13964 RADIUS OF APOGEE

MEAN DIFFERENCE: 2.0611

SIGMA: 2.3298

AFTER 126 COMPARISONS

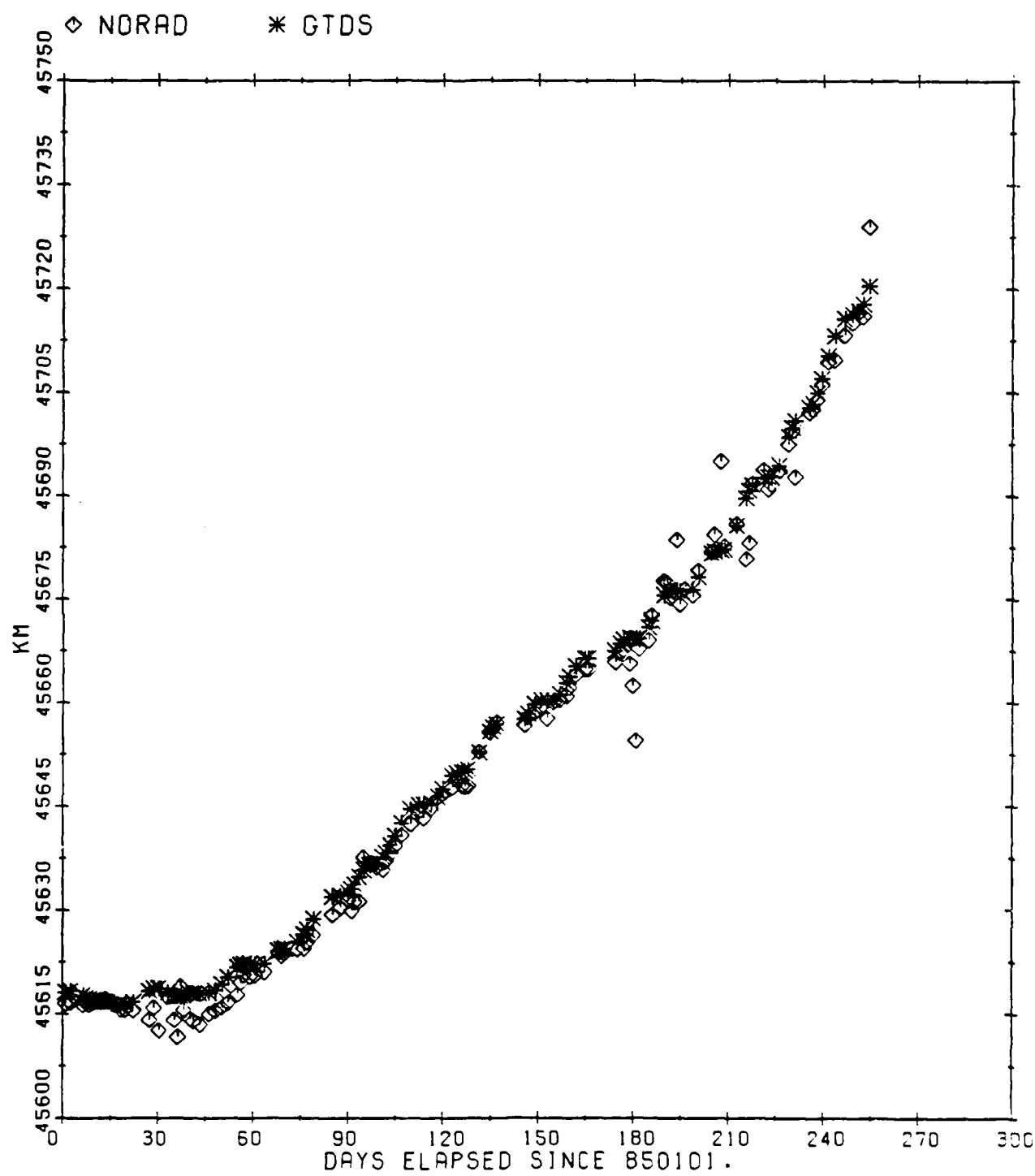


Figure 50. NSSC 13964 Radius of Apogee Comparison

SV13964 SEMIMAJOR AXIS

COMPARISON DIFFERENCE: DELTA = GTDS - NORAD

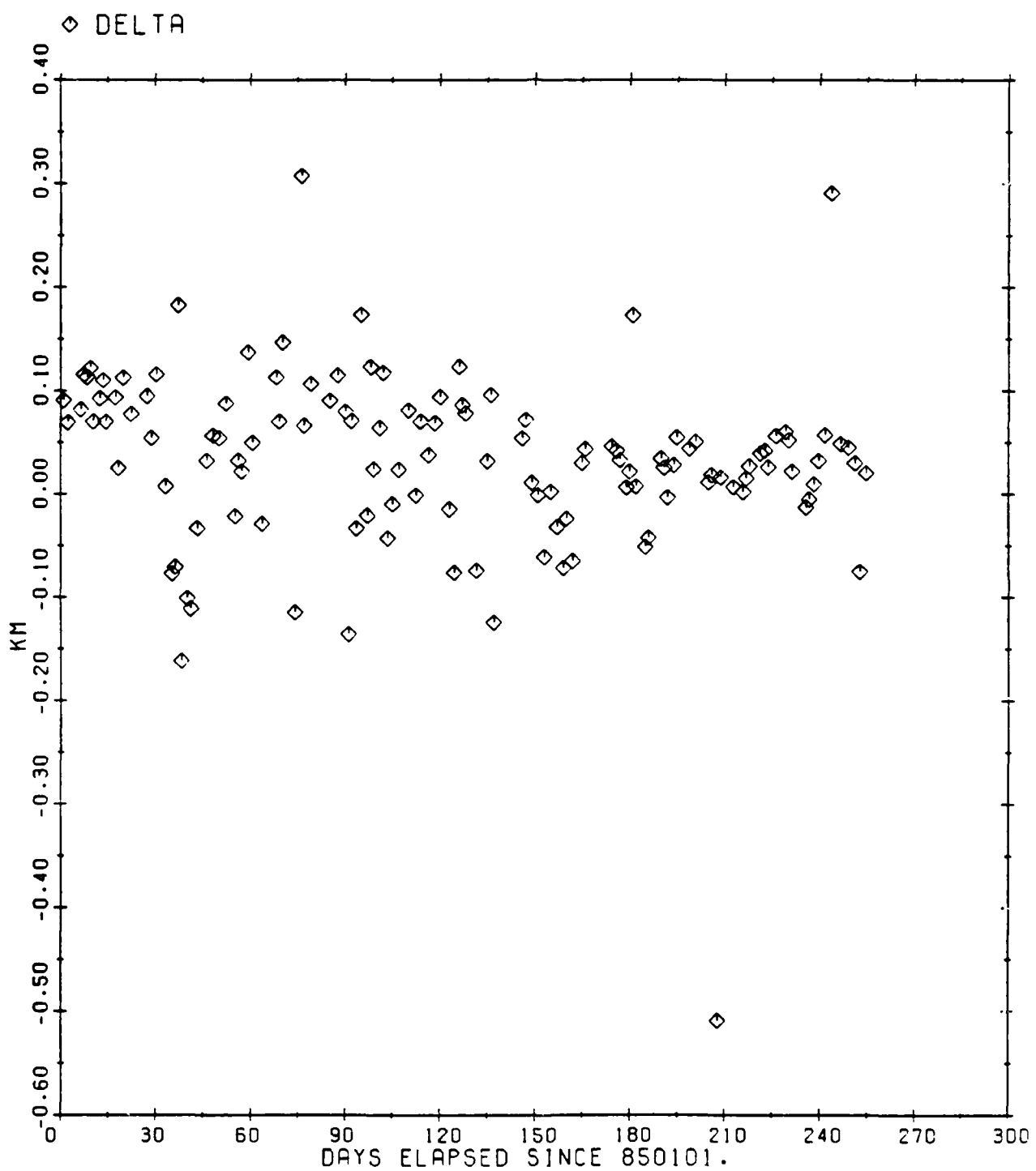


Figure 51. NSSC 13964 Semimajor Axis Difference

SV13964 ECCENTRICITY

COMPARISON DIFFERENCE: DELTA = GTDS - NORAD

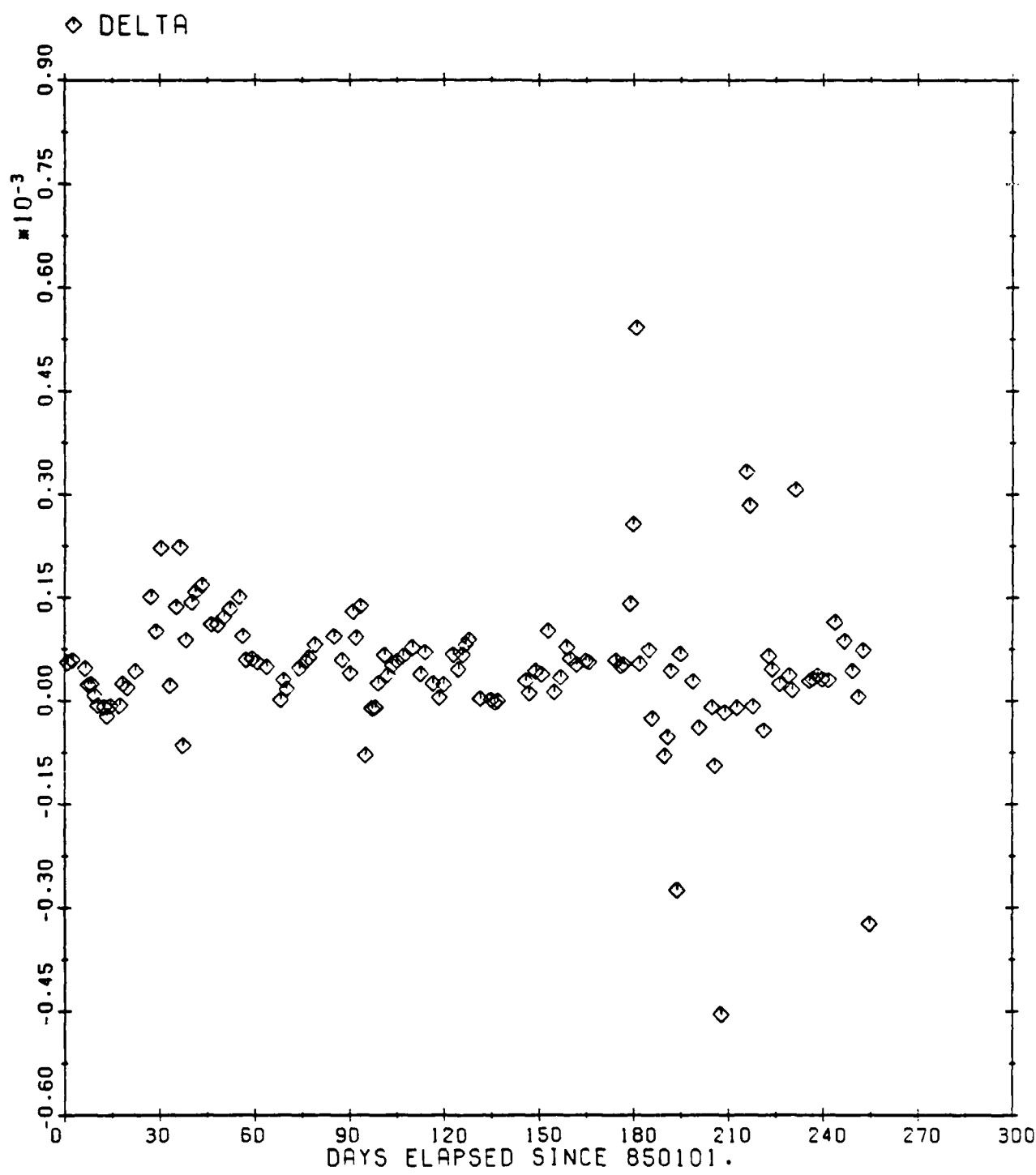


Figure 52. NSSC 13964 Eccentricity Difference

SV13964 INCLINATION

COMPARISON DIFFERENCE: DELTA = GTDS - NORAD

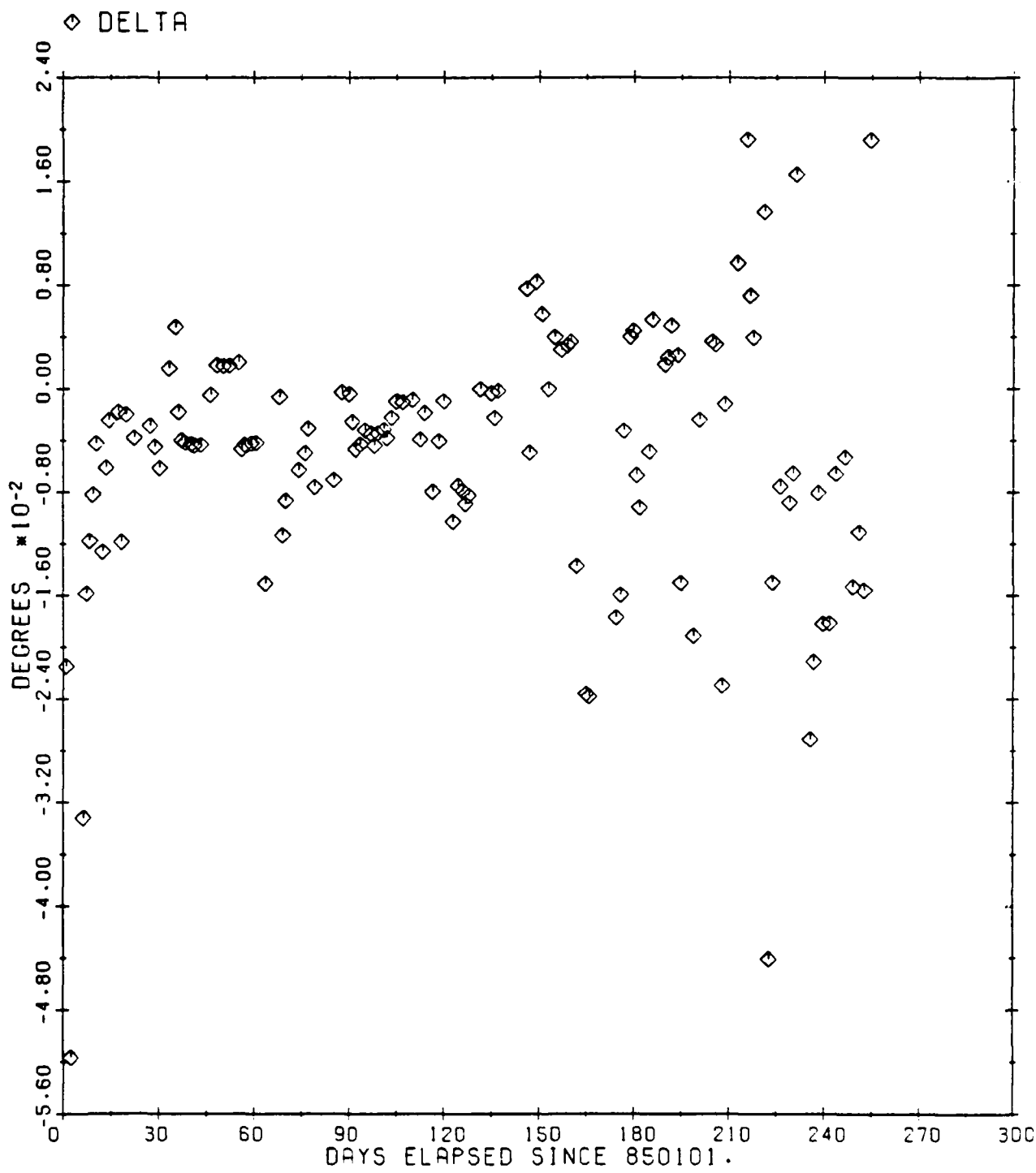


Figure 53. NSSC 13964 Inclination Difference

SV13964 LONGITUDE OF ASCENDING NODE

COMPARISON DIFFERENCE: DELTA = GTDS - NORAD

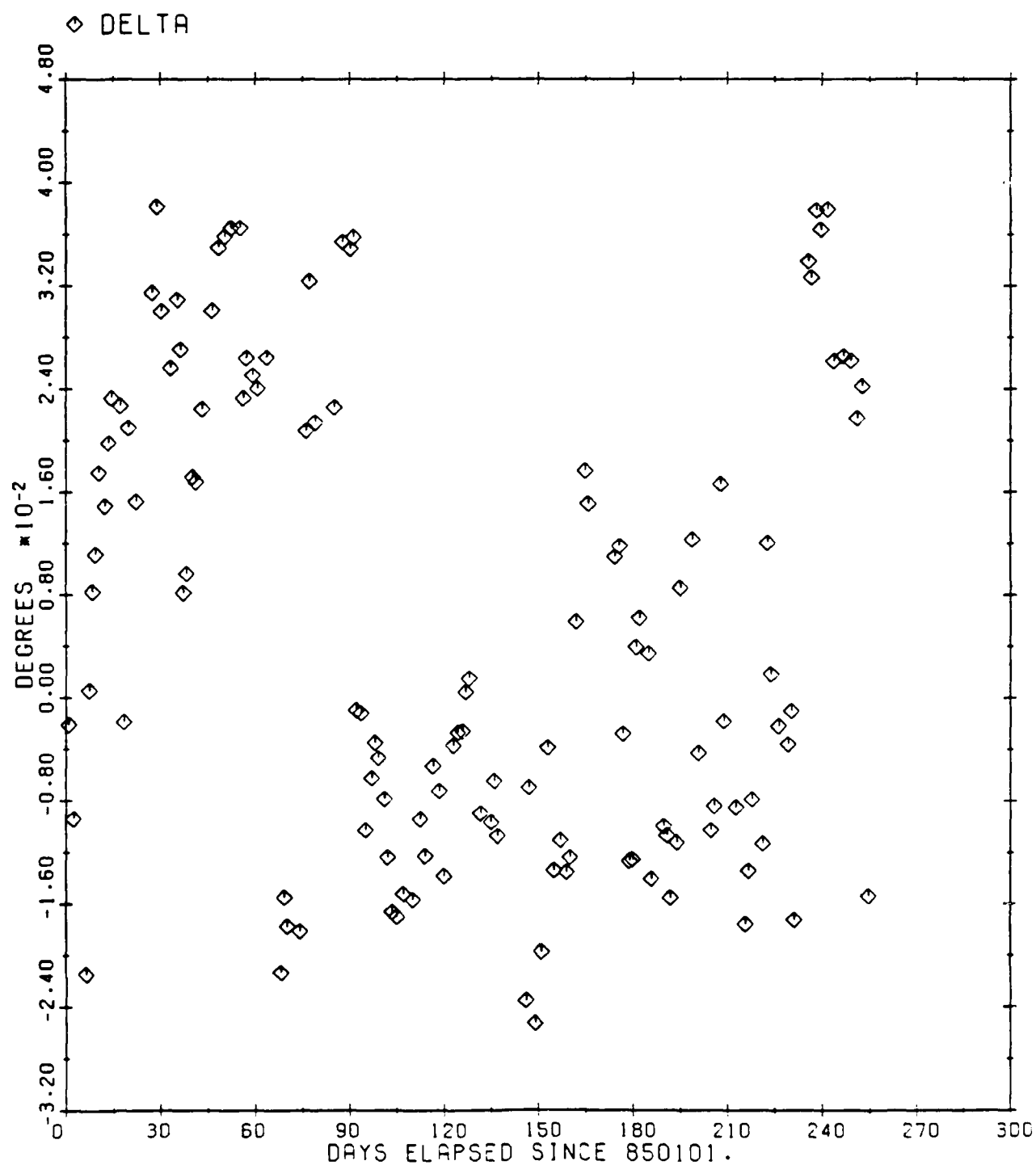


Figure 54. NSSC 13964 Longitude of Ascending Node Difference

SV13964 ARGUMENT OF PERIGEE

COMPARISON DIFFERENCE: DELTA = GTDS - NORAD

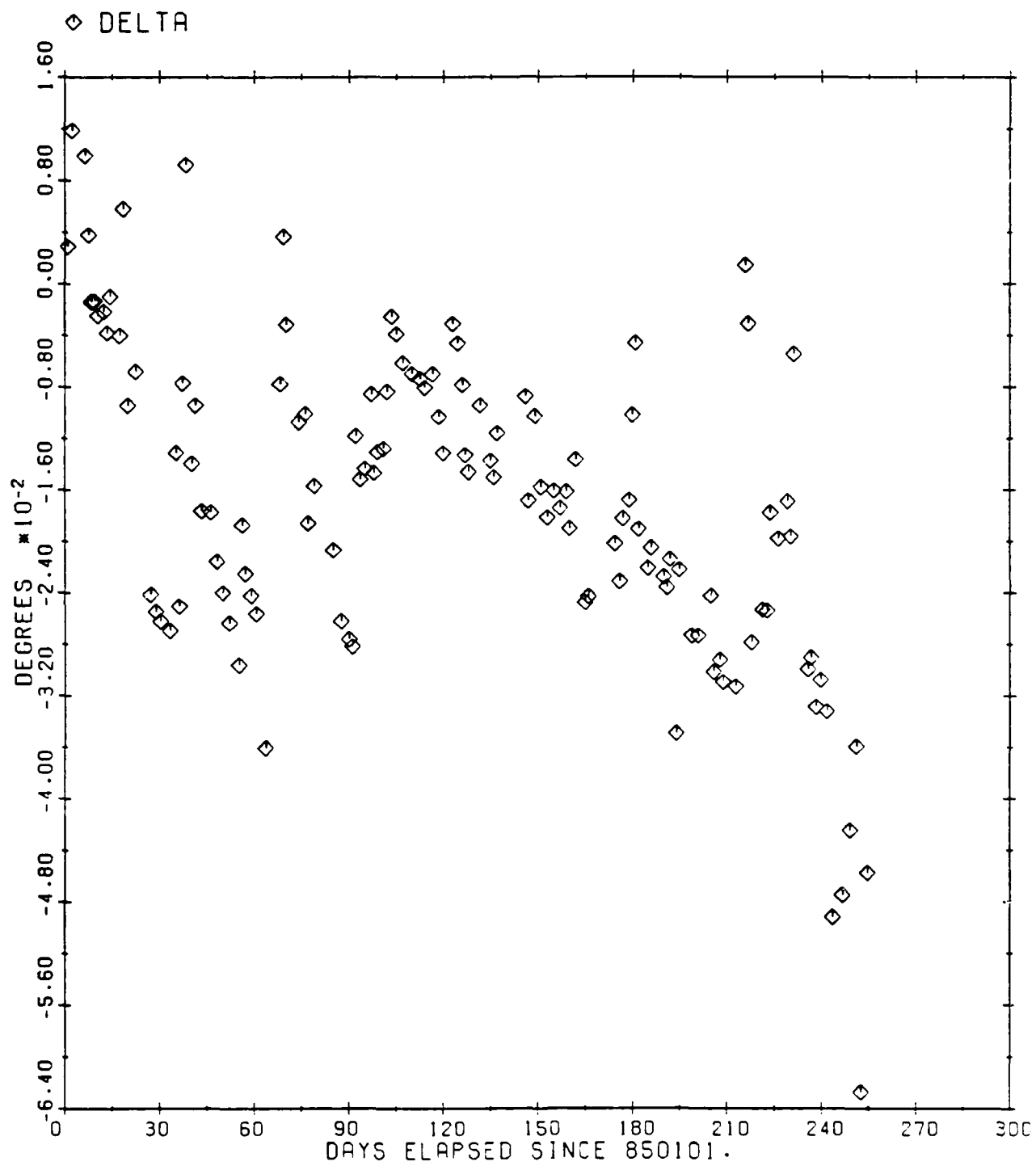


Figure 55. NSSC 13964 Argument of Perigee Difference

SV13964 MEAN ANOMALY

COMPARISON DIFFERENCE: DELTA = GTDS - NORAD

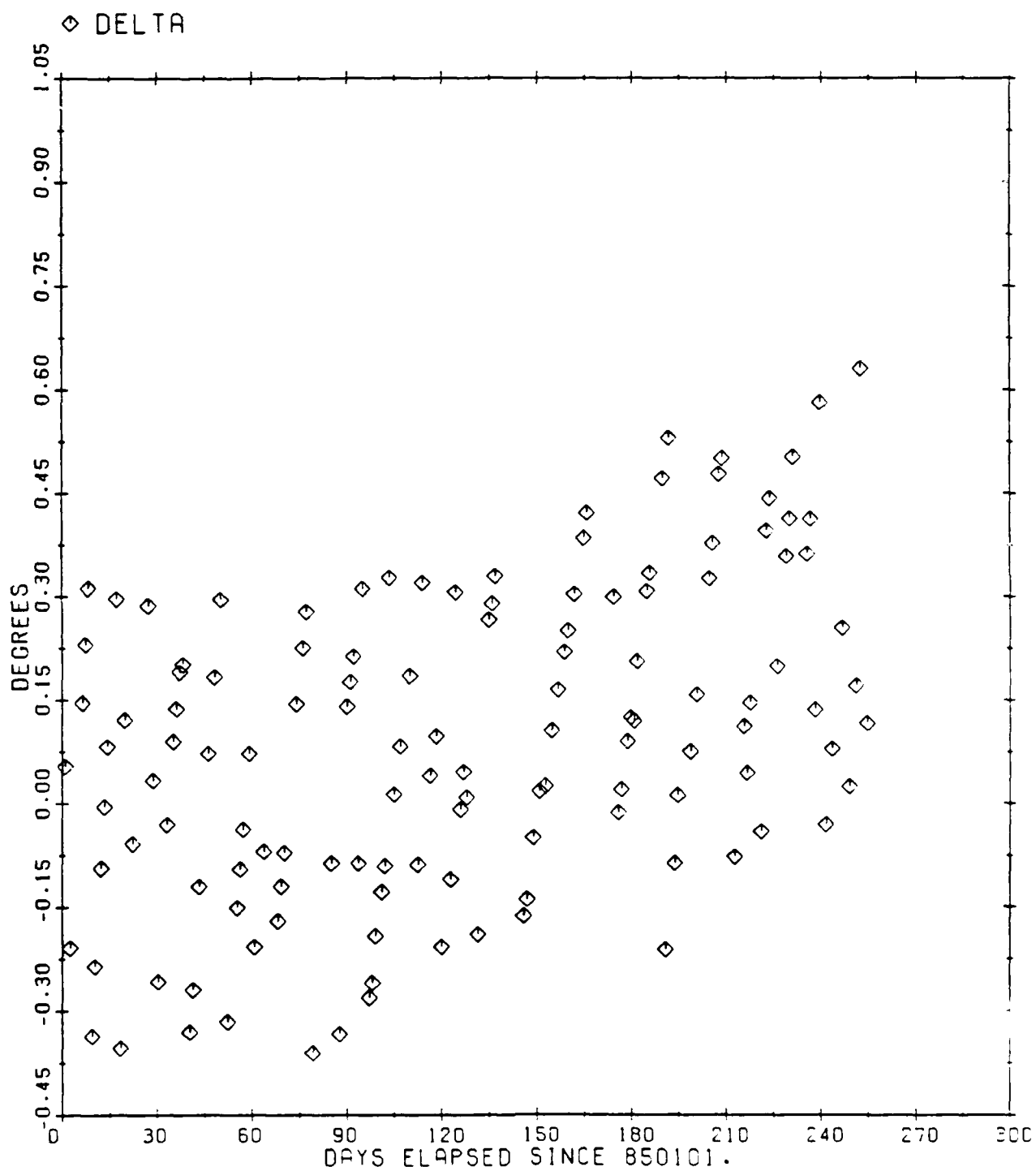


Figure 56. NSSC 13964 Mean Anomaly Difference

SV13964 RADIUS OF PERIGEE

COMPARISON DIFFERENCE: DELTA = GTDS - NORAD

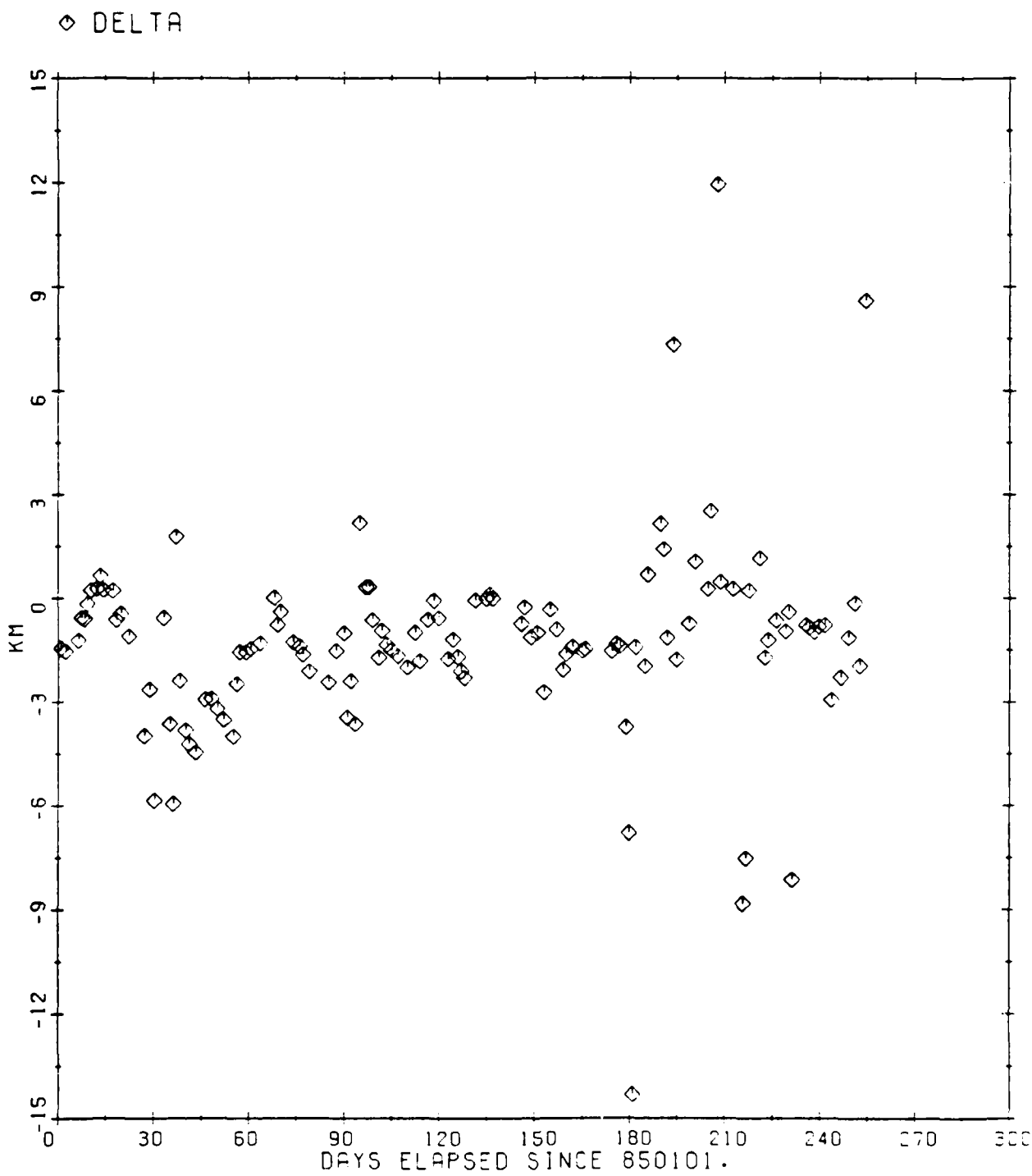


Figure 57. NSSC 13964 Radius of Perigee Difference

SV13964 RADIUS OF APOGEE

COMPARISON DIFFERENCE: DELTA = GTDS - NORAD

◊ DELTA

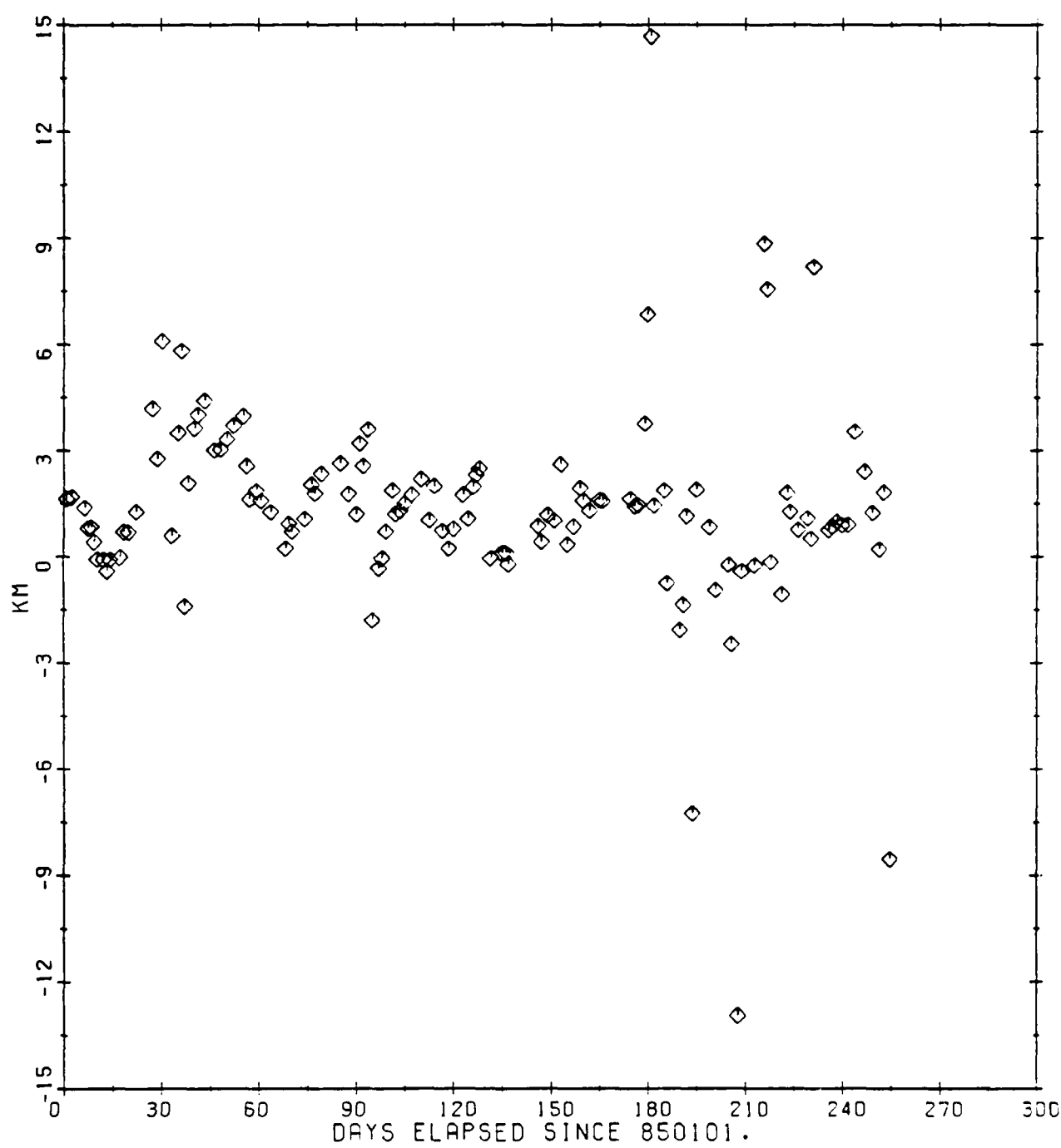


Figure 58. NSSC 13964 Radius of Apogee Difference

NSSC 13964. The resultant initial conditions were used in an "SDP4-simulated" version of SST to create "SDP4-simulated" predictions which were then compared to the fully-modelled SST predictions.

The simulation of SDP4 was accomplished by including in the SST only the dynamic modelling shown in Tables 20 and 21.

Table 20. Mean Force Models in SDP4 Simulation

Zonals: J_2 through J_4 , e^2 , WGS 72 (12x12)

Tesseral Resonance: WGS 72 (12x12), (2,2), (3,2), (5,2),
(4,4), (5,4), e^{20}

Non-Central Bodies:

Moon: $(a/r)^2$, e^2

Sun: $(a/r)^3$, e^3

Drag: off

Solar Pressure: off

Table 21. Short-Periodic Force Models in SDP4 Simulation

Zonals: J_2 only

M-daily Tesseral: off

High-Frequency Tesseral: off

Third-Body: off

J_2^2 : off

Central Body J_2 /M-Daily: off

These models were chosen to simulate the SDP4 dynamics described in [23] and [24]. With this dynamic modelling, the "SDP4-simulated" DC of 20 days of observations for NSSC 13964 resulted in the initial conditions shown in Table 22. Note the final values for mean semimajor axis in Table 22 and Table 16 differ by about 75 meters. Note also the high value of the weighted RMS.

Table 22. Results of the "SDP4-Simulated" DC for NSSC 13964			
Epoch: Jan 1, 1985, 23 hours, 38 min, 17.903 sec			
Element	A priori Value	Final Value	Standard Deviation
a(km)	26554.3000	26554.3768	9.74558E-04
e	0.71790000	0.71787178	1.76389E-06
i(°)	63.0900000	63.0848103	9.71891E-02
Ω(°)	163.313000	163.312091	7.27630E-02
ω(°)	279.650000	279.652677	4.48756E-02
M(°)	12.6270000	12.6445626	1.67609E-02
Weighted RMS: 3.9805			
Mean of 1950.0 Coordinates			

The final values shown in Table 22 were then used to create a 90-day prediction file using the dynamic modelling of Table 20. The first 20 days of prediction (corresponding to the DC fit interval) were compared to the fully-modelled SST predictions. The position and velocity RMS values of the errors in the radial, cross-track, and along-track directions are given in Table 23.

Table 23. Comparison of "SDP4-Simulated" Predictions and Fully-Modelled SST Predictions for NSSC 13964 from 850102 to 850122

Direction	Position RMS (km)	Velocity RMS (km/sec)
Radial	0.15196D+01	0.33271D-03
Cross-Track	0.40188D+01	0.40120D-03
Along-Track	0.25957D+01	0.17127D-03
Total	0.50198D+01	0.54862D-03

An effort was then made to use the fully-modelled version of SST with the shorter fit interval (20 days) to generate initial conditions for the SST predictions. These predictions were then compared to the predictions that resulted from the initialization using the 90-day fit interval. The modelling of Tables 14 and 15 were used along with the converged value for the solar radiation coefficient C_r from Table 16. The same a priori values of the Keplerian elements as Table 16 were used. The results are given in Table 24.

Table 24. Results of SST DC with 20-Day Fit for NSSC 13964

Element	A priori Value	Final Value	Standard Deviation
a (km)	26554.3000	26554.3030	2.24820E-04
e	0.71790000	0.71791564	4.24458E-07
i ($^{\circ}$)	63.0900000	63.0898234	2.41719E-02
Ω ($^{\circ}$)	163.313000	163.314403	1.79993E-02
ω ($^{\circ}$)	279.650000	279.653454	1.11623E-02
M ($^{\circ}$)	12.6270000	12.6279070	4.05857E-02
Weighted RMS: 1.0123			
Mean of 1950.0 Coordinates			

The weighted RMS of 1.0123 from Table 24 compares very favorably with the weighted RMS of 0.92677 from Table 16. Note also that the final values for semimajor axis from Tables 24 and 16 differ by less than 1 meter. These results indicate that satisfactory initial conditions can be determined with the shorter interval of observations.

The final values of the Keplerian elements from Table 24 and the same value of C_r were used to generate a prediction file. The first 20 days of predictions (corresponding to the DC fit interval) were compared to the predictions that resulted from the fully-modelled DC with the 90-day fit interval (Table 16). The position and velocity RMS values of the errors in the radial, cross-track, and along-track directions are given in Table 25.

Table 25. Comparison of SST Predictions (Using 20-Day Fit Interval) and SST Predictions (Using 90-Day Fit Interval) for NSSC 13964 from 850102 to 850122

Direction	Position RMS (km)	Velocity RMS (km/sec)
Radial	0.45229D-01	0.10455D-04
Cross-Track	0.10683D+01	0.11162D-03
Along-Track	0.14532D+00	0.11533D-04
Total	0.10791D+01	0.11270D-03

A comparison of Table 23 and Table 25 demonstrates the effects of reduced dynamic modelling for highly eccentric orbits. The enhanced dynamic modelling in SST resulted in much smaller errors.

The next effort was to evaluate the predictions beyond the fit interval. When the final values of Table 24 were used to generate a prediction in the 850122 to 850212 interval, results were very good, as seen in Table 26.

Table 26. Comparison of SST Predictions (Using 20-Day Fit Interval) and SST Predictions (Using 90-Day Fit Interval) for NSSC 13964 from 850122 to 850212

Direction	Position RMS (km)	Velocity RMS (km/sec)
Radial	0.13058D+00	0.17235D-04
Cross-Track	0.11305D+01	0.78288D-04
Along-Track	0.73424D-01	0.59191D-05
Total	0.11404D+01	0.80380D-04

A comparison of the radial and along-track errors in Tables 25 and 26 demonstrates that position errors beyond the fit interval very closely match the position errors calculated for the fit interval.

Figures 59 through 61 show the radial, cross-track, and along-track errors for the predictions during the DC fit interval. Figures 62 through 64 show the prediction errors for the following 20 days. Each of these figures show two apparent curves because the 1/4 day comparison interval is approximately commensurate with the 12-hr orbital period.

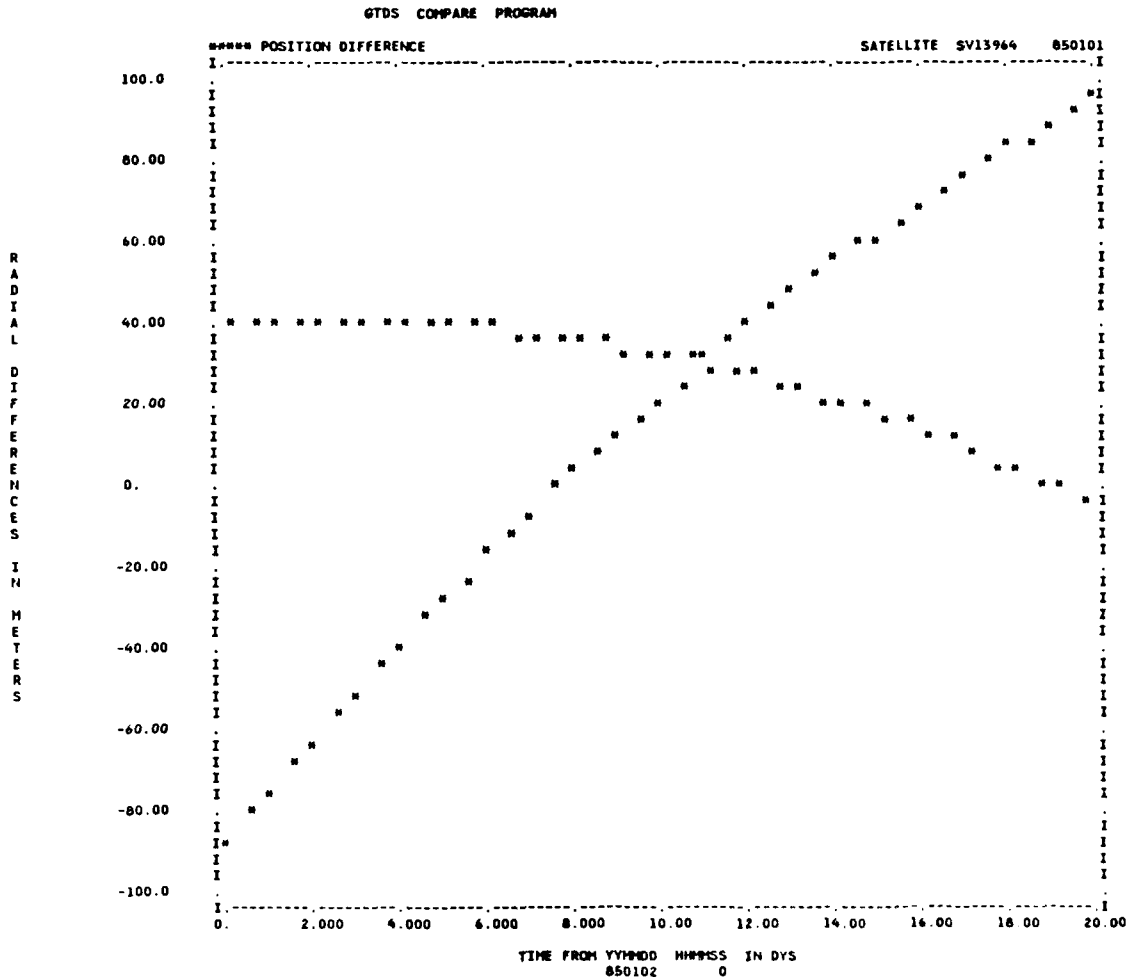


Figure 59. NSSC 13964 Radial Difference

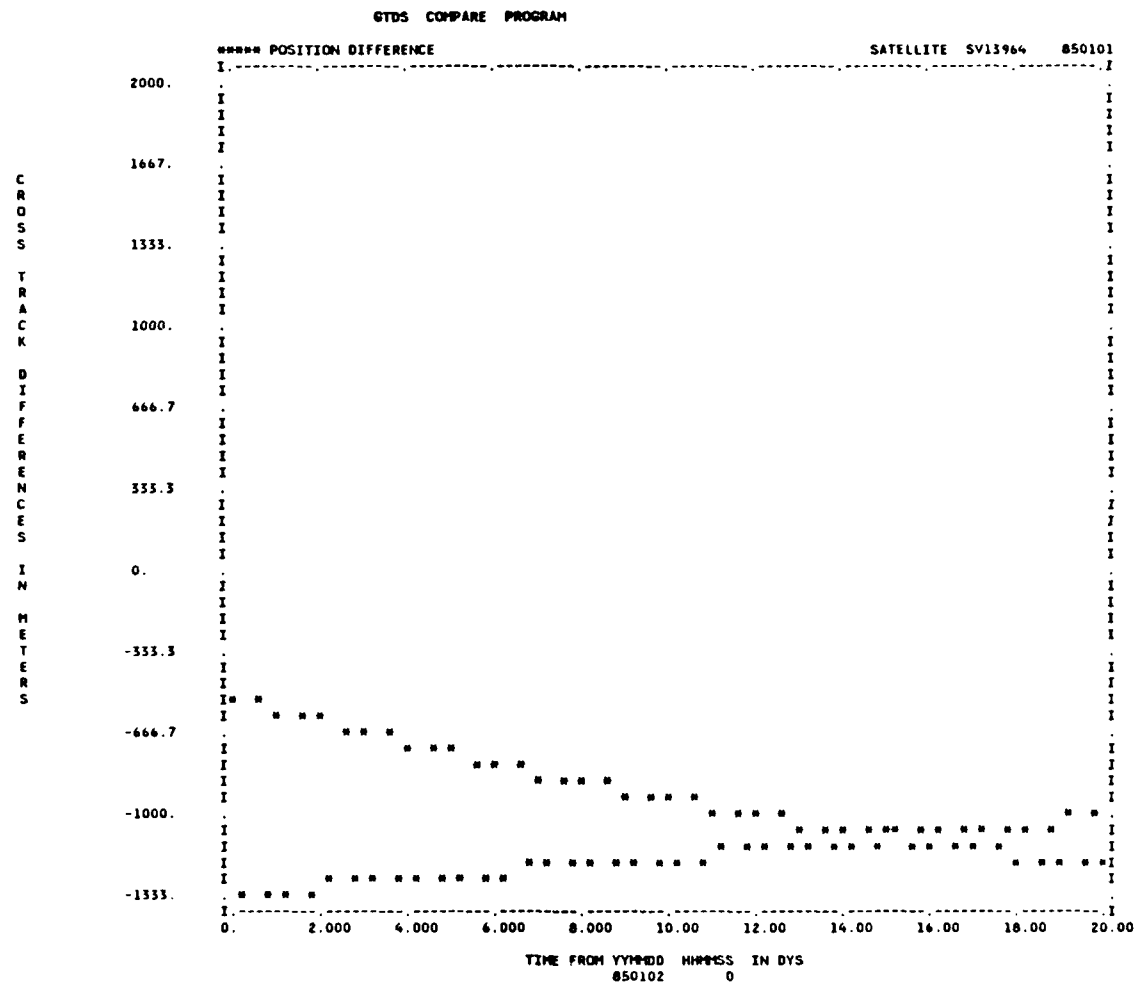


Figure 60. NSSC 13964 Cross-Track Differences

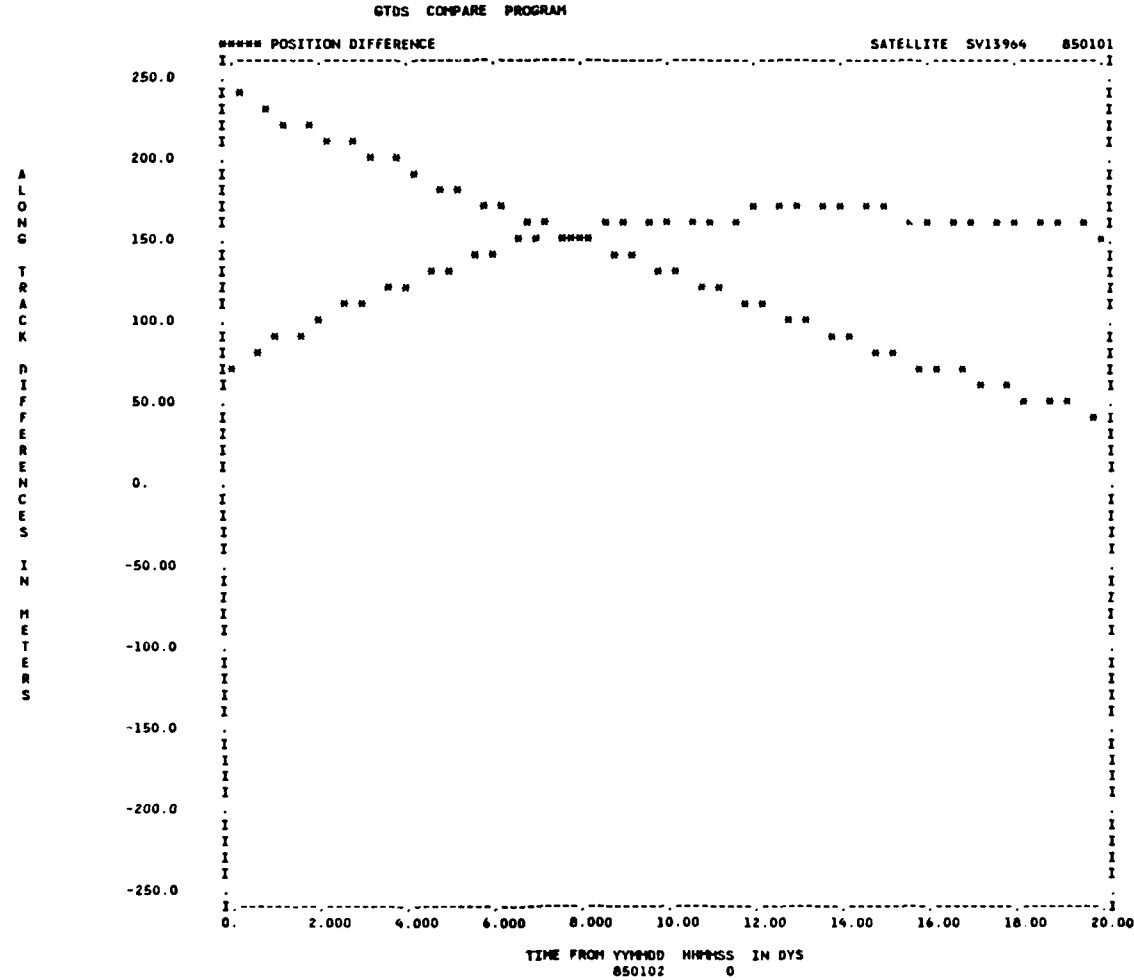


Figure 61. NSSC 13964 Along-Track Differences

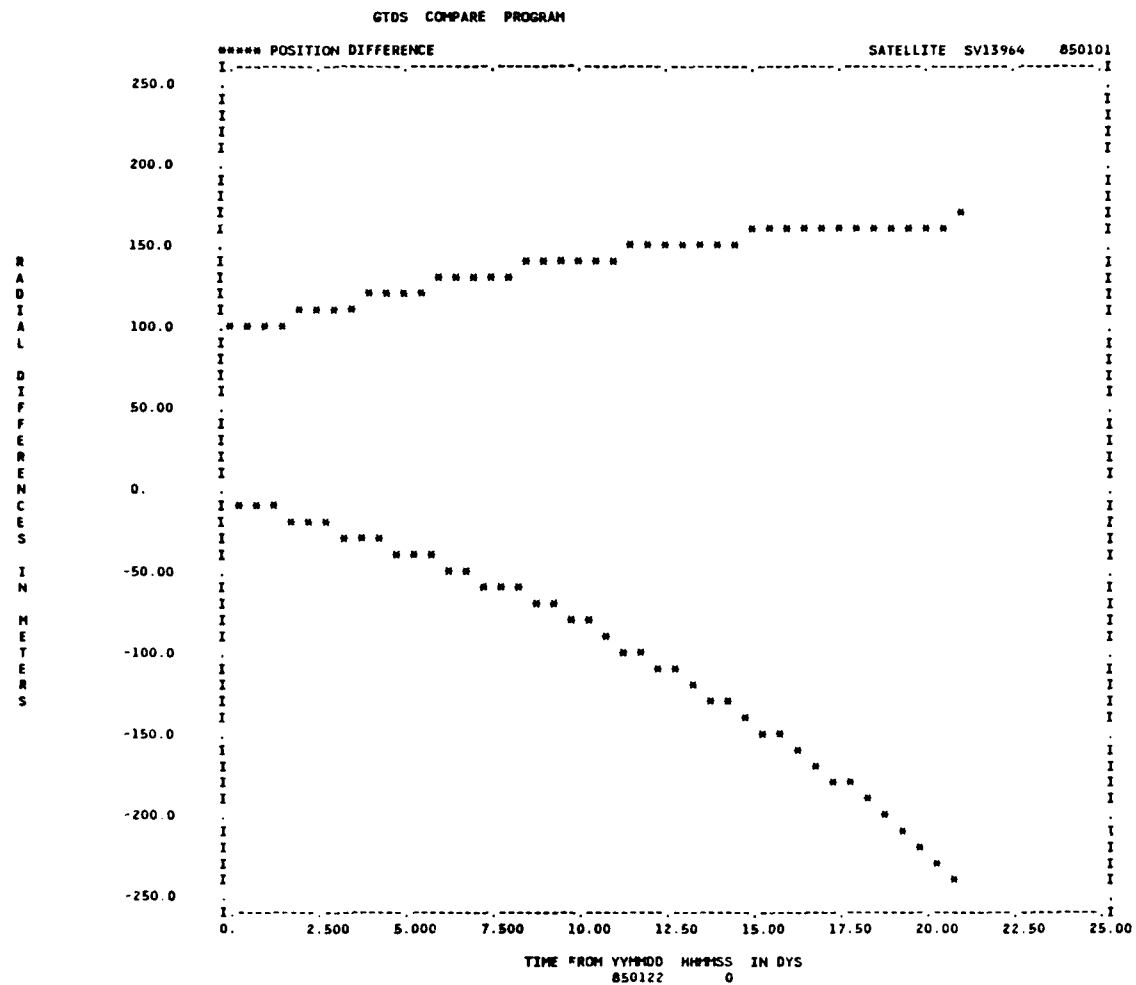


Figure 62. NSSC 13964 Radial Differences

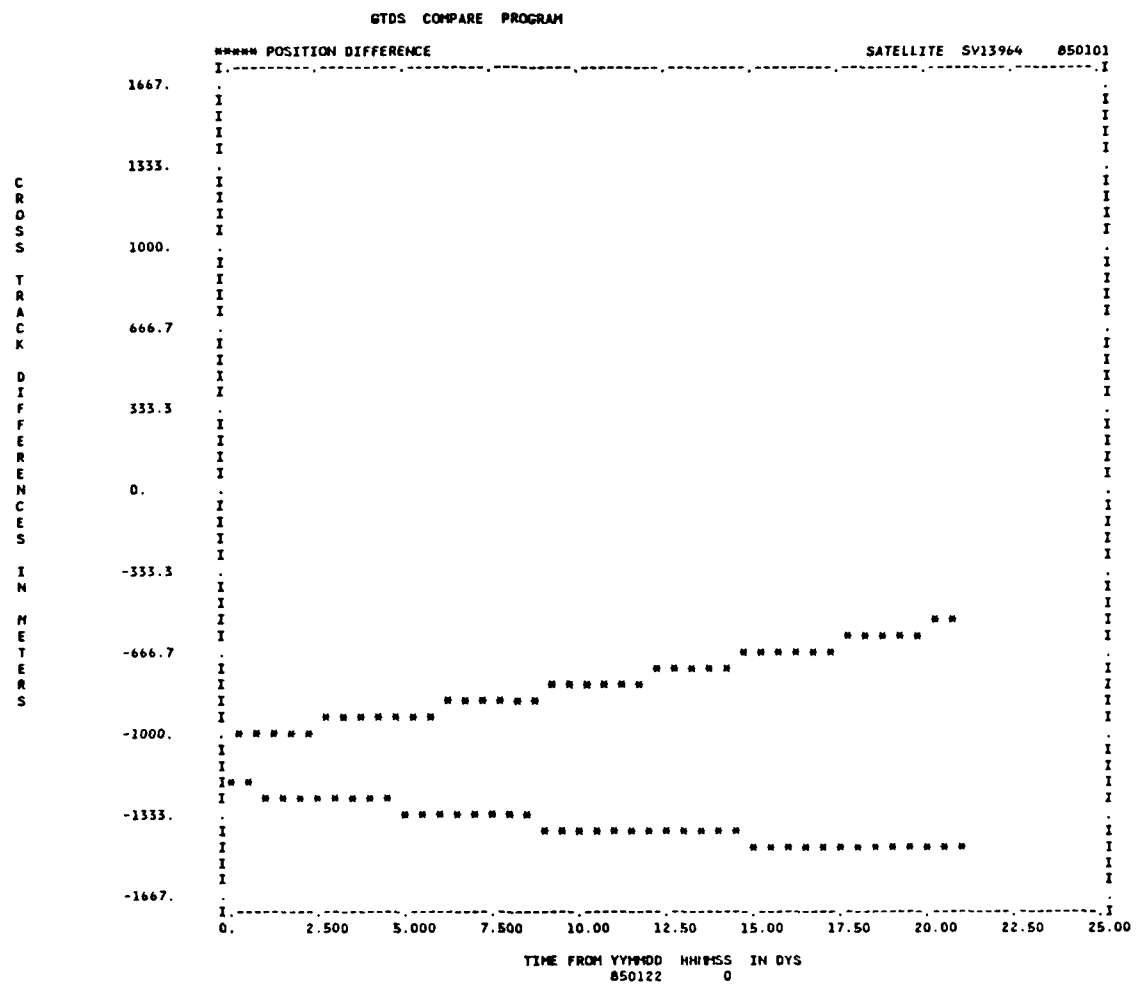


Figure 63. NSSC 13964 Cross-Track Differences

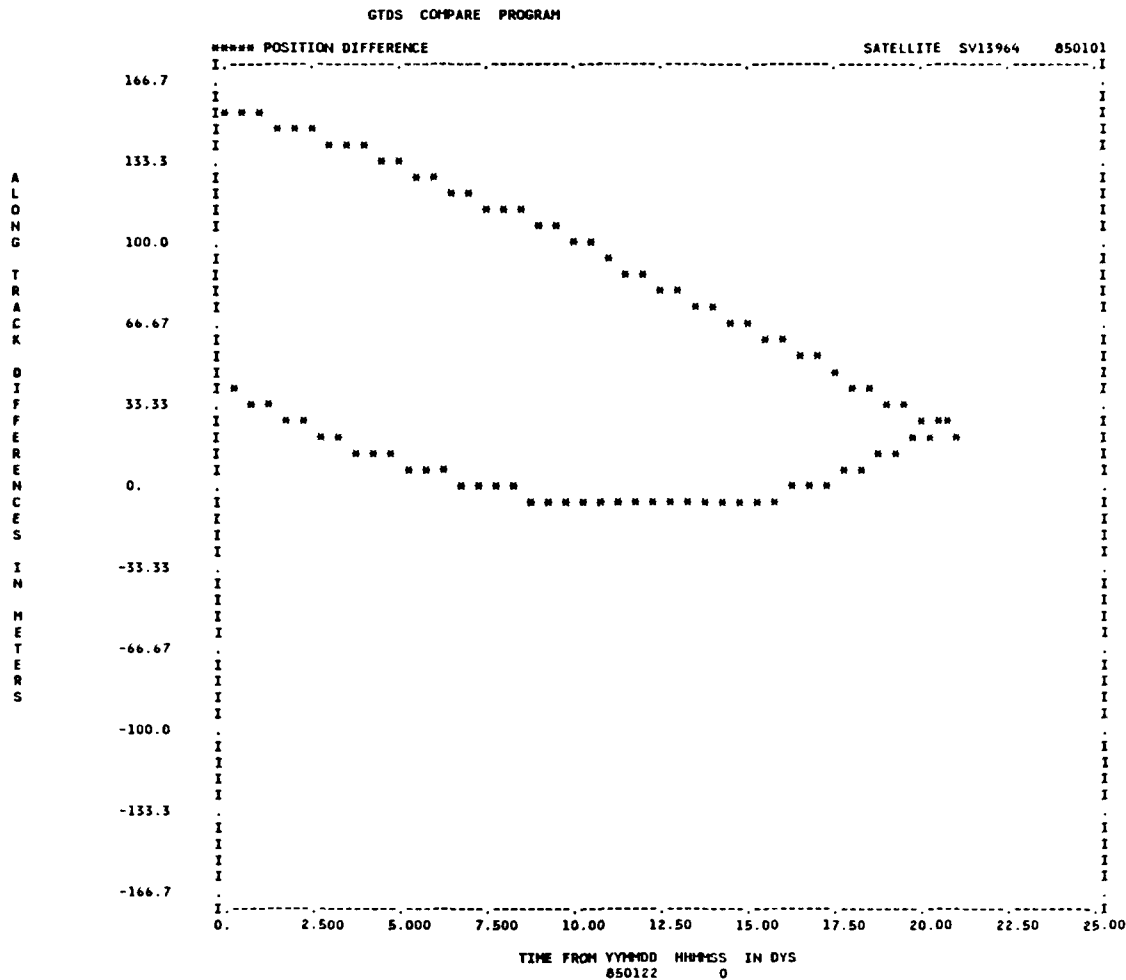


Figure 64. NSSC 13964 Along-Track Differences

CHAPTER 4

CONCLUSIONS AND RECOMMENDATIONS

4.1 CONCLUSIONS

The primary objective of this thesis was to test the semianalytical satellite theory as implemented in the Charles Stark Draper Laboratory version of the Goddard Trajectory Determination System against long arcs of real data of highly eccentric orbits. The real data consisted of a 9-year arc of NORAD element sets for NSSC 9829, the Soviet Molniya 2-17 spacecraft; an 18-month arc of element sets for NSSC 14095, the ESA Exosat; and an 18-month arc of NORAD observations and element sets for NSSC 13964, the Soviet Molniya 1-57 spacecraft.

An introductory chapter reviewed the uses of elliptical orbits and the need for long-term predictions. It also reviewed the application of artificial satellite theory to elliptical orbits, including a summary of the previous applications of satellite theory to highly elliptical orbits.

The overall test methodology involved four main steps:

1. Pre-processing NORAD data
2. Determining an initial state using an SST DC

3. Generating an SST prediction file

4. Evaluating the SST prediction

For NSSC 9829, the Soviet Molniya 2-17, the usage of element sets resulted in an initial vehicle state with a weighted RMS of 0.2893 (Table 4). Best results were obtained using a 6x6 field with GEM 9 coefficients. This initial state was propagated about 2330 days in an SST process to create a 9-year arc of predictions which were compared to the NORAD mean elements. The slowly varying Keplerian element histories and the mean anomaly difference plot clearly demonstrate the ability of the semianalytic theory to predict the dominant motion. Difference plots for semimajor axis exhibited a frequency very similar to the semimajor axis resonance period. Efforts to include an 8x8 field with GEM 9 coefficients resulted in a very unsatisfactory fit (a weighted RMS of 2.071). Exhaustive testing then validated the SST models with the 8x8 field.

Actual observation data was available for NSSC 13964, the Soviet Molniya 1-57. This data was pre-processed to determine the initial state (including the solar radiation coefficient C_r) and resulted in a much improved weighted RMS of 0.92677 (Table 16, with the uncertainties of Tables 12 and 13). These initial conditions were used to generate an SST prediction of about 250 days. Comparison and difference plots exhibited a significant improvement over the NSSC 9829 case as shown in Table 27.

Table 27. Comparison of Prediction Results
Using Element Sets and Observations

Element	NSSC 9829 Mean Difference	NSSC 13964 Mean Difference
a(m)	250.46	67.695
e	0.22437E-03	0.76003E-04
i(°)	0.33941E-01	0.78965E-02
Ω(°)	0.22964	0.15868E-01
w(°)	0.11699	0.17679E-01
M(°)	1.0960	0.19882

The force models used in SDP4, actual observations, and short fit span were included in an SST DC to create "SDP4-simulated" predictions. It was demonstrated that much shorter intervals of observations (20 days) could be used to initialize the SST predictions.

For the Exosat orbit the mean difference between the NORAD and SST predictions for semimajor axis was approximately 77 kilometers over the 250 days of the comparison interval. The mean differences for the eccentricity, inclination, and argument of perigee were 0.0013, 0.102°, and 0.124°, respectively.

This study has shown that the semianalytical theory results in very satisfactory predictions for orbits of high eccentricity. For Molniya-type orbits, the results obtained when using actual observational data were superior to the results obtained when using element sets. For orbits of even higher eccentricity, the SST results were still very satisfactory.

4.2 FUTURE WORK

The use of actual NORAD observations significantly improved the weighted RMS of the differential correction. But there were only about 160 days of element data beyond the fit interval for NSSC 13964 to make comparisons. A longer arc (through 1986) of element sets would permit more meaningful comparisons. Specifically, absence of secular drift in a difference plot for the semimajor axis would confirm that the 8x8 tesseral field was sufficient for long-term predictions of Molniya orbits. Difference plots for a longer interval would also determine if the trends in longitude of ascending node and argument of perigee (Figures 54 and 55) were secular or periodic.

The orbits of the spacecraft in this study were chosen so that the perigee remained outside the main portion of the atmosphere. Thus the drag effects were very slight and the period remained constant. This enabled a single tesseral resonance modelling to remain valid over the entire prediction span.

For some orbits, the lunar-solar perturbations hold the perigee height in the 200 to 350 km range. (An example is NSSC 10723, the International Ultraviolet Explorer rocket body.) The orbit is being continually perturbed by drag and the orbital period decreases significantly over long periods of time. Thus the software modelling for the tesseral geopotential harmonic resonance would have to be variable over the prediction interval, or several shorter intervals could be carefully "piece-mealed" together.

The accurate calculation of drag effects for this type of orbit is also complicated by the long-term changes in atmospheric density. Software modelling of drag would probably require a "smoothed" modelling of density over the solar cycle. Long period variations in both the solar activity and the geomagnetic index should be considered.

Extensions to SDP4 analysis to tie down the particular source of mismodelling which makes the major contribution to error should be considered.

The analysis of the Exosat orbit was based on real data in the form of NORAD element sets. Preliminary analysis of Exosat using observation data has proven unsatisfactory probably due to the sparseness of the data. Long arcs of ESA observation data (with the appropriate error statistics and station locations) could be combined with NORAD observational data. This would probably provide more accuracy in the same manner that NORAD observations improved the Molniya predictions.

Alternatively, we note that our interest in the EXOSAT was motivated by the desire to test the SST for an orbit with an eccentricity much greater than a Molniya. However, the extreme altitude associated with most of the EXOSAT orbit limits the available observation data. Perhaps it would be desirable to choose an orbit with a smaller maximum altitude for this test. The orbits of Elektron 2 and 4 ($e \approx .8$), COS-B ($e \approx .85$), and ISEE1/2 ($e \approx .91$) should be considered in this context.

APPENDIX A

SOURCE CODE FOR UTILITIES

The following pages contain the IBM FORTRAN source code for the utilities used in this study. Listings are available for:

ADCEDIT

RUNADC

SDP4

RDORB1

PLOTTER

RUNADCOB

ASTRON

PRENUT

```
C      PROGRAM      ADCEDIT
C
C
C
C      *****
C      FUNCTION
C      *****
C
C
C
C      This program creates a control deck and a data deck to be used in
C      a CSDL PLOT4B plotting program. It can be used to visually edit
C      NORAD bevel vector data.
C
C
C
C      INPUT *****
C
C          FILE 1      NORAD bevel vector element sets.
C
C      OUTPUT *****
C
C          FILE 40     PLOT4B control deck.
C
C          FILE 41     PLOT4B data set.
C
C      SUBROUTINES CALLED *****
C
C          none
C
C
C          *****
C          USAGE
C          *****
C
C
C      File 1 data, the NORAD bevel vector element sets, can be no more
C      than 2000 lines, i.e., 1000 element sets. After creating the PLOT
C      4B control deck, change all occurrences of 'YR' to the year of
C      the desired graph.
C
C      Invoke the PLOT 4B program by entering the command
C
C      'ADC-----.EDIT.PLOT.FORM IDENT(ADC-----.EDIT.PLOT)'
C
C
C***** HISTORY *****
C
C
C
C      VERSION: September 1986
C              Fortran program for the IBM 3081 and 3033.
C
C      ANALYSIS
```

```

C      Martin E. Fieger, Capt, USAF      AFIT / MIT
C
C      PROGRAMMER
C      Martin E. Fieger, Capt, USAF      AFIT / MIT
C
C
C
C
C***** DECLARATIONS *****
C
C
C
IMPLICIT      DOUBLE PRECISION (A-H,O-Z)
C
C
C      Character Variables *****
C
C      none
C
C      Dimensions *****
C
DIMENSION      ELEM (10000,10)
C
C      Data statements *****
C
C      none
C
C***** BEGIN PROGRAM *****
C
C      Set counter to zero.
C
NUMOBS      =      0
C
C      Read in a new mean element set.
C
100 CONTINUE
C
READ  (1,1000,END=200) NUMSV, DATE, XNDT2, XNDD6,
*           IEXP, BSTAR, IBEXP, XINCL, XNODE, EO, OMEGA,
*           XMO, XNO
C
C      Calculate real values.
C
XNDD6      =      XNDD6 * (10.0D0 ** IEXP)
BSTAR      =      BSTAR * (10.0D0 ** IBEXP)
C
C      Increment counter.
C
NUMOBS      =      NUMOBS + 1
C
C      Store data in array ELEM.
C
ELEM (NUMOBS,1)      =      DATE

```

```

ELEM (NUMOBS,2) = XNDT2
ELEM (NUMOBS,3) = XNDD6
ELEM (NUMOBS,4) = BSTAR
ELEM (NUMOBS,5) = XINCL
ELEM (NUMOBS,6) = XNODE
ELEM (NUMOBS,7) = EO
ELEM (NUMOBS,8) = OMEGA
ELEM (NUMOBS,9) = XMO
ELEM (NUMOBS,10) = XNO

C
C      GO TO 100
C
C      *****
C      PLOT4B DATA DECK
C      *****
C
C      Write the PLOT4B data deck.
C
C      200 CONTINUE
C
C      DO 300 I=1,NUMOBS
C
C      WRITE (41,2000) ELEM (I,1), ELEM (I,2), ELEM (I,3), ELEM (I,4)
C
C      300 CONTINUE
C
C      DO 400 I=1,NUMOBS
C
C      WRITE (41,2000) ELEM (I,1), ELEM (I,5), ELEM (I,6), ELEM (I,7)
C
C      400 CONTINUE
C
C      DO 500 I=1,NUMOBS
C
C      WRITE (41,2000) ELEM (I,1), ELEM (I,8), ELEM (I,9), ELEM (I,10)
C
C      500 CONTINUE
C
C      *****
C      PLOT4B CONTROL DECK
C      *****
C
C      Write the PLOT4B control cards.
C
C
C      WRITE (40,3000) NUMOBS, NUMSV
C
C      WRITE (40,4000)
C
C      WRITE (40,3000) NUMOBS, NUMSV
C
C      WRITE (40,5000)
C
C      WRITE (40,3000) NUMOBS, NUMSV

```

```

C
      WRITE (40,6000)

C
      600 CONTINUE

C
      C           Write final PLOT4B control card.

C
      WRITE (40,7000)

C
      STOP

C
C***** FORMAT STATEMENTS *****
C
C           Input cards ( file 1 ).

C
      1000 FORMAT (2X,I5,11X,F6.0,9X,D10.8,2(1X,D6.5,I2)/
      *           7X,2(1X,D8.4),1X,D7.7,2(1X,D8.4),1X,D11.8)

C
C           Formatted data card

C
      2000 FORMAT ( G12.5,3(2X,G14.7) )

C
C           PLOT4B control card

C
      3000 FORMAT
      * (*DATA    NUMVAR     4          ' /
      *   '       NOREWIND   ',I4          ' /
      *   '       FMTDATA    1          ' /
      *   ' (' G12.5,3(2X,G14.7) )        ' /
      *   ' *TITLE   MAINTITL   0          ' /
      *   ' 'SV',I5.                 ' /
      *   '       SUBTITL    0          ' /
      *   ' 'NORAD MEAN ELEMENTS      ' /
      *   '       AXTITL    1          ' /
      *   ' 'DATE (YYDDD)            ' /
      *   ' '19YR                  ' /
      *   ' *PLOTMOD REMARK         ' /
      *   '       BADPOINT   1002        ' /
      *   ' *PLOT    TITLPLOT   0          ' /
      *   '       LEGEND     0          ' /
      *   '       2                     ')  ' )
C
      4000 FORMAT
      * (*PLOTMOD NOZERO      1          ' /
      *   '       BLKPLOT    201         ' /
      *   ' 'XNDT2                ' /
      *   '   3   1   2             ' /
      *   '       YR001.      YR366.      ' /
      *   ' *PLOTMOD NOZERO      1          ' /
      *   '       BLKPLOT    201         ' /
      *   ' 'XNDD6                ' /
      *   '   3   1   3             ' /
      *   '       YR001.      YR366.      ' /
      *   ' *PLOTMOD NOZERO      1          ' /

```

```
*      BLKPLOT 201      ' /
*      'BSTAR      ' /
*      3 1 4      ' /
*      YR001.     YR366.      ' )
```

C

C

5000 FORMAT

```
* (*PLOTMOD NOZERO      1      ' /
*      BLKPLOT 201      ' /
*      'XINCL      ' /
*      3 1 2      ' /
*      YR001.     YR366.      ' /
* (*PLOTMOD NOZERO      1      ' /
*      BLKPLOT 201      ' /
*      'XNODE      ' /
*      3 1 3      ' /
*      YR001.     YR366.      ' /
* (*PLOTMOD NOZERO      1      ' /
*      BLKPLOT 201      ' /
*      'EO          ' /
*      3 1 4      ' /
*      YR001.     YR366.      ' )
```

C

6000 FORMAT

```
* (*PLOTMOD NOZERO      1      ' /
*      BLKPLOT 201      ' /
*      'OMEGA      ' /
*      3 1 2      ' /
*      YR001.     YR366.      ' /
* (*PLOTMOD NOZERO      1      ' /
*      BLKPLOT 201      ' /
*      'XMO        ' /
*      3 1 3      ' /
*      YR001.     YR366.      ' /
* (*PLOTMOD NOZERO      1      ' /
*      BLKPLOT 201      ' /
*      'XNO        ' /
*      3 1 4      ' /
*      YR001.     YR366.      ' )
```

C

7000 FORMAT ('*END LAST')
END

C PROGRAM RUNADC
C
C
C *****
C FUNCTION
C *****
C
C
C
C This program pre-processes NORAD/ADCOM general-perturbation
C mean orbital elements for use in a GTDS run.
C
C
C INPUT *****
C
C FILE 1 NORAD bovel vector element sets, e.g.,
C
C ADC-----.ELS.DATA
C
C where ----- is the satellite designator.
C
C OUTPUT *****
C
C FILE 2 GTDS observation cards, e.g.,
C
C ADC-----.MEAN.OBS.DATA or
C ADC-----.OSCU.OBS.DATA
C
C FILE 3 NORAD single-averaged elements, e.g.,
C
C ADC-----.NORAD.MEAN.DATA or
C ADC-----.NORAD.OSCU.DATA
C
C FILE 6 Printer messages.
C
C SUBROUTINES CALLED *****
C
C SDP4 ADDTIM CALPAK JULIAN EQUIN KEPEQN
C
C***** HISTORY *****
C
C
C VERSION: September 1986
C Fortran program for the IBM 3081 and 3033.
C
C ANALYSIS
C (unknown) -- NORAD / ADCOM
C
C PROGRAMMER

```

C           (unknown)          -- NORAD / ADCOM
C
C
C
C           MODIFIED ----- Paul J. Cefola
C           October 1981 ----- Charles Stark Draper Laboratory
C
C           1. Constructed double-precision version.
C           2. Modified program to run on IBM at CSDL.
C
C
C           MODIFIED ----- Martin Fieger
C           July 1986 ----- AFIT / USAF
C
C           1. Pre-process NORAD mean element sets.
C           2. Write NORAD mean element sets in GTDS observation card
C              format.
C
C
C           MODIFIED ----- Leo W. Early, Jr.
C           July 1986 ----- Charles Stark Draper Laboratory
C
C           1. Cleaned up code.
C           2. Added debugging write switch.
C
C
C           MODIFIED ----- Martin E. Fieger
C           August 1986 ----- AFIT / USAF
C
C           1. Modified program to write the NORAD elements into
C              a temporary data set to be used for plotting.
C           2. Added switch to subroutine SDP4 to output either mean
C              data (IUPSP=MEAN) or osculating data (IUPSP=OSCU).
C
C
C
C***** DECLARATIONS *****
C
C
C
C           IMPLICIT      DOUBLE PRECISION (A-H,O-Z)
C
C           DOUBLE PRECISION      EQNELM(6) ,KEPELM(6)
C
C
C           Character Variables *****
C
C           CHARACTER *4      ISET,          ITYPE,          IUPSP
C
C
C           Dimensions *****
C
C           DIMENSION      POS(3),        VEL(3)
C
C
C           /C1/ *****
C
C           COMMON /C1/      CK2,          CK4,          E6A,          QOMS2T,
C           *           S,             TOTHRD,        XU3,          XKE,
C           *           XKMPER,        XMNPDA,        AE
C
C

```

```

C   /C2/ *****
C
C   COMMON /C2/    DE2RA      ,PI      ,PIO2      ,TWOPI      ,
C   *           X3PIO2
C
C   /E1/ *****
C
C   COMMON /E1/    XMO      ,XNODEO    ,OMEGAO    ,EO      ,
C   *           XINCL    ,XNO      ,XNDT20    ,XNDD60    ,
C   *           BSTAR    ,X      ,Y      ,Z      ,
C   *           XDOT     ,YDOT    ,ZDOT    ,EPOCH    ,
C   *           DS50
C
C
C
C ***** DATA STATEMENTS *****
C
C
C
C
C   DATA Q0      /    120.      D 0      /
C   DATA S0      /    78.       D 0      /
C   DATA XJ2     /    1.082616   D -3      /
C   DATA XJ4     /    -1.65597   D -6      /
C   DATA GM      /    3.986008   D 5      /
C
C   DATA TIMTOL   /    0. DO      /
C
C
C
C ***** BEGIN PROGRAM *****
C
C   ***** Read control cards  *****
C
C   Read satellite designator, NORAD generator type,
C   card format, type of short-period motion desired,
C   start date of data files, end date for the
C   observation card file, end date for the element
C   data file, search interval, and the suppression
C   interval.
C
C   READ  (5,1000)  INTLSV, ISET, ITYPE, IUPSP, DSTART, ENDOBS,
C   *           DSTOP, INTVL, IDELT
C
C
C   Error on control card?
C
C   IF  (ITYPE .NE. 'TRNS')  THEN
C     WRITE (6,2000)  ITYPE
C     STOP
C   END IF
C   IF  (ISET .NE. 'SDP4')  THEN
C     WRITE (6,2010)  ISET

```

```

STOP
END IF
C
C           Output control cards to printer
C
      WRITE (6,1010) INTLSV, ISET, ITYPE, IUPSP, DSTART, ENDOBS,
      *          DSTOP, INTVL, IDELTA
C
C           *****
C           INITIALIZE
C           *****
C
      IF ( ISET .EQ. 'SDP4' ) IEPT=3
C
C
C           ***** SET FILE PARAMETERS *****
C
C           Compute constants.
C
      CK2      =   .500 * XJ2 * AE**2
      CK4      =   -.37500 * XJ4 * AE**4
      Q0MS2T  =   ((Q0 - S0) * AE / XKMPER) ** 4
      S        =   AE * ( 1.00 + S0 / XKMPER )
C
C           Convert start date, end obs date, stop date
C           to internal units and the interval periods
C           to seconds.
C
      DSTART   =   DSTART * 1.D6
      ENDOBS   =   ENDOBS * 1.D6
      DSTOP    =   DSTOP * 1.D6
      XINTVL   =   INTVL * 86400.D0
      DELTA    =   IDELTA * 3600.D0
C
C           Write first GTDS observation card on file.
C
      WRITE (2,4000) 'OBSCARD'
C
C           Print first GTDS observation card.
C
      WRITE (6,5000) 'OBSCARD'
C
C           *****
C           SET CONTROL VARIABLES *****
C
C           Set computed GO TO switch.
C
      IGO     =   1
C

```

```

C           Set first element set switch.
C
C           NUMOES = 0
C
C
C
C           *****
C           READ MEAN ELEMENT SET
C           *****
C
C
C           ****      READ MEAN ELEMENT SET      ****
C
C           Read in a new mean element set.
C
100 CONTINUE
    READ  (1,3000,END=500)  NUMSV, IYRN, IDOYN, DAYPTN, XNDT2N,
    *          XNDD6N, IEXPN, BSTARN, IBEXPN, XINCLN, XNODEN, EON,
    *          OMEGAN, XM0N, XNON
    IF  (XNON .LE. 0.00)  STOP
C
C           Check satellite designator.
C
    IF  (INTLSV .NE. NUMSV ) THEN
        WRITE (6,2020)
        STOP
    END IF
C
C           Find epoch of new mean element set.
C
    EPOCHN  =  IYRN * 1000 +  IDOYN +  DAYPTN
    SECS    =  86400.00 * DAYPTN
    YEAR    =  IYRN
C
C           Convert format of epoch to YYMMDDHHMMSS.SSS
C
    CALL  JULIAN  (DAYJUL,SECJUL,  YEAR,1.00,0.00,
    *                  0.00,0.00,0.00)
    DAYJUL  =  DAYJUL +  IDOYN
    SECJUL  =  SECJUL +  SECS
    CALL  CALPAK  (YMD,HMS,  DAYJUL,SECJUL)
    EPOKEN  =  YMD * 1.06 +  HMS
C
C           Print epoch times.
C
    WRITE (6,5010)  EPOCHN, EPOKEN
C
C
C           ****      ACCEPT OR REJECT?      ****
C
C           Branch to appropriate part of program.

```

```

C
      GO TO (150,300,400), IGO
C
C           New epoch before beginning of run?
C
      150 IF (EPOKEN .LT. DSTART) GO TO 100
C
C
C           *****
C           FIND NEXT EPOCH
C           *****
C
C
C           Update old mean element set with new mean element
C           set.
C
200 CONTINUE
      EPOKEO = EPOKEN
      EPOCH = EPOCHN
      XNDT20 = XNDT2N
      XNDD60 = XNDDGN
      IEXP = IEXPN
      IBEXP = IBEXPN
      BSTAR = BSTARN
      XINCL = XINCLN
      XNODEG = XNODEN
      EO = EON
      OMEGAO = OMEGAN
      XMO = XMON
      XNO = XNON
C
C           Save epoch time.
C
      DAYSAV = DAYJUL
      SECSAV = SECJUL
      XJUL = DAYSAV + SECSAV / 86400.0D0
      YMDSAV = YMD
      HMSSAV = HMS
C
C           Increment epoch by specified search interval.
C
      CALL ADDTIM (YMD,HMS, DAYJUL,SECJUL, XINTVL, TIMTOL)
      XDATE = YMD * 1.D6 + HMS
C
C           Restore epoch time.
C
      DAYJUL = DAYSAV
      SECJUL = SECSAV
      YMD = YMDSAV
      HMS = HMSSAV
C
C           Increment epoch by specified suppression interval.

```

```

C
      CALL ADDTIM  (YMD,HMS,  DAYJUL,SECJUL,  DELTA,  TIMTOL)
      XDELTA = YMD * 1.D6 + HMS

C
C
C           Read next mean element set.

C
      IGO = 2
      GO TO 100

C
C
C
C           *****
C           FIND POSITION AND VELOCITY
C           *****
C
C
C
C           ***** SET ORBIT GENERATOR *****

C           ***** PARAMETERS *****

C
C
C           New epoch within hourly suppression zone of previous
C           epoch?
C
      300 IF  (EOPEN < .LT. XDELTA)  GO TO 200
C
C           Compute orbit generator parameters.

C
      XNDD60 = XNDD60 * (10.00 ** IEXP)
      XNODEO = XNODEO * DE2RA
      OMEGA0 = OMEGA0 * DE2RA
      XMO = XMO * DE2RA
      XINCL = XINCL * DE2RA
      TEMP = TWOP1 / (XMNPDA * XMNPDA)
      XNO = XNO * TEMP * XMNPDA
      XNDT20 = XNDT20 * TEMP
      XNDD60 = XNDD60 * TEMP / XMNPDA

C
C           Compute more orbit generator parameters.

C
      A1 = (XKE / XNO) ** TOTHRD
      TEMP = 1.500 * CK2 * (3.00 * (DCOS(XINCL)**2.00) - 1.00) /
      * ((1.00 - EO*EO) ** 1.500)
      DEL1 = TEMP / (A1 * A1)
      AO = A1 * (1.00 - DEL1 * (.500 * TOTHRD +
      * DEL1 * (1.00 + (134.00/81.00)*DEL1)))
      DELO = TEMP / (AO * AO)
      XNODP = XNO / (1.00 + DELO)
      BSTAR = BSTAR * (10.00 ** IBEXP) / AE

C
C           Set input parameters for call to orbit generator.

C
      TSINCE = 0.00
      IFLAG = 1

```

```

C
C
C
C           ***** EVALUATE ORBIT GENERATOR *****
C
C           Which analytical orbit theory?
C
C           Note that SDP4 is the only subroutine that has
C           been modified to include the additional parameter
C           IUPSP.
C
C           GO TO (351,352,353,354,355), IEPT
C
C           ----- SGP -----
C
351    CALL SGP  (IFLAG,TSINCE)
GO TO 360
C
C           ----- SGP4 -----
C
352    CALL SGP4 (IFLAG,TSINCE)
GO TO 360
C
C           ----- SDP4 -----
C
353    CALL SDP4 (IFLAG,TSINCE,IUPSP)
GO TO 360
C
C           ----- SGP8 -----
C
354    CALL SGP8 (IFLAG,TSINCE)
GO TO 360
C
C           ----- SDP8 -----
C
355    CALL SDP8 (IFLAG,TSINCE)
C
C
C           ***** WRITE OUTPUT *****
C
C           Compute position in kilometers.
C
360    X      =  X * XKMPER / AE
Y      =  Y * XKMPER / AE
Z      =  Z * XKMPER / AE
C
C           Compute velocity in kilometers/second.
C
C
DX     =  XDOT
DY     =  YDOT
DZ     =  ZDOT
C
DX     =  DX * (XKMPER / AE) * (XMNPDA / 86400.D0)

```

```

      DY      =  DY * (XKMPER / AE) * (XMNPDA / 86400.00)
      DZ      =  DZ * (XKMPER / AE) * (XMNPDA / 86400.00)

C
C
C           Write position on GTDS observation card file.
C
IF ( EPOKEO .LE. ENDOBS ) THEN
C
      WRITE  (2,4010)  21,EPOKEO,X,X
      WRITE  (2,4010)  22,EPOKEO,Y,Y
      WRITE  (2,4010)  23,EPOKEO,Z,Z

C
C           Write velocity on GTDS observation card file.
C
      WRITE  (2,4010)  24,EPOKEO,DX,DX
      WRITE  (2,4010)  25,EPOKEO,DY,DY
      WRITE  (2,4010)  26,EPOKEO,DZ,DZ

C
END IF
C
C
C           Print position in GTDS observation card format.
C
      WRITE  (6,5020)  21,EPOKEO,X,X
      WRITE  (6,5020)  22,EPOKEO,Y,Y
      WRITE  (6,5020)  23,EPOKEO,Z,Z

C
C           Print velocity in GTDS observation card format.
C
      WRITE  (6,5020)  24,EPOKEO,DX,DX
      WRITE  (6,5020)  25,EPOKEO,DY,DY
      WRITE  (6,5020)  26,EPOKEO,DZ,DZ

C
C           Convert to equinoctial elements.
C
      POS(1)  =  X
      POS(2)  =  Y
      POS(3)  =  Z
      VEL(1)  =  DX
      VEL(2)  =  DY
      VEL(3)  =  DZ

C
      RETRO  =  1.00

C
CALL  EQUIN ( EQNELM,RETRO, POS,VEL,  GM, .TRUE. )

C
      SMA    =  EQNELM(1)
      XH    =  EQNELM(2)
      XK    =  EQNELM(3)
      XP    =  EQNELM(4)
      XQ    =  EQNELM(5)
      XML   =  EQNELM(6)

```

```

C          Convert to Keplerian elements.
C
C      CALL    KEPEQN ( KEPELM, EQNELM,RETRO )
C
C          ECC      =  KEPELM(2)
C          XINC    =  KEPELM(3)
C          XLAN    =  KEPELM(4)
C          AP      =  KEPELM(5)
C          XMA     =  KEPELM(6)
C
C          Calculate perigee radius and apogee radius.
C
C          PR      =  SMA * ( 1.00 - ECC )
C          APR     =  SMA * ( 1.00 + ECC )
C
C          Convert angular quantities to degrees.
C
C          XML     =  XML / DE2RA
C          XINC   =  XINC / DE2RA
C          XLAN   =  XLAN / DE2RA
C          AP     =  AP / DE2RA
C          XMA    =  XMA / DE2RA
C
C          Write days elapsed and orbital elements.
C
C          WRITE (3,6000) XJUL, EPOKED,X,Y,Z,DX,DY,DZ,SMA,PR,APR,ECC,
C          *           XINC,XLAN,AP,XMA,XH,XK,XP,XQ,XML
C
C          Increment the counter.
C
C          NUMOBS =  NUMOBS + 1
C
C          *****
C          END LOOP
C          *****
C
C          New epoch beyond end of run?
C
C          400 IF  (EPOKEN .GT. DSTOP)  GO TO 500
C
C          New epoch beyond weekly suppression zone of previous
C          epoch?
C
C          IF  (EPOKEN .GT. XDATE)  GO TO 200
C
C          Read next mean element set
C
C          IGO   =  3
C          GO TO 100
C
C

```

```

C      *****
C      END RUN
C      *****
C
C      500 CONTINUE
C
C          Write final observation card on file.
C
C          WRITE (2,4000) 'END'
C
C          Print final observation card.
C
C          WRITE (6,5000) 'END'
C
C          STOP
C
C***** FORMAT STATEMENTS *****
C
C          Input cards.
C
C          1000 FORMAT (33X,I5/3(31X,A4/),3(31X,F7.0/),31X,I2/31X,I2 )
C
C          1010 FORMAT (1X,'SV',I5,2X,3(A4,2X),3(F7.0,2X),2(I2,2X) )
C
C          Error messages.
C
C          2000 FORMAT( ' A card type of ',A4,' is illegal.' /
C                  *       ' You must use a transmission card to input data.')
C          2010 FORMAT( ' Ephemeris type ',A4,' not legal; will skip this case.' )
C
C          2020 FORMAT( ' Satellite designators do not match.' )
C
C
C          Input cards ( file 5 ).
C
C          3000 FORMAT (2X,I5,11X,I2,I3,D9.8,1X,D10.8,2(1X,D6.5,I2)/
C                  *       7X,2(1X,D8.4),1X,D7.7,2(1X,D8.4),1X,D11.8)
C
C          GTDS observation cards ( file 2 ).
C
C          4000 FORMAT( AB )
C          4010 FORMAT( 8X, I3,6X, G21.15, 2G21.14 )
C
C          Debugging print ( file 6 ).
C
C          5000 FORMAT( 1X, AB )
C          5010 FORMAT( ' NORAD: ',G19.13,5X, 'GTDS: ',G21.15 )
C          5020 FORMAT( 9X, I3,5X, G21.15,5X, G21.14,5X, G21.14 )
C
C          Temporary data set ( file 3 ).
C
C          6000 FORMAT('DAY',G19.10,8X,G21.15      /

```

```

*   'X  ',G19.10,7X,'Y  ',G19.10,7X,'Z  ',G19.10 /
*   'DX  ',G19.10,7X,'DY  ',G19.10,7X,'DZ  ',G19.10 /
*   'SMA ',G19.10,7X,'PR ',G19.10,7X,'APR ',G19.10 /
*   'ECC ',G19.10,7X,'INC ',G19.10,7X,'LAN ',G19.10 /
*   'TAP ',G19.10,7X,'MA ',G19.10,7X,'H  ',G19.10 /
*   'K  ',G19.10,7X,'P  ',G19.10,7X,'Q  ',G19.10 /
*   'ML ',G19.10          )

C
C      END
C      BLOCK DATA
C
C      PURPOSE
C          INITIALIZE PORTION OF COMMON BLOCK /C1/ USED IN THE
C          NORAD/ADCOM GENERAL PERTURBATION SATELLITE THEORY
C          PACKAGE.
C
C
C      VARI-    DIMEN-  LOCA-
C      ABLE     SION    TION   DESCRIPTION
C      -----  -----
C
C      E6A           10**(-6)
C      TOTHRD        2 / 3
C      XKE           GRAVITATIONAL CONSTANT,(ER/MIN)**3/2
C      XKMPER        KM PER EARTH RADIUS
C      XMNPDA        TIME UNITS PER DAY
C      AE            EQUATORIAL RADIUS OF EARTH,(D.U./E.R.)
C      XJ3           NUMERICAL VALUE OF J3 ZDNAL HARMONIC
C
C
C      -----
C
C      VERSION OF OCTOBER 1981
C          FORTRAN SUBROUTINE FOR THE AMDAHL 470/V8 AND THE IBM 3033.
C
C      ANALYSIS
C          P. CEFOLA      -- CHARLES STARK DRAPER LABORATORY
C
C      PROGRAMMER
C          P. CEFOLA      -- CHARLES STARK DRAPER LABORATORY
C
C
C***** DECLARATIONS *****
C
C      IMPLICIT      REAL*8 (A-H,O-Z)
C
C      COMMON/C1/CK2,CK4,E6A,Q0MS2T,S,TOTHRD,
C      *           XJ3,XKE,XKMPER,XMNPDA,AE
C
C
C      DATA   E6A      /   1.D-6      /
C      DATA   TOTHRD   /   .66666667D0   /
C      DATA   XKE      /   .743669161D-1   /

```

```

DATA XKMPER / 6378.135D0 /
DATA XMNPDA / 1440.D0 /
DATA AE / 1.D0 /
DATA XJ3 / -.253881D-5 /

C
END
BLOCK DATA

C
C PURPOSE
C     INITIALIZE COMMON BLOCK /C2/. THIS BLOCK DATA IS FOR USE
C     WITH THE NORAD/ADCOM GENERAL PERTURBATION PACKAGE.

C
C
C VARI-   DIMEN- LOCA-
C ABLE    SION   TION  DESCRIPTION
C -----  -----  -----
C
C     descriptive heading
C
C DE2RA           DEGREES TO RADIANS CONVERSION
C PI              MATHEMATICAL CONSTANT PI
C PIO2             PI / 2
C TWOPI            2 * PI
C X3PIO2           3 * PI / 2
C
C -----
C
C VERSION OF OCTOBER 1981
C FORTRAN SUBROUTINE FOR THE AMDAHL 470/V8 AND THE IBM 3033.

C
C ANALYSIS
C     P. CEFOLA      -- CHARLES STARK DRAPER LABORATORY
C
C PROGRAMMER
C     P. CEFOLA      -- CHARLES STARK DRAPER LABORATORY
C
C
C***** DECLARATIONS *****
C
C     IMPLICIT      REAL*8 (A-H,O-Z)
C
C COMMON/C2/DE2RA,PI,PIO2,TWOPI,X3PIO2
C
C     DATA DE2RA    / .174532925D-1   /
C     DATA PI       / 3.14159265D0   /
C     DATA PIO2    / 1.57079633D0   /
C     DATA TWOPI   / 6.28318530D0   /
C     DATA X3PIO2  / 4.71238898D0   /
C
C END

```

SUBROUTINE SDP4(IFLAG,TSINCE,IUPSP)

C

C

C

C PURPOSE

C SDP4 IS THE 12 HR, HIGH ECCENTRICITY AND 24 HR

C GEOSYNCHRONOUS NORAD/ADCOM GENERAL PERURBATION THEORY.

C THIS SUBROUTINE IS TAKEN FROM THE PROJECT SPACETRACK

C REPORT NO.3, DECEMBER 1980, "MODELS FOR THE

C PROPAGATION OF NORAD ELEMENT SETS", F.R.HOOTS AND

C R. L. ROEHRICH.

C

C METHOD

C BROUWER - HOMI - LANE

C

C

C

C CALLING SEQUENCE

C SDP4(IFLAG,TSINCE)

C

C PHYSICAL PARAMETERS USED IN THE COMMENTS

C parm1 meaning

C parm2 meaning

C parm3 meaning

C parm4 meaning

C

C SUBROUTINES CALLED

C DEEP FMOD2P ACTAN

C

C

C ADCOM/D06 VERSION OF DECEMBER 1980

C FORTRAN SUBROUTINE FOR THE AMDAHL 470/V8 AND THE IBM 3033.

C THIS IS A DOUBLE PRECISION VERSION CONSTRUCTED BY P. CEFOLA.

C

C

C ANALYSIS

C ANALYST -- P. CEFOLA

C

C PROGRAMMER

C PROGRAMMER -- P. CEFOLA

C

C MODIFICATIONS

C Version of September 1986

C Martin E. Fieger ----- Captain, USAF/AFIT/MIT

C

C Added a subroutine parameter IUPSP to enable selection of

C a mean output without the update for short periodics

C (IUPSP=1), or an osculating output with the update for

C short periodics (IUPSP=0).

C

```

C***** DECLARATIONS *****
C
C      IMPLICIT      REAL*8 (A-H,O-Z)
C
C      CHARACTER*4 IUPSP
C
C
C      COMMON/E1/XMO,XNODE0,OMEGA0,E0,XINCL,XNO,XNDT20,
C      1           XNDD60,BSTAR,X,Y,Z,XDOT,YDOT,ZDOT,EPOCH,DS50
C
C      COMMON/C1/CK2,CK4,E6A,QOMS2T,S,TOTHRD,
C      1           XJ3,XKE,XKMPER,XMNPDA,AE
C
C***** BEGIN PROGRAM *****
C
C
C
C      IF (IFLAG .EQ. 0) GO TO 100
C
C          Recover original mean motion (XNODP) and semimajor
C          axis (AODP) from input elements.
C
C      A1 = (XKE/XNO)**TOTHRD
C
C      COSIO = DCOS(XINCL)
C
C      THETA2 = COSIO * COSIO
C
C      X3THM1 = 3.0D0 * THETA2 - 1.0D0
C
C      EOSQ = E0 * EO
C
C      BETAQ2 = 1.0D0 - EOSQ
C
C      BETAO = DSQRT(BETAQ2)
C
C      DEL1 = 1.5D0 * CK2 * X3THM1 / (A1 * A1 * BETAO * BETAQ2 )
C
C      AO = A1 * ( 1.0D0-DEL1 * (.5D0 * TOTHRD + DEL1*(1.0D0+134.0D0/81.0D0*
C      1           DEL1 )))
C
C      DELO = 1.5D0 * CK2 * X3THM1 / (AO * AO * BETAO * BETAQ2)
C
C      XNODP = XNO / ( 1.0D0 + DELO )
C
C      AODP = AO / ( 1.0D0 - DELO )
C
C
C          Initialization
C
C
C          For perigee below 156 km, the values of
C          S and QOMS2T are altered.
C
C      S4 = S

```

```

C
      QOMS24 = QOMS2T
C
      PERIGE = ( AODP * ( 1.0D-ED ) - AE ) * XKMPER
C
      IF ( PERIGE.GE.156.D0) GO TO 10
C
      S4 = PERIGE - 78.D0
C
      IF ( PERIGE.GT. 98.D0 ) GO TO 9
C
      S4 = 20.D0
C
      9 QOMS24 = ((120.D0 - S4) * AE / XKMPER)**4.D0
C
      S4 = S4 / XKMPER + AE
C
      10 PINVSQ = 1.D0 / (AODP * AODP * BETA02 * BETA02)
C
      SING = DSIN(OMEGAO)
C
      COSG = DCOS(OMEGAO)
C
      TSI = 1.D0 / (AODP - S4)
C
      ETA = AODP * EO * TSI
C
      ETASQ = ETA * ETA
C
      EETA = EO * ETA
C
      PSISQ = DABS (1.D0 - ETASQ)
C
      COEF = QOMS24 * TSI**4.D0
C
      COEF1 = COEF / PSISQ**3.5D0
C
      C2 = COEF1*XNODP*(AODP*(1.D0 + 1.5D0 * ETASQ + EETA *
      * (4.D0 + ETASQ)) + .75D0 * CK2 * TSI / PSISQ *
      * X3THM1 * ( 8.D0 + 3.D0 * ETASQ * ( 8.D0 + ETASQ)))
C
      C1 = BSTAR * C2
C
      SINIO = DSIN(XINCL)
C
      A30VK2 = - XJ3 / CK2 * AE **3.D0
C
      X1MTH2 = 1.D0 - THETA2
C
      C4 = 2.D0 * XNODP * COEF1 * AODP * BETA02 * ( ETA *
      * (2.D0 + .5D0 * ETASQ ) + EO * (.5D0 + 2.D0 * ETASQ)
      * -2.D0 * CK2 * TSI /
      * (AODP*PSISQ)*(-3.D0 *X3THM1*(1.D0 -2.D0 * EETA + ETASQ *
      * (1.5D0-.5D0*EETA))+.75D0*X1MTH2 * (2.D0 * ETASQ - EETA *

```

```

*      ( 1.0D + ETASQ) ) * DCOS(2.0D * DMEGAO)))
C
C      THETA4 = THETA2 * THETA2
C
C      TEMP1 = 3.0D * CK2 * PINVSQ * XNODP
C
C      TEMP2 = TEMP1 * CK2 * PINVSQ
C
C      TEMP3 = 1.250D * CK4 * PINVSQ * PINVSQ * XNODP
C
C      XMDOT = XNODP + .50D * TEMP1 * BETA0 * X3THM1
*          + .06250D * TEMP2 * BETA0 *
*          ( 13.0D - 78.0D * THETA2 + 137.0D * THETA4 )
C
C      X1M5TH = 1.0D - 5.0D * THETA2
C
C      OMGDOT = -.50D * TEMP1 * X1M5TH + .06250D * TEMP2 *
*          ( 7.0D - 114.0D * THETA2 +
*          395.0D * THETA4 ) + TEMP3 * ( 3.0D - 36.0D * THETA2 +
*          49.0D * THETA4 )
C
C      XHDOT1 = - TEMP1 * COSIO
C
C      XNODOT = XHDOT1 + (.50D * TEMP2 * ( 4.0D - 19.0D * THETA2 )
*          + 2.0D * TEMP3 * ( 3.0D - 7.0D * THETA2 )) * COSIO
C
C      XNODCF = 3.50D * BETA02 * XHDOT1 * C1
C
C      T2COF = 1.50D * C1
C
C      XLCOF = .1250D * A30VK2*SINIO*(3.0D + 5.0D * COSIO)/(1.0D + COSIO)
C
C      AYCOF = .250D * A30VK2 * SINIO
C
C      X7THM1 = 7.0D * THETA2 - 1.0D
C
C
90 IFLAG = 0
C
C      CALL DPINIT(E0SQ,SINIO,COSIO,BETA0,A0DP,THETA2,
1           SING,COSG,BETAD2,XMDOT,OMGDOT,XNODOT,XNODP)
C
C
C          Update for secular gravity and
C          atmospheric drag.
C
C
100 XMDF = XMD + XMDOT * TSINCE
C
C      OMGADF = OMEGA0 + OMGDOT * TSINCE
C
C      XNODEO = XNODE0 + XNODOT * TSINCE
C
C      TSQ = TSINCE * TSINCE
C

```

```

XNODE = XNODEDF + XNODECF * TSQ
C
TEMPA = 1.00 - C1 * TSINCE
C
TEMPE = BSTAR * C4 * TSINCE
C
TEMPL = T2COF * TSQ
C
XN = XNODEP
C
C
C
CALL DPSEC(XMDF,OMGADF,XNODE,EM,XINC,XN,TSINCE)
C
A = (XKE/XN)**TOTHRD * TEMPA**2.00
C
E = EM - TEMPE
C
XMAM = XMDF + XNODEP * TEMPL
C
CALL DPPER(E,XINC,OMGADF,XNODE,XMAM)
C
XL = XMAM + OMGADF + XNODE
C
BETA = DSQRT(1.00 - E * E)
C
XN = XKE / A ** 1.500
C
C
Long period periodics.
C
C
AXN = E * DCOS (OMGADF)
C
TEMP = 1.00 / ( A * BETA * BETA )
C
XLL = TEMP * XLCOF * AXN
C
AYNL = TEMP * AYCOF
C
XLT = XL + XLL
C
AYN = E * DSIN(OMGADF) + AYNL
C
C
Solve Keplers equation.
C
C
CAPU = FMOD2P( XLT - XNODE )
C
TEMP2 = CAPU
C
DD 130 I = 1,10
C
SINEPW = DSIN(TEMP2)
C

```

```

COSWP = DCOS(TEMP2)
C
    TEMP3 = AXN * SINEPW
C
    TEMP4 = AYN * COSEPW
C
    TEMP5 = AXN * COSEPW
C
    TEMP6 = AYN * SINEPW
C
    EPW = (CAPU - TEMP4+TEMP3-TEMP2) / (1.00 - TEMP5 - TEMP6) +
          TEMP2
C
        IF(DABS(EPW - TEMP2) .LE. E6A) GO TO 140
C
130 TEMP2 = EPW
C
C
C           Short period preliminary quantities.
C
C
140 ECOS = TEMP5 + TEMP6
C
    ESINE = TEMP3 - TEMP4
C
    ELSQ = AXN * AXN + AYN * AYN
C
    TEMP = 1.00 - ELSQ
C
    PL = A * TEMP
C
    R = A * (1.00 - ECOS)
C
    TEMP1 = 1.00 / R
C
    RDOT = XKE * DSQRT(A) * ESINE * TEMP1
C
    RFDOT = XKE * DSQRT(PL) * TEMP1
C
    TEMP2 = A * TEMP1
C
    BETAL = DSQRT(TEMP)
C
    TEMP3 = 1.00 / (1.00 + BETAL)
C
    COSU = TEMP2 * (COSEPW - AXN + AYN * ESINE * TEMP3)
C
    SINU = TEMP2 * (SINEPW - AYN - AXN * ESINE * TEMP3)
C
    U = ACTAN( SINU, COSU )
C
    SIN2U = 2.00 * SINU * COSU
C
    COS2U = 2.00 * COSU * COSU - 1.00

```

```

C
C      TEMP = 1.0D / PL
C
C      TEMP1 = CK2 * TEMP
C
C      TEMP2 = TEMP1 * TEMP
C
C          Update for short periodics if required by input card.
C
C      IF ( IUPSP .EQ. 'OSCU' ) THEN
C
C          RK = R*(1.0D-1.5D0*TEMP2*BETAL*X3THM1)+.5D0*TEMP1*X1MTH2*COS2U
C
C          UK = U - .25D0 * TEMP2 * X7THM1 * SIN2U
C
C          XNODEK = XNODE + 1.5D0 * TEMP2 * COSIO * SIN2U
C
C          XINCK = XINC + 1.5D0 * TEMP2 * COSIO * SINIO * COS2U
C
C          RDOTK = RDOT - XN * TEMP1 * X1MTH2 * SIN2U
C
C          RFDOBK = RFDOBK + XN * TEMP1 * (X1MTH2 * COS2U + 1.5D0 * X3THM1)
C
C      ELSE
C
C          RK = R
C
C          UK = U
C
C          XNODEK = XNODE
C
C          XINCK = XINC
C
C          RDOTK = RDOT
C
C          RFDOBK = RFDOBK
C
C      END IF
C          Orientation vectors.
C
C          SINUK = DSIN(UK)
C
C          COSUK = DCOS(UK)
C
C          SINIK = DSIN(XINCK)
C
C          COSIK = DCOS(XINCK)
C
C          SINNOK = DSIN(XNODEK)
C
C          COSNOK = DCOS(XNODEK)
C
C          XMX = - SINNOK * COSIK
C

```

```
C XMY = COSNOK * COSIK
C UX = XMX * SINUK + COSNOK * COSUK
C UY = XMY * SINUK + SINNOK * COSUK
C UZ = SINIK * SINUK
C VX = XMX * COSUK - COSNOK * SINUK
C VY = XMY * COSUK - SINNOK * SINUK
C VZ = SINIK * COSUK
C Position and velocity.
C C
C X = RK * UX
C Y = RK * UY
C Z = RK * UZ
C XDOT = RDOTK * UX + RFDDOTK * VX
C YDOT = RDOTK * UY + RFDDOTK * VY
C ZDOT = RDOTK * UZ + RFDDOTK * VZ
C
RETURN
END
```

```
C      PROGRAM RDORB1
C
C
C
C      *****
C      FUNCTION
C      *****
C
C
C      This program reads a GTDS ORB1 file and converts position and
C      velocity to Keplerian and equinoctial elements and then writes
C      the elements into a data set.
C
C
C      INPUT *****
C
C
C          FILE 24      GTDS ephemeris run orbital elements, e.g.,
C
C                          ADC----ORB1.DATA
C
C          FILE 5       Gravitational constant of GTDS EPHEM ORB1 file
C
C      OUTPUT *****
C
C          FILE 4       Temporary file, e.g.,
C
C                          ADC----EPHEM.DATA
C
C      SUBROUTINES CALLED *****
C
C          OPNORB      RDORB      EQUIN      KEPEQN
C
C
C      ***** HISTORY *****
C
C
C
C      VERSION: September 1986
C              Fortran subroutine for the IBM 3081 and 3033.
C
C      ANALYSIS
C          Martin E. Fieger ----- Captain, USAF/AFIT/MIT
C
C      PROGRAMMER
C          Martin E. Fieger ----- Captain, USAF/AFIT/MIT
C
C
C      ***** DECLARATIONS *****
```

```

C
C
C
    IMPLICIT      DOUBLE PRECISION (A-H,O-Z)
C
    LOGICAL      DONE
C
C Dimensions *****
C
    DIMENSION      POS(3),          VEL(3)
C
    DOUBLE PRECISION EQNELM(6),     KEPELM(6)
C
C***** DATA STATEMENTS *****
C
    DATA           DE2RA / .174532925D-1 /
C
C***** BEGIN PROGRAM *****
C
C           Read the gravitational constant used on the
C           ORB1 file.
C
    READ   (5,900)  GM
C
C           Open the GTDS-generated ORB1 file 24.
C
    CALL   OPNORB  ( DAYBEG, SECBEG, DAYEND, SECEND, TIMDIF,
*                  ICENT, ICOORD, DAYREF, SECREF, DONE, 24 )
C
C           Read another data record.
C
    100 CONTINUE
C
    CALL   RDORB  ( TIME, POS, VEL, DONE )
C
    IF (DONE) STOP
C
C           Calculate the Julian date of the record
C
    XJUL      =  DAYBEG + ( SECBEG + TIME ) / 86400.0D0
C
C           Calculate the YYMMDDHHMMSS. form of the date.
C
    IJUL      =  XJUL
    SECJUL    =  ( XJUL - IJUL ) * 86400.0D0
    DAYJUL    =  IJUL
C
    CALL CALPAK (YMD,HMS, DAYJUL,SECJUL)
C
    EPOKE    =  YMD * 1.0D6 + HMS
C
C           Save the position and velocity vectors.
C
    X      =  POS(1)

```

```

Y      = POS(2)
Z      = POS(3)
DX     = VEL(1)
DY     = VEL(2)
DZ     = VEL(3)

C
C           Convert to equinoctial elements.
C
RETRO   = 1.0D0

C
CALL EQUIN ( EQNELM, RETRO, POS, VEL, GM, .TRUE. )

C
SMA     = EQNELM(1)
XH      = EQNELM(2)
XK      = EQNELM(3)
XP      = EQNELM(4)
XQ      = EQNELM(5)
XML     = EQNELM(6)

C
C           Convert to Keplerian elements.
C
CALL KEPEQN ( KEPELM, EQNELM, RETRO )

C
ECC     = KEPELM(2)
XINC    = KEPELM(3)
XLAN    = KEPELM(4)
AP      = KEPELM(5)
XMA     = KEPELM(6)

C
C           Calculate the perigee radius and apogee radius.
C
PR      = SMA * ( 1.0D0 - ECC )
APR    = SMA * ( 1.0D0 + ECC )

C
C           Convert angular quantities to degrees.
C
XML     = XML / DE2RA
XINC    = XINC / DE2RA
XLAN    = XLAN / DE2RA
AP      = AP / DE2RA
XMA     = XMA / DE2RA

C
C           Write the Julian day and orbital elements.
C
WRITE (4,1000) XJUL,EPOKE,X,Y,Z,DX,DY,DZ,SMA,PR,APR,ECC,
*                  XINC,XLAN,AP,XMA,XH,XK,XP,XQ,XML

C
GO TO 100

C **** Format statements ****
C
900 FORMAT(31x,F10.2)
C
1000 FORMAT('DAY',G19.10,BX,G21.15) /

```

```
* 'X ',G19.10,7X,'Y ',G19.10,7X,'Z ',G19.10 /  
* 'DX ',G19.10,7X,'DY ',G19.10,7X,'DZ ',G19.10 /  
* 'SMA',G19.10,7X,'PR ',G19.10,7X,'APR',G19.10 /  
* 'ECC ',G19.10,7X,'INC',G19.10,7X,'LAN',G19.10 /  
* 'AP ',G19.10,7X,'MA ',G19.10,7X,'H ',G19.10 /  
* 'K ',G19.10,7X,'P ',G19.10,7X,'Q ',G19.10 /  
* 'ML ',G19.10 )
```

C

END

```
C      PROGRAM      PLOTTER
C
C
C      *****
C      FUNCTION
C      *****
C
C
C      This program reads a set of nineteen orbital elements from a
C      file of GTDS EPHEM program elements and performs a five-point
C      Lagrangian interpolation of the elements to the times of a set of
C      NORAD mean elements (which served as the GTDS DBS card deck).
C      In a general application, this program reads a data set of up to
C      nineteen functions of a single variable, which need not be given
C      at regular intervals; reads a second data set containing nineteen
C      functions of the same variable; and interpolates the values of the
C      functions of the second data set to the values of the independent
C      variable of the first data set.
C
C      *****
C      USAGE
C      *****
C
C
C      This program creates the formatted data set and the control card
C      deck to perform the CSDL PLOT4B program.
C      The GTDS EPHEM interval is the interval (in seconds) between data
C      points on the ORB1 file.
C
C
C      SUBROUTINES CALLED *****
C
C          LAGRAN     INTERP     RCAERR     LINANG     CARTES
C
C***** HISTORY *****
C
C      VERSION: OCTOBER 1986
C          Fortran program for the IBM 3081 and 3033.
C
C      ANALYSIS
C          Martin E. Fieger, Capt, USAF -- AFIT / MIT
C
C      PROGRAMMER
C          Martin E. Fieger, Capt, USAF -- AFIT / MIT
C
C
C***** DECLARATIONS *****
C
C
C          IMPLICIT      DOUBLE PRECISION (A-H,O-Z)
C
C          Character variables *****
C
C          CHARACTER * 7   SVDESG
```

```

CHARACTER * 7 YTITLE (20)
CHARACTER * 28 MTITLE (20)
CHARACTER * 28 DTITLE (3)
CHARACTER * 7 ETITLE (3)
CHARACTER * 5 STITLE (2)

C
C Dimensions *****
C
DIMENSION DAYCNT (5)
DIMENSION COEF (11,5), I (11,5), POLY (11)
DIMENSION POS (3), VEL (3)
DIMENSION ELEM (1000,23,2), DIFF (1000,20)
DIMENSION XMEAN (20), SIGMA (20)
DIMENSION VECT1 (6), VECT2 (6), ERROR (6)
DIMENSION ANGLIN (4,5), ANGSAW (4,5), ANGVEL(4)
DIMENSION EQNELM (6)

C
C Data statements *****
C
DATA MTITLE /'X-COMPONENT OF POSITION',
*'Y-COMPONENT OF POSITION',
*'Z-COMPONENT OF POSITION',
*'X-COMPONENT OF VELOCITY',
*'Y-COMPONENT OF VELOCITY',
*'Z-COMPONENT OF VELOCITY',
*'SEMITMAJOR AXIS',
*'RADIUS OF PERIGEE',
*'RADIUS OF APOGEE',
*'ECCENTRICITY',
*'INCLINATION',
*'LONGITUDE OF ASCENDING NODE',
*'ARGUMENT OF PERIGEE',
*'MEAN ANOMALY',
*'H',
*'K',
*'P',
*'Q',
*'MEAN LONGITUDE'/

C
DATA YTITLE /'KM',
*'KM',
*'KM',
*'KM/SEC',
*'KM/SEC',
*'KM/SEC',
*'KM',
*'KM',
*'KM',
*'DEGREES',
*'DEGREES',
*'DEGREES'/

```

```

*          'DEGREES' ,
*
*
*
*
*
*          'DEGREES' /
C
DATA DTITLE    / ' POSITION RADIAL ERROR      ' ,
*                  ' POSITION CROSS-TRACK ERROR ' ,
*                  ' POSITION ALONG-TRACK ERROR ' /
C
DATA ETITLE    / 'KM      ' ,
*                  'KM      ' ,
*                  'KM      ' /
C
DATA TWOP1     / 6.2831 85307 17958 65 DO /
DATA DE2RA     / 0.1745 3292  5 D-1 /
C
C***** Begin program *****
C
C
C***** INPUT CONTROL CARDS *****
C
C
C      Read satellite designator, the GTDS EPHEM program
C      time interval, the comparison start date, the first
C      day of the plot and the final day of the plot (in
C      days since the start date), the Fortran file number
C      of the irregularly-spaced data and the legend name to
C      be used on the plots, and the Fortran file number
C      of the regularly-spaced data and the legend name to
C      be used on the plots.
C
READ (5,2000) SVDESG,GINTVL,START,FIRST,FINAL,IRN1,STITLE(1),
*                 IRN2,STITLE(2)
C
C      Read the gravitational constant used on the
C      ORB1 file.
C
READ (5,2100) GM
C
C      Convert the interval to days.
C
HAFWID = ( GINTVL * 2.0D ) / 86400.0D
C
C      Convert the start date to a Julian date.
C
CALL JULPAK ( DAYJUL,SECJUL, START,0.0D )
C
DAYREF = DAYJUL + SECJUL / 86400.0D
C
C      *****

```

```

C           INTERPOLATOR
C   ****
C
C           Set flags and counters to initial conditions.
C
C           NUMADC = 0
C
C           ISHIFT = 0
C
C           Read in first data record from the GTDS predictions
C           on file IRN2.
C
C           READ (IRN2,3000,END=800) DAYCNT(1), X,YY,Z,DX,DY,DZ,SMA,PR,APR,
C           *          ECC,XINC,XLAN,AP,XMA,XH,XK,XP,XQ,XML
C
C           Save the Keplerian and equinoctial elements for
C           interpolation; convert angular quantities to radians.
C
C           Y( 1,1) = SMA
C           Y( 2,1) = ECC
C           Y( 3,1) = XINC * DE2RA
C           Y( 4,1) = XLAN * DE2RA
C           Y( 5,1) = AP    * DE2RA
C           Y( 6,1) = XMA   * DE2RA
C           Y( 7,1) = XH
C           Y( 8,1) = XK
C           Y( 9,1) = XP
C           Y(10,1) = XQ
C           Y(11,1) = XML   * DE2RA
C
C           100 CONTINUE
C
C           Read in the next four records.
C
C           DD 200 J=2,5
C
C           READ (IRN2,3000,END=800) DAYCNT(J), X,YY,Z,DX,DY,DZ,SMA,PR,APR,
C           *          ECC,XINC,XLAN,AP,XMA,XH,XK,XP,XQ,XML
C
C           Save the Keplerian and equinoctial elements for
C           interpolation; convert angular quantities to radians.
C
C           Y( 1,J) = SMA
C           Y( 2,J) = ECC
C           Y( 3,J) = XINC * DE2RA
C           Y( 4,J) = XLAN * DE2RA
C           Y( 5,J) = AP    * DE2RA
C           Y( 6,J) = XMA   * DE2RA
C           Y( 7,J) = XH
C           Y( 8,J) = XK
C           Y( 9,J) = XP
C           Y(10,J) = XQ
C           Y(11,J) = XML   * DE2RA
C

```

```

200 CONTINUE
C
C          Calculate the angular velocity of mean anomaly
C          and mean longitude.
C
        AVGSMA      =  ( ( Y(1,1) + Y(1,5) ) / 2.0D0 ) ** 3.0D0
        ANGVEL(1)   =  DSQRT ( GM / AVGSMA )
        ANGVEL(2)   =  ANGVEL(1)

C
C          To calculate the linearized values of the angular
C          elements, assume the longitude of ascending node
C          and argument of perigee are constant.
C
        ANGVEL(3)   =  0.0D0
        ANGVEL(4)   =  0.0D0

C
C          Store the sawtooth values of the angular values.
C
        DO 250 J=1,5
C
        ANGSAW(1,J)  =  Y( 6,J)
        ANGSAW(2,J)  =  Y(11,J)
        ANGSAW(3,J)  =  Y( 4,J)
        ANGSAW(4,J)  =  Y( 5,J)

C
        250 CONTINUE
C
C          Calculate the linearized values of the angles.
C
        CALL LINANG ( ANGLIN, ANGSAW, ANGVEL, GINTVL, 4, 5)

C
C          Store the new values of the angular values in the
C          array Y.
C
        DO 270 J=1,5
C
        Y( 6,J)      =  ANGLIN(1,J)
        Y(11,J)     =  ANGLIN(2,J)
        Y( 4,J)      =  ANGLIN(3,J)
        Y( 5,J)      =  ANGLIN(4,J)

C
        270 CONTINUE
C
C          Set a flag to show interpolator coefficients have
C          not been calculated.
C
        ICOEF      =  0

C
C          Calculate the center and upper bound of the
C          interpolation interval.
C
        CENTER    =  ( DAYCNT(5)+DAYCNT(1) ) / 2.0D0
C
        UPRBND   =  CENTER + HAFWID
C

```

```

C           If the interpolation interval is being shifted,
C           omit the next read step (data was previously read).
C
C           IF (ISHIFT .EQ. 1) GO TO 400
C
C           Read in the NORAD observations on file IRN1.
C
C           300 READ (IRN1,3000,END=900) DAYADC,X,YY,Z,DX,DY,DZ,SMA,PR,APR,
C               *           ECC,XINC,XLAN,AP,XMA,H,XK,P,Q,XML
C
C           Check that the date of the data is within the time
C           period for this plot.
C
C           IF ( (DAYADC-DAYREF) .LT. FIRST ) GO TO 300
C
C           IF ( (DAYADC-DAYREF) .GT. FINAL ) GO TO 900
C
C           Increment the counter.
C
C           NUMADC = NUMADC + 1
C
C           Convert angular values to radians and store all
C           the NORAD mean elements in array ELEM.
C
C           ELEM ( NUMADC, 1,1 ) = DAYADC - DAYREF
C           ELEM ( NUMADC, 2,1 ) = X
C           ELEM ( NUMADC, 3,1 ) = YY
C           ELEM ( NUMADC, 4,1 ) = Z
C           ELEM ( NUMADC, 5,1 ) = DX
C           ELEM ( NUMADC, 6,1 ) = DY
C           ELEM ( NUMADC, 7,1 ) = DZ
C           ELEM ( NUMADC, 8,1 ) = SMA
C           ELEM ( NUMADC, 9,1 ) = PR
C           ELEM ( NUMADC,10,1 ) = APR
C           ELEM ( NUMADC,11,1 ) = ECC
C           ELEM ( NUMADC,12,1 ) = XINC * DE2RA
C           ELEM ( NUMADC,13,1 ) = XLAN * DE2RA
C           ELEM ( NUMADC,14,1 ) = AP * DE2RA
C           ELEM ( NUMADC,15,1 ) = XMA * DE2RA
C           ELEM ( NUMADC,16,1 ) = H
C           ELEM ( NUMADC,17,1 ) = XK
C           ELEM ( NUMADC,18,1 ) = P
C           ELEM ( NUMADC,19,1 ) = Q
C           ELEM ( NUMADC,20,1 ) = XML * DE2RA
C
C           Is the time within bounds of the current
C           interpolator interval? If so, calculate the
C           independent variable for the interpolator and
C           increment the counter. If not, shift the
C           interpolator interval by saving the last element
C           set and reading four more element sets. Set a flag
C           to denote a shift is in progress.
C
C           400 IF ( DAYADC .LE. UPRBND ) GO TO 600

```

```

C      ISHIFT      =   1
C      DAYCNT(1)    =   DAYCNT(5)
C
C      DO 500 I=1,11
C
C          Y(I,1)    =   Y(I,5)
C
C      500 CONTINUE
C
C      GO TO 100
C
C      600 CONTINUE
C
C          A new interpolator interval has been found.
C          Calculate the new value of the independent
C          variable and reset the shift flag.
C
C          XVAR      =   (DAYADC - CENTER ) / HAFWID
C
C          ISHIFT     =   0
C
C          Calculate the interpolator coefficients for this
C          period if the coefficient flag is off. Then turn
C          the flag on.
C
C          IF ( ICOEF .EQ. 0 ) THEN
C
C              CALL LAGRAN ( COEF, Y, 11, 5 )
C
C              ICOEF     =   1
C
C          END IF
C
C          Interpolate the equinoctial and Keplerian
C          elements for the date DAYADC.
C
C          CALL INTERP ( POLY, COEF, XVAR, 11, 5 )
C
C          Convert from equinoctial elements to Cartesian
C          elements.
C
C          EQNELM (1)    =   POLY ( 1)
C          EQNELM (2)    =   POLY ( 7)
C          EQNELM (3)    =   POLY ( 8)
C          EQNELM (4)    =   POLY ( 9)
C          EQNELM (5)    =   POLY (10)
C          EQNELM (6)    =   POLY (11)
C
C          RETRO        =   1.00
C
C          CALL CARTES (POS, VEL, EQNELM, RETRO, GM)
C

```

```

C           Store the interpolated elements in array ELEM.
C
C           ELEM (NUMADC, 2,2) = POS(1)
C           ELEM (NUMADC, 3,2) = POS(2)
C           ELEM (NUMADC, 4,2) = POS(3)
C           ELEM (NUMADC, 5,2) = VEL(1)
C           ELEM (NUMADC, 6,2) = VEL(2)
C           ELEM (NUMADC, 7,2) = VEL(3)
C           ELEM (NUMADC, 8,2) = POLY(1)
C           ELEM (NUMADC, 9,2) = POLY(1) * ( 1.00 - POLY(2) )
C           ELEM (NUMADC,10,2) = POLY(1) * ( 1.00 + POLY(2) )
C           ELEM (NUMADC,11,2) = POLY(2)
C           ELEM (NUMADC,12,2) = POLY(3)
C           ELEM (NUMADC,13,2) = POLY(4)
C           ELEM (NUMADC,14,2) = POLY(5)
C           ELEM (NUMADC,15,2) = POLY(6)
C           ELEM (NUMADC,16,2) = POLY(7)
C           ELEM (NUMADC,17,2) = POLY(8)
C           ELEM (NUMADC,18,2) = POLY(9)
C           ELEM (NUMADC,19,2) = POLY(10)
C           ELEM (NUMADC,20,2) = POLY(11)

C
C           Calculate the differences between the GTDS
C           predictions and the NORAD mean elements.
C
C           DO 660 J=2,20
C
C           DIFF(NUMADC,J) = ELEM(NUMADC,J,2) - ELEM(NUMADC,J,1)
C
C           Filter the angular elements....
C
C           IF ( J.EQ.12 .OR. J.EQ.13 .OR. J.EQ.14
C                .OR. J.EQ.15 .OR. J.EQ.20 ) THEN
C
C               Calculate the modulus by two pi and convert to
C               degrees.
C
C               I = ELEM(NUMADC,J,1) / TWOPI
C               ELEM(NUMADC,J,1) = ELEM(NUMADC,J,1) - I * TWOPI
C
C               ELEM(NUMADC,J,1) = ELEM(NUMADC,J,1) / DE2RA
C
C               IF ( ELEM(NUMADC,J,1) .LT. 0.00 )
C                    ELEM(NUMADC,J,1) = ELEM(NUMADC,J,1) + 360.00
C
C               Calculate the modulus by two pi and convert to
C               degrees.
C
C               I = ELEM(NUMADC,J,2) / TWOPI
C               ELEM(NUMADC,J,2) = ELEM(NUMADC,J,2) - I * TWOPI
C
C               ELEM(NUMADC,J,2) = ELEM(NUMADC,J,2) / DE2RA
C
C               IF ( ELEM(NUMADC,J,2) .LT. 0.00 )

```

```

*           ELEM(NUMADC,J,2) = ELEM(NUMADC,J,2) + 360.D0
C
C           Calculate the modulus by two pi and convert to
C           degrees.
C
I = DIFF(NUMADC,J) / TWOPI
DIFF(NUMADC,J) = DIFF(NUMADC,J) - I * TWOPI
C
DIFF(NUMADC,J) = DIFF(NUMADC,J) / DE2RA
C
C           Constrain the difference to be between
C           minus pi and plus pi.
C
IF ( DIFF(NUMADC,J) .GT. 180.D0 )
*     DIFF(NUMADC,J) = DIFF(NUMADC,J) - 360.D0
C
IF ( DIFF(NUMADC,J) .LT. -180.D0 )
*     DIFF(NUMADC,J) = DIFF(NUMADC,J) + 360.D0
C
ENDIF
C
660 CONTINUE
C
C           Save the four position and velocity vectors in a
C           separate array.
C
DO 700 I=1,6
C
VECT2(I) = ELEM (NUMADC, I+1, 2 )
C
VECT1(I) = ELEM (NUMADC, I+1, 1 )
C
700 CONTINUE
C
C           Call the subroutine RCAERR to calculate the
C           radial, cross-track, and along-track errors in
C           position .
C
CALL RCAERR ( VECT1, VECT2, ERROR )
C
C           Store the errors in the array ELEM.
C
DO 750 I=1,3
C
ELEM (NUMADC, I+20, 1) = ERROR (I)
C
750 CONTINUE
C
C           Read the next DAYADC date.
C
GO TO 300
C
C           If there are insufficient ORB1 data records to

```

```

C           interpolate for every NORAD mean element record,
C           reduce the number of element sets plotted.
C
C     800 NUMADC = NUMADC - 1
C
C     900 CONTINUE
C
C           ****
C           PLOT4B DATA CARDS
C           ****
C
C           Write the array ELEM into the data set
C           formatted by the control card for the
C           plotting program.
C
C     DO 1200 J=2,20
C
C           XMEAN(J) = 0.0D0
C           SIGMA(J) = 0.0D0
C
C     DO 1000 I=1,NUMADC
C
C           Write element comparisons into file 41.
C
C           WRITE (41,4000) ELEM (I,1,1), ELEM (I,J,1), ELEM (I,J,2)
C
C           Calculate the mean difference.
C
C           XMEAN(J) = XMEAN(J) + DABS ( ELEM(I,J,2) - ELEM(I,J,1) )
C
C     1000   CONTINUE
C
C           XMEAN(J) = XMEAN(J) / NUMADC
C
C           Calculate the standard deviation.
C
C     DO 1100 I=1,NUMADC
C
C           SIGMA(J) = SIGMA(J) +
C           *      ( DABS( ELEM(I,J,2)-ELEM(I,J,1) ) -
C           *      XMEAN(J) ) ** 2
C
C     1100   CONTINUE
C
C           SIGMA(J) = DSQRT ( SIGMA(J) / (NUMADC-1) )
C
C     1200 CONTINUE
C
C           Write the radial, cross-track, and along-track
C           errors into file 41.
C
C     DO 1300 J=21,23
C
C           DO 1300 I=1,NUMADC

```

```

C
      WRITE (41,4100) ELEM (I,1,1), ELEM (I,J,1)
C
1300 CONTINUE
C
C           Write the difference between the GTDS-generated
C           elements and the NORAD mean elements into file 41.
C
      DO 1400 J=2,20
C
      DO 1400 I=1,NUMADC
C
      WRITE (41,4100) ELEM (I,1,1), DIFF (I,J)
C
1400 CONTINUE
C
C           ****
C           PLOT4B CONTROL CARDS
C           ****
C
C           Write the PLOT4B control cards for the
C           comparison plots.
C
C
      DO 1500 J=2,20
C
C
      WRITE (40,5000) NUMADC, SVDESG, MTITLE(J), START,
      *                   STITLE(1),STITLE(2),
      *                   XMEAN(J), SIGMA(J), NUMADC
C
      WRITE (40,5010) FIRST, FINAL, YTITLE(J)
C
C
1500 CONTINUE
C
C           Write the PLOT4B control cards for the
C           error plots.
C
C
      DO 1600 J=1,3
C
      WRITE (40,5100) NUMADC, SVDESG, DTITLE(J), START,
      *                   STITLE(1),STITLE(2)
C
      WRITE (40,5110) FIRST, FINAL, ETITLE(J)
C
C
1600 CONTINUE
C
C           Write the PLOT4B control cards for the
C           difference plots.
C
C
      DO 1700 J=2,20
C

```

```

        WRITE (40,5200) NUMADC,SVDESG, MTITLE(J), START,
        *                      STITLE(2),STITLE(1)
C
C           WRITE (40,5210) FIRST, FINAL, YTITLE(J)
C
1700 CONTINUE
C
C           Write final PLOT4B control card.
C
C           WRITE (40,5400)
C
C           STOP
C
C***** Format statements *****
C
C           Control cards
C
2000 FORMAT ( 49X,A7/49X,F7.0/49X,F7.0/49X,F7.0/49X,F7.0/
        *          49X,I2/49X,A5/49X,I2/49X,A5 )
C
2100 FORMAT ( 49X,F10.2 )
C
C           Input files
C
3000 FORMAT ( 3X,G19.10/ 6 (3X,G19.10,10X,G19.10,10X,G19.10/ ),
        *          3X,G19.10 )
C
C           PLOT4B data cards
C
4000 FORMAT ( F8.3,2(3X,G19.10) )
C
4100 FORMAT ( F8.3,3X,G19.10 )
C
C           PLOT4B control cards
C
5000 FORMAT
        * (*DATA      NUMVAR      3                  ' /
        *      '       NOREWIND   ',I4                  /
        *      '       FMTDATA    1                  ' /
        *      ' ( F8.3,2(3X,G19.10) )                ' /
        *      ' *TITLE    MAINTITL   0                  ' /
        *      ' A7,A28                                /
        *      '       AXTITL    0                  ' /
        *      ' DAYS ELAPSED SINCE ',F7.0              /
        *      ' A5                                    /
        *      ' A5                                    ' /
        *      '       SUBTITL                           ' /
        *      ' MEAN DIFFERENCE: ',G11.5,1X,'SIGMA: ',G11.5,1X,
        *      ' AFTER ',I4,' COMPARISONS'                 )
C
5010 FORMAT
        * (*PLOTMOD YSCALE                   ' /
        *      '          0.          0.                  ' /
        *      '          XSCALE                   ' /

```

```

*      0.      0.      ' '
*      XLIMIT      ' '
*      ,F7.0,'     ,F7.0      ' '
*      NOZERO      1      ' '
*      BADPOINT    1002      ' '
*      SCATTER      1      ' '
*      /*PLOT      TITLPLOT      ' '
*      LEGEND      1      ' '
*      2 3      ' '
*      BLKPLOT    200      ' '
*      A7      ' '
*      1 1 2 3      ' ')

```

C

5100 FORMAT

```

* /*DATA  NUMVAR    2      ' '
*      NOREWIND ',I4      ' '
*      FMTDATA    1      ' '
*      '( F8.3,3X,G19.10 )      ' '
*      /*TITLE  MAINTITLE  0      ' '
*      A7,A28      ' '
*      AXTITLE    0      ' '
*      'DAYS ELAPSED SINCE ',F7.0      ' '
*      'ERROR      ' '
*      SUBTITLE      ' '
*      A5,' (ESTIMATED); ,A5,' (TRUTH)      ' ')

```

C

5110 FORMAT

```

* /*PLOTMOD YSCALE      ' '
*      0.      0.      ' '
*      XSCALE      ' '
*      0.      0.      ' '
*      XLIMIT      ' '
*      ,F7.0,'     ,F7.0      ' '
*      NOZERO      1      ' '
*      BADPOINT    1002      ' '
*      SCATTER      1      ' '
*      /*PLOT      TITLPLOT      ' '
*      LEGEND      1      ' '
*      2      ' '
*      BLKPLOT    200      ' '
*      A7      ' '
*      1 1 2      ' ')

```

C

5200 FORMAT

```

* /*DATA  NUMVAR    2      ' '
*      NOREWIND ',I4      ' '
*      FMTDATA    1      ' '
*      '( F8.3,3X,G19.10 )      ' '
*      /*TITLE  MAINTITLE  0      ' '
*      A7,A28      ' '
*      AXTITLE    0      ' '
*      'DAYS ELAPSED SINCE ',F7.0      ' '
*      'DELTA      ' '
*      SUBTITLE      ' '

```

```
* 'COMPARISON DIFFERENCE: DELTA = ',A5,'--',A5 )  
C  
5210 FORMAT  
* (*PLOTMOD YSCALE /  
* ' 0. 0. /  
* XSCALE /  
* ' 0. 0. /  
* XLIMIT /  
* ',F7.0,',F7.0 /  
* NOZERO 1 /  
* BADPOINT 1002 /  
* SCATTER 1 /  
* **PLOT TITLPLOT /  
* LEGEND 1 /  
* 2 /  
* BLKPLOT 200 /  
* A7 /  
* 1 1 2 / )  
C  
5400 FORMAT (*END LAST)  
END
```

C PROGRAM RUNADCOB
C
C
C
C *****
C FUNCTION
C *****
C
C
C This program reads an ADCOM observation card file and writes a
C GTDS card file.
C
C
C INPUT *****
C
C File 5 ADCOM observation cards.
C
C File 8 Station acronyms.
C LWE1122.ORBIT.STATFILE.DATA
C
C OUTPUT *****
C
C File 6 Printer messages.
C
C File 7 GTDS observation cards.
C
C
C /OBSDAT/ *****
C
C Observation time computed in subroutine DATE.
C
C DAYOBS I Julian date at noon on day of observation.
C SECOPS I Time of observation in seconds from noon.
C (Range: -43200 to almost 43200)
C
C YMDOBS I Calendar date packed in the form YYMMDD.
C HMSOBS I Time of day packed in the form HHMMSS.SSSSS
C
C YEAR I Year - 1900.
C MONTH I Month.
C DAY I Day.
C
C HOUR I Hour.
C MINUTE I Minute.
C SECOND I Second.
C
C
C SUBROUTINES CALLED *****
C

C DATE RANGES AZIMUT ELEVAT RANGER ASTRON
C
C
C
C ***** HISTORY *****
C
C
C
C
C VERSION: October 1986
C Fortran main program for the IBM 3090.
C
C ANALYSIS
C Joe F. Lombardo -- Charles Stark Draper Laboratory
C
C PROGRAMMER
C Joe F. Lombardo -- Charles Stark Draper Laboratory
C
C
C MODIFIED ----- Leo W. Early, Jr.
C Oct 1986 ----- Charles Stark Draper Laboratory
C
C 1. Converted from FORTRAN 66 to FORTRAN 77.
C 2. Replaced algorithm used to find station acronym. Old
C algorithm searched entire station array. New algorithm
C uses a single array reference.
C 3. Improved code structure.
C 4. NEW -- Print lists of known stations used and unknown
C stations used.
C
C MODIFIED ----- Leo W. Early, Jr.
C Dec 1986 ----- Charles Stark Draper Laboratory
C
C 1. Output GTDS observation cards in standard GTDS observation
C card order.
C 2. Transform coordinates of optical observations (right ascen-
C sion and declination) from NORAD to mean-of-1950.0 coordinate
C system.
C 3. Suppress output of observation cards for unknown stations.
C
C MODIFIED ----- Leo W. Early, Jr.
C Dec 1986 ----- Charles Stark Draper Laboratory
C
C 1. Add coordinate system for optical observations. See subrou-
C tine ASTRON.
C
C
C ***** DECLARATIONS *****
C
C
C IMPLICIT DOUBLE PRECISION (A-H,O-Z)
C

```

C      /OBSDAT/ *****
C
C      INCLUDE      (OBSDAT)
C
C
C      Constants *****
C
C          Maximum station ID number.
C
C          PARAMETER      (NSTAT      =    999
C
C
C
C      Character Variables *****
C
C          CHARACTER * 1    LEL           ,LRA
C          CHARACTER * 1    LELR          ,LAXR
C          CHARACTER * 1    LAC           ,EQNYR
C          CHARACTER * 4    STANAM        ,STNAME (0:NSTAT)
C          CHARACTER * 4    NULSTA
C
C      Numeric Data Types *****
C
C          LOGICAL         OBSERV (0:NSTAT)
C
C
C
C***** DATA STATEMENTS *****
C
C
C
C          Null station acronym.
C
C          DATA NULSTA    / '****' /
C
C          Number of observations ignored.
C
C          DATA NACC      / 0 /
C          DATA NCOS      / 0 /
C          DATA NCOSR     / 0 /
C
C
C
C***** BEGIN PROGRAM *****
C
C
C
C          *****
C          READ STATION LIST
C          *****
C
C
C

```

```

C           Fill station list with null acronyms.
C
C
DO 10 ISTNUM = 0,NSTAT
STNAME (ISTNUM)    =  NULSTA
10 CONTINUE
C
C           Read station acronyms from station file.
C
20 CONTINUE
READ  (8,4000,END=30)  ISTNUM,STANAM
STNAME (ISTNUM)    =  STANAM
GO TO 20
C
C           Set station observation indicators -- there are no
C           observations for any station.
C
30 DO 40 ISTNUM = 0,NSTAT
OBSERV (ISTNUM)    =  .FALSE.
40 CONTINUE
C
C
C
C           *****
C           WRITE GTDS OBSERVATION CARDS
C           *****
C
C
C           *****
C           BEGIN FILE   *****
C
C           Write OBSCARD card.
C
WRITE  (7,3000)  'OBSCARD '
C
C
C           *****
C           READ ADCOM CARD   *****
C
C           Read ADCOM observation card.
C
100 CONTINUE
READ  (5,1000,END=300)  ISTNUM,  IYR, IDAY, IHR, IMIN, SEC,
*      LEL,ELEV,  IAZORA,  RNGE,IRX,  LRA,RATR,
*      LELR,ELRR,  LAXR,AZRR,  LAC,ACC,  ITYPE,EQNYK
C
C           Find character codes.
C
ILEL    =  ICHAR (LEL)
ILRA    =  ICHAR (LRA)
ILELR   =  ICHAR (LELR)
ILAXR   =  ICHAR (LAXR)
ILAC    =  ICHAR (LAC)
C
C           Compute Julian date and GTDS calendar date.

```

```

C
      CALL DATE (IYR, IDAY, IHR, IMIN, SEC)
C
C           Compute GTDS observation card date.
C
C           OBSTIM = YMDOBS * 1.D6 + HMSOBS
C
C           Find station name.
C
C           STANAM = STNAME (ISTNUM)
C
C           Branch to code for this observation type.
C
C           GO TO (200,205,210,215,220, 225,230,235,240,245),
C           * ITYPE + 1
C
C
C           **** WRITE GTDS CARDS ****
C
C           ----- ADCOM type 0 -----
C
C           Range rate.          (GTDS type 9)
C
C
200     IF (STANAM .NE. NULSTA) THEN
      CALL RANGER (ILRA,RATR, RATE, STANAM,OBSTIM)
      END IF
      OBSERV (ISTNUM) = .TRUE.
      GO TO 100
C
C           ----- ADCOM type 1 -----
C
C           Azimuth.          (GTDS type 4)
C           Elevation.        (GTDS type 5)
C
C
205     IF (STANAM .NE. NULSTA) THEN
      CALL AZIMUT (IAZORA, AZMTH, STANAM,OBSTIM)
      CALL ELEVAT (ILEL,ELEVR, ELEV, STANAM,OBSTIM)
      END IF
      OBSERV (ISTNUM) = .TRUE.
      GO TO 100
C
C           ----- ADCOM type 2 -----
C
C           Range.            (GTDS type 1)
C           Azimuth.          (GTDS type 4)
C           Elevation.        (GTDS type 5)
C
C
210     IF (STANAM .NE. NULSTA) THEN
      CALL RANGES (RNGE,IRX, RANGE, STANAM,OBSTIM)
      CALL AZIMUT (IAZORA, AZMTH, STANAM,OBSTIM)
      CALL ELEVAT (ILEL,ELEVR, ELEV, STANAM,OBSTIM)
      END IF
      OBSERV (ISTNUM) = .TRUE.

```

```

GO TO 100
C
C          ----- ADCOM type 3 -----
C
C          Range.           (GTDS type 1)
C          Azimuth.         (GTDS type 4)
C          Elevation.       (GTDS type 5)
C          Range rate.     (GTDS type 9)
C
215      IF (STANAM .NE. NULSTA) THEN
    CALL  RANGES  (RNGE,IRX,      RANGE,  STANAM,OBSTIM)
    CALL  AZIMUT  (IAZORA,       AZMTH,  STANAM,OBSTIM)
    CALL  ELEVAT  (ILEL,ELEVR,   ELEV,   STANAM,OBSTIM)
    CALL  RANGER  (ILRA,RATR,   RATE,   STANAM,OBSTIM)
END IF
OBSERV (ISTNUM) = .TRUE.
GO TO 100
C
C          ----- ADCOM type 4 -----
C
C          Range.           (GTDS type 1)
C          Azimuth.         (GTDS type 4)
C          Elevation.       (GTDS type 5)
C          Range rate.     (GTDS type 9)
C          Range acceleration.
C          Azimuth rate.
C          Elevation rate.
C
220      IF (STANAM .NE. NULSTA) THEN
    CALL  RANGES  (RNGE,IRX,      RANGE,  STANAM,OBSTIM)
    CALL  AZIMUT  (IAZORA,       AZMTH,  STANAM,OBSTIM)
    CALL  ELEVAT  (ILEL,ELEVR,   ELEV,   STANAM,OBSTIM)
    CALL  RANGER  (ILRA,RATR,   RATE,   STANAM,OBSTIM)
END IF
OBSERV (ISTNUM) = .TRUE.
NACC      = NACC + 1
GO TO 100
C
C          ----- ADCOM type 5 -----
C
C          Right ascension.   (GTDS type 6)
C          Declination.      (GTDS type 7)
C
225      IF (STANAM .NE. NULSTA) THEN
    CALL  ASTRON  (IAZORA,ILEL,ELEVR,  EQNYR,  STANAM)
END IF
OBSERV (ISTNUM) = .TRUE.
GO TO 100
C
C          ----- ADCOM type 6 -----
C
C          Range.           (GTDS type 1)
C
230      IF (STANAM .NE. NULSTA) THEN

```

```

        CALL    RANGES  (RNGE,IRX,      RANGE,   STANAM,OBSTIM)
END IF
OBSERV (ISTNUM) = .TRUE.
GO TO 100
C
C          ----- ADCOM type 7 -----
C
C          Direction cosines.
C
235    NCOS   =   NCOS + 1
GO TO 100
C
C          ----- ADCOM type 8 -----
C
C          Range.           (GTDS type 1)
C          Direction cosines.
C
240    IF     (STANAM .NE. NULSTA) THEN
        CALL    RANGES  (RNGE,IRX,      RANGE,   STANAM,OBSTIM)
END IF
OBSERV (ISTNUM) = .TRUE.
NCOSR       =   NCOSR + 1
GO TO 100
C
C          ----- ADCOM type 9 -----
C
C          Range.           (GTDS type 1)
C          Range rate.      (GTDS type 9)
C          Direction cosines.
C
245    IF     (STANAM .NE. NULSTA) THEN
        CALL    RANGES  (RNGE,IRX,      RANGE,   STANAM,OBSTIM)
        CALL    RANGER  (ILRA,RATR,     RATE,    STANAM,OBSTIM)
END IF
OBSERV (ISTNUM) = .TRUE.
NCOSR       =   NCOSR + 1
GO TO 100
C
C
C          ***** END FILE *****
C
C          Write END card.
C
300 WRITE (7,3000) 'END'
C
C
C          *****
C          PRINT STATISTICS
C          *****
C

```

```

C           ***** LIST OF KNOWN STATIONS *****
C
C           Print heading -- List of known stations used.
C
WRITE (6,2000)
LINE = 5
C
C           Are there observations for this station?
C           Is this station known?
C
DO 410 ISTNUM = 0,NSTAT
  IF (OBSERV (ISTNUM) .AND.
*     STNAME (ISTNUM) .NE. NULSTA) THEN
C
C           Print blank line after every five station names.
C
LINE = LINE + 1
IF (LINE .GT. 5) THEN
  LINE = 1
  WRITE (6,2110)
END IF
C
C           Print station number and acronym.
C
WRITE (6,2100) ISTNUM, STNAME (ISTNUM)
END IF
410 CONTINUE
C
C
C           ***** LIST OF UNKNOWN STATIONS *****
C
C           Print heading -- List of unknown stations used
C
WRITE (6,2010)
LINE = 5
C
C           Are there observations for this station?
C           Is this station unknown?
C
DO 420 ISTNUM = 0,NSTAT
  IF (OBSERV (ISTNUM) .AND.
*     STNAME (ISTNUM) .EQ. NULSTA) THEN
C
C           Print blank line after every five station names
C
LINE = LINE + 1
IF (LINE .GT. 5) THEN
  LINE = 1
  WRITE (6,2110)
END IF
C
C           Print station number and acronym
C

```

MD-R105 825

AN EVALUATION OF SEMIANALYTICAL SATELLITE THEORY
AGAINST LONG ARCS OF REA. (U) AIR FORCE INST OF TECH
WRIGHT-PATTERSON AFB OH M E FIEGER JAN 87

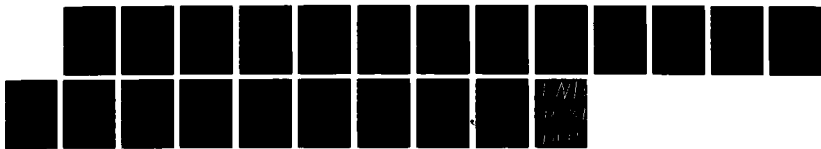
3/3

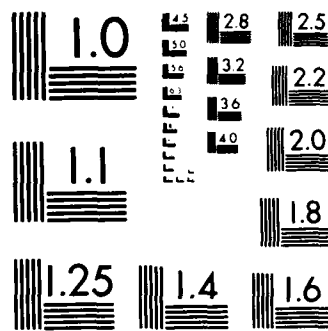
UNCLASSIFIED

AFIT/CI/NR-87-52T

F/G 22/3

NL





MICROCOPY RESOLUTION TEST CHART
NATIONAL BUREAU OF STANDARDS 1963 A

```

        WRITE (6,2100) ISTNUM, NULSTA
        END IF
420 CONTINUE
C
C
C
C           ***** IGNORED OBSERVATIONS *****
C
C           Print number of non-GTDS observations ignored.
C
        WRITE (6,2200) NACC,NCOSR,NCOS
        STOP
C
C
C
C***** FORMAT STATEMENTS *****
C
C
C
C           ADCOM observation cards.
C
1000 FORMAT( T7, I3, I2,I3,I2,I2,F5.3,
           *      A1,F5.4,1X,   I7,1X,   F7.5,I1,1X,   A1,F6.5,1X,
           *      A1,F4.4,1X,   A1,F4.4,1X,   A1,F4.4,2X,   I1,A1)
C
C           Printer messages.
C
2000 FORMAT( /// '***** Known Stations Used *****',
           *      '***** //'
           *      ' This list includes all known stations in the ',
           *      'ADCOM observation file which generated GTDS-usable' /
           *      ' observations.' )
2010 FORMAT( /// '***** Unknown Stations Used *****',
           *      '***** //'
           *      ' This list includes all unknown stations in the ',
           *      'ADCOM observation file which generated GTDS-usable' /
           *      ' observations.' )
2100 FORMAT( 1X,I5,   10X,A4 )
2110 FORMAT( 1X )
2200 FORMAT( /// '***** Non-GTDS Observations Found *****',
           *      '***** //'
           *      '1X,I5,' Elevation rate, azimuth rate, and range ',
           *      'acceleration triples were found.' /
           *      '1X,I5,' Direction cosine pairs were found on range'',
           *      'range-rate/direction-cosine cards.' /
           *      '1X,I5,' Direction cosine only cards were found.' //
           *      ' All non-GTDS observations found were ignored.' )
C
C           GTDS observation cards.
C
3000 FORMAT( A8 )
C
C           Station acronyms.
C

```

```
4000 FORMAT( 2X,I3,    5X,A4 )
      END
```

```

SUBROUTINE ASTRON (IAZORA,IILEL,ELEVR, EQNYR, STANAM)
C
C
C
C      *****
C      FUNCTION
C      *****
C
C
C
C      This subroutine writes an ADCOM optical observation pair
C      (right ascension and declination) onto a pair of standard
C      GTDS observation cards.
C
C
C      CALLING SEQUENCE *****
C
C      CALL ASTRON (IAZORA,IILEL,ELEVR, EQNYR, STANAM)
C
C      PARAMETERS *****
C
C          IAZORA   I    Right ascension.           (HHMMSS.S)
C          IILEL    I    Declination -- first digit with overpunch.
C          ELEVR    I    Declination -- later digits. (D.DDDD)
C
C          EQNYR   I    Coordinate system of observation.
C
C          '0'     NORAD true of date at time of obser-
C                  vation
C
C          '1'     mean of 1900.0
C          '2'     mean of 1920.0
C          '3'     mean of 1950.0
C          '4'     mean of 1975.0
C          '5'     mean of 2000.0
C          '6'     mean of 1850.0
C          '7'     mean of 1855.0
C          '8'     mean of 1875.0
C          '9'     mean of 1960.0
C
C          'X'     NORAD true of date at beginning of
C                  Besselian year of observation
C
C          'Y'     NORAD true of date at midnight, Jan 0,
C                  of year of observation
C
C          STANAM  I    Station name.
C
C
C      /OBSDAT/ *****

```

C Observation time computed in subroutine DATE.
C
C DAYOBS I Julian date at noon on day of observation.
C SEC OBS I Time of observation in seconds from noon.
C (Range: -43200 to almost 43200)
C
C YMDOBS I Calendar date packed in the form YYMMDD.
C HMSOBS I Time of day packed in the form HHMMSS.SSSSS
C
C YEAR I Year - 1900.
C MONTH I Month.
C DAY I Day.
C
C HOUR I Hour.
C MINUTE I Minute.
C SECOND I Second.
C
C
C SUBROUTINES CALLED *****
C
C PRENUT VEMA33
C
C
C***** HISTORY *****
C
C
C
C VERSION: December 1986
C Fortran subroutine for the IBM 3090.
C
C ANALYSIS
C Leo W. Early, Jr. -- Charles Stark Draper Laboratory
C
C PROGRAMMER
C Leo W. Early, Jr. -- Charles Stark Draper Laboratory
C
C
C***** DECLARATIONS *****
C
C
C
C IMPLICIT DOUBLE PRECISION (A-H,O-Z)
C
C /OBSDAT/ *****
C
C INCLUDE (OBSDATA*)
C
C
C Constants *****
C

```

C          Number of mean-of-reference coordinate systems used
C          for optical observations.
C
C          PARAMETER      (NCOORD = 9 ) )
C
C
C          Character Variables *****
C
C          CHARACTER * 1   EQNYR
C          CHARACTER * 4   STANAM
C
C          Numeric Data Types *****
C
C          LOGICAL        INIT
C
C          Dimensions *****
C
C          DIMENSION      UNIT (3)           ,YRCORD (NCOORD)
C          DIMENSION      ROTATE (3,3)
C
C          Saved Variables *****
C
C          SAVE          INIT
C
C
C          ***** DATA STATEMENTS *****
C
C
C
C          ***** MATHEMATICAL CONSTANTS *****
C
C          Ratio of circumference of circle to diameter.
C
C          DATA HALFPI    / 1.5707 96326 79489 66 D 0 /
C          DATA TWOPI     / 6.2831 85307 17958 65 D 0 /
C
C          Degrees to radians.
C
C          DATA DEGREE    / 1.7453 29251 99432 96 D -2 /
C
C
C
C          ***** TIME PARAMETERS *****
C
C
C          Reference epoch and Julian date of mean-of-1950.0
C          coordinate system.
C
C          DATA YRREF     / 1950.          D 0 /
C          DATA DAYREF    / 24332 82.423   D 0 /
C          DATA SECREF    / 0.            D 0 /
C
C          Reference epochs of observation coordinate systems.

```

```

C
DATA YRCORD (1)      / 1900.  D 0  /
DATA YRCORD (2)      / 1920.  D 0  /
DATA YRCORD (3)      / 1950.  D 0  /
DATA YRCORD (4)      / 1975.  D 0  /
DATA YRCORD (5)      / 2000.  D 0  /
DATA YRCORD (6)      / 1850.  D 0  /
DATA YRCORD (7)      / 1855.  D 0  /
DATA YRCORD (8)      / 1875.  D 0  /
DATA YRCORD (9)      / 1960.  D 0  /

C
C           Length of the tropical year.   (seconds)
C
DATA TROPIC      / 31556.925.97 47  D 0  /

C
C           Secular acceleration constant used to convert from
C           Besselian years to tropical years.   (inverse years)
C
DATA BESACC      / 2.345  D -11  /

C
C
C
C           ***** CONTROL PARAMETERS *****
C
C           Initialize this subroutine on the next call.
C
DATA INIT      / .TRUE.  /

C
C
C
C           ***** BEGIN PROGRAM *****
C
C
C
C           *****
C           INITIALIZE
C           *****
C
C
C
C           Initialize subroutine?
C
C
IF  (INIT)  THEN
C
C           Compute unit used to measure right ascension
C
TENSEC  *  DEGREE / 2400.00
C
C           Compute length of tropical year in ephemeris days
C
TROPIC  =  TROPIC / 86400.00
C
C           Compute reference epochs of coordinate systems in
C           years since 1900

```

```

C
      YRREF = YRREF - 1900.00
      DO 10 I = 1,NCOORD
         YRCORD (I) = YRCORD (I) - 1900.00
10    CONTINUE

C
C           This subroutine has been initialized.

C
      INIT = .FALSE.
      END IF

C
C
C
C           *****
C           CONVERT ANGLES
C           *****
C
C
C           *****
C           RIGHT ASCENSION *****
C
C
C           Unpack right.
C
      ISEC = IAZORA
      IMIN = ISEC / 1000
      IHOUR = IMIN / 100

C
C           Unpack left.

C
      RAHOUR = IHOUR
      RAMIN = IMIN - 100 * IHOUR
      RASEC = ISEC - 1000 * IMIN

C
C           Convert to tenth-seconds of time.

C
      ALPHA = RAHOUR + RAMIN + 600.00 + RASEC

C
C           Convert to radians.

C
      ALPHA = ALPHA * TENSEC

C
C
C           *****
C           DECLINATION *****
C
C
C           Convert initial blank to + 0

C
      IF (ILEL .EQ. 64) ILEL = 240

C
C           Convert initial minus sign to - 0

C
      IF (ILEL .EQ. 96) ILEL = 208

C
C           Declination is positive -- first digit numeric.

```

```

C
IF (ILEL .GE. 240) THEN
    DELTA = (ILEL - 240) * 10 + ELEVR
C
C           Declination is negative -- first digit overpunched.
C
ELSE
    DELTA = - (ILEL - 208) * 10 - ELEVR
END IF
C
C           Convert to radians.
C
DELTA = DELTA * DEGREE
C
C
C           *****
C           COMPUTE ROTATION MATRIX
C           *****
C
C
C           ***** NORAD TRUE-OF-DATE *****
C
C           Does observation use NORAD true-of-date coordinate
C           system?
C
IF (EONYR'.EQ. '0') THEN
C
Compute time of observation in ephemeris days since
C           1950.0.
C
WARNING: This computation ignores leap seconds.
C
TIME = (DAYOBS - DAYREF) +
       (SEC OBS - SECREF) / 86400.00
C
Compute transformation matrix from mean-of-1950.0
C           coordinates to NORAD true-of-date coordinates.
C
CALL PRENUT (ROTATE, TIME,'FULL')
C
C
C           ***** NORAD TRUE-OF-BESSELIAN *****
C
C           Does observation use the NORAD true-of-date coord-
C           inate system at the beginning of the Besselian
C           year?
C
ELSE IF (EONYR'.EQ. 'X') THEN
C
Compute time at beginning of Besse an year in
C           ephemeris days since 1950.0

```

```

C
      AVRYR = 1.0D - BESACC * (YRREF + YEAR)
      TIME = (YEAR - YRREF) * AVRYR * TROPIC
C
C          Compute transformation matrix from mean-of-1950.0
C          coordinates to NORAD true-of-Besselian coordinates.
C
      CALL PRENUT (ROTATE, TIME,'FULL')

C
C
C          **** NORAD TRUE-OF-JAN-0.0 ****
C
C          Does observation use the NORAD true-of-date coord-
C          inate system at midnight on Jan 0 of the year of
C          observation?
C
      ELSE IF (EQNYR .EQ. 'Y') THEN
C
C          Compute Julian date of Jan 0.0 of year of
C          observation.
C
      CALL JULIAN (DAYJUL,SECJUL, YEAR,1.0D,C.0D,
                    0.0D,0.0D,0.0D)

C
C          Compute time of Jan 0.0 of year of observation in
C          ephemeris days since 1950.0.
C
C          WARNING: This computation ignores leap seconds.
C
      TIME = (DAYJUL - DAYREF) +
              (SECJUL - SECREF) / 86400.0D
C
C          Compute transformation matrix from mean-of-1950.0
C          coordinates to NORAD true-of-Jan-0.0 coordinates.
C
      CALL PRENUT (ROTATE, TIME,'FULL')

C
C
C          **** MEAN-OF-REFERENCE ****
C
C          Does observation use a mean-of-reference coordinate
C          system?
C
      ELSE IF (EQNYR .GE. '1' .AND. EQNYR .LE. '9') THEN
C
C          Find reference epoch of observation coordinate
C          system.
C
      READ (EQNYR, '(I1)') IYEAR
C
C          If reference epoch of observation coordinate system
C          is 1950.0 then leave observation unchanged.

```

```

C
IF      (YRCORD (IYEAR) .EQ. YRREF)   GO TO 400
C
C           Compute time of reference epoch in ephemeris days
C           since 1950.0.
C
AVRYR  =  1.0D - BESACC * (YRREF + YRCORD (IYEAR))
TIME   =  (YRCORD (IYEAR) - YRREF) * AVRYR * TROPIC
C
C           Compute transformation matrix from mean-of-1950.0
C           coordinates to mean-of-reference coordinates.
C
CALL    PRENUT  (ROTATE,    TIME,'PRECES')
C
C
C           **** NO COORDINATE SYSTEM *****
C
C           Write error message.
C
ELSE
WRITE  (6,1000)  ALPHA,YMDOBS,   DELTA,HMSOBS,   EQNYR
C
C           Leave observation unchanged.
C
GO TO 400
END IF
C
C
C           *****
C           TRANSFORM OBSERVATION
C           *****
C
C
C           **** FIND UNIT VECTOR *****
C
C           Compute cosine of declination.
C
COSDEL  =  COS (DELTA)
C
C           Compute unit vector from right ascension and
C           declination.
C
UNIT (1)  =  COS (ALPHA) * COSDEL
UNIT (2)  =  SIN (ALPHA) * COSDEL
UNIT (3)  =  SIN (DELTA)
C
C
C           **** TRANSFORM COORDINATES *****
C
C           Transform unit vector from observation coordinate

```

```

C           system to mean-of-1950.0 coordinate system.
C
C           CALL    VEMA33   (UNIT,   UNIT,ROTATE)
C
C
C           **** FIND ANGLES ****
C
C           Compute magnitude of equatorial component of unit
C           vector.
C
C           UNIEQU = UNIT (1) * UNIT (1) + UNIT (2) * UNIT (2)
C           UNIEQU = SQRT (UNIEQU)
C
C           Compute right ascension and declination.
C
C           IF     (UNIEQU .EQ. 0.00)  THEN
C               ALPHA = 0.00
C               DELTA = SIGN (HALFPI, UNIT (3))
C           ELSE
C               ALPHA = ATAN2 (UNIT (2), UNIT (1))
C               IF     (ALPHA .LT. 0.00)  ALPHA = ALPHA + TWOPI
C               DELTA = ATAN2 (UNIT (3), UNIEQU)
C           END IF
C
C
C           ****
C           WRITE OBSERVATION CARDS
C           ****
C
C           Compute GTDS observation card date
C
C           400 OBSTIM = YMDOES * 1.06 + HMSOBS
C
C           Write right ascension card
C
C           WRITE (7,2000) STANAM,6, OBSTIM, ALPHA,ALPHA
C
C           Write declination card
C
C           WRITE (7,2000) STANAM,7, OBSTIM, DELTA,DELTA
C
C           Return
C
C           RETURN
C
C
C           **** FORMAT STATEMENTS ****
C
C

```

```
C
C           Error message.
C
1000 FORMAT( /'*****      ERROR      *****      Observa ,
*           'tion card uses unknown coordinate system.  /)
*           ' Right ascension = ',1PG17.10,20X,   'Calendar date = ,
*           OPF10.0 /
*           ' Declination    = ',1PG17.10,20X,   'Time of day,    = ,
*           OPF13.3 /
*           ' Coordinate system indicator = ',A )
C
C           GTDS observation cards.
C
2000 FORMAT( A4,5X,    I2,6X,    3G21.14 )
END
```

```

SUBROUTINE PRENUT (ROTATE, TIME,TRANS)
C
C
C
C      *****
C      FUNCTION
C      *****
C
C
C
C      This subroutine computes precession and nutation matrices for the
C      Earth at a given time and returns in parameter ROTATE the
C      coordinate transformation matrix requested in parameter TRANS:
C
C      Value of
C      TRANS          Coordinate Transformation in ROTATE
C      -----
C
C      'FULL'        MEAN OF 1950.0    to    TRUE OF DATE
C      'PRECES'       MEAN OF 1950.0    to    MEAN OF DATE
C      'NUTATE'       MEAN OF DATE     to    TRUE OF DATE
C
C
C
C      CALLING SEQUENCE *****
C
C      CALL PRENUT (ROTATE, TIME,TRANS)
C
C      PARAMETERS *****
C
C      ROTATE  D   Coordinate transformation matrix.
C
C      TIME    I   Time since 1950.0 in ephemeris days.
C      TRANS   I   Coordinate transformation requested.
C                  'FULL'        MEAN OF 1950.0    to    TRUE OF DATE
C                  'PRECES'       MEAN OF 1950.0    to    MEAN OF DATE
C                  'NUTATE'       MEAN OF DATE     to    TRUE OF DATE
C
C      SUBROUTINES CALLED *****
C
C      MSET33      MAMA33
C
C
C
C***** HISTORY *****
C
C
C
C      VERSION: February 1985
C              Fortran subroutine for the IBM 3090.
C
C      ANALYSIS
C              (unknown)

```

```
C
C      PROGRAMMER
C          (unknown)
C
C
C      MODIFIED ----- Leo W. Early, Jr.
C      Feb 1985 ----- Charles Stark Draper Laboratory
C
C          1. Converted code to Fortran 77.
C          2. Improved code structure.
C
C
C
C***** DECLARATIONS *****
C
C
C
C      IMPLICIT      DOUBLE PRECISION (A-H,O-Z)
C
C      Character Variables *****
C
C      CHARACTER * (*) TRANS
C
C      Dimensions *****
C
C      DIMENSION      XP (3,3)           ,ROTATE (3,3)
C      DIMENSION      XN (3,3)
C
C
C
C***** DATA STATEMENTS *****
C
C
C
C      Degrees to radians.
C
C      DATA DEGREE    /   1.7453 29251 99432 96   D -2   /
C
C      Sine of obliquity of ecliptic.
C
C      DATA SINEPS    /   3.978 3951   D -1   /
C
C      Constant part of nutation matrix.
C
C      DATA XN (1,1)  /   1. DO   /
C      DATA XN (2,2)  /   1. DO   /
C      DATA XN (3,3)  /   1. DO   /
C      DATA XN (1,2)  /   0 .DO   /
C      DATA XN (2,1)  /   0 .DO   /
C
C
C
C***** BEGIN PROGRAM *****
```

```

C
C
C
C      *****
C      PRECESSION MATRIX
C      *****
C
C
C      Is precession matrix needed?
C
IF    (TRANS .NE. 'NUTATE')   THEN
C
C          Compute time parameters.
C
T     =    TIME / 36524.22D0
TT   =   T * T
C
C          Compute precession matrix -- 1950.0 to requested
C          Date.
C
XP (1,1)  =  1.0D - (1.3D-7*T + 2.9696D-4) * TT
XP (1,2)  =  ((2.21D-6*T - 6.76D-6) * T - 2.234941D-2) * T
XP (1,3)  =  ((9.6D-7*T + 2.07D-6) * T - 9.7169D-3) * T
XP (2,1)  =  - XP(1,2)
XP (2,2)  =  1.0D - (1.5D-7*T + 2.4975D-4) * TT
XP (2,3)  =  - 1.0858D-4*TT
XP (3,1)  =  - XP(1,3)
XP (3,2)  =  XP(2,3)
XP (3,3)  =  1.0D - 4.721D-5*TT
END IF
C
C
C
C      *****
C      NUTATION MATRIX
C      *****
C
C
C      Is nutation matrix needed?
C
IF    (TRANS .NE. 'PRECES')   THEN
C
C          Compute time parameters.
C
DC   =   (TIME - .077D0) + 18262.5D0
TC   =   DC / 36525.D0
C
C          Compute auxiliary angles.
C
O   =   (((4.6D-20*DC + 1.557D-12) * DC + 5.2953922D-2) * DC
*       + 259.18327D0) * DEGREE
P   =   (((7.8D-20*DC + 1.700D-12) * DC + 2.6352793D+1) * DC

```

```

*      + 540.86823D0) * DEGREE
Q = ((4.52D-13*DC + 1.9712947D0) * DC
*      - 160.60664D0) * DEGREE
TWOO = 0 + 0
C
C          Compute nutation matrix at requested date.
C
XN (1,3) = (SIN(O) * (17.2327D0 + 0.01737D0*TC) -
*      SIN(TWOO) * (0.2088D0 + 0.2D-4*TC) +
*      SIN(Q) * (1.2729D0 + 0.13D-3*TC) +
*      SIN(P) * (0.2037D0 + 0.2D-4*TC)) * SINEPS / 206264.8D0
XN (3,1) = - XN(1,3)
XN (3,2) = (COS(O) * (9.21D0 + 0.91D-3*TC) -
*      COS(TWOO) * (0.0904D0 - 0.4D-4*TC) +
*      COS(Q) * (0.5522D0 - 0.29D-3*TC) +
*      COS(P) * (0.0884D0 - 0.5D-4*TC)) / 206264.8D0
XN (2,3) = - XN(3,2)
END IF
C
C
C
C          *****
C          TRANSFORMATION MATRIX
C          *****
C
C
C          Nutation.
C
IF (TRANS .EQ. 'NUTATE') THEN
    CALL MSET33 (ROTATE, XN)
C
C          Precession.
C
ELSE IF (TRANS .EQ. 'PRECES') THEN
    CALL MSET33 (ROTATE, XP)
C
C          Precession and nutation.
C
ELSE
    CALL MAMA33 (ROTATE, XN,XP)
END IF
C
C
C          *****
C          RETURN
C          *****
C
C
C          RETURN
END

```

LIST OF REFERENCES

1. King-Hele, D.G., The Royal Aircraft Establishment Table of Earth Satellites, 1957-1982, John Wiley & Sons, New York, 1983.
2. National Aeronautics and Space Administration, Interplanetary Monitoring Platform: Engineering History and Achievements, NASA TM-80758, May 1980.
3. Frazier, B., Stone, R., and Thompson, P.R., "Selection of Orbits for the CRRES Dual-Mission Satellite," AAS/AIAA pre-print 85-403, presented at the AAS/AIAA Astrodynamics Specialist Conference, Vail, Colorado, August 1985.
4. Johnson, N.L., The Soviet Year in Space: 1985, Teledyne Brown Engineering, Colorado Springs, Colorado, January 1986, (copy available from author).
5. Janin, G., "How Long Do Our Satellites Live?," ESA Bulletin, Number 45, February 1986.
6. Carter, A.B., "Satellites and Anti-Satellites, The Limits of the Possible," International Security, Volume 10, Number 4, Spring 1986.
7. Richelson, J.T., "The Satellite Data System," Journal of the British Interplanetary Society, Volume 37, 1984, pp 226-228.
8. Johnson, N.L., The Soviet Year in Space: 1984, Teledyne Brown Engineering, Colorado Springs, Colorado, January 1985, (copy available from author).
9. Johnson, N.L., The Soviet Year in Space: 1983, Teledyne Brown Engineering, Colorado Springs, Colorado, January 1984, (copy available from author).
10. Adams, J.D., Jr., "The Evolution of Eccentric Satellite Orbits," AIAA pre-print 69-928.
11. Hagesawa, G.K., A FORTRAN Program for Deep Space Sensor Analysis, AFIT/GSO/OS/84D-5, M.S. Thesis, Air Force Institute of Technology, December 1984.
12. Roth, E.A., "Space Debris - A Hazard for the Space Station," ESA Bulletin, Number 44, November 1985.
13. Lang, T.J., and Hanson, J.M., "Orbital Constellations which Minimize Revisit Time," AAS 83-402, Advances in the Astronautical Sciences, 1983, Vol 54, Part 2.

14. Suddeth, D.H., "Debris in the Geostationary Orbit Ring, The Endless Shooting Gallery, The Necessity for a Disposal Policy," Orbital Debris, NASA Conference Publication CP-2360, March 1985.
15. May, M.M., "Safeguarding Our Military Space Systems," Science, Volume 232, 18 April 1986.
16. U.S. Congress, Office of Technology Assessment, Anti-Satellite Weapons, Countermeasures, and Arms Control, OTA-ISC-281, Washington, DC: U.S. Government Printing Office, September 1985.
17. Cook, G.E., and Scott, D.W., "Lifetime of Satellites in Large Eccentricity Orbits," Planetary Space Sciences, Vol. 15, No. 10, 1967, pp. 1549-56.
18. Allan, R.R., "Commensurable Eccentric Orbits Near Critical Inclination," Celestial Mechanics, Vol. 30, No. 3, 1971, pp. 320-330.
19. Wagner, C.A., "Stable Longitudes for 12-hr Eccentric Orbit Satellites," Journal of Spacecraft and Rockets, Vol. 9, No. 10, 1972, pp. 757-763.
20. Cook, G.E., "Basic Theory for PROD, a Program for Computing the Development of Satellite Orbits," Celestial Mechanics, Volume 7, 1972, pp. 301-314.
21. King-Hele, D.G., "The Orbital Lifetimes of Molniya Satellites," Journal of the British Interplanetary Society, Vol. 28, No. 12, 1975, pp. 783-796.
22. King-Hele, D.G., "Methods for Predicting Satellite Orbital Lifetimes," Journal of the British Interplanetary Society, Vol. 31, No. 5, 1978, pp. 181-196.
23. Hoots, F.R., and Roehrich, R.L., Models for Propagation of NORAD Element Sets, Spacetrack Report No. 3, December 1980, Aerospace Defense Command, United States Air Force.
24. Hujasak, R.S., "A Restricted Four-Body Solution for Resonating Satellites with an Oblate Earth," AAS/AIAA pre-print 79-136, presented at the AAS/AIAA Astrodynamics Specialist Conference, Provincetown, Massachusetts, June 1979.
25. Kaula, W.M., Theory of Satellite Geodesy, Blaisdell Publishing, Waltham, Massachusetts, 1966.
26. Hoots, F.R., Models for Propagation of Space Command Element Sets, Spacetrack Report No. 6, July 1986, USAF Space Command.
27. Hoots, F.R., and France, R.G., "Performance of an Analytic Satellite Theory in a Real World Environment," AAS/AIAA pre-print 83-395, presented at the AAS/AIAA Astrodynamics Specialist Conference, Lake Placid, New York, August 1983.

28. Jacchia, L.G., New Static Models of the Thermosphere and Exosphere with Empirical Temperature Profiles, SP-3313, Smithsonian Astrophysical Observatory, Cambridge, Massachusetts, May 1970.
29. McClain, W.D., A Recursively Formulated First Order Semianalytical Artificial Satellite Theory Based on the Generalized Method of Averaging, Vol. 1, NASA CR-156782, N78-28147, November 1977.
30. McClain, W.D., A Recursively Formulated First Order Semianalytical Artificial Satellite Theory Based on the Generalized Method of Averaging, Vol. 2, CSC/TR-78/6001, NASA CR-156783, N78-28148, May 1978.
31. Cappellari, J.O., et al, Mathematical Theory of the Goddard Trajectory Determination System, X-582-76-77, Goddard Spaceflight Center, Greenbelt, Maryland, April 1976.
32. Green, A.J., Orbit Determination and Prediction Processes for Low Altitude Satellites, Ph.D. Dissertation, Department of Aeronautics and Astronautics, Massachusetts Institute of Technology, December 1979.
33. Taylor, S.P., Semianalytical Satellite Theory and Sequential Estimation, S.M. Thesis, Department of Aeronautics and Astronautics, Massachusetts Institute of Technology, September 1981.
34. Wagner, E.A., Application of the Extended Semianalytical Kalman Filter to Synchronous Orbits, S.M. Thesis, Department of Aeronautics and Astronautics, Massachusetts Institute of Technology, February 1983.
35. Early, L.W., "A Portable Orbit Generator using Semianalytical Satellite Theory," AIAA/AAS pre-print 86-2164-CP, presented at the AIAA/AAS Astrodynamics Conference, Williamsburg, Virginia, August 1986.
36. Charles Stark Draper Laboratory, Plotting System PLOT4B, DCD 696, August 1984.
37. Long, A.C., and Early, L.W., System Description and User's Guide for the GTDS R&D Averaged Orbit Generator, CSC ISD-7816020, Computer Science Corporation, November 1978.
38. Taylor, B.G., Andresen, R.D., Peacock, A., Zobl, R., "The European X-Ray Observatory Satellite - Exosat," ESA Journal 1982, Volume 6, 1982.
39. Peacock, A., Taylor, B.G., "Reflections on Two Years of Exosat Operations," ESA Bulletin, Number 44, November 1985.
40. Kling, R., of Teledyne Brown Engineering, personal correspondence with P.J. Cefola, dated July 23, 1986.

41. Sridharan, R., "Status of Network," presentation at 1986 Space Surveillance Workshop, Lincoln Laboratory, April 8, 1986.
42. Major, P.E., Spacetrack Sensor Accuracies, NORAD D06 Technical Note TN 79-4, October 1979.
43. Major, P.E., of USAF Space Command, personal correspondence with P.J. Cefola, December 1986.
44. Cefola, P.J., "Preliminary Test of the Extended Semianalytical Kalman Filter (ESKF) for the 12 hour, High Eccentricity Orbit," Charles Stark Draper Intralab Memorandum IR&D-012-15Z-PJC, 26 April 1982.

REPORT DOCUMENTATION PAGE		READ INSTRUCTIONS BEFORE COMPLETING FORM
1. REPORT NUMBER AFIT/CI/NR 87-52T	2. GOVT ACCESSION NO.	3. RECIPIENT'S CATALOG NUMBER <i>4115 895</i>
4. TITLE (and subtitle) An Evaluation Of Semianalytical Satellite Theory Against Long Arcs Of Real Data For Highly Eccentric Orbits		5. TYPE OF REPORT & PERIOD COVERED THESIS/11/1987/11/1987
7. AUTHOR(S) Martin Earl Fieger		6. PERFORMING ORG. REPORT NUMBER
9. PERFORMING ORGANIZATION NAME AND ADDRESS AFIT STUDENT AT: Massachusetts Institute of Technology		10. PROGRAM ELEMENT PROJECT, TASK AREA & WORK UNIT NUMBERS
11. CONTROLLING OFFICE NAME AND ADDRESS AFIT/NR WPAFB OH 45433-6583		12. REPORT DATE January 1987
14. MONITORING AGENCY NAME & ADDRESS (if different from Controlling Office)		13. NUMBER OF PAGES 211
		15. SECURITY CLASS. (of this report) UNCLASSIFIED
		15a. DECLASSIFICATION/DOWNGRADING SCHEDULE
16. DISTRIBUTION STATEMENT (of this Report) APPROVED FOR PUBLIC RELEASE; DISTRIBUTION UNLIMITED		
17. DISTRIBUTION STATEMENT (of the abstract entered in Block 20, if different from Report)		
18. SUPPLEMENTARY NOTES APPROVED FOR PUBLIC RELEASE: IAW AFR 190-1		<i>Lynn E. Wolaver May 87</i> Lynn E. WOLAVER Dean for Research and Professional Development AFIT/NR
19. KEY WORDS (Continue on reverse side if necessary and identify by block number)		
20. ABSTRACT (Continue on reverse side if necessary and identify by block number) ATTACHED		

END

12 - 87

DTIC